THE EFFECT OF GREEN ROOIBOS EXTRACT ON RAT HEARTS IN A PRE-DIABETIC MODEL: AN EVALUATION OF THE FUNCTION AND MECHANISMS INVOLVED

by

SYBRAND ENGELBRECHT SMIT

Dissertation presented for the Degree of
Doctor of Philosophy
in the Faculty of Medicine and Health Sciences
at Stellenbosch University

Supervisor: Prof. Barbara Huisamen
Co-supervisor: Dr. Erna Marais
Co-supervisor: Dr. Rabia Johnson

April 2019

DECLARATION

By submitting this dissertation electronically, I declare that the entirety of the work contained therein is my own, original work, that I am the sole author thereof (save to the extent explicitly otherwise stated), that reproduction and publication thereof by Stellenbosch University will not infringe any third party rights and that I have not previously in its entirety or in part submitted it for obtaining any qualification.

Signature: ..... **Date:** 31 October 2018

ABSTRACT

Background— Cardiovascular diseases (CVD) remains the leading cause of death globally, with a rising prevalence of individual risk factors such as obesity and insulin resistance. Furthermore, diabetic patients are particularly at risk for developing ischemic heart disease and strokes. In patient suffering an ischemic event, most of the myocardial damage incurred happens once blood flow is restored – a phenomena known as reperfusion injury. Mitochondrial ROS production is implicated as one of the major contributors to cell death in the reperfused heart and the importance of mitophagic processes (mitochondrial housekeeping) could be a potential therapeutic target to prevent ischemia/reperfusion injury (I/R-I). *Aspalathus linearis* (commonly known as rooibos) is an indigenous South African plant grown exclusively in the Western Cape fynbos region. Rooibos is rich in bioactive phenolic compounds, including aspalathin, a C-linked dihydrochalcone glucoside unique to rooibos, known for its hypoglycemic and strong antioxidant potential.

Methods— The present study made use of 300 Wistar rats randomly allocated into controls and rats receiving a 16-week high-fat, high-caloric diet (HCD). After 10 weeks on the respective diets, half of each group received 60 mg/kg/day Afriplex green rooibos extract (GRT), containing 12% aspalathin, for 6 weeks. The primary aim was to investigate its therapeutic potential in treating 20 min global ischemia/reperfusion injury (I/R-I) in rats with increased susceptibility for CVD, as well as determine the mitochondrial oxidative phosphorylation (OxPhos) during four stages of I/R-I. The secondary aim was to elucidate GRT's effect on cardiac signaling and mitophagy with regards to I/R-I.

Results— HCD over 16 weeks resulted in daily increased food intake (22.30±1.27 g vs 18.00±0.54 g = ↑24%; $p<0.001$), decreased daily water intake (19.55±0.58 mL vs 29.74±0.74 mL = ↓34%; $p<0.001$), leading to increased body weight (403.9±5.1 vs373.6±4.8 g = ↑8%; $p<0.001$) and increased intraperitoneal fat (23.69±0.89 vs 13.98±0.43 g = ↑69%; $p<0.001$) compared to age-matched controls. Furthermore, HCD increased fasting blood glucose (5.75±0.16 vs 5.21±0.16 mM = ↑10%; $p<0.05$), fasting blood insulin (6.20±0.57 vs 4.31±0.54 ng/mL = ↑44%; $p<0.05$) and insulin resistance through raised HOMA-IR (3.52±0.35 vs 2.30±0.28 = ↑53%; $p<0.05$) compared to age-matched controls. GRT supplementation for 6 weeks had no significant effect on biometric parameters in either controls or HCD. Pre-ischemia, HCD rats presented with worse functional heart parameters, such as diastolic and systolic pressure, aortic output (AO), cardiac output (CO) and total work (W_T) (10.69±0.14 vs 12.6±0.19 mW = ↓15%; $p<0.001$) compared to controls, while GRT supplementation was able to significantly improve these parameters in both controls (13.91±0.23 mW = ↑10%; $p<0.001$) and HCD (11.98±0.20 mW = ↑12%; $p<0.001$). GRT administration also lowered the heart rate during stabilization in both control and HCD by an average 10 bpms ($p<0.05$). Post-ischemia, HCD hearts were weaker than controls and had a lower W_T recovery (55.51±2.28 vs 64.8±2.04% = ↓14%; $p<0.01$), while GRT restored W_T recovery in HCD (63.35±2.49% = ↑14%; $p<0.05$). HCD rats also had a greater infarct size compared to controls (34.99±11.56 vs 16.42±8.71% = ↑113%; $p<0.01$) following a 35 min regional ischemia protocol. GRT supplementation led to a remarkable reduction in infarct size (13.22±6.66% = ↓62%; $p<0.001$), while conferring no added protection to controls (14.58±5.43%). Regarding cardiac and mitochondrial signaling, prior to ischemia HCD heart had a decreased dependence on insulin-dependent AMPK and increased inflammation via upregulated p38, whereas GRT treatment presented with decreased insulin-dependent PKB and AS160 signaling (together with increased FA OxPhos compared to carbohydrates,

however showed more mitochondrial uncoupling, decreasing basal metabolic rate and thereby potentially less ROS production), inhibited GSK3β and conferred an anti-inflammatory effect by significantly reducing p38 activation. HCD also had higher mitophagy rates through Parkin and LC3 signaling. After 20 min ischemia, in HCD, ATM and AMPK were upregulated and insulin-dependent PKB downregulated with GSK3β. Mitophagy signals, such as PINK1 and p62 were elevated, but autophagic flux remained low during ischemia in all groups. GRT supplementation resulted in an opposite profile with AMPK downregulated and showing inhibition of ERK1/2. In early reperfusion, all protective signaling were downregulated in HCD including AMPK, PKB, AS160, GSK3b and ATM. Mitophagy was also activated through Parkin, p62 and LC3 while having increased OxPhos potential in FA compared to carbohydrates. GRT supplementation reduced oxidative stress and inflammation through downregulation of JNK1/2 and p38, and initiated mitophagy through an AMPK-dependent mechanism and Parkin. GRT supplementation also inhibited mitochondrial OxPhos after reperfusion culminating in a potentially decreased ROS production.

Conclusion— This study showed the cardioprotective effect of Afriplex GRT supplementation by improving functional heart recovery and reducing infarct size post-ischemia in rats with elevated risk for CVD. Another novel find is the reduction in heart rate induced by GRT treatment through inhibition of pacemaking cells. This could have potential therapeutic application in patients suffering from ischemic heart disease. GRT ilicits a cardiotonic effect in I/R-I through anti-inflammatory mechanisms pre- and post-ischemia. In early reperfusion, GRT treatment resulted in decreased oxidative stress, inhibition of mitochondrial OxPhos and enabled AMPK-dependent mitophagy. GRT shows promise as a strong antioxidant and anti-inflammatory agent in managing adverse outcomes in patients at risk for CVD.

ABSTRAK

Agtergrond- Kardiovaskulêre siektes (CVD) is steeds die wêreld se nommer een oorsaak van sterftes. Die teenwoordigheid hiervan kan grotendeels toegeskryf word aan ‘n toenemende voorkoms van individuele risikofaktore, insluitende vetsug en insulienweerstandigheid. Verder, diabetiese pasiënte in besonder dra hoë risiko vir die ontwikkeling van iskemiese hartsiektes en beroertes. In pasiënte wat 'n iskemiese gebeurtenis ly, word die meeste van die myokardiale skade eers opgedoen wanneer bloedvloei herstel word - 'n verskynsel bekend as reperfusiebesering. Mitochondriale reaktiewe oksidant spesie (ROS)-produksie word geïmpliseer as een van die belangrikste bydraers tot seldood tydens reperfusie en die belangrikheid van mitofagiese prosesse (mitochondriale huishouding) kan 'n potensiële terapeutiese doelwit dien in voorkoming van iskemie/reperfusiebesering (I/R-I). *Aspalathus linearis* (algemeen bekend as rooibos) is 'n inheemse Suid-Afrikaanse plant wat uitsluitlik in die Wes-Kaapse fynbosstreek gegroei word. Rooibos is ryk aan bioaktiewe fenoliese verbindings, insluitende aspalatien, 'n C-gekoppelde dihidrochalcoon-glukosied, uniek aan rooibos, en bekend vir sy sterk anti-inflammatoriese antioksidant en vermoë om bloedsuiker te verlaag.

Metodes- In die teenwoordigende studie het ons gebruik gemaak van 300 Wistar-rotte wat lukraak verdeel is in ‘n 16-week hoë-vet, hoë-kalorie-dieet (HCD) groep, en ‘n ouderdom-gekontroleerde beheergroep wat slegs standard rotkos ontvang het. Na 10 weke op die onderskeie diëte het die helfte van elke groep vir 6 weke 60 mg / kg / dag Afriplex Green Rooibos Extract (GRT), wat 12% aspalatien bevat, ontvang. Die primêre doel was om die terapeutiese potensiaal as behandeling van 20 min globale ischemie / reperfusiebesering (I /R-I) te ondersoek in rotte met verhoogde vatbaarheid vir KVS, asook om die mitochondriale oksidatiewe fosforilering (OxPhos) tydens vier stadiums van I/R-I te bepaal. Die sekondêre doelwit was om GRT se effek op hart seintransduksie en mitofagie met betrekking tot I/R-I te verduidelik.

Resultate-HCD administrasie, teenoor kontrole dieet, vir 16 weke het gelei tot verhoogde daaglikse voedselinname (22,30±1,27 g teenoor 18,00±0,54 g = ↑ 24%; p<0.001) en verhoogde daaglikse waterinname (19.55±0.58 mL vs 29.74±0.74 mL = ↓ 34%; p<0.001) wat gelei het tot verhoogde liggaamsgewig (403.9±5.1 vs 373.6±4.8g = ↑ 8%; p<0.001) en verhoogde intraperitoneale vet (23.69±0.89 teenoor 13.98±0.43g = ↑ 69%; p<0.001). Daarbenewens het HCD ook verhoogde vastende bloedglukose (5.75±0.16 vs 5.21±0.16 mM = ↑10%; p<0.05), vastende bloedinsulien (6.20±0.57 vs 4.31±0.54 ng / mL = ↑44%; p<0.05) en insulienweerstandigheid deur verhoogde HOMA-IR (3.52±0.35 vs 2.30± 0.28 = ↑53%; p<0.05) in vergelyking met ouderdom-gekontroleerde kontrole groepe. GRT-aanvulling vir 6 weke het geen beduidende effek gehad op biometriese parameters in beide die kontroles en HCD nie. Tydens stabilisering van die geïsoleerde harte, het dié van HCD-rotte verswakkende funksionele hartparameters getoon, soos diastoliese en sistoliese druk, aorta-uitset (AO), hartuitset (CO) en totale werk (W_T) (10.69±0.14 teenoor 12.6±0.19 mW = ↓15%; p<0.001) in vergelyking met kontroles, terwyl GRT-aanvulling hierdie parameters aansienlik kon verbeter in beide kontroles (13.91±0.23 mW = ↑10%; p<0.001) en HCD (11.98±0.20 mW = ↑12%; p<0.001). GRT-administrasie het ook die hartklop verlaag tydens stabilisering met 'n gemiddelde 10 hartkloppens per minuut in beide beheer en HCD groepe (p<0.05). Tydens reperfusie het HCD harte swakker gevaar as kontroles met 'n verlaagde W_T herstelling (55.51±2.28 teenoor 64.8±2.04% = ↓14%; p<0.01), terwyl GRT W_T kon herstel in HCD (63.35±2.49% = ↑14%; p<0.05). HCD-rotte het ook groter

infarkt-groottes gehad in vergelyking met beheer groepe (34,99±11,56 teenoor 16,42±8,71% = ↑113%; p<0.01) na aanleiding van 'n 35 min streeks-ischemie protokol. GRT-aanvulling het gelei tot 'n merkwaardige vermindering in infarkt-grootte (13.22±6.66% = ↓62%; p<0.001), terwyl dit geen ekstra beskerming aan kontroles verleen het nie (14.58±5,43%). Met betrekking tot die hart- en mitochondriale seintransduksie het die HCD-hart 'n afname in afhanklikheid van insulien-afhanklike AMPK en toename van inflammasie via opgereguleerde p38 getoon. GRT-behandeling het ‘n beduidende verlaging van insulien-afhanklike PKB- en AS160-sein geïnduseer (saam met verhoogde vetsuur teenoor koolhidraat oksidatiewe fosforilasie (OxPhos) vertoning, maar terselfdertyd verhoogde mitochondriale ontkoppeling wat gevolglik ‘n stadiger basale metaboliese tempo tot volg het en moontlik minder reaktiewe oksidante spesie (ROS)-produseer). GRT-behandeling het ook GSK3β geïnhibeer en 'n anti-inflammatoriese effek toegedien deur die p38-aktivering aansienlik te verminder. HCD het ook hoër mitofagiese prosesse getoon deur Parkin- en LC3-seine te opreguleer. Na 20 min van iskemie in HCD harte is ATM en AMPK opgereguleer en insulien-afhanklike PKB is afgereguleer saam met GSK3β. Mitofagiese seine, soos PINK1 en P62, was verhef, maar autofagie as ‘n geheel was laag gedurende ischemie in alle groepe. GRT aanvulling het gelei tot 'n teenoorgestelde profiel met ‘n afname in AMPK aktivering asook inhibisie van ERK1/2. Tydens vroeë reperfusie is alle beskermende seinwerk in HCD afgestel, insluitende AMPK, PKB, AS160, GSK3β en ATM. Mitofagie is ook geaktiveer deur Parkin, P62 en LC3, terwyl OxPhos potensiaal toegeneem het in vetsure in vergelyking met koolhidrate. GRT-aanvulling het verder oksidatiewe stres en inflammasie verminder deur JNK1/2 en p38 af te reguleer, en verhoging in mitofagie teweeg gebring deur middel van 'n AMPK-afhanklike meganisme en Parkin. GRT-aanvulling het ook mitochondriale OxPhos geïnhibeer na reperfusie wat 'n potensiële verlaagde ROS-produksie tot volg gehad het.

Gevolgtrekking - Hierdie studie het die hartbeskermende effek van Afriplex GRT-aanvulling getoon deur die verbetering van funksionele hartherstel en die vermindering van infarkt-grootte na ‘n ischemiese episode uit te wys in pre-diabetiese rotte met verhoogde risiko vir CVD. Nog 'n nuwe bevinding is die verlaging in hartklop geïnduseer deur GRT behandeling deur inhibisie van pasaangee selle en kan potensiële terapeutiese toediening hê by pasiënte wat aan iskemiese hartsiektes ly. GRT gee 'n kardiotoniese effek in I/R-I deur middel van anti-inflammatoriese meganismes voor- en na-ischemie. In vroeë reperfusie het GRT-behandeling gelei tot verminderde oksidatiewe stres, inhibisie van mitochondriese OxPhos en AMPK-afhanklike mitofagie. GRT toon belowende effekte as 'n sterk antioksidant en anti-inflammatoriese middel in die hantering van nadelige uitkomste vir pasiënte met 'n risiko vir CVD.

ACKNOWLEDGEMENTS

Holy Bible : New Living Translation

1 Corinthians 13:1 - 13

Love Is the Greatest

"[1]If I could speak all the languages of earth and of angels, but didn't love others, I would only be a noisy gong or a clanging cymbal. [2] If I had the gift of prophecy, and if I understood all of God's secret plans **and possessed all knowledge**, and if I had such faith that I could move mountains, **but didn't love others, I would be nothing.** [3] If I gave everything I have to the poor and even sacrificed my body, I could boast about it; but if I didn't love others, I would have gained nothing.

[4] Love is patient and kind. Love is not jealous or boastful or proud [5] or rude. It does not demand its own way. It is not irritable, and it keeps no record of being wronged. [6] It does not rejoice about injustice but rejoices whenever the truth wins out. [7] Love never gives up, never loses faith, is always hopeful, and endures through every circumstance.

[8] Prophecy and speaking in unknown languages and special knowledge will become useless. But love will last forever! [9] **Now our knowledge is partial and incomplete**, and even the gift of prophecy reveals only part of the whole picture! [10] **But when the time of perfection comes,** these partial things will become useless.

[11] When I was a child, I spoke and thought and reasoned as a child. But when I grew up, I put away childish things. [12] Now we see things imperfectly, like puzzling reflections in a mirror, but then we will see everything with perfect clarity. All that I know now is partial and incomplete, but then **I will know everything completely, just as God now knows me completely.**

[13] **Three things will last forever—faith, hope, and love—and the greatest of these is love."**

- Paul, the Apostle of Jesus Christ

My thanks be to **God** for blessing me with opportunity to study, to advance my career, to enquire into things I'm curious about, to grant me with favour so I can focus on completing the task at hand - all while I'm searching for my place in the Kingdom and learning to submit to His Will. My God is an awesome God. His Name is **Jesus**. He is Worthy of All Praise! And I will sing of His Love Forever. Amen!! Thank you, Jesus, for saving me from my brokenness and my addictions. And for filling me with life!! That I may testify of Your Name. I pray that whoever read this, may they know that in my own strength this thesis would've been incoherent scribbles and half a completed diagram. When I had 2 months to go, a Literature Review to finish writing, a conference to attend abroad, and an ENTIRE results and discussion section to complete – God took my hand, slapped the cigarettes and alcohol and grass out of my hand, and taught me how to persevere to finish a job. God is Good. And He is open to show anyone who seek Him how much He loves you. He is in the game of miracles and He WILL meet you at your expectation! Therefore, ALL the Thanks and Praise be to YOU, **Jesus**!

I would also like to thank the **Division of Medical Physiology** (Stellenbosch University) and the **National Research Foundation** for financial support. Thanks to the efforts of both I was able to experience a lifelong

goal of mine to have gone abroad and visit Israel, to go to China, Sun City, conferences at places that I would not have had the privilege to experience had it not been for the fortunate set of circumstance that allowed me the opportunity to pursue my Doctoral studies in such a peaceful environment. I would forever recommend the department because of its people. It makes life's choices more difficult because you guys are so deep in my heart, yet we have to move on… It was a true honour to have spend my every day the past 5 years at Medical Physiology. May you all be blessed and continue to lift up the medical scientists of tomorrow!

I would like to thank **Prof. Barbara Huisamen**. She put a lot of trust in me to do my own thing, and there were days where the freedom got the best of me, but she always had a gentle approach to encourage me, inform me of opportunities, to make suggestions, and to assist with all my questions. I would not have been finished had it not been for your encouragement to make the necessary arrangements to get my reviewers to concede getting the dissertation both late and still full of rash writing that would require soft understanding eyes. You are a good supervisor, researcher, speaker, teacher and mother! I am very proud that I made the right choice 5 years ago to put my trust in you as a supervisor. I have not regretted it once. I hope it's mutual even with all my stubbornness :') But for that I also want to thank you – for bearing with me. I was a very… "eie-wys' tipe student… "At times". But I loved being proven wrong or being set straight with one quick answer! And of that there was many! Everytime I wanted to deviate from the plan, you were quick to just give me what I want most – the Why! Understanding. Thank you, Prof. May your years of research and teaching be as many as you desire! And may you continue to be a blessed supervisor. Emotionally, financially and skillfully. Thank you to my co-supervisors, **Dr. Erna Marais and Dr. Rabia Johnson**: especially towards the end I appreciate all the late nights editing and extra hours pushing through to make the submission possible! It would not have been possible without you! I wish you all of the best with your current and prospective students! May they find solace in your steed.

I would like to thank **Dr. Mignon van Vuuren**. We started this PhD journey together, we were young and hopeful and confused about everything. But even when procrastination was at its peak, experiments at its worst, and our hair messy from blowing cells – I still knew it would be a good day at the office if we were near! I wish you all the best and I look forward to your business one day! Whatever it may be, it will fly! Cause you can add sparkle to anything.

I would like to thank **Frans Everson**. Mister! Ja-nee niks wat Frans doen is mainstream nie, so nou sit hy in België! Haha, maar nee dis tydelike treffers daai! Een van die dae is jy terug en dan is dit net vasbyt tot die einde. Hopelik bring hulle elke maand 'n nuwe McFlurry of Krusher flavor uit… want broer, jy gaan 'n soetigheid begin crave! Lol, nee ek spot, maar ek waardeer regtig al die wyse woorde deur die dae en aande… en vroeë oggendure! En ek is jammer vir my een song wat ek aanhou sing het hier van begin einde se tyd (beide studies en verhoudings), mens gaan mos maar deur die motions (as jy jonk is… haha, ek hoop dis once). Maar ek waardeer jou geselskap, ons mannewales in Parys en Sun City, al die lawwigheid en ernstige sit en werk, en voorsiening… Jy't my vrygewigheid geleer. Om vir mense sommer net te seen met kos en geskenke en choclits. Dit is 'n voorreg en 'n plesier om jou vriend te wees! Mag dit juig vorentoe. Ek staan op aandag om te sien hoe die toekoms uitspeel! Sterkte, buddy!

I would like to thank **Claudine Manirafasha**. We started in the deepend together! Learning how to animal, finding out adult-onset rat allergy is a thing. Lol. But I really enjoyed getting to know and taking care of babies. You've taught me a lot about taking life by the horns and jumping on opportunities as they come. I take my hat of for you and what you've accomplished, and I hope your studies will finish soon! I hope you're writing as I type xD. Good luck! And I hope to see you soon, roomie! And blessings be upon, Mugisha!! May he grow up strong and steadfast in the Lord! You have a beautiful boy, Claudine!

I want to thank **Elina Kamanga (Alzie)**… For supporting me to start this degree. Even though it became the most difficult time of my life in so many aspects. From having too much freedom, to having none at all, and fighting through so many personal battles… I wouldn't trade these 3 years, along with the experience, friendships I made, lessons I learnt, mistakes I made (a lot) - they were all necessary in the grander scheme God has planned for each of us. As I'm writing this, I am excited. SO excited. I've made it to 30 and I still have the excitement of a kid when I picture what God can do in people's lives! And it will always be my hope that He will lift you up and bless you and restore all the honour that you deserve. I just want to see when it happens… I wanna sing How Great is Our God with you. In honest worship. Thank you for being part of my life, Alzie. And congratulations on completing your Psychology Masters degree Cum LAUDE!! You the boss, baby girl! And you were meant to flap your wings! May God keep you safe till you find home!!

I want to thank **Sibo Mzezewa**. You are one of the most genuine people I have ever met. You supported me through everything. You had your hands full with my drama and "new-person" hopes and all my excuses and listening to my deepest fears. And I thank God that He taught you how to persevere and pray your way through the storms of life! You encouraged me more than anyone has ever done before. In return, I will be exponentially nice to you for the rest of my life! Haha, I will continue to try and pay you back. But I really owe you. And I truly believe we will be friends for life. You have an amazing anointing on your life to care deeply for people, to commit to people and to stand in the gap between their problems and God. So, may you run and not grow weary, and may God strengthen both your heart and hand to keep on encouraging people. Even when they are being… Two and a Half Men… Sorry. But done with that, here's to personal testimonies of victory and growth! May the curve never plato! Let's run! Catch me! xD

I want to thank **Junaid Koopman**. Sup buddy! Thank you Jay for all your sacrifices after long days at work and then still having to deal with my thesis whining, and making me food (EVERY DAY.. wow), and always being willing to relax when I need a friend. You are such a caring person, Kleinboet. I'm so hopeful that your breakthrough is naby. And by that I mean just working for and with people that appreciate you! Basics, you know? But we've come a long way you and I… We've been through two new year's eves… We were there! Haha. I've really enjoyed spending time with you, and even with the uncertainties of the future, one thing is certain and that is that we will always be friends. Because… you stuck with me man :') You bring out the random in me, and I bring out the frustration in you!! But it's good. Cause you need to be challenged. I challenge you to a duel some. Hehe. Nah, just wanna say I love you man, and I look forward to seeing what on the horisons! 4 Directions! You decide ;)

I want to thank my dad, **Yan Smit**, for all his sacrifices. You have supported me since child's leg, and thanks to you I have had all the personal freedom in the world to choose my own future. You've always encouraged me to do what feels right to me. Not just verbally, but backing your word with finances and support in ways I never expect. From paying my undergrad studies, to helping me with living cost and then giving me gradually more responsibility – a student house so I can stay with people I care about… This is the life I get to lead because of one man's faithfulness. You are a great dad. And I feel guilty to have had such a loving father.. who fears the Lord, gives credit where credit is due, always tries to make every gettogether special and memorable. Who tells me he loves me and is proud of me. Continuously. These are goals for any parents, and you are doing them on autopilot. Dankie Pa… Ek is baie life vir PA!

I want to thank my mum, **Solje Smit**, for being the best mother ever. From starting to fill my sponge brain as a baby, to providing my every need as a child and then 'advising' me what to do as a student :') always encouraging me to go out, see places, do stuff! Haha, and that is exactly who you are! I have so much respect for mum and the courage to have started, persevered, and even cumming your Psych-Ed Honours studies, pursuing a love for children having successfully raised her own 4! Next! Haha, a real go-getter. And I'm proud of your leap of faith to go all the way to Dubai!! I love this side of you, and I want mum to have the most adventurous life ahead. I hope there an extra bed ready for when we come visit please! Dubai sounds just around the corner! Baie lief vir MA!!

I want to also thank **Enid Mulder**, for being the most selfless person I know. Dankie vir elke liewe opoffering en voorsiening wat jy gemaak het in my lewe gedurende die afgelope 10 jaar. Van die optellende gesprekke, tot die afsloof in kombuis, tot die opoffer van jou laptop op 'n crucial tyd wat myne nie meer wou nie… Almal kan altyd meer gerus wees as jy naby is, want jy doen almal se werk!! En dis regtig my hoop dat mense dit sal begin raaksien en jou waardeer vir wie jy is, ver bo net vir wat jy doen! Ek wil partykeer uitbasuin "Jy is GENOEG!", want sjoe iewers moet iemand anders bietjie slack optel en vir jou treat! Die boot was heerlik, dankie!! :') Besef ek nou! Haha, maar nee, ek bedoel dit. Jy is 'n goeie mens. En goeie mense verdien 'n break! Dankie vir al jou liefde!! Ek waardeer jou ontsaglik baie!! Baie lief vir jou!

Die res van die Smulders gesin!! **Jean, Gerrie, Mia, Trudie, Marichelle, Andy**… Julle weet ek is eksponensiëel lief vir julle elkeen! Dis nou 05:00 op Maandag 25 Februarie… En ek kon seker nog, maar… ek sien julle nou-nou, so dus same thing! 0:)

To all the people of 10 Ricketts and 6 Groeneweide!! **Zibele, Festus, Nyiko, Yaw, Kojo, Lieze, Jess, Thembi**!!! You guys have been there at my best and worst!! And you've loved me all the way! I really appreciate you guys and know that I will move stones for all of you one day! Just say when and I'll bring the bakkie! :')

And lastly, a special shout-out to **everyone who prayed for me** during this season of mine! May God double your portion, and may you walk in favour all the days of your life! You have an amazing heart, and we serve an amazing God. **Every blessing for every person in this acknowledgement, I pray and bind in the Name of Jesus, our Lord and Saviour! Amen.**

x

PUBLICATIONS DURING THE STUDY

1. **Smit, S.E.**, Johnson, R., Van Vuuren, M.A. & Huisamen, B. Myocardial Glucose Clearance by Aspalathin Treatment in Young, Mature, and Obese Insulin-Resistant Rats. Planta Med. **2018** Jan;84(2):75-82. doi: 10.1055/s-0043-117415.

PRESENTATIONS AT SCIENTIFIC MEETING

1. **Smit, S.E.**, Huisamen, B. & Marais, E. The metabolic changes within the heart of rats subjected to a high-fat, low-carbohydrate diet and the functional recovery of the heart after ischemia reperfusion. Oral presentation, Biomedical Research and Innovation Platform, Medical Research Council Journal Symposium, Cape Town, South Africa, **2016**.
2. **Smit, S.E.** Shining light on heart matters. Oral presentation, Medical Physiology Journal Symposium, Stellenbosch University, South Africa, **2016**.
3. **Smit, S.E.,** Huisamen, B., Marais, E. & Johnson, R. Afriplex GRT Progress Lecture. Oral Presentation. Biomedical Research and Innovation Platform. South African Medical Research Council, Cape Town, South Africa, **2017**.
4. **Smit, S.E.** Antioxidants in cardiovascular research therapy. Oral presentation, Medical Physiology Journal Symposium, Stellenbosch University, South Africa, **2017**
5. **Smit, S.E.,** Huisamen, B., Marais, E. & Johnson, R. Green rooibos extract (Afriplex GRT) protects rat hearts against high-fat, high-caloric diet-induced comorbidities. Oral presentation, Annual Academic Year Day, Stellenbosch University, South Africa, **2017**
6. **Smit, S.E.,** Huisamen, B., Marais, E. & Johnson, R. Green rooibos extract's cardioprotective properties and potential mechanisms. Oral presentation, South African Rooibos Council Funding Symposium, Agricultural Research Council, Stellenbosch, South Africa, **2017**
7. **Smit, S.E.,** Huisamen, B., Marais, E. & Johnson, R. Afriplex green rooibos extract and post-ischemic heart recovery in diet-induced pre-diabetic rats. Oral presentation, The 66th Annual Meeting of the Society for Medicinal Plant and Natural Product Research (GA) jointly with the 11th Shanghai International Conference on Traditional Chinese Medicine and Natural Medicines (S-TCM), Parkyard Hotel, Shanghai, China, **2018**
9. **Smit, S.E.,** Huisamen, B., Marais, E. & Johnson, R. Cardioprotective properties of Afriplex green rooibos extract in diet-induced obese wistar rats. Oral presentation, SA Heart, Sun City, South Africa, **2018**

TABLE OF CONTENT

LIST OF ILLUSTRATIONS

FIGURES

APPENDIX

TABLES

CHAPTER FOUR

CHAPTER FIVE

APPENDIX

LIST OF ABBREVIATIONS

I. UNITS OF MEASUREMENT

% : percentage
°C : degree celcius
bpm : beats per minute
cm : centimeter
g : gram
h : hour
Hg : mercury
IU : International unit
kg : kilogram
kJ : kilojoules
L : litre
M : molar
mA : milliampere
mg : milligram
min : minute
mm : millimeter
mM : millimolar
p : pico
rpm : revolutions per minute
sec : second
V : volt
W : work
v : volume
α : alpha
β : beta
ζ : zeta
λ : lambda
μ : micro
μL : microlitre
μm : micrometer

II. CHEMICAL COMPONENTS

Acrylamide : N,N'-Methylenebisacrylamide
Ca^{2+} : calcium
$CaCl_2$: Calcium chloride
CO_2 : Carbon dioxide
$CuSO_4$: Copper sulfate
dH_2O : Distilled water
DMSO : Dimethyl sulfoxide
$DPPH^{\bullet}$: 2,2-diphenyl-1-picrylhydrazyl free radical
e^- : electron
EDTA : Ethylenediaminetetraacetic acid
EGTA : Ethyleneglycoltetraacetic acid
H^+ : protons / hydrogen ions
H_2O : water
H_2O_2 : hydrogen peroxide
HO2• : hydroperoxyl radical
HCl : hydrochloric acid
KCl : Potassium chloride
KH : Krebs-Henseleit buffer
KH_2PO_4 : Potassium dihydrogen phosphate
$MgSO_4$: Magnesium sulphate
Na^+ : sodium ion
Na^+K^+-tartrate : Sodium potassium tartrate
Na_2CO_3 : Disodium carbonate
Na_2HPO_4 : Disodium hydrogen phosphate
Na_2SO_4 : Sodium sulphate
Na_3VO_4 : Sodium orthovanadate
NaCl : Sodium chloride
NaH_2PO_4 : Sodium dihydrogen phosphate
$NaHCO_3$: Sodium bicarbonate
NaOH : Sodium hydroxide
NO : Nitric oxide
O_2 : oxygen
$O_2^{\bullet}$: superoxide radical
PMSF : Phenylmethyl sulfonyl fluoride
SDS : Sodium dodecyl sulfate
STZ : Streptozotocin
TBS : Tris-buffered saline
TCA : Trichloroacetic acid
TEMED : N,N,N',N',-tetramethylethylendiamin
TMB : 3,3,5,5'-tetramethylbenzidine

TTC : Triphenyl tetrazolium chloride

III. PROTEIN ABBREVIATIONS

ADP : adenosine diphosphate
AGE : Advanced glycation end products
AMP : adenosine monophosphate
AMPK : AMP-activated protein kinase
AS160 : Akt substrate of 160 kDa
Atg : autophagy-related protein
ATP : adenosine triphosphate
BAD : Bcl-2-associated death promoter
Bak : Bcl2 homologous antagonist/killer
Bax : Bcl2-like protein 4
Bcl2 : B-cell lymphoma 2
Bid : BH3 interacting-domain death agonist
BNIP3 : Bcl2 nineteen kilodalton interacting protein
BSA : Bovine serum albumin
CaMKKβ : Ca2+-calmodulin-dependent kinase kinase β
cAMP : Cyclic adenosine monophosphate
CPT-1 : Carnitine palmitoyl transferase-1
DDP-4 : dipeptidyl peptidase-4
ERK : extracellular signal regulated kinase
FA : Fatty acids
FFA : Free fatty acids
G-1-P : Glucose-1-phosphate
G-6-P : glucose-6-phosphate
GAP : GTPase-activating protein
GLUT1/4 : glucose transporter 1/4
GLP-1 : glucagon-like peptide-1
GSH : Glutathione
GSK-3 : glycogen synthase kinase-3
GSSG : Glutathione disulfide
GTP : Guanosine triphosphate
HbA1c : glycohemoglobin
HDL : High-density lipoproteins
HDL-C : High-density lipoprotein cholesterol
HRP : Horseradish Peroxidase
IgG : Immunoglobulin G
IL-1β : Interleukin-1β
IL-6 : Interleuken-6
IR : Insulin receptor
IRS : Insulin receptor substrate
JAK : Janus kinases
JNK : c-Jun N-terminal kinase
LDL-C : Low-density lipoprotein cholesterol
LKB1 : liver kinase B1
MAPK : mitogen activated protein kinase
MCP1 : monocyte chemoattractant protein-1
MCT1/4 : monocarboxylate transporters 1/4
mPTP : mitochondrial permeability transition pore
mTOR : mammalian target of rapamycin
NADH Nicotinamide adenine dinucleotide
p22phox : human neutrophil cytochrome b light chain
PDH : Pyruvate dehydrogenase
PH : Pleckstrin homology
PI3K : Phosphatidylinositol 3 kinase
PIP2 : (Ptdlns(4,5)P2) Phosphatidylinositol (4,5) bisphosphate
PIP3 : (Ptdlns(3,4,5)P3) Phosphatidylinositol (3,4,5) triphosphate
PKA : Protein kinase A (cyclic AMP-dependent protein kinase)
PKB : protein kinase B (or Akt)
PDK1 : phosphoinositide-dependent kinase-1
PIP2 : phosphatidylinositol phosphate
PKC : Protein kinase C
PPAR-γ : Peroxisome proliferator-activated receptor γ
PTEN : Phosphatase and tensin homolog deleted on chromosome 10
Puma : p53 upregulated modulator of apoptosis
RIP : receptor-interacting proteins
Ser : Serine
SOD : superoxide dismutase
SR : Sarcoplasmic reticulum

STAT : Signal transducers and activators of transcription
TAG : Triacylglycerols
TBARS : thiobarbituric acid reactive substances
Thr : Threonine
TMB : 3,3',5,5'-Tetramethylbenzidine
TNFα : Tumor necrosis factor α
VIP : vasoactive intestinal peptide

IV. OTHER ABBREVIATIONS

$\Delta\psi_m$: mitochondrial membrane potential
%RR : Percentage respiratory recovery
AAR : Area at risk
AO : Aortic output
ARC : Agricultural Research Council
AUC : Area under curve
BC : Before Christ
BMI : Body Mass Index
BW : Body weight
CDC : Center for Disease Control and Prevention
CF : Coronary flow rate
CO : Cardiac output
CT : Computerized Tomography
CVD : Cardiovascular disease
DEXA : Dual X-ray
DiaP : Diastolic pressure
ECL : Enhanced chemiluminescence
ETC : electron transport chain
FA : Fatty acids
FAME : fatty acid methyl esters
FFA : Free fatty acids
FRE : Fermented rooibos extract
GC : gas-liquid chromotography
GRE : Green rooibos extract
GRT : Afriplex green rooibos extract
HCD : High-caloric diet
HOMA-IR : Homeostasis model assessment of insulin resistance
HR : Heart rate
IHD : Ischemic heart disease
IP : Intraperitoneal
IPC : Ischemic preconditioning
InsR : Insulin resistance
I/R-I : Ischemia/reperfusion injury
KH : Krebs-Henseleit buffer
MRC : Medical Research Council
MRI : Magnetic Resonance Imaging
NIH : National Institutes of Health
OGTT : Oral glucose tolerance test
OxPhos : Oxidative phosphorylation
OxPhos S3 : Oxidative phosphorylation of S3
OxPhos S4 : Oxidative phosphorylation of S4
PVDF : Polyvinylidene fluoride
QC : Quality Control
RCI : Respiratory control index
RISK : Reperfusion-injury salvage kinase
ROS : Reactive oxygen species
RSA : Republic of South Africa
S3 : State 3 respiration
S4 : State 4 respiration
S5 : State 5 respiration
SAFE : Survivor activating factor enhancement
SDS-PAGE : Sodium dodecyl sulphate-polyacrylamide gel electrophoresis
SEM : Standard error of the mean
SS : Soluble solids
SysP : Systolic pressure
T1D : Type 1 Diabetes
T2D : Type 2 Diabetes
UK : United Kingdom
USA : United States of America
W_T : total work
WHO : World Health Organization

Chapter 1
LITERATURE REVIEW
Cardiovascular Disease

1.1 INTRODUCTION

"The Heartfelt Truth"

Cardiovascular diseases (CVD) are the leading cause of death worldwide, constituting 31% of all annual global deaths (17.7 million people) ("WHO | Cardiovascular diseases", 2018). The two major contributing factors are obesity (excessive energy storage) and insulin resistance (reduced glucose clearance). Under normal physiological conditions, the heart's contractile function enables circulation of nutrient rich blood through the arteries and veins of the entire body. The heart also relies on these nutrients, including glucose and free fatty acids (FFA), as energy substrates for its contracting cardiomyocytes. The rate at which nutrients are transported into all cells and used as substrates is primarily dependent on the action of the hormone, insulin. Insulin induces anabolic processes through activating energy consumption, while simultaneously counterbalancing blood glucose levels. However, in diseased conditions, such as type 2 diabetes (T2D), various complications start to arise hindering the heart's performance. Ineffective clearing of blood glucose, primes the pancreas to increase insulin production in order to compensate for elevated blood glucose levels, and when this state progresses, insulin receptors become so desensitized that the pancreas cannot maintain sufficient insulin levels (Shanik *et al.*, 2008). The effect of a decreased potential to effectively utilize insulin in peripheral insulin sensitive organs, such as the muscle, heart, fat and liver, and is collectively known as insulin resistance (InsR). According to Kannel and McGee (1979), a prolonged insulin desensitized state leads to a 4-fold increase for the risk of developing ischemic heart disease (IHD), also known as coronary heart disease, and strokes. Furthermore, as a direct consequence of obesity, or excess fat mass, higher levels of circulating FFA and cholesterol are also present in the blood potentially resulting in a plaque build-up inside arteries, and thereby narrowing or completely blocking blood flow (Kwan *et al.*, 2014). Understandably, the slightest reduction in blood flow to the heart is severely detrimental to the heart's function. Therefore, effective cardioprotective therapies remains one of the most clinically relevant research fields in cardiology today (Fuster, 2014).

1.2 THE HEART

"The Conductor"

1.2.1 Overview of the Heart

The heart is the conductor of all human beings. It sets the tempo for the entire circulatory system, transporting nutrients, oxygen (O_2), waste, heat, hormones, and immune cells throughout the body – over, and over. The heart beats an average 100,000 times per day, pumping 10,000 liters of blood through 95,000 km of veins and arteries (Raff, 2003; Watson, 2009). It is as big as a human fist and constitute only 0.5% of our entire body weight, averaging 280 g in men and 230 g in women ("The Normal Size of the Heart Muscle Weight", 1951).

From a mechanical point of view, the heart's only function is to maintain blood pressure. This is achieved by generating high hydrostatic pressure to pump blood out of the heart, while also creating low pressure to bring it back. This gradient of force is known as blood pressure, also defined as the amount of strain put on the arteries by flowing blood. The amount of blood circulated per minute can be increased as much as 6-fold during exercise (Baggish & Wood, 2011), and heart rate can range from 40 beats per minute (bpm) at rest to more than 200 bpm (Uusitalo *et al.*, 1998) depending on genetics and age (Jose & Collison, 1970).
Even though regular exercise is strongly associated with good health, it does not exclude cardiovascular complications, as is evident from pro-athletic patients with CVD, stemming from various structural and functional heart abnormalities (Baggish & Wood, 2011). Furthermore, overexertion can lead to an overload of cardiovascular pressure and increased blood volume which can result in acute heart failure, or trigger a pre-existing heart condition (Carbone *et al.*, 2017).

Interestingly, heart cells can regenerate, albeit at a renewal rate of 1% of all heart cells per year from age 20, declining to as little as 0.3% by age 75 - effectively equating to less than 50% turnover of heart cells during an entire lifespan (Bergmann *et al.*, 2009). Understandably, any damage inflicted to this organ, albeit via damage to the heart's chambers, veins or valves, or in the circulatory system via occlusions, constrictions, or loss of blood, forces the system to overcompensate to maintain the body's functional demand for nutrient rich blood. Once all else fails, heart transplantation remains the final therapeutic option for heart failure (Wilhelm, 2015), with the latest available global statistics in 2008 indicating 5,400 heart transplants performed annually ("WHO | GKT1 Activity and Practices", 2013).

1.3 OBESITY

"Energy can never be created or destroyed – it only changes form".

1.3.1 Overview of Obesity

The human body constitutes the same materials found in food, albeit in different proportions according to genetics and lifestyle choices. The average healthy lean man comprises of 62% water, 16% fat, 16% protein, 6% minerals and less than 1% carbohydrate, with women having 6% more fat and slightly less of the rest (Carpenter *et al.*, 2018). A body fat percentage of at least 3-5% in men and 12-15% in women is considered essential for healthy functioning (Kang, 2012). In particular, stored adipose tissue play a significant role during pregnancy and facilitates the regulation of hormones (Kotecki, 2011). Excess fat not only serve as extra energy storage but can also protect internal organs from impact trauma and help regulate body temperature through heat generation in response to cold and overfeeding (Stanford *et al.*, 2012). Furthermore, adipose tissue is also a metabolically active endocrine organ and produces biologically active substances, including pro-inflammatory cytokines, angiotensin II, leptin, resistin and adiponectin (Kershaw & Flier, 2004).

Obesity and overweight are defined as abnormal or excessive fat accumulation that presents a risk to health ("WHO | Obesity", 2014). These two related conditions can severely alter metabolism and contribute to a cluster of pathophysiological conditions, collectively called the metabolic syndrome (Grundy, 2004). Furthermore, as obesity increases, the risk for IHD, ischemic stroke, T2D and cancer also rise (Chamie *et al.*, 2013; Eckel, 1997; Saboor Aftab *et al.*, 2014).

1.3.2 Cause of Obesity

The law of conservation of energy states that energy can never be created or destroyed – it can only change forms. The process of metabolism involves the conversion of energy, either through catabolism (breaking down molecules and releasing energy), or anabolism (constructing new molecules and consuming energy). All the energy from foods consumed will either be released or stored within the body. Maintaining a healthy body weight range is subject to balancing energy intake (consumption of food and O_2) and energy output (dissipation through body heat, motility and energy storage). The basal metabolic rate, defined as the energy required in a resting condition, accounts for 60-70% of total energy expenditure in most individuals (Merghani *et al.*, 2015). Persistently consuming more calories (energy) than your daily metabolic demand results in excess fat storage contributing to body weight gain and eventually obesity (Heymsfield *et al.*, 2002). Baseline metabolism rate also decreases with age, gender (women < men), ethnicity and increased free fat mass (obese < non-obese) further complicating the obesity epidemic (Mcmurray *et al.*, 2015). Moreover, lower consumption of O_2, through not partaking in regular aerobic exercise, also leads to a decrease in basal metabolic rate (Mcmurray *et al.*, 2015). Broadly speaking, factors that contribute to the obesity epidemic encompass a decrease in physical activity, unhealthy diet, lack of sleep, as well as certain medical conditions, such as pregnancy and medications with known lipid dystrophy side-effects.

1.3.3 Assessment

Health experts use body mass index (BMI) together with body proportions and percentage body fat to classify obesity. BMI is a crude calculation through which a person's weight (in kg) is divided by the square of their height (in meters) (Global Diabetes Community, 2015). A BMI between 25 and 30 kg/m^2 is considered overweight, whereas a BMI of above 30 kg/m^2 is classified as obese (**Figure 1.1**).

BMI (kg/m^2)	Weight Status
Below 18.5	Underweight
18.5-24.9	Normal
25.0-29.9	Overweight
30.0-34.9	Obese (Class I)
35.0-39.9	Obese (Class II)
40.0+	Morbidly Obese (Class III)

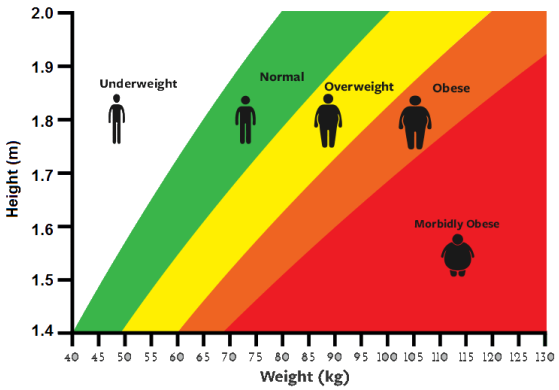

Figure 1.1 Body mass index classification according to metric height and weight. Obtained from Global Diabetes Community (2015).

However, BMI cannot discriminate between fat and lean body mass (muscles, bones, organs and blood) and is therefore unreliable in diagnosing obesity in young people, pregnant women and muscular patients. Additionally, the following measures can be implemented:

- waist circumference (circumference of natural waist)
- waist-to-hip ratio (waist circumference divided by hip circumference) (Noble, 2001)
- skinfold thickness (measure subcutaneous fat using calipers) (Gray *et al.*, 1990)
- underwater weighing (body density measurement) (Kotecki, 2011)
- bio-electrical impedance (total body fat resistance measured by electrical current) (Gray *et al.*, 1990).

- dual energy X-ray absorptiometry (DEXA) (measure fat-free mass, fat mass and bone mineral density)
- computerized tomography (CT) (cross-sectional and three-dimensional imaging of internal organs and structures)
- magnetic resonance imaging (MRI) (construct three-dimensional image of entire body composition) (Hu, 2008).

To date, the most accurate assessment of body composition is given by DEXA and Rapid-MRI scans (Borga *et al.*, 2018).

1.3.4 Epidemiology

Annually, 2.8 million people die as a consequence of being overweight or obese ("WHO | Obesity", 2015). Even though being underweight places you at a higher risk for early death (Anjana *et al.*, 2018), obesity is still associated with a higher prevalence of deaths world-wide. In 2016, 1.9 billion (39%) adults over the age of 18 were overweight, and an estimated 650 million (13%) were obese ("WHO | Obesity and overweight", 2018), of which 11% were male and 15% female (**Figure 1.2**). Furthermore, the prevalence of obesity has nearly tripled over the past 40 years.

1.3.4.1 Children and Adolescents

Annually, more children and adolescents are becoming obese. The global prevalence of overweight and obese infants and young children (0 to 5 years old) has increased from 32 million to 41 million between 1990 and 2016 ("WHO | Obesity and overweight", 2018). In developing African nations, the prevalence of overweight and obesity in young children have doubled, from 4 million to 9 million children. In developed countries, childhood obesity (6 – 11 years old) increased from 7% to 18% between 1980 and 2012, while adolescent obesity (12 – 19 years old) also increased from 5% to 21% in this period. According to literature, an estimated third of American children and adolescents are overweight or obese (Ogden *et al.*, 2014). No current data exists for the developing world, but regardless, without therapeutic intervention, obesity will likely proceed into childhood, adolescence and adulthood.

1.3.4.2 Socio-economic Status

In a study done by Pampel and colleagues (2012) they found that a country's socio-economic status influences the prevalence of obesity. They found that the higher the country's income level, the higher the prevalence of raised BMI's. Higher income countries had an overweight prevalence of more than double that of lower income countries. For obesity, the prevalence more than triples from 7% obesity in low-income countries to 24% in high-income countries. Obesity was also twice as prevalent in women in low-income countries compared to men, whereas it was similar in high-income countries.

Furthermore, an increase in overweight individuals negatively impact the overall health of a country as these individuals present with chronic conditions and are more prone to premature death. This trend is also becoming more prominent in the developing countries (Popkin, 2009). Socio-economic development results in better health management, but at the same time also results in new problems such as the gradual replacement of malnutrition with overconsumption (Pampel *et al.*, 2012). Arguably, the group to be most severely impacted by this growing trend of obesity, will be those least financially advantaged.

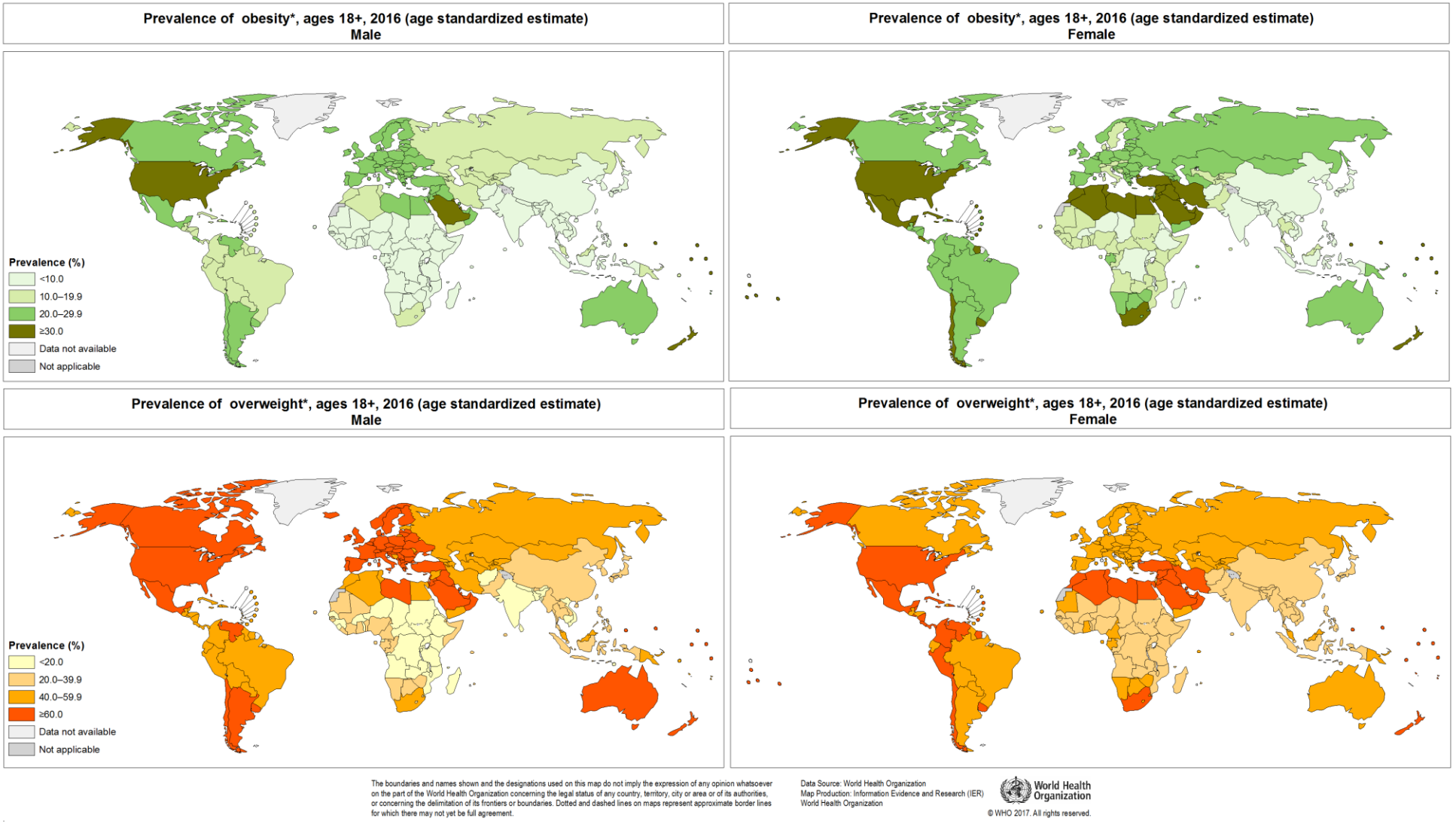

Figure 1.2 Global prevalence of obesity and overweight in male and female populations. Note that Polynesian countries have similar prevalence of overweight and obesity in males and females.

1.4 INSULIN RESISTANCE

"Use it or Lose it"

1.4.1 Overview of Insulin Resistance

Insulin resistance (InsR) describes a state of decreased insulin sensitivity experienced by insulin-hardened tissue – effectively resulting in poorer glucose utilization (Beale, 2013). As a result, glucose accumulates in the blood instead of being taken up by the muscles, fat and liver. Chronic hyperglycemia would result in augmented insulin production by the pancreatic β-cells to increase glucose clearance (Leibiger *et al.*, 2008). However, this progresses to hyperinsulinemia and the inability of insulin to decrease high circulating blood glucose (DeFronzo & Tripathy, 2009). Thus, hyperinsulinemia is both a response and a contributor to InsR (Cavaghan *et al.*, 2000a). When left untreated, prolonged InsR can overburden β-cells and result in T2D and increase the risk for CVD (Cavaghan *et al.*, 2000b).

1.4.2 Overview of Insulin

Insulin is a peptide hormone that plays a crucial role in tissue development, growth and maintaining energy homeostasis (Sesti, 2006). Insulin is produced within the pancreatic β-cells and housed in mature secretory granules. After consuming a meal, blood glucose spikes, which stimulates the release of insulin into the systemic circulation. Insulin secretion can also be induced by various other factors, ranging from amino acids (such as leucine and arginine) and lipids (non-esterified fatty acids (FA)) (Fu *et al.*, 2013) to gastrointestinal hormones called incretins (Baggio & Drucker, 2007) and other hormones (growth hormone, glucagon, secretin, cholecystokinin, gastrin, vasoactive intestinal peptide (VIP), gastrin-releasing peptide) (Wilcox, 2005), as well as in response to vagal nerve stimulation (Ahrén & Taborsky, 1986).

- **Insulin Function**

Insulin plays a multifunctional role within the body, eliciting a specific response for each organ or tissue target (Benito, 2011). Primarily, it facilitates the absorption of glucose into muscle, fat and liver cells, through promoting glucose transporter 4/2 (GLUT4/2) translocation from an intracellular reservoir compartment to the plasma membrane (Bertrand *et al.*, 2008) lowering blood glucose levels (Wilcox, 2005). Alternatively, it aids in the conversion of glucose to glycogen (glycogenesis) in muscle tissues and liver, and also prevents the production of endogenous glucose (gluconegogenesis) within the liver (Bazotte *et al.*, 2014). All three of these mechanisms result in lowered blood glucose. Other than glucose, insulin also influences lipid metabolism by regulating lipid synthesis in liver cells and adipocytes and inhibiting the breakdown of FA in adipose tissue (Sesti, 2006). In the heart, insulin is mainly responsible for substrate utilization but can furthermore augment cardiomyocyte contraction, influence myocardial relaxation, promote angiogenesis and cell survival, downregulate apoptosis, enhance myocardial microcirculation and reduce coronary artery resistance, which improves blood perfusion of the myocardium (Iliadis *et al.*, 2011).

1.4.3 Assessment

InsR can be assessed by either measuring the blood insulin levels or the blood glucose response to insulin (Bray & Hamman, 2015). The first test, known as a hyperglycemic clamp, requires keeping blood glucose levels constantly elevated through hyperinfusion of glucose and measuring the response of pancreatic β-cells to produce insulin. The second test, known as an euglycemic clamp, consists of intravenously infusing high levels of insulin into a patient's blood, while simultaneously measuring the fluctuating blood glucose levels for up to 24 h (Heise *et al.*, 2016). The euglycemic clamp is the gold standard in human trials and pharmacodynamic studies of drug interactions in diabetes patients (Bray & Hamman, 2015). However, the test is too costly and impractical to be used for clinical assessment of diabetes pathology. Rather, blood tests such

as fasting lipograms and glycohemoglobin tests are performed to determine the likely presence of insulin resistance, a strong indicator for prediabetes.

1.4.3.1 Fasting Plasma Glucose Test

Measuring fasting blood glucose in people who have not eaten for at least 8 h, can serve as a strong indicator of prediabetes (Jeon *et al.*, 2013). Normal fasting blood sugar is considered between 2.8-5.6 mmol/L (50 and 100mg/dL), whereas 5.6-6.9 mmol/L (100 and 125 mg/dL) is indicative of prediabetes - known as impaired fasting glucose – and a fasting blood glucose exceeding 7 mmol/L (126 mg/dl) is considered diabetic (Mayo Foundation for Medical Education and Research, 2018). The test is most reliable when performed in the morning hours following sleeping and fasting. In a study done by a Chinese group led by Wang and colleauges (2010) they analysed the fasting blood glucose of 500 Wistar rats, specifically comparing the method (glucose oxidation method vs glucose strips), fasting vs non-fasting blood glucose, the site of blood glucose collection and the duration of fasting (5h vs 11h). They found that the rats averaged fasting 3.95 mmol/L vs 5.65 mmol/L non-fasting, the difference between 5h vs 11h was 0.8 mmol/L and blood glucose taken from the abdominal aorta was up to 40% higher than in the tail. Furthermore, they found the glucose oxidation method to be more reliable, whereas glucose strips potentially show erroneous readings, which need to be double-checked when suspicious readings are monitored. In conclusion, they found that the criteria for using blood glucose as indicator for diabetes in rats are similar to that of humans.

1.4.3.2 Oral Glucose Tolerance Test

Similar to the fasting plasma glucose test, the oral glucose tolerance test (OGTT) also entails 8 h of fasting, but additionally, at the start of the test, a person receives glucose bolus to consume, succeeded by follow-up blood glucose tests to determine how quickly the blood glucose is cleared (Bray & Hamman, 2015). Traditionally, prediabetes have been diagnosed in patients showing impaired glucose tolerance after a 2h OGTT (American Diabetes Association, 2014). However, prediabetes does not always result in T2D, and similarly, people without prediabetes can also spontaneously develop T2D (Unwin *et al.*, 2002). As such, it has been shown that blood glucose levels 1h post OGTT can be a stronger indicator of future diabetic complications and mortality (Pareek *et al.*, 2018).

1.4.3.3 Lipograms

Various components of the lipogram is linked to InsR and consequent CVD risk, however they are not always well understood (Bertsch & Merchant, 2015). For instance, a high triglyceride to high-density lipoprotein cholesterol (HDL-C) ratio greater than 3.0 has been correlated to 64% sensitivity for InsR and 68% specificity for InsR compared to euglycemic clamp established InsR (McLaughlin *et al.*, 2003). On the contrary, it used to be postulated for over half a century that high concentrations of low-density lipoprotein cholesterol (LDL-C) was associated with CVD (Ravnskov *et al.*, 2018). However, this statement has only recently been deemed incorrect and was verified in a study done by Bertsch & Merchant (2015) who found no corrolation between CVD risk and LDL-C levels in an 8-year follow-up of 103,646 non-CVD and non-T2D members between the age of 50 to 75 years old.

1.4.3.4 Hemoglobin A1c

Hemoglobin A1c (HbA1c), or glycohemoglobin, is used as an indicator of average blood glucose over the past 3 months (Nam *et al.*, 2018). The test is based on binding of glucose to hemoglobin, the O_2 -carrier protein present in red blood cells, which typically have a lifespan of 3 months. The percentage of bound HbA1c can be used to determine a person's diabetic status. A percentage between 5.7 and 6.4 is considered prediabetic. It is the most reliable test to date, but not always the most sensitive to recent developments in prediabetes and

diagnosing prediabetes in people of African, Mediterranean or Southeast Asian descent, as well as people having a known familial history of sickle cell anemia, due to possessing a hemoglobin variant that interferes with the results of the HbA1c test.

1.4.4 Insulin-resistant Conditions

1.4.4.1 Metabolic Syndrome

Metabolic syndrome (or insulin resistance syndrome) is defined as a range of characteristics prevalent in overweight and obese individuals resulting in increased CVD and T2D prevalence, and all-cause mortality (Kaur, 2014). These conditions include at least 3 of the following:

- large waist size (≥102 cm for men, ≥89 cm for women)
- elevated blood triglycerides (≥150 mg/dL)
- abnormal blood cholesterol (HDL cholesterol of ≤40 mg/dL for men or ≤50 mg/dL for women)
- high blood pressure (≥130/85)
- high blood glucose levels (fasting blood glucose level ≥100 mg/dL or ≥5.6 mmol/L)

Although many of these abnormalities can also occur in non-InsR subjects (McLaughlin *et al.*, 2004), they are closely related to obesity (Cornier *et al.*, 2008) and are strongly associated with increased risk for cardiac diseases and lowered life expectancy (Vella *et al.*, 2013). The mechanism underlying InsR is still not completely understood. One of the major indicators of InsR is an inhibition of glycogen synthesis (Bonadonna *et al.*, 1993). Glycogen synthesis results in almost 80% of glucose clearance entering skeletal muscles under normal conditions and understandably any decrease in this rate can detrimentally influence blood glucose levels (DeFronzo & Tripathy, 2009). Furthermore, a sustained positive or surplus energy balance leads to expanded adipose tissue (obesity) and obesity-related disorders, which are commonly associated with InsR in 41% of patients even in the absence of diabetes (Tewari *et al.*, 2015). Adipose tissue not only stores additional calories, but as an endocrine organ, also secretes pro-inflammatory cytokines, such as tumour necrosis factor alpha (TNFα), interleukin-1-beta (IL-1β) and monocyte chemoattractant protein-1 (MCP1) (Wieser *et al.*, 2013). In the case of obesity, adipose tissue undergoes a phenotypical change which attracts more macrophages that can account for up to 40% of the total cells in adipose tissue (Kang *et al.*, 2016; Xu *et al.*, 2003), which further increases pro-inflammatory cytokine secretion, resulting in chronic inflammation, and has been implicated in InsR (Olefsky & Glass, 2010). Lastly, fat cell lipolysis (the process of adipocyte triacylglycerol breakdown into FA and glycerol resulting in elevated blood triglyceride) is also elevated in obesity and associated with InsR (Morigny *et al.*, 2016).

1.4.4.2 Ischemic Heart Disease and Strokes

Increasing obesity poses a rising risk to ischemic heart disease (IHD) – the leading cause of CVD (Gregory *et al.*, 2017). IHD is the result of sustained plaque build-up due to cholesterol deposits in the coronary arteries – normally supplying the heart with O_2-rich blood (National Institute of Health, 2009). The narrowing of coronary arteries results in reduced blood flow to the heart causing chest discomfort and when completely blocked triggers a heart attack. Finally, a plaque region can also rupture or dislodge and form blood clots anywhere within in the vascular system, called an embolism. Most notably, a blood clot resulting in complete blockage of blood flow to the brain is known as a brain embolism or stroke, causing irreversible damage and potential premature death. Strokes are the second leading cause of death worldwide, and approximately 240 new cases are identified daily in South Africa, often resulting in lingering disabilities (Akinrinmade *et al.*, 2017). Furthermore, the relationship between lipid displacement, InsR and the subsequent development of serious

disorders including T2D, hypertension, dyslipidemia and disorders of coagulation and fibrinolysis are well established and can lead to CVD (Boden, 2011).

1.4.4.3 Diabetes

- ***Diabetes Overview***

Diabetes mellitus is the most common metabolic disease worldwide with an estimated 425 million diabetic adults (1 in 11 adults), an additional 352 million having impaired glucose tolerance, and an estimated 212 million still undiagnosed ("International Diabetes Foundation", 2018). Consequently, $727 billion (12% of global health expenditure) is spent on diabetes – equivalent to the entire gross domestic product of either Switzerland or Saudi Arabia ("World Economic Outlook", 2018).

Diabetes can be divided into three distinct forms, namely Type 1, Type 2 or gestational diabetes. Type 1 diabetes (T1D) is characterised by selective autoimmune destruction of pancreatic β-cells responsible for insulin secretion, thereby detrimentally affecting insulin secretion required for normal energy metabolism. T2D in contrast, is the result of acquired insulin insensitivity in the liver, adipose tissue and muscle cells, initially resulting in overexpression of insulin which overexerts β-cell function, and eventually becomes a full blown inability to effectively clear blood glucose (DeFronzo, 1999). It was first proposed that diabetic patients present with InsR only, as opposed to insulin deficiency (Himsworth, 1936), however it is now recognized that both conditions are essential in the disease progression of T2D. Gestational diabetes is also an acquired form of diabetes prevalent in 7% of all pregnancies (especially during the 24th to 28th week of gestation) and presents with a degree of glucose intolerance that can result in T2D post-pregnancy (Association American Diabetes, 2003; Metzger & Coustan, 1998). T2D has a much higher incidence (about 95% of all cases of diabetes) and obesity is the most common risk factor for developing of T2D (Ghasemi & Jeddi, 2017), resulting in elevated serum triglycerides, hypertension and InsR. T1D is primarily diagnosed in younger individuals, whereas T2D used to be considered a disease of the aged. However, in recent years there has been an upward trend of younger people also presenting with T2D (Huang *et al.*, 2009). Genetics have also been shown to be involved in diabetic development, as the disease is often dependent on genetic changes, especially epigenetic changes brought upon by environmental factors. In extreme cases (<2%) genetics has shown direct involvement in conditions such as maturity-onset diabetes (Fajans *et al.*, 2001) and neonatal diabetes (Støy *et al.*, 2010).

- ***Treatment***

The primary agenda in treating diabetes is the maintenance of blood glucose levels within normal physiological ranges (Polonsky, 2012). Diet and exercise are effective in the treatment and management of both type 1 and 2 diabetes (Eiselein *et al.*, 2004), while injectable insulin is also considered as a safe alternative to deal with diabetic episodes (McCall, 2012). Additionally, T2D treatments include non-insulin oral anti-diabetic medications, comprising of biguanides, sulfonylureas, α-glucosidase inhibitors, and thiazolidinediones. Each class of medication has a unique mechanism of action (**Figure 1.3**):

- Biguanides (such as metformin) is the most prescribed drug in treating T2D and acts by increasing the liver's insulin sensitivity and restoring its glucose metabolism (Viollet *et al.*, 2012). The molecular action of metformin is heavily dependent on the treatment dose and duration, and was initially thought to occur only through an AMPK-dependent inhibition of mitochondrial respiration, however AMPK-independent mechanisms has now also been implicated (Rena *et al.*, 2017). Metformin is considered to have few side effects, but the most common occurrence is gastrointestinal complications in 20-30% of patients resulting

in nausea and vomiting (Diabetes Prevention Program Research Group, 2012). Furthermore, patients with liver and kidney dysfunction has also shown to be prone to fatal lactic acidosis (Salpeter *et al.*, 2006).

- Sulfonylureas are the most widely used anti-diabetic drug due to its low cost and acts through increasing insulin production by the pancreatic β-cells (Sola *et al.*, 2015). This mechanism occurs through binding to a sulphonylurea-specific receptor causing the inhibition of ATP-senstive K^+ channels on the pancreatic β-cells plasma membrane. This inhibition prevents K^+ from exciting the cell, leading to a depolarization that opens voltage-gated Ca^{2+} channels (therefore intracellular Ca^{2+} buildup) triggering more insulin granulae fusion with the cell membrane and subsequent insulin secretion (Ashcroft, 1996; Levine & Sobel, 1957). Prolonged used has been associated with hypoglycemic episodes and decreased insulin secretion, through desensitization of the sulphonylurea-specific receptors (Sola *et al.*, 2015).
- α-glucosidase inhibitors (such as acarbose) delay the absorption of carbohydrates from the gastro-intestinal tract (Willms *et al.*, 1991). Through competitive inhibition of α-glucosidases, acarbose delays carbohydrate digestion, extending the total carbohydrate digestion time and thereby reduce the rate of glucose absorption, subsequently also lowering hyperinsulinemia (Bischoff, 1995). As a secondary effect, acorbose also reduces triglyceride uptake into adipose tissue and hepatic lipogenesis, reducing triglyceride content. Acarbose was also shown to have a resensitizing effect on GLUT4 (Ledwig *et al.*, 2002). Due to the inhibition of complex carbohydrate breakdown into glucose, some carbohydrates remain undegraded till the colon, where bacterial digestion takes over. This results in gastrointestinal side-effects including flatulence (in 78% of patients) and diarrhea (in 14% of patients) (Derosa & Maffioli, 2012). Furthermore, there has been reported incidences of liver inflammation whereby treatment had to be ceased (Derosa & Maffioli, 2012).
- Thiazolidinediones (or glitazones) increase insulin sensitivity in peripheral tissues, such as the muscles and fat cells (Kahn *et al.*, 2000). They act by binding peroxisome proliferator-activator receptor gamma in adipocytes to stimulate peripheral adipogenesis and FA uptake (Greenfield *et al.*, 2004). This reduction of circulating FA's and lipid substrate availability for liver and muscle tissue results in improved insulin sensitivity. Furthermore, thiazolidinediones also favourably impact adipocyte hormone secretions, such as adiponectin, which also independently aids in insulin resensitization (Achari & Jain, 2017). Given the involvement of thiazoledinediones in adipocyte functioning, it is not surprising that the treatment results in weight gain and increased peripheral fat mass (but not visceral fat) (Greenfield *et al.*, 2004). Furthermore, thiazolidinediones is also not suitable for patients with heart failure as the drug causes fluid retention, resulting in increased plasma volume and therefore decreased haemoglobin concentrations causing anemia. As blood oxygen is lowered, the heart has to compensate to retain the oxygen demand of peripheral tissues (Coats, 2004).

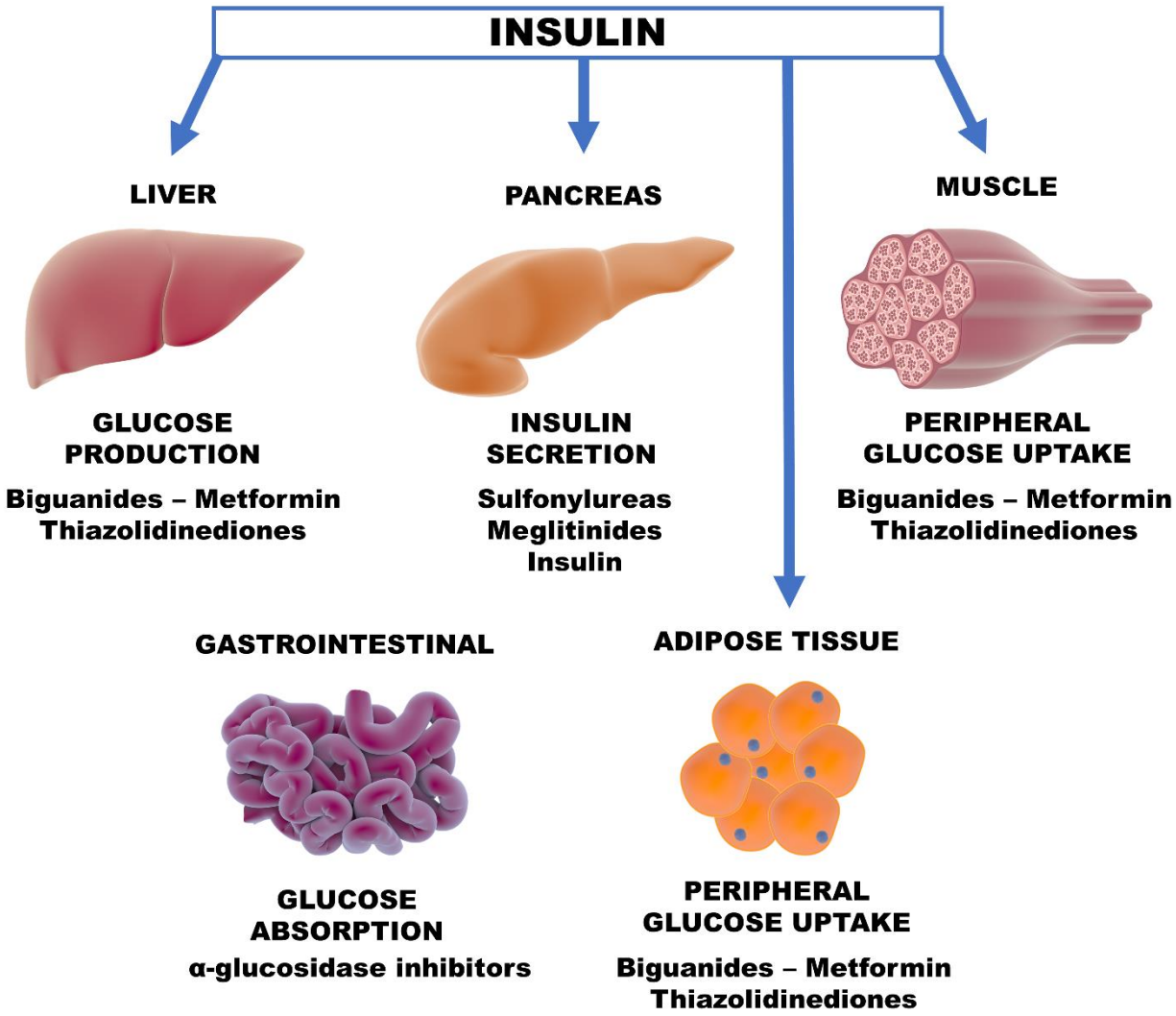

Figure 1.3 Anti-diabetic therapies and the mode of action. Adapted from Beaser et al. (2015).

The different oral agent classes have different effects on basal insulin and postprandial glucose – effects which only become apparent as T2D progresses. The latest drugs available for treating T2D are incretins, such as glucagon-like peptide-1 (GLP-1) – a gastrointestinal hormone that increases insulin production in β-cells (Kjems *et al.*, 2003). Similarly, dipeptidyl peptidase-4 (DDP-4) inhibitors can be used to delay the breakdown of GLP-1 (Dicker, 2011). All of the above have, however, been linked to a variety of serious adverse health effects, prompting a search for safer, natural hypoglycemic agents to be used (Patel *et al.*, 2012).

1.4.5 Summary of Insulin Resistance

The increased prevalence of obesity in the general population is evident. This burden of disease also contributes to a rise in insulin resistant patients. However, insulin resistance is only viewed as an adaptive mechanism (to protect cells against acute lipid overload and inflammation) which becomes ineffective and leads to multiple metabolic abnormalities in the chronic state (Tsatsoulis *et al.*, 2013).

1.5 ISCHEMIA-REPERFUSION INJURY

"Turning it off and on again".

1.5.1 Overview of Ischemia

During prolonged ischemia, metabolism switches over to anaerobic metabolism and lactate accumulation, leading to a decrease in adenosine triphosphate (ATP) levels and intracellular pH (**Figure 1.4**). Consequently, ATPase-dependent ion transport mechanisms cease to work properly, causing a buildup of ROS, intracellular and mitochondrial calcium (Ca^{2+}) (a phenomenon known as Ca^{2+} overload), contributing to the opening of the mPTP leading to swelling and rupture of cells, and ultimately cell death through necrotic, necroptosis, apoptotic or autophagic mechanisms.

Short durations of ischemia (typically < 5 min) followed by reperfusion activates cell survival signaling cascades protecting the heart from the consequences of longer periods of ischemia – a phenomenon known as ischemic conditioning. Extending ischemia to 20 min results in myocardial stunning, meaning upon reperfusion contractility is impaired, but will eventually improve without resulting in infarction or significant inflammatory responses. Prolonged ischemia beyond 20 min results in cell damage which will lead to myocardial infarctions, and re-establishing blood flow further aggravates tissue injury through inflammatory signaling. Ischemic periods between 5 and 20 minutes induce myocardial stunning (Kalogeris *et al.*, 2017).

1.5.2 Causes of Ischemic Episodes

Ischemic episodes can occur in myocardial infarction, stroke, and peripheral vascular disease (Kalogeris *et al.*, 2017). The major uncontrollable risk factors for ischemic episodes include advancing age, male gender and hereditary factors. Controllable risk factors for myocardial infarction and ischemic stroke include acute (and chronic) consumption of 4 or more servings of alcohol per day, smoking of tobacco, hyperlipidemia, hypertension, sedentary lifestyle, obesity, metabolic syndrome and diabetes mellitus (Kalogeris *et al.*, 2012). The most common underlying cause for ischemic episodes in the western world can be attributed to thromboembolic or atherothrombotic vaso-occlusive disease (Kalogeris *et al.*, 2012). Increasingly, studies are suggesting that conditions like diabetes, hyperlipidemia and aging can influence the progression of I/R-I independent of the vascular aspects (Boengler *et al.*, 2009; Ferdinandy *et al.*, 2007).

1.5.2.1 Fetal Programming

The importance of fetal programming is a vital contributor of ischemic disease in later adulthood. Studies have reported a "U"-shaped correlation between placental-to-fetal weight ratio and heart disease, which indicates that factors inhibiting placental development can severely promote myocardial vulnerabilities later in adulthood (Thornburg *et al.*, 2010). It has been found that fetal exposure to a wide variety of environmental triggers, including hemodynamic effects, growth factors, cocaine (Meyer & Zhang, 2009) and tobacco smoke exposure, hypoxia (Patterson & Zhang, 2010) and nutrient status all contribute towards CVD progression in later age (Langley-Evans & McMullen, 2010; Reynolds *et al.*, 2010). Intrauterine stress results in gene-activated responses, called fetal programming, and is found to increase risk for CVD. Furthermore, the risk for IHD can also be subject to birth weight (Barker, 2007; Reynolds *et al.*, 2010). It was noted that mortality from ischemic disease in adults increased as birth weight decreased from 4.1 kg to 2.3 kg, and the same association was found for increasing birth weights above 4.3 kg. However, regardless of genetic predisposition, caloric restriction and exercise can confer cardioprotection and improve ischemic tolerance even in aged hearts (Boengler *et al.*, 2009).

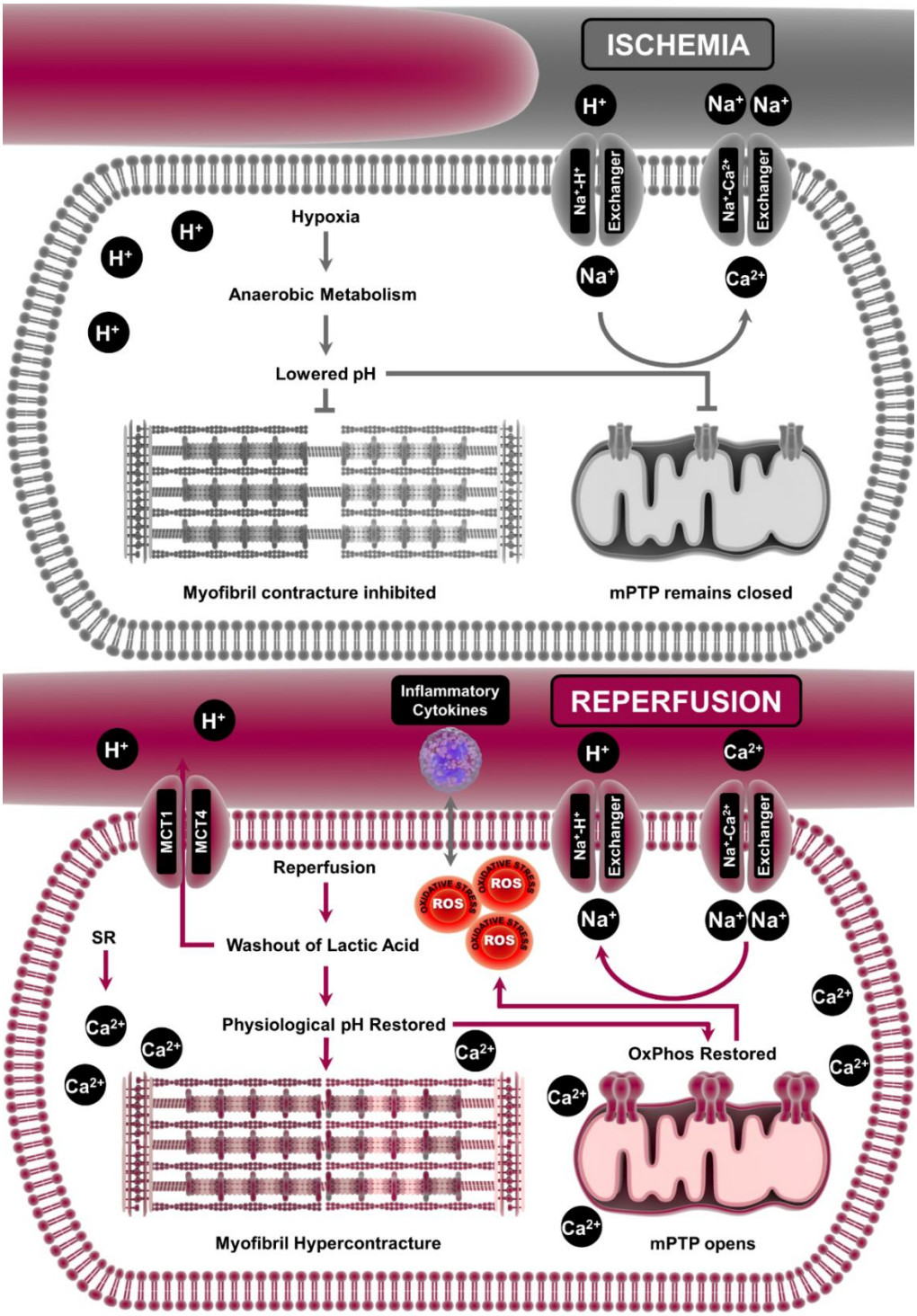

Figure 1.4 Changes within cardiomyocyte during ischemia/reperfusion. When O_2 supply is ceased to myocardial tissue, the metabolism switches from aerobic to anaerobic, causing lactate accumulation and lowering of intracellular pH. This drives H^+ out of the cell in exchange for a rising intracellular Na^+ (facilitated by the Na^+ / H^+ exchanger), which then drives intracellular Na^+ to be transported out of the cell in exchange for Ca^{2+} (facilitated by the 2 Na^+ / Ca^{2+} exchanger). During ischemia, Na^+ / K^+ ATPase loses functionality which further exacerbates intracellular Na^+ overload. Once blood flow is restored, O_2 and aerobic substrates flood into ischemic tissue and the electron transport chain (ETC) is restarted, leading to a surge in ROS and consequently proinflammatory neutrophils, which worsens ischemic injury. Adapted from Hausenloy & Yellon (2013). SR: sarcoplasmic reticulum; mPTP: mitochondrial permeability transition pore; OxPhos: oxidative phosphorylation; ROS: reactive oxygen species; MCT1/4: Monocarboxylate transporters 1/4.

1.5.3 Overview of Reperfusion Injury

Ischemia/Reperfusion-Injury (I/R-I) refers to the damage incurred to ischemic tissue upon re-establishing blood flow. Myocardial reperfusion is essential in protecting viable myocardium, however it is also the cause for up to 50% additional damage done to the susceptible post-ischemic myocardium (Javadov *et al.*, 2018; Yellon & Hausenloy, 2007). The severity of the damage to tissues is dependent on the degree of obstruction and the duration of ischemia (Heusch & Gersh, 2016). Cell death can still occur 3 days after reperfusion was reinstated (Zhao *et al.*, 2000). Therefore, swift restoration of blood flow remains the primary therapeutic approach to all incidences of ischemia.

I/R-I is especially prevalent in myocardial infarctions, strokes and peripheral vascular disease. Cardioprotective therapies are aimed at targeting myocardial injury to prevent damage done during I/R-I (Rossello & Yellon, 2016). Interventions performed during ischemia and reperfusion can decrease infarct size by as much as 50% (Yellon & Hausenloy, 2007). Improving our understanding of I/R-I enables the development of new therapies and would extend the amount of time an organ can remain ischemic without irreversible I/R-I occurring. This could potentially implicate our modes of organ transplantation and even aid in performing bloodless operation where visual acuity is important (Yellon & Hausenloy, 2007).

The mechanisms involved in I/R-I are complex with the net result being damage to all biomolecules in exposed cells and tissues (Kalogeris *et al.*, 2017), with eventual cell death ensuing if left untreated. The fundamental characteristics of reperfusion injury entails the release of reactive oxygen species (ROS), cytokines and chemokines from surrounding endothelium, macrophages and mast cells, recruitment of neutrophils and endothelial dysfunction (**Figure 1.4**) (Wu *et al.*, 2018). The opening of the mitochondrial permeability transition pore (mPTP) induced by ROS from both intracellular and extracellular sources also leads to sarcoplasmic reticulum dysfunction resulting in Ca^{2+} overload, lipid peroxidation of cell membranes, denaturing of enzymes and ultimately also DNA damage (Hausenloy & Yellon, 2013). Furthermore, ATP generation also facilitates the clearing of accumulated intracellular H^+ by flushing out lactic acid through the monocarboxylate transporters 1 and 4 (MCT1/4) and through the 2 Na^+ / Ca^{2+} exchanger – however, this has also shown to be detrimental (Zhu *et al.*, 2013). Hours after reperfusion, neutrophils are still attracted in response to ROS from the infarcted myocardium (Wu *et al.*, 2018)

Relevant to this study, focus will remain on the following key mechanisms present in cardiac I/R-I: Oxidative stress, Ca^{2+} overload, mPTP opening and pronounced inflammatory responses resulting in cell death.

1.5.4 Oxidative Stress

As necessary as reoxygenation is for re-establishing aerobic ATP production, it also gives rise to an increase in ROS generation. ROS is highly reactive to all surrounding biomolecules and paradoxically induces cell dysfunction. This state of elevated ROS signaling has been deemed oxidative stress – an imbalance between pro-oxidants and antioxidants, in favor of the former – and is an important contributory factor to I/R-I induced damage (Zhou, Prather, *et al.*, 2018). Many conditions linked to CVD are associated with excessive pro-oxidant production and/or depression of endogenous antioxidant status, including diabetes, hyperlipidemia, hypertension, and obesity.

ROS is generated in multiple compartments and by multiple enzymes within the cell, such as NADPH oxidase at the plasma membrane, lipid oxidation within peroxisomes, oxidative phosphorylation (OxPhos) within mitochondria, and various cyclooxygenases and xanthine oxidase in the cytoplasm (Goszcz *et al.*, 2015). Although these sources contribute to the overall oxidative burden, the majority of ROS are produced during OxPhos and ATP generation within the mitochondria. Mitochondrial ROS might attack various mitochondrial constituents, causing mitochondrial DNA mutations and oxidative damage to respiratory enzymes (Goszcz *et al.*, 2015). Furthermore, a defect in mitochondrial respiratory enzymes would increase mitochondrial production of ROS, causing further mitochondrial damage and dysfunction (Kalogeris *et al.*, 2017).

The major ROS radical formed during I/R-I is superoxide anion ($O_2^{\bullet}$) by reduction of molecular O_2 (Granger, 1988). Furthermore, all other reactive species is either directly or indirectly derived from $O_2^{\bullet}$ through its dismutation or interaction with other related reactive species further inducing tissue damage. $O_2^{\bullet}$ is generated by various cytosolic and membrane enzymes as well as by the ETC, and capable of directly oxidizing enzymes with iron-sulfur cores, including aconitase, fumarase, NADH dehydrogenase, creatine kinase and calcineurin (Raedschelders *et al.*, 2012). Under normal physiological conditions, $O_2^{\bullet}$ spontaneously converts into hydrogen peroxide (H_2O_2) – a reaction that can be accelerated up to 10,000 times by superoxide dismutase (SOD) (Kalogeris *et al.*, 2012). However, in low pH conditions, such as during ischemia, $O_2^{\bullet}$ can spontaneously convert to its conjugate acid, the strong oxidant hydroperoxyl radical ($HO_2^{\bullet}$).

- ***p22phox***

p22phox, also known as the human neutrophil cytochrome b light chain, is a crucial constituent of the plasma membrane enzyme NADPH-oxidase (Dinauer *et al.*, 1990). NADPH-oxidase, consists of 5 isoforms (Nox1-5) and facilitates the transfer of one electron (e^-) from NADH or NADPH to O_2 to produce $O_2^{\bullet}$, with p22phox being the final e^- transporter in the chain (Xu, Yuan, *et al.*, 2014). This can be useful as in the case of phagocytes which kills foreign microbes by trapping them in a high ROS compartment (Dahlgren & Karlsson, 1999). However, during cardiac I/R-I, NADPH-oxidase has been identified as a major source of $O_2^{\bullet}$ overproduction (Nediani *et al.*, 2007). It has been found that increased p22phox levels are related to lipid peroxidation after acute myocardial infarction in rats (Fukui *et al.*, 2001).

1.5.5 Calcium Overload

Under ischemic conditions, cells need to resort to anaerobic glycolysis to meet their demand for ATP. This results in a buildup of lactate, H^+ and NAD^+ reducing cytosolic pH levels. To counter-balance, cells exchange H^+ for Na^+ by means of the plasmalemmal Na^+ / H^+ exchanger (Murphy & Steenbergen, 2007), which is then in turn exchanged for Ca^{2+} via the plasmalemmal Na^+ / Ca^{2+} exchanger. Upon reperfusion, the buildup of Ca^{2+} is worsened as H^+ removal increases the H^+ gradient across the plasmalemma and effectively speeds up Na^+/H^+ exchanger action (Sanada *et al.*, 2011). Furthermore, Ca^{2+} reuptake into the sarcoplasmic reticulum is also impaired during I/R-I further contributing to the lethality of elevated intracellular Ca^{2+}. This results in cardiomyocyte hypercontracture causing sarcolemmal rupture and eventually cell death through contraction band necrosis (Miyazaki *et al.*, 1987).

Lethal increases in Ca^{2+} is normally dealt with by mitochondrial Ca^{2+} uptake via a Ca^{2+} uniporter – a transmembrane protein that makes use of the negative mitochondrial membrane potential ($\Delta\psi_m$) compared to the cytosol to attract positively charged Ca^{2+} (Contreras *et al.*, 2010). However, once the Ca^{2+} is too overwhelming it can trigger the mPTP opening response. Furthermore, ischemic Ca^{2+} buildup can also result

in overactivation of Ca^{2+} / calmodulin-dependent protein kinases which can contribute to cell death. Increased intracellular Ca^{2+} can also signal the activation of inflammasomes, which mediate increased cytokine production, including IL-1β and TNFα, giving rise to an entire cytokine and chemokine cascade complicating I/R-I injury (Slegtenhorst *et al.*, 2014).

1.5.6 Mitochondrial Permeability Transition Pore Opening

I/R-I induces the opening of the mPTP, a common end-effector (**Figure 1.4**). Normally, the mPTP serve as a highly conductive pore permeable to molecules smaller than ±1.5 kDa in size, including H^+, but remains closed during ischemia in the presence of low pH (Hausenloy & Yellon, 2013). However, reperfusion causes dramatic increases in mitochondrial Ca^{2+} and ROS inducing the opening of the mPTP (Ong & Gustafsson, 2012), and whilst open allows H^+ to move freely between the inner mitochondrial membrane and the matrix, effectively dissipating the $\Delta\psi_m$, uncoupling ETC and inhibiting ATP synthesis (Halestrap, 2010). Additionally, the increase in intramitochondrial H^+ also draws water inside, causing the mitochondria to swell and rupture. When mitochondria are destroyed, necrosis of the cardiomyocyte will occur (Cohen & Downey, 2015). The molecular makeup of the mPTP still remains unknown (Javadov *et al.*, 2018), but it has been shown to entail the protein complexes adenine translocase, mitochondrial phosphate carrier, and most prominently cyclophilin-D. This composition led to the discovery of chemical inhibitors for cyclophilin-D, such as cyclosporine-A, sanglifehrin-A, and Debio-025, which have shown to protect against I/R-I-induced cell death in various organs, including the heart (Clarke *et al.*, 2002; Di Lisa *et al.*, 2009). Cardioprotective therapies are thus aimed at keeping the mPTP closed. Mitochondrial dysfunction and signaling is discussed in more detail in **Chapter 2 (Section 2.3)**.

1.5.7 Mechanisms of Cell Death

Signal transduction is crucial for maintaining cellular processes in response to I/R-I with various kinases displaying critical involvement in I/R-I pathogenesis (Vassalli *et al.*, 2012). In the past, cell death associated with I/R-I has been attributed to reduced energy supply, inflammation and a buildup of toxic molecules and mechanical injury inducing necrosis (Kalogeris *et al.*, 2012). Necrosis refers to a form of cell death resulting from extensive cell damage, characterised by disruption of organelles and membrane rupture independent of ATP supply (Konstantinidis *et al.*, 2012). However, cell death in I/R-I can also occur through various other mechanisms, each with their own mode of action (Kalogeris *et al.*, 2017) (See **Figure 1.5**). As part of this review we will only focus on necrosis and necroptosis, apoptosis and autophagy.

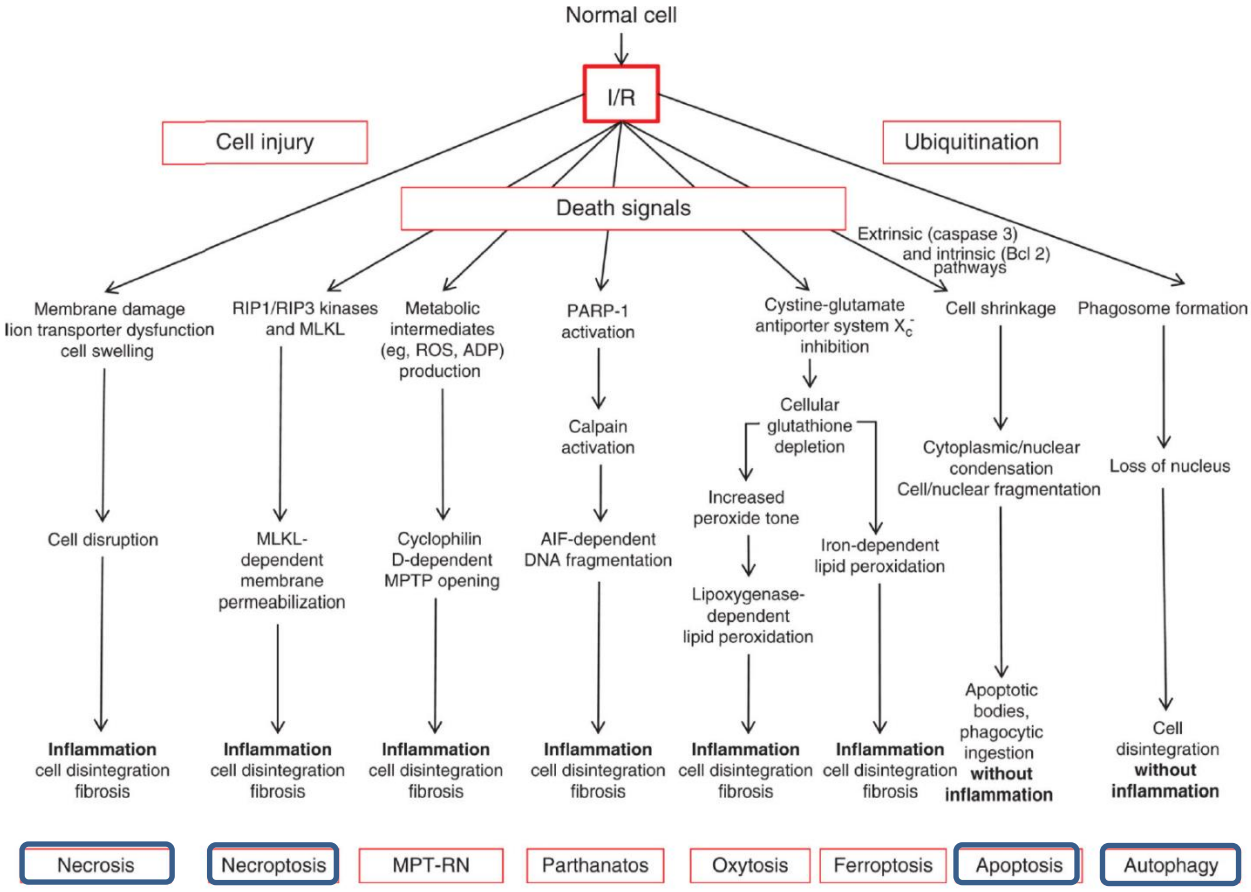

Figure 1. 5 Different modes of cell death known to date. Taken from Kalogeris et al. (2017) to illustrate the complexity of cell death mechanisms. In this review we only focus on necrosis, necroptosis, apoptosis and autophagy.

1.5.7.1 Necrosis and necroptosis

Necrosis is characterized by dysfunctional ion transport mechanisms causing the swelling of cells and organelles, mitochondrial dysfunction, lack of nuclear fragmentation, plasma membrane rupture and leakage of intracellular contents in the extracellular space (Kalogeris *et al.*, 2017). Necrosis was initially thought to be the random consequence of overwhelming stress resulting in cell death. However, likewise to apoptosis and autophagy, necrosis can also be programmed, especially in response to I/R-I, in a process referred to as necroptosis. In this regard, extreme cellular stress or the activation of death receptors recruits a group of serine/threonine kinases called receptor-interacting proteins (RIP), which target the opening of the mPTP (Karch *et al.*, 2015). Activation of RIP1 and RIP3 also results in increased ROS production via NADPH oxidases (Morgan *et al.*, 2008) or through mitochondrial complex I (Vandenabeele *et al.*, 2010).

1.5.7.2 Apoptosis

Apoptosis is an ATP-dependent programmed cell death, which causes cell shrinkage and condensing of the cytosol and nucleus to form apoptotic bodies. It is characterised by both cytochrome-c release from damaged mitochondria, or autocoid (localized hormones) cell-surface receptor (Fas ligand) activation, resulting in downstream signaling via caspases and other signaling proteins which cause non-selective pore formation on the outer membrane of the mitochondria, the opening of the mPTP, DNA cleavage and nuclear degradation (Konstantinidis *et al.*, 2012). Apoptosis, unlike necrosis, does not release cellular content into the extracellular

space as the apoptotic bodies are surrounded by cell membranes. This also enable apoptotic bodies to be digested by phagocytes without creating an inflammatory response (Kalogeris *et al.*, 2012).

Apoptosis can result through extrinsic or intrinsic mechanisms (Whelan *et al.*, 2010). The extrinsic pathway occurs through activation of the Fas, TNFα and TRAIL receptors, which recruit death domain-containing proteins to the receptor complex. The formation of this death-inducing signaling complex activates protease caspase-8, resulting in activation of caspase-3. Caspase-3 serves as a protein slayer within cells lysing various cellular proteins (Whelan *et al.*, 2010). The intrinsic pathway, or mitochondrial apoptotic pathways, is activated in response to cytotoxic stimuli by I/R-I or oxidative stress, resulting in translocation and integration of the cell death regulator, B-cell lymphoma 2 (Bcl2), which can either result in apoptosis inhibition or induction by recruiting Bcl2-like protein 4 (Bax), Bcl2 homologous antagonist/killer (Bak), BH3 interacting-domain death agonist (Bid), p53 upregulated modulator of apoptosis (Puma) and Bcl2 nineteen kilodalton interacting protein (BNIP3) into the outer mitochondrial membrane (Whelan *et al.*, 2010). Ischemia by itself is not sufficient to activate the redox sensitive Bcl2 proteins and requires reperfusion. Once these proteins have permeabilized the outer membrane they signal the release of various pro-apoptotic proteins, such as cytochrome c, from the intermembrane space. Cytochrome c attaches to the cytosolic protein, apoptosis protease activating factor 1, resulting in an apoptosome which further activates the caspase-3, caspase-9 system (Whelan *et al.*, 2010).

Cardioprotective research is aimed at finding pro-apoptotic proteins and signals which can be targeted during I/R-I to possibly salvage cardiomyocytes destined for degradation. It has been demonstrated that inhibiting caspases during reperfusion can decrease infarct size in animal models (Mocanu *et al.*, 2000). However, in Bcl2 knockout mice, they found greater damage in response to I/R-I occurring in the absence of pro-apoptotic proteins than simply induced by apoptosis. This reaffirms that these proteins are not just involved in apoptosis, but their role in regulating normal cell function, such as their role in Ca^{2+} homeostasis, is of greater importance than initially realized (Scorrano *et al.*, 2003).

1.5.7.3 Autophagy

Autophagy is the cell's mechanism of housekeeping which disposes of old and damaged proteins and organelles. It can also be protective in response to cellular stress induced by starvation, hypoxia, mitochondrial dysfunction and infection, by recycling amino acids and FA's from damaged organelles and removing intracellular pathogens (Kalogeris *et al.*, 2017). Autophagy is thus considered a cell survival mechanism rather than a mechanism of cell death. However, uncontrollable autophagy can result in cell death and potentially exacerbate I/R-I (Kalogeris *et al.*, 2012).

The morphology of autophagy starts with a phagophore, an expanding isolation membrane which starts to surround a cell organelle or compartment to be processed (Gottlieb & Mentzer, 2010). Once the contents are completely engulfed it is known as an autophagosome, which will go on to fuse with a lysosome to degrade all the enclosed material, additionally also inducing an inflammatory cascade (Kalogeris *et al.*, 2017). This process is narrowly regulated by the mammalian target of rapamycin (mTOR) protein which inhibits autophagy. However, in response to a decreased nutritional status or stress, mTOR can be inactivated, resulting in autophagy activation (Gottlieb & Mentzer, 2010). This activates the kinase autophagy-related protein 1 (Atg1), which recruits Atg13 and Atg17 to start the phagophore formation. Another complex comprising of the class III PI3-Kinases vps34, vps15, and Beclin-1 then continues phagophore formation and recruits Atg12, Atg5 and

Atg8 (also called LC-3) which is essential for phagophore elongation and autophagosome completion. Once completed, fusion of the autophagosome to the lysosome is facilitated by the small GTPase Rab7 and the lysosomal membrane protein, LAMP2A (Gottlieb & Mentzer, 2010).

Autophagy is essential during ischemia, however its role in reperfusion remains uncertain (Ma *et al.*, 2015; Sciarretta *et al.*, 2011). The general consensus during I/R-I, is that inhibition of autophagy results in aggravated tissue damage (Jiang *et al.*, 2010), whereas activation of autophagy can confer cardioprotection (Carloni *et al.*, 2010). However, contrastingly it has been shown that AMPK upregulation during prolonged I/R-I can result in mTOR inhibition and thereby upregulate autophagy which resulted in a harmful response (Takagi *et al.*, 2007). To the contrary again, suppression of autophagy during reperfusion by administration of autophagosome formation inhibitor, 3-MA, or a Beclin1 inhibitor, urocortin, has shown to reduce neonatal and adult rat cardiomyocyte cell death following I/R-I (Valentim *et al.*, 2006). It thus remains that more research is needed to identify the appropriate status for autophagy during the critical events of reperfusion injury.

1.5.8 Mechanisms of Cell Protection

1.5.8.1 RISK Pathway

Reducing cell death in ischemic and reperfused myocardium can be accomplished through activation of growth factors, or pro-survival proteins, such as the upstream PKB activator, PI3K, and ERK1/2 (Baxter *et al.*, 2001; Yellon & Baxter, 1999). Protection relying on these two key protein cascades was coined the “Reperfusion injury salvage kinase (RISK) pathway”, first described by Schulman and colleagues (2002). They made use of the growth factor urocortin, which when administered during reperfusion upregulated ERK1/2 and decreased myocardial infarct size. When urocortin was co-treated with an ERK1/2 inhibitor, the protection was completely abolished. Since then, the importance of the RISK pathway has been thoroughly investigated by testing the protective effect of various cardioprotective therapies. The RISK-pathway can be summarised as a group of pro-survival protein kinases able to be cardioprotective when activated from the point of reperfusion (Hausenloy *et al.*, 2005).

The efficacy of the RISK pathway can be summarized in three characteristics:

Early kinase activation is Protective

It has been shown that, in response to ischemic pre-conditioning, the RISK pathway is activated at 2 distinct time points:

1) The “Trigger phase” - upon administration of the preconditioning cycles just before the ischemic episode,
2) Early reperfusion – at the onset of reperfusion (Rossello & Yellon, 2016)

It is speculated that closing the mPTP in the first 15 min of reperfusion is the main target for intervention in reducing cardiac I/R-I (Hausenloy *et al.*, 2003). This link between the RISK pathway and the mPTP has also been shown in rat myocytes before (Davidson *et al.*, 2006). Also, when the mPTP inhibitors, such as cyclosporin, sanglifehrin or insulin, is administered more than 15 min into reperfusion the protection is lost (Hausenloy *et al.*, 2003; Jonassen *et al.*, 2001).

Temporary kinase activation is Protective

Pro-survival kinases are only beneficial when acutely activated, whereas chronic activation of growth factors is considered harmful. Chronic activation of the PI3K-PKB cascade induces cardiac hypertrophy (Nagoshi *et al.*, 2005). Clinically it has been shown that ERK and PKB is chronically activated in a failing heart (Haq *et al.*, 2001). The heart can control phosphorylation of ERK and PKB through activation of PTEN – an important trigger for switching growth-induced pathways on and off (Rossello *et al.*, 2017). Clinically, this is an ideal treatment for a patient with acute myocardial infarction as it would only require inhibitory intervention prior to reperfusion, to prevent severe I/R-I (Rossello *et al.*, 2017).

Common cardioprotective pathway

The RISK pathway is not solely activated during ischemic conditioning but can also be activated in response to various pharmacological agents including insulin, bradykinin adenosine or statins (Rossello & Yellon, 2016). Our understanding of the RISK pathway has mostly been acquired from work done on small rodent models of acute myocardial infarction, but its role in larger animals, including humans still need to be better established (Rossello & Yellon, 2018). RISK has clearly been shown to be involved in cardioprotection in rats and rabbits but is of lesser importance in pigs (Hausenloy & Yellon, 2004; Hausenloy *et al.*, 2005; Skyschally *et al.*, 2009). The link between ischemic preconditioning and RISK activation has been shown in human atrial trabeculae, but remote conditioning still needs to be clearly established in large animals and humans (Heusch *et al.*, 2012).
The MAPK pathway cooperates with the PI3K/PKB pathway to control cell proliferation. MAPK's consists of 3 groups of serine threonine kinases: extracellular signal-regulated kinases (ERK1/2/3), c-Jun amino-terminal kinase/stress-activated protein kinases (JNK), and p38 MAPK's. Depending on the extracellular stimuli, these kinases can initiate a network of cell signaling cascades with various responses. The different isoforms of ERK, JNK, and the p38 MAPK's are expressed in nearly all types of tissues and cells (Deng et al., 2012).
There exist numerous downstream targets induced by pro-death kinases capable of contributing to I/R-I. JNK and p38 activation results in a surge of inflammatory cytokines, including TNFα and IL-1 shown to be key players in the damage incurred during I/R-I (King *et al.*, 2009). Furthermore, p38, and JNK, along with PKC, have shown to translocate to the mitochondria and increase complex I ROS production by up to 80% (Chambers & LoGrasso, 2011) making it more prone to mitophagy. p38 and JNK's exact role in apoptosis remain unclear, as they have both shown to inactivate anti-apoptotic Bcl2 proteins (De Chiara *et al.*, 2006; Fan *et al.*, 2000) and also activate pro-death Bcl2 proteins (Bright *et al.*, 2004; Metukuri *et al.*, 2009).

1.5.8.2 Insulin-Dependent Mechanisms

Insulin signaling is well established to be cardioprotective in insulin resistance and CVD (Ji *et al.*, 2010). The PI3K/PKB pathway is the primary signaling cascade mediating metabolic effects induced by insulin. Once the insulin receptor is activated, tyrosine phosphorylation of insulin receptor substrates (IRS) 1-4 occurs, resulting in PI3K activation at it's p85 regulator subunit. PI3K then activates the membrane-bound phosphatidylinositol phosphate, PIP2, transforming it to PIP3 resulting in downstream activation of phosphoinositide-dependent kinase-1 (PDK1) and recruitment of PKB/Akt – responsible for insulin's metabolic effects.

- ***PKB***

Protein Kinase B (PKB) or Akt is a serine/threonine kinase which plays a diverse cellular signaling role in especially insulin metabolism. 3 major isoforms have been identified, namely PKB1, PKB2 and PKB3, all of which are activated after PI3K recruitment. PKB1 is the most researched isoform, whereas it is known that PKB2 is highly expressed in the heart, and PKB3 is severely upregulated in a stressed heart (Altomare *et al.*, 1995; Taniyama *et al.*, 2005; Walsh, 2006). When PI3K is inhibited through pharmacological inhibition by

wortmannin for instance, PKB activation is also inhibited (Burgering & Coffer, 1995). In the heart, PKB is upregulated in response to insulin and nutritional status (Shiojima *et al.*, 2002), exercise training (Konhilas *et al.*, 2005), pressure overload (Naga Prasad *et al.*, 2000) and advanced heart disease (Taniyama *et al.*, 2005). PKB1 furthermore plays a protective role in the myocardium of both acute and chronic cardiac ischemic injuries (Fujio *et al.*, 2000). PKB's prominence as a multipurpose pro-survival protein signal has made it a prominent therapeutic target in treating cancer, diabetes, strokes and neurodegenerative diseases.

- ***ERK***

ERK (extracellular-signal-regulated kinases) are intracellular protein kinases which play a diverse role in cell differentiation and cell division. The ERK pathway is activated in response to a multitude of extracellular effectors, including growth factors, cytokines, viral infections, transforming agents, GPCR ligands and carcinogens (Shaul & Seger, 2007). The best understood MAPKs are ERK1 (p44 MAPK) and ERK2 (p42 MAPK) which are distributed in all tissue types. ERK p42/p44 are MAPK subtypes that mediate the mitogenic and the pro-inflammatory effects of insulin (Sasaoka *et al.*, 2006). Once resting cells are stimulated, ERK1/2 first accumulates in the nucleus through active and passive processes to phosphorylate nuclear transcription factors involved in early gene responses. The activation of the ERK cascade is mediated by upstream mitogen-activated protein kinase kinase 1/2 (MEK1/2). Once activated, ERK1/2 also phosphorylate hundreds of other substrates, such as the membrane proteins, CD120a, Syk and calnexin, the nuclear substrates, SRC-1, Pax-6, Elk-1, MEF2, c-Fos, c-Myc and STAT3, several MAPK-activating protein kinases (MK's), MAPK-interacting (MNK's) and cytoskeletal proteins (Roskoski, 2012). Due to the magnitude of influence of the ERK pathway, it has been seen to play conflicting roles in cellular processing, including proliferation, differentiation, metabolism, morphology, survival and programmed cell death (Deng et al., 2012). The ERK cascade consists of Ras, Rafs, MEK1/2, ERK1/2 and the MAPKAPK's (MAPK-activating protein kinases), Elk-1, Sap1a and c-Fos.

1.5.8.3 Insulin-Independent Mechanisms

- ***AMPK***

AMP-activated protein kinase (AMPK) plays a key role as a master regulator of cellular energy homeostasis (Hardie *et al.*, 2006). The kinase is activated in response to stresses that deplete cellular ATP supplies such as low glucose, hypoxia (Mungai *et al.*, 2011), ischemia, and heat shock (Frederich & Balschi, 2002). AMPK is a heterotrimeric protein that contains a catalytic subunit (α) and two regulatory subunits (β and γ). AMPKα2 is most commonly expressed in liver, skeletal muscle and heart tissues (Hardie & Carling, 1997). Binding of AMP to the γ subunit allosterically activates the complex, making it a more attractive substrate for its major (but not sole) upstream AMPK kinase, liver kinase B1 (LKB1) (Woods *et al.*, 2003). Increased intracellular Ca^{2+} concentration leads to the activation of Ca^{2+}-calmodulin-dependent kinase kinase β (CaMKKβ) which phosphorylates and activates AMPK (Woods, 2003). Activation of AMPK in response to Ca^{2+} fluxes provide a mechanism for cells to anticipate the increased demand for ATP. In contrast, insulin inhibits AMPK activation in response to an excess of nutrients. Insulin promotes glycogen, triglyceride and protein synthesis, while AMPK inhibits these energy consuming processes (Towler & Hardie, 2007). However, AMPK can play a protective role in cardiac ischemia as an energy generator in response to fat-cell derived hormones such as adiponectin and leptin (Shibata et al., 2005).

AMP-activated protein kinase has been shown to directly stimulate glucose uptake in skeletal muscle, thereby improving insulin insensitivity (Fisher et al., 2002). Activation of AMPK enhances both the transcription and translocation of GLUT4, resulting in an increase in otherwise insulin-stimulated glucose uptake. In addition, it

also stimulates catabolic processes such as FA oxidation and glycolysis via inhibition of acetyl-CoA carboxylase and activation of phosphofructokinase 2 in the heart (Hopkins et al., 2003). AMPK negatively regulates several proteins central to ATP consuming processes such as, glycogen synthase, HMG-CoA reductase, glycerol-3-phosphate acyltransferase and elongation factor 2, resulting in the down-regulation or inhibition of gluconeogenesis, glycogen, lipid and protein synthesis.

Due to its role as a central regulator of both lipid and glucose metabolism, AMPK is considered a key therapeutic target for the treatment of obesity, T2D, myocardial I/R-I and atherosclerosis (Li, Zhong, *et al.*, 2017).

- ***AS160***

Both insulin-dependent (PKB) and insulin-independent (AMPK) signaling can result in PKB substrate of 160kDa (AS160) activation. Typically, insulin signaling leads to the activation of PKB, which in turn phosphorylates AS160 on 5 suggested sites, of which the Ser588 and Thr642 are the most prominent (Manning & Cantley, 2007), resulting in stimulation of GLUT4 translocation to the cell membrane. Mutations at these two sites significantly inhibit insulin-induced GLUT4 translocation (Sano et al., 2003). Currently, the mechanism proposed for PKB-AS160 mediation of GLUT4 translocation, states that PKB activation on the various binding sites of AS160 inhibits GTPase-activating protein (GAP) activity, requiring a Rab-family GTPase to become GTP loaded. Rabs are small G-proteins that in their GTP-bound form can participate in vesicle movement and fusion (Mîinea *et al.*, 2005). Upon stimulation, GLUT4 vesicles translocate to the plasma membrane and facilitate the uptake of glucose from the blood stream (Mîinea, 2005) (**Figure 2.11**). Alternatively, AMPK has also been found to phosphorylate AS160 independent of insulin at its Ser473 site, which results in the same downstream activation and recruitment of GLUT4 (Treebak et al., 2006).

1.5.8.4 Stress Sensing

- ***JNK***

JNK (c-Jun N-terminal kinases) or SAPK (Stress-activated protein kinases) are kinases that form part of the MAPK family and are activated in response to cytokines and cellular stress. The JNK family comprises 3 different isoforms, JNK1, JNK2 and JNK3, also known as SAPKγ, SAPKα and SAPKβ respectively. JNK1 and 2 can be found in all tissue types, but JNK3 is mainly a brain protein (Bode & Dong, 2007). JNK can be activated in response to inflammatory cytokines or I/R-I (Deng *et al.*, 2012), via upstream MAPK kinase (MKK4 and MKK7) phosphorylation at its Ser63 and Ser73 residues, resulting in downstream signaling leading to inflammation (Ip & Davis, 1998). Alternatively, JNK can also be inhibited via Ser/Thr or Tyr protein phosphatases. Selective JNK inhibition have shown to be cardioprotective in I/R-I in kidneys and lungs (Wang *et al.*, 2007; Wolf *et al.*, 2008), however the same effect could not be mimicked in hearts and resulted in aggravated damage (Jang & Javadov, 2014; Shvedova *et al.*, 2018). The current trend argues that JNK1 and 2 is essential in I/R-I prevention, while an ongoing search for selective JNK3 inhibitors are underway (Shvedova *et al.*, 2018).

1.5.8.5 Inflammation Markers

- ***p38***

p38's, also called CSBP (cytokinin specific binding proteins), is a class of MAPK's sensitive to cytokines and stress signals. They play a role in cell differentiation, apoptosis and autophagy. The p38 family has 4 different isoforms, p38α, p38β, p38γ and p38δ, of which p38α and p38γ are most abundant in the heart (Deng *et al.*, 2012). Similar to JNK, the p38 cascade can be activated in response to inflammatory cytokines and I/R-I

(Harding *et al.*, 2010), starting with the upstream MAPK kinase (MEKK3 and MKK3/4/6) phosphorylation of p38 in turn activates MK2/3/5, Elk-1, CHOP, ATF2 and MEF2A (Deng *et al.*, 2012).

Within the isolated-perfused rat heart, p38 have been shown to double in kinase activity following 20 min of ischemia and 15 min of reperfusion, which proved to be detrimental (Milano *et al.*, 2007). In our own labs, we have also demonstrated that preconditioning in an isolated rat heart model resulted in attenuated p38 activation levels following reperfusion, which resulted in increased heart function (Marais *et al.*, 2001). Similarly, an *in vivo* I/R-I in rat hearts found p38 activation can abolish insulin's cardioprotective effect (Chai *et al.*, 2008). Furthermore, p38 activation in I/R-I exacerbates TNFα-induced tissue damage in response to elevated ROS, such as H_2O_2 (Meldrum *et al.*, 1998). p38 MAPK inhibition in I/R-I mouse hearts led to a decrease infarct size (Gao *et al.*, 2002).

1.5.8.6 Auxiliary Metabolic Regulation

- ***GSK-3***

GSK-3 (glycogen synthase kinase-3) is a protein kinase responsible for glycogen synthase regulation and plays a prominent role in glucose homeostasis (Ali *et al.*, 2001). Cardiac GSK-3 consists of two isoforms, GSK-3α (51 kDa) and GSK-3β (37 kDa) (Woodgett, 1990). GSK-3 plays a multifunctional role in cell signaling involved in proliferation, migration, inflammatory responses, glucose transport, glycogen synthesis, apoptosis and muscle contractility (Huisamen & Flepisi, 2014; Huisamen & Lochner, 2010). In response to insulin stimulation, PI3K and PKB are activated which in turn inactivates GSK-3 via phosphorylation of the Ser21 site in GSK-3α and Ser9 site in GSK-3β (Cohen *et al.*, 1997). Inactivation of GSK-3 resulting in the activation of glycogen synthase and inhibiting the mPTP formation. This has made GSK-3 β inhibitors attractive targets in ischemic preconditioning (Förster *et al.*, 2006). In contrast, GSK-3 activation through casein kinase 2 signaling (Rayasam *et al.*, 2009), results in IRS-1 and -2 phosphorylation at their Ser307 and Ser332 sites resulting in an inhibition of these signals and subsequently inhibits PI3K (Eldar-Finkelman & Krebs, 1997). This has negatively implicated GSK-3 as a glucose uptake inhibitor and a contributor to insulin resistance (Aguirre *et al.*, 2000; Flepisi *et al.*, 2013).

- ***ATM***

Ataxia-telangiectasia mutated kinase (ATM) is a key regulator of several signaling pathways in response to DNA damage, leading to cell cycle arrest, DNA repair or apoptosis (Smith *et al.*, 1999). ATM is denoted after the symptoms experienced when ATM is deficient (the AT-syndrome: "poor coordination" and "small dilated blood vessels") (Lee & Paull, 2007). Interestingly, lack of PKB function *in vivo* presents with phenotypical similarities to the AT-syndrome. ATM has also been shown to mediate PKB's insulin stimulated response (Viniegra *et al.*, 2005). Furthermore, ATM also plays a crucial role in the heart by controlling myocardial fibrosis and preventing myocyte hypertrophy (Foster *et al.*, 2012). In ATM-knockout mice, no activation of pro-apoptotic factors such as p53 and JNKs were observed, however a decrease in the anti-apoptotic factor, PKB, resulted in increased myocyte apoptosis (Foster *et al.*, 2012). Cardiac ATM have been shown to be upregulated in response to acute ischemic damage and reperfusion incurred during cardiopulmonary bypass surgery (Corbucci *et al.*, 2004).

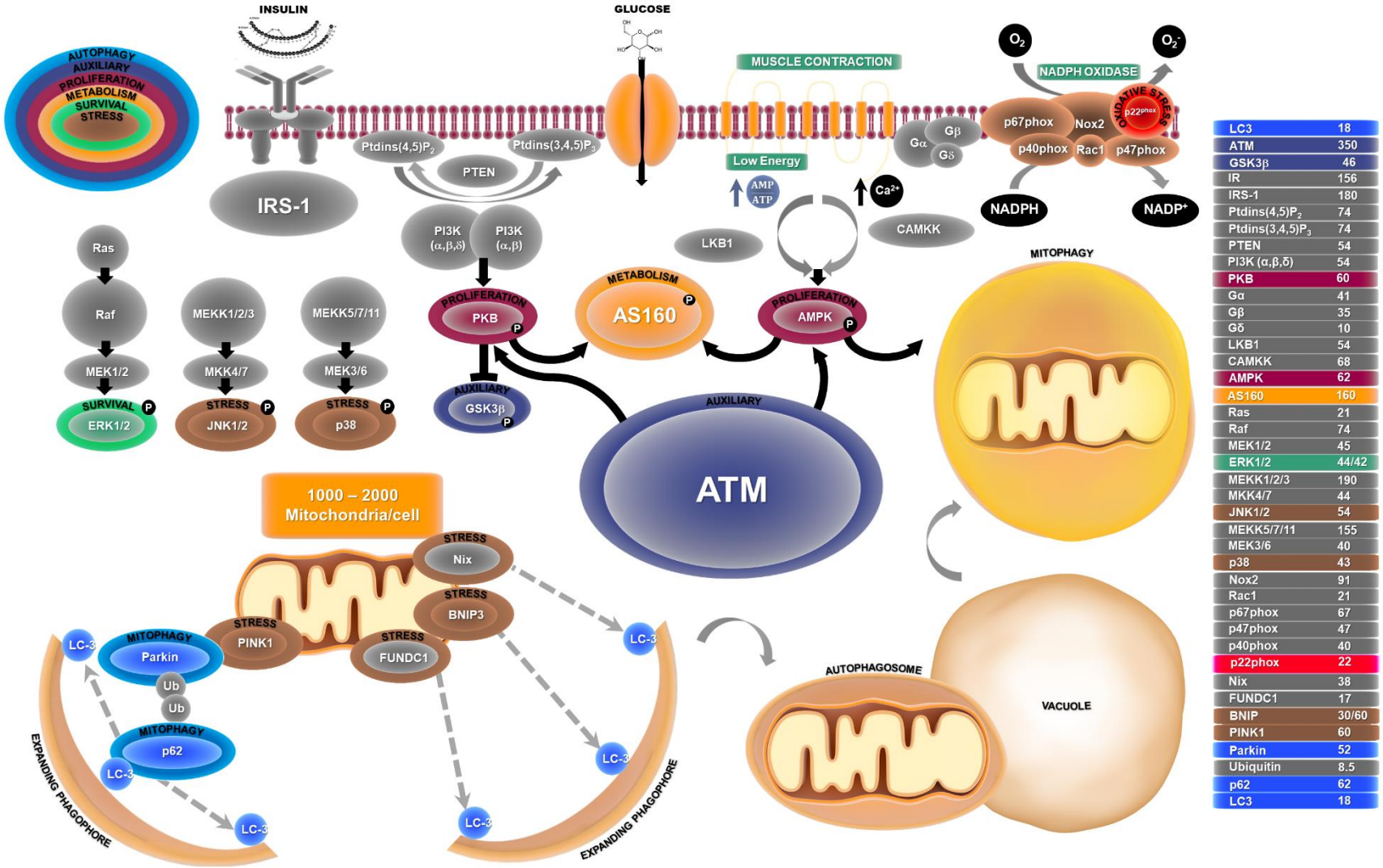

Figure 1.6 Proposed cell signaling mechanisms involved in cardioprotection. Cell signaling is narrowly regulated by a network of proteins working together to to resolve homeostatic imbalances in response to extracellular stresses and metabolic status. To investigate the efficacy of novel cardioprotective therapies aimed at improving I/R-I, it is important to have a clear understanding of the phosphorylation and expression state of key proteins as I/R-I progress. These proteins undergo state changes in response to varying levels of cellular stress, such as induced during ischemia, upon reperfusion and during prolonged reperfusion.

1.5.8.7 Alternative Pathways

- ***SAFE Pathway***

Alternative pathways not investigated in this dissertation have been suggested to be in part responsible for mediating ischemic preconditioning-induced cardioprotective effect, including the survivor activating factor enhancement (SAFE), and the NO/PKG pathway. It has been shown that administration of TNFα before ischemia can be cardioprotective without activation of the RISK pathway (Lecour *et al.*, 2005). This alternative pathway was coined 4 years later as the SAFE pathway and has been linked to preconditioning (Lecour, 2009). The SAFE pathway has been identified in rodent and porcine hearts (Bhatt *et al.*, 2013; Lecour, 2009; Lecour *et al.*, 2005). Individual steps have been identified but not nearly as thorough as the RISK pathway. As such, evidence supporting the involvement of the SAFE pathway is very fragmented, and wholly not as compelling yet (Cohen & Downey, 2015). The pathway provides a mechanism by which extracellular factors control gene expression (O'Shea *et al.*, 2015). Briefly, once engaged with a ligand (TNFα, interleukin-6 (IL-6) or growth factors), receptor-associated Janus Kinases (JAK) are activated and induce a functional change in the cytokine receptor allowing the cytoplasmic transcription factor, signal transducers and activators of transcription-3 (STAT-3) to be phosphorylated on its tyrosine residues. Activated STAT-3 forms a dimer that translocates to the nucleus and in turn regulate gene expression and targets the inhibition of the mPTP opening (Lecour, 2009; O'Shea *et al.*, 2013).

Chapter 2
LITERATURE REVIEW
Mitochondrial Dysfunction

2.1 INTRODUCTION

"Power from Within"

Mitochondria was coined from the Greek 'mitos' ("thread-like") and 'khondrion' ("granule-like") according to their appearance. A mitochondrion is enclosed by two membranes containing specialized proteins, dividing the organelle into a narrow intermembrane space and a broader internal matrix. The outer membrane contains various channels made by the protein porin, and acts as the first barrier to large molecules entering the mitochondrion, while the highly convoluted inner membrane, containing specific transport proteins, further limits only selected molecules from entering the internal matrix. The inner mitochondrial membrane also has a unique folding-configuration (called cristae), which aligns oxidative phosphorylation complexes in close proximity to each other (Youle & van der Bliek, 2012). The number of mitochondria in a cell type is dependent on the metabolic demand and can range from a single mitochondrion to thousands. Within cardiac tissue, mitochondria comprise 40% of the cell weight (Papadopoulou *et al.*, 1999) and cell volume (Murphy & Steenbergen, 2007), but accounts for 90% of ATP generation – enabling the cell to generate 15 times more ATP than it would have otherwise (Davidson, 2015). Mitochondria are quite flexible and have been shown to rapidly change shape and remain in constant motion throughout the cell. They are thought to be moved by motor proteins along the microtubule networks within cells and appear as a mixture of fragmented and tube-like structures within specific cell-types. For instance, in neurons they form mitochondrial networks throughout the cytosol, while in cardiomyocytes they form populations within intermyofibrillar or subsarcolemmal compartments (**Appendix A1**) (Ong & Hausenloy, 2010). Mitochondria also contains its own circular DNA (different from its host) (Gray *et al.*, 1998), comprising about 1% of the total cellular DNA (Trifunovic, 2006) and can reproduce independently of the cell and translate its own proteins. Mitochondria are primarily inherited from the maternal lineage, as the only mitochondria present in sperm is situated in the mid-section of the sperm tail (used to fuel the journey to the egg), but once fertilization is successful the tail falls off (**Appendix A2**). Therefore, all mitochondria prevalent in the development of the new organism comes from the mother's egg. This makes mitochondrial DNA different from nuclear DNA, which is shuffled every generation. Mitochondrial DNA has been shown to be involved in various genetic diseases, including Alzheimer's disease and diabetes (Davidson, 2015).

2.2 ENERGY METABOLISM

"The heart is all about non-stop energy".

2.2.1 Overview of Myocardial Energy Metabolism

The heart consists of specialized muscle cells and has the unique feature of uninterrupted contraction and relaxation (An & Rodrigues, 2006). This also makes the heart the most metabolically active organ in the body (Neubauer, 2007), needing a high supply of energy equating to 6 kg of adenosine triphosphate (ATP) ($1/8^{th}$ of total requirement per day) (Kühlbrandt, 2015) to sustain cellular maintenance and contractile function (Shah &

Shannon, 2003). The heart has very little stored ATP content (5 μmol/g of wet weight) and therefore a high turnover of ATP (~30 μmol/g of wet weight per minute at rest) allowing the entire pool of ATP to be recycled every 10 sec (Bing *et al.*, 1954; Opie, 1968, 1969a). The heart can utilize various substrates for energy generation (An & Rodrigues, 2006), but the most prominent are FA's, which account for 60-90% of ATP production (Lopaschuk, Ussher, *et al.*, 2010). The remaining energy is derived from glucose, amino acids, lactate and ketones. The heart switches between these substrates to facilitate optimal energy production during different physiological (post-prandial and fasted) or pathological conditions (Abdurrachim *et al.*, 2015). These conditions can influence the demand for energy, the amount of O_2 supplied to the heart, the amount of fatty acid supplied to the heart and the prevalence of the competing substrates, as well as change the mechanisms of substrate uptake and utilization within the cell (Lopaschuk, Folmes, *et al.*, 2010).

2.2.2 ATP

Food molecules, such as carbohydrates, fat and protein are metabolized through stepwise oxidation to produce the chemical energy molecule ATP. ATP is the main molecular energy source used to support contractile proteins, facilitate ion transport and enable enzymes to be functional. It is majorily generated when phosphate ions are linked to adenosine diphosphate (ADP) by the enzyme, ATP synthase (Lodish, 2000). However, it is also important to mention that ATP can be produced by direct transfer of a high-energy phosphate group to ADP during catabolic breakdown of high-energy transfer compounds during glycolysis and aerobic respiration (Lambeth, 2006). Therefore, ATP can either be produced through anaerobic metabolism of carbohydrates (in the cytoplasm), or via aerobic metabolism of fats, carbohydrates and proteins (in the mitochondria). Aerobic metabolism in the heart account for up to 95% of total ATP yield (Nsiah-Sefaa & McKenzie, 2016) due to its high density of mitochondria (Berg *et al.*, 2002). Metabolism can also be broken up into three separate stages, which all proceed in series: The first process is either glycolysis (in the cytosol) or fatty acid β-oxidation (in the mitochondrial matrix), followed by the citric acid cycle (CAC) (in the mitochondrial matrix), and ending in oxidative phosphorylation (on the inner mitochondrial membrane).

2.2.3 Glucose Metabolism

Glucose, a monosaccharide carbohydrate, is one of the major fuels utilized by the heart under normal physiological conditions. Glucose can either be derived from carbohydrates, such as sugars and starches after being processed by the digestive tract, or endogenously made by the body through breakdown of muscle and liver glycogen, or by de novo synthesis from lactate, glycerol, alanine and glutamine (Newsholme *et al.*, 2003). It enters cells through 14 different glucose transporters (GLUT's) depending on the tissue type (Augustin, 2010), and within the heart GLUT4 is the most prominent transporter of glucose intake. The rate at which glucose can be used is always limited by the rate of uptake, rather than the processing of glucose (Manchester *et al.*, 1994). Once inside the heart cell, glucose can be metabolised via glycolysis (in the cytosol) and glucose oxidation (in the mitochondria) or stored as glycogen in small quantities.

- ***Glycolysis***

The initial stage of glucose metabolism, known as glycolysis, occurs in the absence of O_2 in the cytosol of cells. The first step in glycolysis is the phosphorylation of glucose to glucose-6-phosphate (G-6-P) by hexokinase, leaving a negative charge and effectively trapping G-6-P inside the cell (Reddy & Reddy, 2015). Under physiological conditions, an estimated two-thirds of G-6-P is converted to glycogen (DeFronzo & Tripathy, 2009), whereas the rest enters glycolytic pathways to generate ATP. Each glucose molecule produces 2 ATP and 2 three-carbon pyruvate compounds, to be used subsequently in the CAC (**Figure 2.1**).

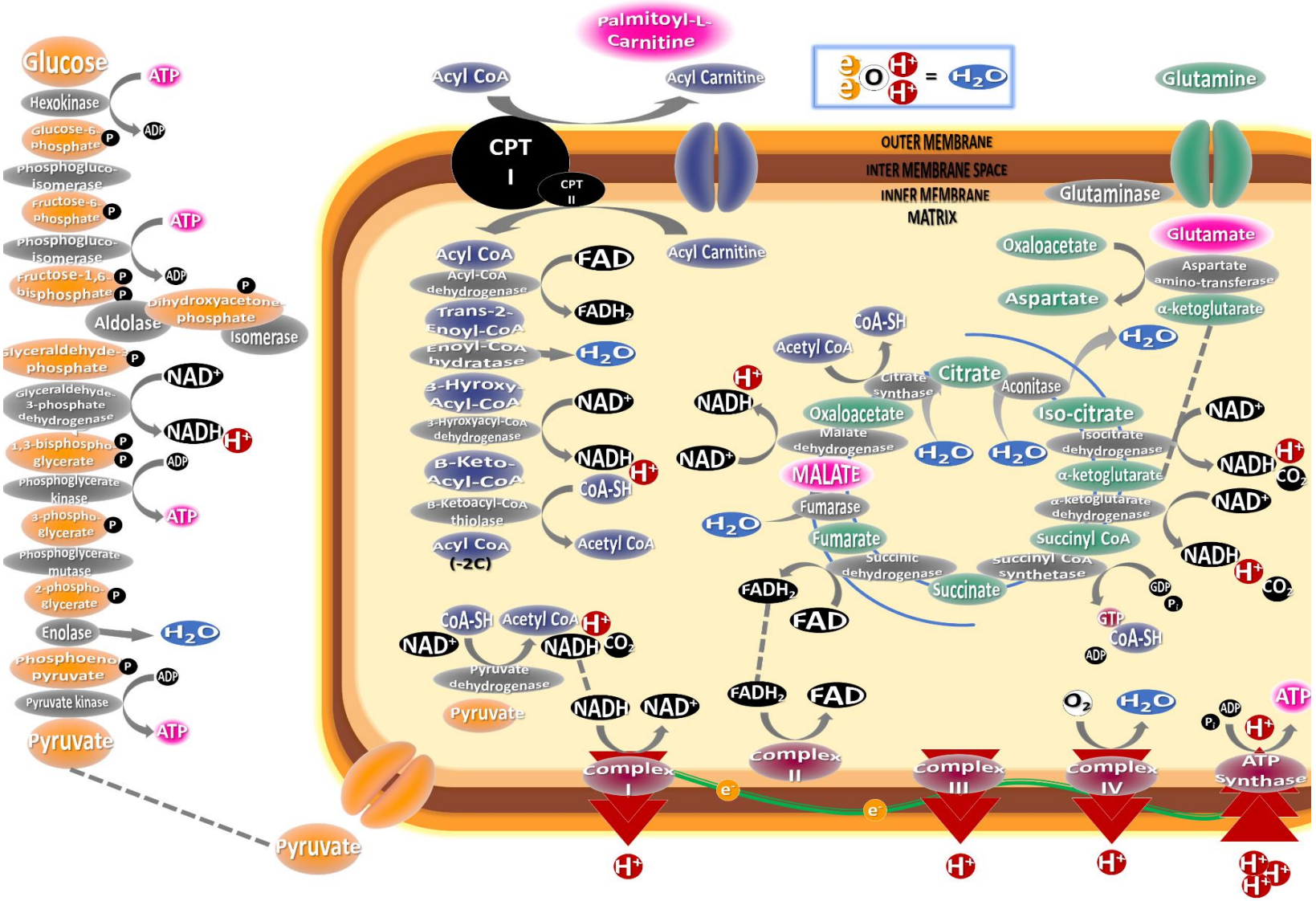

Figure 2.1 Energy metabolism pathways involved in generating ATP from either glucose or fatty-acid substrate in mitochondria

- ***Citric Acid Cycle***

CAC, also known as the tricarboxylic cycle or the Krebs cycle, is the metabolic junction between carbohydrates, fat and protein (Yang et al., 2014). After glycolysis, pyruvate and FA's are redirected to the mitochondria for conversion to acetyl CoA. The CAC oxidizes about 66% of all acetyl-CoA to produce CO_2 as waste product, and NADH and $FADH_2$ which passes electrons to the ETC to facilitate ATP production during OxPhos (Nsiah-Sefaa & McKenzie, 2016). The CAC does not directly require O_2 to cycle, but it is reliant on O_2 to recycle NAD^+ by accepting e^- from NADH. However, the 2-carbon acetyl group is not oxidized directly but transferred to the 4-carbon oxaloacetate to form a 6-carbon, citric acid – from where the name for the cycle is derived. This is followed by the gradual oxidation of citric acid to produce energy-rich activated carrier molecules, such as NADH and $FADH_2$, to be used for ATP production during OxPhos. The first step is the synthesis of citrate by citrate synthase from acetyl-CoA and oxaloacetate. Oxidising citrate produces 'reducing equivalents' NADH and $FADH_2$ to drive ATP production during OxPhos. During the cycle, carbon is also released in the form of CO_2, which further facilitates the replenishing of oxaloacetate. Carbon-containing CAC intermediates, such as oxaloacetate and a-ketoglutarate can also be used as alternative sources of energy or transported back into the cytosol to serve as precursors for amino biosynthesis (Owen *et al.*, 2002). This creates a higher demand for oxaloacetate which becomes a rate-limiting step, unless produced from an alternative pathway not derived from mitochondrial citrate. These alternative pathways are known as anaplerosis, allowing the CAC cycle to function as both a bioenergetic and biosynthetic pathway (Owen *et al.*, 2002). At the end of the cycle oxaloacetate is reproduced and the cycle can start again. In the end, the majority of glucose (80 – 90%) undergoing glycolysis is converted to 34 ATP molecules, carbon dioxide and water, while the remainder is converted to lactate (DeFronzo & Tripathy, 2009)

- *Glutamate*

Glutamate is a major precursor for oxaloacetate, a CAC intermediate, important in citrate synthesis (Bhatti *et al.*, 2017). Glutamate is either derived from glutamine via glutaminase, producing also nitrogen containing ammonia, or by nitrogen-donating reactions involved in nucleotide synthesis (Matés *et al.*, 2013). Glutamate is then converted to α-ketoglutarate by one of two reactions:

  - Under high-glucose conditions, transaminases transfer the amino group from glutamate to ketoacid, resulting in α-ketoglutarate and an amino acid (Yang *et al.*, 2014).
  - Under glucose-starved conditions (and impaired PKB signaling), glutamate dehydrogenase deaminates glutamate resulting in ammonia and α-ketoglutarate (Yang *et al.*, 2009)

- *Malate*

During OxPhos, pyruvate, glutamate and aspartate can all be derived from glutamine via glutaminolysis, which replenish the metabolic substrates of the CAC and support the synthesis of alanine and NADPH (DeBerardinis *et al.*, 2007). However, using glutamate or pyruvate in isolation can result in lower O_2 consumption rates (Puchowicz *et al.*, 2004). In the absence of malate, acetyl CoA accumulation inhibits pyruvate dehydrogenase via feedback inhibition and can also result in a decrease in CAC intermediates through dicarboxylate carriers (Salabei *et al.*, 2014). Therefore, when investigating mitochondrial oxidative phosphorylation, the addition of malate removes feedback inhibition by increasing oxaloacetate production thereby clearing acetyl CoA - essential for normal pyruvate dehydrogenase functioning.

2.2.4 Fatty Acid Metabolism

In the heart, utilizing FA for energy metabolism is very dynamic and can account for nearly 100% of total energy requirements or feature only in a minor capacity (Bing *et al.*, 1954; Opie, 1968, 1969b). FA's reach the heart in one of two forms: FFA's bound to albumin or FA's released from triacylglycerol (TAG) found in chylomicrons or very-low-density lipoproteins (VLDL) (Van Der Vusse *et al.*, 2000). Furthermore, excess body fat can be broken down and release as FFA's to meet energy requirements - one kg body fat contains 7,740 calories of potential energy (Jennings & Lesser, 2012), which is double the amount of energy stored in equal amounts of glycogen (Kotecki, 2011). Furthermore, interestingly, for every 10 kg of fat broken down into energy in the presence of O_2, 8.4 kg is exhaled as a CO_2 byproduct through the lungs, and only 1.6 kg turns to H_2O which may be excreted in urine, faeces, sweat, breath, tears and other bodily fluids (Meerman & Brown, 2014). The rate of utilization is largely dependent on a variety of factors; ranging from the specific demand for energy, the availability of energy substrates, the type of FA's available and its transport into the cell and mitochondria, the amount of O_2 supplied, the rate at which FA's can be esterified to Coenzyme A (an essential step to prime FA;s for lipid oxidation), the health of mitochondria and the rate at which new enzymes involved in FA's metabolism can be generated (Lopaschuk, Folmes, *et al.*, 2010).

- ***Fatty Acid β-Oxidation***

Beta-oxidation is the breakdown process through which FA's are converted into substrate products in the mitochondria to be used for energy generation. FFA's are negatively charged, making it impossible to diffuse across cell membranes without specific transport proteins. Once inside the cell, FA's need to be transported into the mitochondrial matrix for β-oxidation to occur. Products formed in this process include NADH and $FADH_2$, co-enzymes involved in ETC, and acetyl-CoA - a type of acetate whereby most of the useful energy stored in sugars, fats and amino acids is extracted from.

- ***Oxidative Phosphorylation***

OxPhos is the final step in cellular respiration and refers to the phosphorylation of ADP to ATP while oxidizing an energy substrate. It is the only step in substrate metabolism that directly requires atmospheric O_2 derived from water to process acetyl into CO_2. OxPhos comprises two closely connected components – the ETC and chemiosmosis. ETC drives the majority of ATP synthesis in most cells. NADH and $FADH_2$ transfer the e^- generated from the previous oxidation steps to the ETC located on the inner membrane of the mitochondrion. As e^- pass through this long chain of specialized e^- acceptors and donor molecules, the overall energy state is gradually lowered. The released energy is used to create a H^+ gradient, by pumping H^+ out of the mitochondrial matrix into the intermembrane space. This gradient can, in turn, be used to store potential energy (likened to a battery) to drive energy-requiring reactions – such as the phosphorylation of ADP to generate ATP. The last step in the ETC is the transfer of e^- to O_2 gas molecules (having diffused into the mitochondrion), which combines with the excess H^+ in solution to produce a water molecule. With this action, the e^- reach their lowest energy state, and no more energy can be extracted from the oxidized food molecule. The complete oxidation of a glucose molecule to H_2O and CO_2 results in 34 molecules of ATP produced. Of the 30, only 2 molecules of ATP are produced in the absence of O_2 during glycolysis (Lodish, 2000). ETC is the final step in metabolism of food molecules, and the site where the most chemical energy is generated.

2.2.5 Lactate Metabolism

- ***Cori Cycle***

During prolonged contraction of skeletal muscles, O_2 supply grows limited, inhibiting complete oxidation of glucose. In this scenario, glucose is fermented to two molecules of ATP and lactic acid, rather than pyruvate (Lodish, 2000). Lactic acid accumulates in skeletal muscle (arguably contributing to muscle and joint aches (Miles & Clarkson, 1994) until it is cleared by secretion into the blood. Once in circulation, it is either taken up by the heart or liver, where it can be reprocessed to pyruvate and further metabolized to ATP and CO_2 or converted back to glucose (Lodish, 2000). Monocarboxylates, such as pyruvate, lactate and ketone bodies are transported across the cell and organelle membranes via H^+ -linked monocarboxylate transporters (Halestrap & Wilson, 2012).

2.2.6 Ketone Metabolism

Technically, heart muscle prefers acetoacetate as energy substrate over glucose (Berg *et al.*, 2002). During periods of fasting or strenuous exercise, acetoacetate is produced in the liver, along with other ketone bodies to be used as energy substrate within organs.

2.2.7 Glycogen Metabolism

The heart contains very limited supplies of glycogen reserves, comprising about 2% of the adult heart cell volume (Berg *et al.*, 2002), and 30% of fetal and newborn cardiomyocytes (Shelley, 1961). Cardiac glycogen concentration can vary based on training status, exercise and diet (Depre *et al.*, 1998). In contrast to liver and skeletal muscle cells, cardiomyocytes produce glycogen during fasting (Schneider *et al.*, 1991). In times of fasting, fatty acids become the predominant fuel for the heart, whilst glucose uptake and glycolysis are decreased. This leads to a repurposing of glucose for glycogen synthesis. Glycogen stores can be further expanded in response to insulin, which simultaneously stimulates glucose transport and glycogen synthase activity (Moule & Denton, 1997). Glycogen synthesis is also upregulated when lactate is used as the primary fuel for the heart (Laughlin & Taylor, 1994). Furthermore, heart glycogen can also be broken down in response to adrenaline or O_2 deprivation to produce glucose (Morgan & Parmeggiani, 1964).

2.3 MITOCHONDRIAL DYSFUNCTION

“Load-shedding…”

The role of mitochondria in human health have been extensively studied for the past 60 years (Calvo & Mootha, 2010), yet new questions resulting in new insights are still being raised. As mentioned in the previous section, mitochondria are involved in energy-production (ATP, NADH and GTP) and bio-synthesis (amino acids, heme groups, iron sulfur clusters), but also play an important role in membrane biogenesis (phospholipid construction) (Kühlbrandt, 2015), cellular signaling (Ca^{2+}) (Chandel, 2014; Rizzuto *et al.*, 2012) and cellular stress (Pellegrino & Haynes, 2015). Thus, retaining mitochondrial quality is essential as dysfunctional mitochondria cause an array of pathological effects. Mitochondrial quality control revolves around a cycle of fission, fusion, mitophagy and biogenesis (Anzell *et al.*, 2018). Stressful conditions such as acute I/R-I influence mitochondrial structural integrity (through swelling or disruption of cristae), ideally resulting in mitophagy of dysfunctional mitochondria (Anzell *et al.*, 2018).

2.3.1 Mitochondrial Fission and Fusion

Mitochondria are often pictured as rigid, inflexible structures, but they form intercommunicating networks linked to the cytoskeleton which are constantly undertaking fission (division) and fusion (joining) subject to

intracellular stresses (Chen & Knowlton, 2010; Wong *et al.*, 2000). Mitochondrial fission and fusion maintain mitochondrial homeostasis, by regulating turnover of new mitochondria or recycling of old (Seo *et al.*, 2010), re-establishing electrical and biochemical connectivity, and preserving mitochondrial DNA (Youle & van der Bliek, 2012). Regardless of which cell-type, the balance between fission and fusion is induced by cellular stress and energy requirements (Ong & Gustafsson, 2012). Alterations in mitochondrial morphology occurs when too much fusion gives way to giant networks of clumped mitochondria, or too much fission results in tiny, mitochondrial pieces (Song *et al.*, 2015). During I/R-I, low ATP levels and elevated mitochondrial ROS production causes upregulation of fission inducing extrinsic apoptosis, resulting in increased post-ischemic cell death. Inhibiting mitochondrial fission during I/R-I reduced mitochondrial fragmentation and presented cardioprotective properties by inhibiting the mPTP opening (Ong & Hausenloy, 2010). These findings have implicated mitochondrial fission and fusion regulation as a promising therapeutic target in I/R-I.

2.3.2 Mitophagy

Obesity and insulin resistance are associated with changes in cardiac mitochondrial function, including reduced OxPhos and therefore decreased ATP synthesis (Essop *et al.*, 2009). To deal with these added stressors, cells undergo mitophagy, a specialized form of autophagy responsible for elimination of mitochondria in response to starvation and other forms of metabolic stress (Dolman *et al.*, 2013). Two distinct mitophagy pathways are known which can be categorized into either Parkin-independent or Parkin-dependent pathways. Parkin-dependent mitophagy results from a loss in $\Delta\psi m$ leading to rapid attenuation of the proteolysis of PTEN-induced putative kinase 1 (PINK1), increasing PINK1 accumulation on the surface of damaged mitochondria (**Figure 1.6**). In turn, PINK1 promotes phosphorylation of Parkin (PARK2), which then ubiquitinates SQSTM1 (p62) resulting in proteosomal degradation of p62 (Song *et al.*, 2015). P62 serve as the link between tagging of the damaged mitochondria and ligation of the autophagy-specific adaptor protein MAP1LC3 (LC3) – targeting mitochondria for degradation by autophagosomal fusion with lysosomes. Alternatively, independent of parkin (as is evident in Parkinson's Disease where Parkin-signaling is disrupted), mitophagy can also occur through either the BNIP3/Nix or FUNDC1 pathway (Novak *et al.*, 2010). For instance, Nix (BNIP3L), located on the outer membrane of mitochondria, can serve as an autophagy receptor by binding LC3, which then recruits mitochondria to the autophagosome (Novak & Dikic, 2011). BNIP3L's homolog, BNIP3 (in addition to FUNDC1 and NIX) can also localize to the mitochondria to mediate non-apoptotic cell death, leading to mitophagy (Campello *et al.*, 2014). As these pathways can be programmed individually, yet often influence each other's actions (Zorzano, 2017), it is safe to say that a lot more research is needed to improve our understanding of when specific mitophagy pathways are favoured.

2.3.3 Mitochondrial ROS production

Mitochondria are the single biggest source of intracellular $O_2^{\bullet}$ (Perrelli *et al.*, 2011). The ECT reduces over 90% of O_2 entering cells to water, while 1-2% is reduced to $O_2^{\bullet}$ due to e^- leakage at Complex I and Complex III, normally neutralized by SOD. However, mitochondrial ROS generation is elevated in I/R-I, partly due to a decrease in endogenous mitochondrial antioxidant potential (Stowe & Camara, 2009). These results were confirmed using specific inhibitors of various steps in the ETC, selective targeting of antioxidants to the mitochondria, and transgenic overexpression of mitochondrial versus cytosol-specific isoforms of antioxidant enzymes (e.g., MnSOD vs CuZnSOD) (Perrelli *et al.*, 2011). In other studies, pharmacological protection against I/R-I-induced vascular dysfunction and tissue injury have been found to dependent on inhibition of mitochondrial ROS production (Perrelli *et al.*, 2011).

2.3.4 Alterations in Diseased Conditions

- ***Obesity (Elevated FAO)***

Under normal physiological conditions, excess supply of energy not utilized for immediate energy needs, are stored in the form of triacylglycerols (TAG) in adipocytes, as ATP is too unstable to use for stockpiling energy. FFA's usually circulate at concentrations between 0.2 and 0.6 mM and the release of FFA's is acutely regulated to meet the energy requirements (Kurien & Oliver, 1971). When this balance is disturbed through mechanisms such as persistent overconsumption of food, adipose hypertrophy and hyperplasia, leading to greater release of FFA into circulation at concentrations above 2 mM in diabetes (Boden, 2008; Kurien & Oliver, 1971). Elevated FFA in circulation leads to increased VLDL-TAG synthesis in the liver, further exacerbating hyperlipidemia. In both experimental animals and humans, elevated circulating FA's and TAG induced by obesity and insulin resistance are important contributors to high rates of FA uptake and β-oxidation in the heart (Alberts *et al.*, 2002; Koutsari & Jensen, 2006; Lopaschuk, Folmes, *et al.*, 2010). Myocardial triglyceride content has been found to proportionally increase with BMI (Szczepaniak *et al.*, 2003) and is a strong indicator of cardiac dysfunction and heart failure (Sharma *et al.*, 2004). In diabetic patients without heart disease, an increase in FA circulation has also been correlated with a decrease in heart metabolism and diastolic functioning (stiff heart muscles leading to slower filling of the ventricles after a contractile cycle) (Leichman *et al.*, 2006; Lopaschuk, Folmes, *et al.*, 2010), and decreasing glucose oxidation can result in lower cardiac mechanical efficiency (How *et al.*, 2006). As a therapeutic option it has been shown that pharmacologically inhibiting fatty acid metabolism and activating glucose metabolism can result in improved heart function in diabetic patients (Stanley, 1997).

- ***Insulin Resistance***

In a failing heart, metabolism switches to glucose as the preferred substrate due to the efficiency of glucose oxidation in the generation of high-energy phosphates (Shah & Shannon, 2003). Increasing the amount of energy derived from glucose requires the upregulation of glucose transport and glucose oxidation. However, in the case of insulin resistance, glucose uptake and oxidation are both impaired, leading to less ATP generated from glucose. In diseased conditions, cells need to make use of alternative energy sources, including amino acids and fatty acid, to meet their metabolic demand. In this regard, glutamate and carnitoyl-L-palmitate are potential metabolic fuels used to investigate OxPhos potential in isolated cardiac mitochondria.

- ***Ischemia***

Without O_2, mitochondrial OxPhos ceases and greater emphasis is placed on glycolysis to maintain cellular ATP demand. Initially, the glycolytic rate increases for the first 60 to 120 sec, after which it slows down to a steady state for up to 90 min, depending on the severity of ischemia (Jennings & Reimer, 1981). If ischemia persists beyond this point, all remaining ATP levels will be spent resulting in compromised transmembrane ion gradients which will trigger cell death. Electron flow through the respiratory chain is mediated by the presence of O_2 and thus inhibited during ischemia. Therefore, F_1F_0 ATP synthase is unable to phosphorylate ADP to produce ATP (Di Lisa *et al.*, 2009). Secondly, to maintain the $\Delta\psi m$, ATP synthase runs in the opposite direction and starts to hydrolyze the remaining ATP (Di Lisa *et al.*, 2009). This quickly depletes ATP levels in the presence of ischemia. It has been shown that inhibiting ATP synthase during ischemia can effectively prevent ATP loss and prevent cell death in isolated rat hearts (Grover *et al.*, 2004). However, OxPhos inhibition during ischemia can also inhibit fatty acid breakdown, resulting in a toxic intracellular buildup of fatty acids, recruiting inflammatory metabolites and stimulating the mPTP opening (Di Paola & Lorusso, 2006). Mitochondrial

dysfunction has also been associated with heart failure (Rosca *et al.*, 2008). In mitochondria isolated from these hearts, OxPhos was severely decreased. As the individual activities of ETC enzymes remained normal, this dysfunction was attributed to a decrease in supermolecular assembly of ETC components (respirasomes) – dimerization of Complex I and Complex III assembled to Complex IV (Rosca *et al.*, 2008).

- ***Summary***

Mitochondria dysfunction is synonymous with a change in substrate oxidation. Impaired oxidation of energy substrates, especially FA, result in lipid accumulation and deposition of lipid mediators such as diacylglycerol and ceramides, both of which have shown to reduce insulin signaling. Insulin resistance increases susceptibility to cell death following I/R-I, as the anaerobic metabolism is firstly compromised during ischemia due to a decrease in glucose oxidation. This results in a decreased ability to maintain homeostasis at the onset of reperfusion while myocardial stunning prevails. After reperfusion, cardiac cells become overburdened by ROS and calcium, which can lead to dysregulated autophagic mechanisms. As impaired autophagy results in a failure to clear abnormal mitochondria, dysfunctional mitochondria proceed to open the mPTP leading to cell death. Therefore, therapies aimed at improving substrate utilization, supressing ROS production and preventing lethal calcium increases can effectively block the mPTP from opening and thereby prevent reperfusion-induced cell death.

Chapter 3
LITERATURE REVIEW
Rooibos

3.1 INTRODUCTION

"THE PURPOSE OF POLYPHENOLS"

Nature is the master craftsman of molecules used in drug development. In drug discovery, natural products remain an inexhaustible resource of therapeutic potential with an estimated 35,000-70,000 plant species having been screened for their medicinal use to date (Veeresham, 2012). Interestingly, the first purely natural therapeutic product was morphine in 1826, marketed by Merck, whereas the first semi-synthetic pure drug was aspirin (isolated from *Salix alba*) in 1899 by Bayer (Veeresham, 2012). Surprisingly, today only 11% of the 252 drugs listed as essential by the WHO and only 50% of cancer drugs used in the past 30 years are either directly or indirectly derived from natural products (Veeresham, 2012). This while even the most popular anti-diabetic medication, metformin, finds its origins in the French lilac or goat's rue (*Galega officinalis*), a plant that has been used for its medicinal properties since 1,500 B.C. (Witters, 2001). The search for novel synthetic chemicals, defined as compounds produced by man whereas natural products are made by nature, has often led us down a path of uncertainty and minor improvements at best as was asserted by Olfson & Marcus (2013) who compared the effect size of novel treatments published in 4 of the top journals around the world between 1966 and 2010. This is not to say that these research avenues should be stopped, but it is refreshing to know that the simpler way can often be more effective. Furthermore, up to 80% of the world's population still rely on natural medicines to treat ailments due to their time trialed safety and efficacy (Ekor, 2014). In search of more effective therapies in managing CVD progression, polyphenols and related phenolic compounds have been identified as prominent targets (Pandey & Rizvi, 2009). Polyphenolic compounds are abundant in plants and are readily found in fruit and vegetables. In addition, they are important components of herbs and spices and are likely to be critical ingredients in most Chinese medicines (Goszcz *et al.*, 2015). There are three major mechanisms by which polyphenols might impact on CVD, acting as antioxidants, anti-inflammatory agents, and/or anti-thrombotic agents. Together with their antioxidant properties, they can also generate ROS. The pro-oxidant effects of polyphenols can also be beneficial, since, by imposing a mild degree of oxidative stress, they can induce endogenous antioxidant defense mechanisms and serve as a means of preconditioning (Goszcz *et al.*, 2015). This can be thought of as how small bouts of exercise, followed by periods of rest, can increase your endurance and strengthen muscles in the long run. Unfortunately, the amount of research on the antioxidant potential of polyphenols far overshadows the lesser number of studies on the biological implications of their pro-oxidant properties. As a new role player to the field of CVD therapies, we turn our attention to the polyphenol-rich Rooibos, a plant exclusively cultivated in South Africa. In recent years Rooibos has shown promise as a strong antioxidant, anti-inflammatory and cardioprotective agent when administered orally. It is thus worthwhile to explore Rooibos' potential in treating CVD risk in a model of obesity and insulin resistant co-morbidities.

3.2 ROOIBOS

"FROM ROOIBOS TO GREENBOS"

3.2.1 Overview of Rooibos

Aspalathus Linearis (from the Latin *aspalathus* or Greek *aspalathos* – a scented and spiny bush) (Burm.f.) Dahlg. (Fabaceae, Tribe Crotalarieae), is an endemic South African fynbos species cultivated to produce the well-known herbal tea, rooibos (Johnson *et al.*, 2018; Quattrocchi, 2012). In the past 100 years, rooibos tea went from zero commercial value to being the most sought after herbal tea in at least 37 countries worldwide, including Germany, the Netherlands, the United Kingdom, Japan and the United States of America representing 86% of the export market in 2010 (Joubert & de Beer, 2012a; Joubert & De Beer, 2011). After ordinary black tea (*Camellia sinensis*), rooibos is reported to be the second most consumed tea beverage in the world (Anonymous, 2007). Its caffeine-free and comparatively low tannin status, combined with its potential health-promoting properties, most notably antioxidant activity, contributes to its popularity. The use of rooibos has also moved beyond herbal tea to intermediate value-added products such as extracts for the beverage, food, nutraceutical and cosmetic markets. Traditionally, rooibos has been used as a treatment or ointment for alleviating stress-related ailments such as insomnia and anxiety. Rooibos polyphenols also exhibit similar properties to the polyphenols of honeybush (*Cyclopia intermedia*), black and green (*Camellia sinensis*) teas when comparing antioxidant potential and antimutagenicity (van der Merwe *et al.*, 2006). Furthermore, increased antioxidant levels in unfermented rooibos compared to fermented rooibos (FRE), led to the development of green rooibos (GRE) (**Figure 3.1**). This has become a prominent product for nutraceutical industries isolating rooibos compounds for its anti-oxidant properties.

3.2.2 Composition

Rooibos' potential health benefits are a direct result of its phenolic compounds (Joubert & De Beer, 2011). Of therapeutic value, rooibos contains two unique polyphenolic compounds, aspalathin (Koeppen & Roux, 1965), a dihydrochalcone C-glucoside and aspalalinin (Shimamura *et al.*, 2006), a cyclic dihydrochalcone – occurring exclusively in *Aspalathus Linearis*. Rooibos also contains nothofagin, a rare dihydrochalcone C-glucoside which was first identified in the heartwood of *Nothofagus fusca* (Hillis & Inoue, 1967) and subsequently in the Chinese medicinal plant *Schoepfia chinensis* (Huang *et al.*, 2008). The remaining major phenolic compounds prevalent in rooibos include the flavones (orientin, iso-orientin, vitexin, isovitexin, luteolin and chrysoeriol), the flavanones (dihydro-orientin, dihydro-iso-orientin and hemiphlorin, and the flavonols (quercetin, hyperoside, isoquercitrin and rutin) (Ferreira *et al.*, 1995; Koeppen *et al.*, 1962; Marais *et al.*, 2000; Rabe *et al.*, 1994; Shimamura *et al.*, 2006). Rooibos also contains the phenolic acids, lignans, flavone diglycosides, (+)-catechin, a phenylpyruvic acid glycoside, and the coumarins, esculetin and esculin (Beltrán-Debón *et al.*, 2011; Breiter *et al.*, 2011; Krafczyk & Glomb, 2008; Marais, C., Steenkamp, J.A., Ferreira, 1996; Shimamura *et al.*, 2006).

3.2.3 Processing

Commercially, rooibos shoots are shredded and bruised, and left to enzymatically and chemically oxidize. This is followed by fermentation and sun drying (Joubert & Schulz, 2006). Finally, the tea is steam pasteurized to ensure that the final product is microbiologically safe. However, steam pasteurization significantly reduces the soluble solids, total polyphenols, total colour and most importantly, aspalathin contents of rooibos infusions (Koch *et al.*, 2013). The polyphenolic content (specific chemical structures with strong anti-oxidant capacity occurring naturally in plants) in rooibos extracts, especially the aspalathin and nothofagin content, are dependent on the concentration present in the plant (Schulz *et al.*, 2003) and the extent to which the plant

material is fermented (Joubert, 1996). Fermenting rooibos plant material to procure oxidized rooibos herbal tea results in a significant loss of phenolic composition (**Figure 3.1**), with 98% loss in aspalathin content reported in some cases (Schulz *et al.*, 2003).

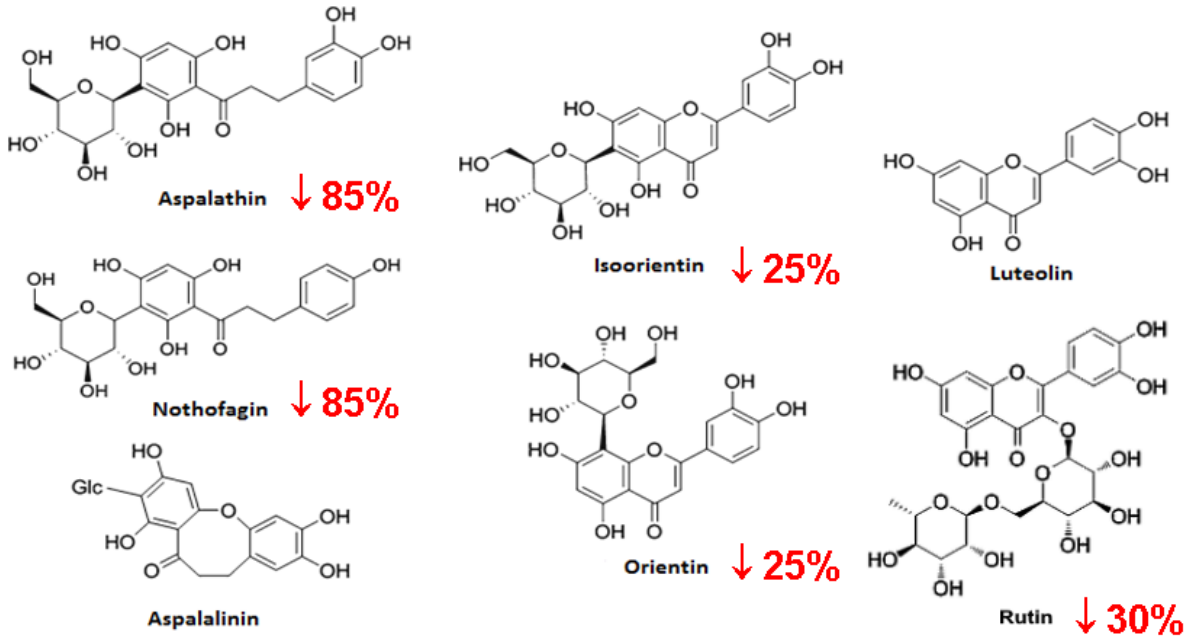

Figure 3.1 Reduction in major compounds present in rooibos following fermentation

3.2.4 Bioavailability

Polyphenols have very low bioavailability with less than 1% ingested reaching the plasma at concentrations rarely exceeding 1 μM when 10-100 mg of a single polyphenol is ingested (depending on the specific type) (Breiter *et al.*, 2011; Goszcz *et al.*, 2015; Scalbert & Williamson, 2000). Polyphenols are firstly metabolized by phase I and II liver enzymes, as well as the kidneys, resulting in conjugates forming in the blood plasma and urine (McGurk *et al.*, 1998). Peak concentrations in human plasma are usually achieved within 2h of ingesting polyphenols and baseline concentration restored within 12h (Scalbert & Williamson, 2000). The biological properties of most polyphenolic metabolites remain unknown (Scalbert *et al.*, 2002). Through conjugation, the biological effects of the parent compound can be either reduced or completely inhibited (Day *et al.*, 2000). Flavonoids bind to proteins, such as albumin, effectively lowering the detectable free flavonoid levels in the plasma (Manach *et al.*, 1997), while most flavonoids remain unabsorbed until it reaches the large intestine or is broken down by colonic microflora (Thilakarathna & Rupasinghe, 2013). Glucoronidation of aspalathin dissipates its antioxidant potential, but it can still elicit other biological properties, as compared with the conjugation of another rooibos compound, quercetin (Day *et al.*, 2000; O'Leary *et al.*, 2003).

Aspalathin (2',3,4,4',6'-pentahydroxy-3-C-β-D-glucopyranosyldihydrochalcone) is a C-glycosyl dihydro-chalcone and soluble in water and other polar solvents, but insoluble in non-polar media. It is the primary polyphenol and flavonoid present in the leaves of Rooibos or *Aspalathus linearis,* whilst also biogenetically related to other flavonoids isolated from rooibos tea (Koeppen & Roux, 1966). Aspalathin has a very low estimated absorption rate between 0.1% and 0.9% in pigs and humans (Courts & Williamson, 2009; Kreuz *et al.*, 2008; Stalmach *et al.*, 2009). Unmetabolized aspalathin is also detectable in human plasma (Laue *et al.*,

2009). After ingestion of aspalathin, the glycoronyl and sulphate conjugates are present in rat liver extracts (Van Der Merwe *et al.*, 2010) and O-linked methyl-, sulphate-, glucoronide-, and O-methyl-O-glucoronide derivates in human urine and plasma (Courts & Williamson, 2009; Stalmach *et al.*, 2009). Even though polyphenolic conjugation is well recognized, most biological studies still incorporate unmetabolized, natural, plant polyphenols. The unconjugated polyphenols as well as the remaining conjugates, could possibly aggregate in the body and elicit pharmacological activities (Zhang *et al.*, 2007), especially anti-diabetic effects (Sequeira & Poppitt, 2017).

3.2.5 Safety and Toxicity

Marnewick and coleagues (2003) treated ten Fisher 344 rats with 2 g/100 ml GRE and FRE for 10 weeks and found no adverse effects on body weight, liver, kidney or serum parameters (including aspartate transaminase, alanine transaminase (ALT), alkaline phosphatase (ALP), creatinine, bilirubin, total protein, cholesterol and iron status). In a follow-up study, they gave 40 volunteers 6 cups of fermented rooibos per day for six weeks (essentially ~1.5 L of tea per day) and some individuals presented with minor elevations in liver enzymes, albeit not enough to be clinically significant (Marnewick *et al.*, 2011).

In contrast, in 2010, Sinisalo and colleagues (2010) reported a case study on a 42-year-old woman who presented with elevated liver enzymes, ALT, ALP and γ-glutamyl transferase, indicators of possible liver toxicity after consuming 1L of rooibos tea per day for 2 weeks. As this was an isolated incident it was argued that the specific brand of rooibos might've been poorly processed or laced with hepatotoxic compounds (Sinisalo *et al.*, 2010). Poorly processed rooibos contains high amounts of Salmonella, a gram-negative bacteria which can cause severe diarrhea, fever and abdominal cramps in infected patients (Gouws *et al.*, 2014), which can be avoided through proper processing insuring the tea is microbially safe (Joubert & Schulz, 2006). Overall, rooibos has been confirmed as safe for human consumption by at least 3 studies (Breet *et al.*, 2005; Hesseling *et al.*, 1979; Marnewick *et al.*, 2011).

3.3 ROOIBOS FUNCTION

"ALL-IN-ONE NATURAL REMEDY"

Rooibos is gaining more popularity as a dietary antioxidant supplement and drinking merely 2 cups of either fermented or unfermented rooibos has the potential to raise plasma anti-oxidant levels in healthy adults (Villaño *et al.*, 2010). Furthermore, in adults susceptible to CVD, consuming 6 cups of fermented rooibos infusions per day for 6 weeks has been shown to improve lipid profiles and redox status (Marnewick *et al.*, 2011). It is gaining increasing popularity in research as a potent anti-oxidant (Dludla *et al.*, 2014; Sinjman *et al.*, 2009), cardioprotective agent (Pantsi *et al.*, 2011), stimulant of glucose clearance in muscle and cardiac cells (Muller *et al.*, 2012; Smit *et al.*, 2018), regulator of energy metabolism (Kawano *et al.*, 2009; Son *et al.*, 2013) and lipid lowering agent (Marnewick *et al.*, 2011).

3.3.1 Antioxidant Potential

The balance between internal and external ROS production in response to stress, is at the core of the ageing process and many age-related diseases (Liochev, 2013). Under baseline conditions, cells have a natural scavenging capacity to balance ROS production through anti-oxidants such as glutathione (GSH). However, during diseased conditions such as diabetes or myocardial infarction, there is an increased vulnerability for cellular damage and apoptosis due to an imbalance in the antioxidant to oxidative stress ratio. It has repeatedly been shown that diets consisting of primarily plant-based foods and beverages can lower the risk of developing

chronic diseases (Hu, 2003). Consuming flavonoids reduces the incidence of CVD and cancer (Arts & Hollman, 2005; Knekt *et al.*, 2002). Also, dietary interventions consisting of polyphenol-rich foods, have shown to improve plasma antioxidant capacity and total phenolic content (Lotito & Frei, 2006) Conversely, as shown by (Prior *et al.*, 2007), consuming nutrients without anti-oxidants, results in a loss of anti-oxidant potential in the blood. Moreover, strong antioxidant polyphenols have been researched in treating diabetic-associated complications (Zang *et al.*, 2006). Aspalathin is implicated as one of the main contributors of rooibos' antioxidant potential (Joubert *et al.*, 2009) (**Figure 3.2**), which is partly due to the relatively high content of aspalathin in rooibos, compared to the other compounds, and its radical scavenging activities.

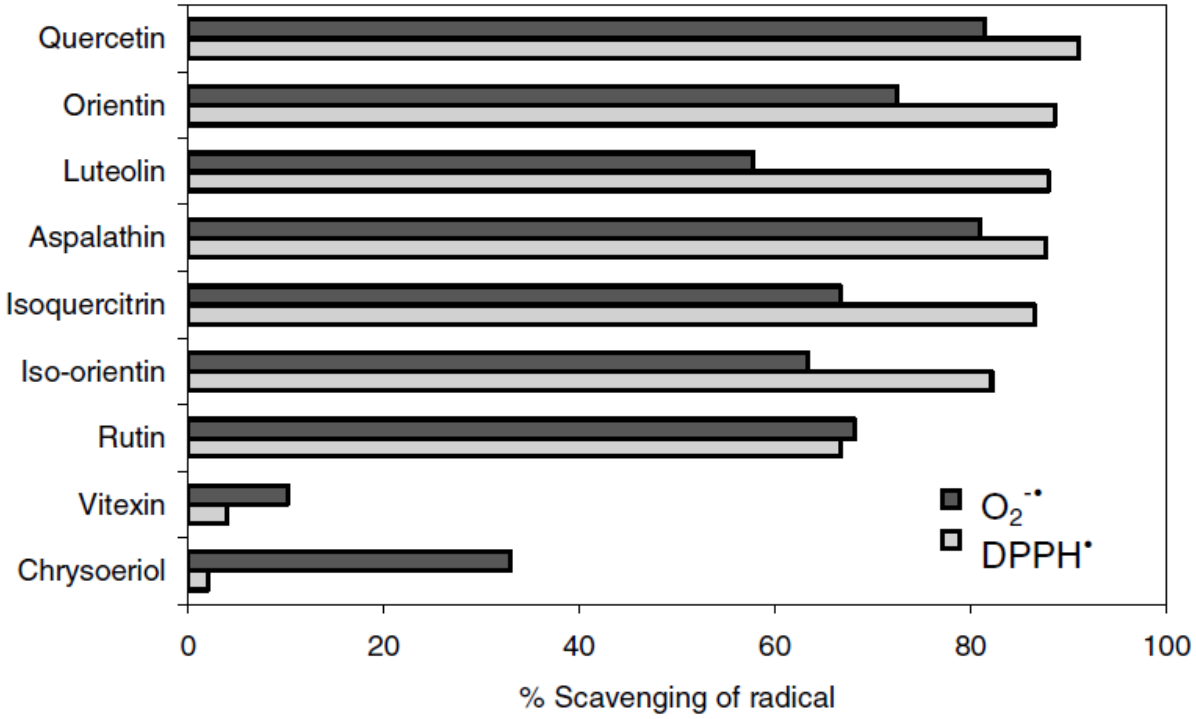

Figure 3.2 Comparison of the aspalathin's free radical scavenging ability compared to other rooibos flavonoids. DPPH•: 2,2-diphenyl-1-picrylhydrazyl free radical, O2•: superoxide radical (Joubert et al., 2006).

- ***In vitro***

Dludla and colleagues (2014) showed that FRE pretreatment in ischemic cardiomyocytes with a pro-oxidant insult (exogenous H_2O_2) preserved GSH and ATP content, improving anti-oxidant status and thereby reduced intracellular ROS and cell death. The protective effect of FRE was also more pronounced than that of vitamin E (a strong anti-oxidant used in radiotherapy treatment) (Prasad *et al.*, 2002). Chen and colleagues (2013) investigated the protective properties of aspalathin, GRE and FRE in *C.elegans* - an invertebrate organism used for investigating hyperglycemic conditions, ageing and longevity through simulation of a high glucose environment. They found that both rooibos and aspalathin prevents damage induced by juglone toxicity (used in high dosages to generate intracellular superoxides, $O_2^{\bullet}$ and H_2O_2). Similarly, in RIN-5F cells, GRE and aspalathin was able to protect against juglone toxicity by scavenging the $O_2^{\bullet}$ radicals (Son *et al.*, 2013). Furthermore, aspalathin display greater antioxidant potential than the commercial standard EGCG (epigallocatechin gallate), the most abundant catechin in green tea (Snijman *et al.*, 2007).

However, high dosages of polyphenols are known to exhibit pro-oxidant, rather than anti-oxidant effects (Mennen *et al.*, 2005). This was verified by Dludla and colleagues (2014) as high doses of FRE reduced its protective effect against exogenous H_2O_2.

- ***In vivo***

Rats treated with both GRE and FRE displayed increased myocardial total GSH content and reduced oxidative stress, which was also associated with improved aortic output recovery after ischemia/reperfusion (Pantsi *et al.*, 2011). In a study done on 40 human adults at risk for CVD, consuming 6 cups of fermented rooibos for 6 weeks improved redox status, lipid profile and elevated plasma GSH levels (Marnewick *et al.*, 2011). Likewise, Villaño and colleagues (2010) found that 2 cups of either fermented or unfermented rooibos tea in healthy adults increased plasma antioxidant capacity for 1 h similarly to other purported strong antioxidants, such as black tea (Widlansky *et al.*, 2005), green tea (Coimbra *et al.*, 2006) and cranberry juice (Duthie *et al.*, 2005). Lastly, rats receiving fermented rooibos tea for 7 weeks had increased antioxidant capacity and reduced lipid peroxidation, and after I/R-I in the brain, presented with reduced brain oedema and neuronal apoptosis compared to controls (Akinrinmade *et al.*, 2017).

- ***Synergy between related compounds in rooibos***

Interestingly, Simpson and colleagues (2013) showed that reconstituting an artificial infusion from the two most active dihydrochalcones, aspalathin and nothofagin, using the same concentrations had a greater antioxidant potential than the sum of either alone, or when compared to natural green and fermented infusions.

3.3.2 Cardioprotection

Pretreatment of cardiomyocytes with fermented rooibos prevented damage induced by ischemia, as indicated by a reduced amount of high fatty acid binding protein leakage (Dludla et al., 2014). Pantsi and colleagues (2011) showed that both GRE and FRE fed to rats for 7 weeks, were able to significantly improve heart function following ischemia/reperfusion and decrease poly ADP ribose polymerase (PARP) cleavage (a pro-apoptotic protein), while only FRE was able to decrease caspase-3 (also a pro-apoptotic protein) activity, inhibiting apoptosis and thereby having a cardioprotective effect. In a lipid toxic H9c2 cardiomyocyte model, established by exposure to 33 mM glucose for 48 h, treatment of 1 μM aspalathin for 6 h could reverse metabolic abnormalities through modulation of lipid metabolism (PPARγ and Srebf1/2), inflammation (IL-6/Jak2 pathway) and increased Bcl2 expression potentially preventing myocardium apoptosis (Johnson *et al.*, 2017).

3.3.3 Hypoglycemic agent

Aspalathin has been found to dose-dependently increase glucose uptake in rat L6 skeletal myotubes at concentrations between 1 and 100 μM (Kawano et al., 2009; Son et al., 2013). In our previous studies, we found that aspalathin had no observable effect on glucose uptake prior to 1.5 h *in vitro* administration to isolated cardiomyocytes, attributable to its role in upregulating gene expression first, resulting in GLUT4 translocation to membranes to facilitate glucose uptake into cells (Smit et al., 2018). Aspalathin also suppressed elevated fasting blood glucose and improved impaired glucose tolerance in *ob/ob* mice (Son et al., 2013) and *db/db* mice (Kawano et al., 2009).

- ***AMPK-dependent mechanism***

Kawano and colleagues (2009) first showed in RIN-5F pancreatic β-cells that 100 μM aspalathin treatment can increase insulin secretion, potentially leading to improved glucose homeostasis. Mazibuko and colleagues (2013) found that treating palmitate-induced insulin-resistant C2C12 skeletal muscle cells with either FRE or GRE enhanced glucose uptake, mitochondrial activity and ATP production, and resulted in the activation of

the insulin-independent AMPK pathway which culminated in increased levels of GLUT4. Similarly, Son and colleagues (2013) found that *ob/ob* mice fed a diet substituted with 0.1% aspalathin for 5 weeks (effective aspalathin dose 100 mg/kg/day/mouse) suppressed gene expression of enzymes related to gluconeogenesis and glycogenolysis, while upregulating glycogenesis in the liver resulting in improved glucose homeostasis. This effect was shown to manifest in activated AMPK signaling promoting endogenous GLUT4 translocation to the plasma membrane without effecting PKB activation. In C2C12 mouse skeletal muscle cells, Muller et al. (2012) also showed aspalathin improved glucose uptake, while this same effect could not be mimicked in Chang liver cells, which does not contain GLUT4. This strongly implicates GLUT4 and AMPK as essential role players in eliciting rooibos' response.

- ***PKB-dependent mechanism***

The role of rooibos' flavonoids on PKB signaling remain controversial. In rats supplemented for 7 weeks with GRE and FRE, there was little to no significant difference in total cardiac PKB levels (Pantsi *et al.*, 2011). In another study done by Son and colleagues (2013), rooibos also did not activate PKB in normal L6 myocytes. However, Mazibuko and colleagues (2013) was able to show activation of PKB in insulin resistant C2C12 myocytes when treated with rooibos. They observed that chronic exposure to saturated FFA, such as palmitate, reduces downstream activation of IRS-1 resulting in decreased PKB activation and GLUT4 translocation, effectively producing more insulin resistant cells (Bhattacharya *et al.*, 2007). However, when treated with rooibos, the P-PKB levels of the palmitate treated cells resembled that of normal P-PKB levels when stimulated by insulin, suggesting that rooibos can activate downstream insulin signaling.

- ***Synergy between related compounds in rooibos***

Muller and colleagues (2012) showed that Streptozotocin (STZ)-induced T1D Wistar rats (STZ used to ablate insulin producing pancreatic β-cells) pretreated for 1 h with aspalathin-enriched fractions suppressed blood glucose level increases. Purified aspalathin was unable to elicit the same response, but when aspalathin was combined with rutin (another prominent flavanoid present in rooibos), blood glucose was effectively suppressed for up to 6 h. Furthermore, it's been shown that GRE has a post-prandial blood glucose lowering effect in rats through suppressing intestinal α-glucosidase activity (Mikami *et al.*, 2015). Recently, it's been shown that 200 µg/mL GRE was required to have the same α-glucosidase inhibitory effect as 42 µg/mL of the anti-diabetic drug, acarbose (Miller *et al.*, 2018).

3.3.4 Lipid Profile

A person's lipid profile is determined by screening the blood for abnormalities in lipids, including cholesterol and triglycerides. In adults at risk for CVD, it was found that 6 cups of fermented rooibos per day for 6 weeks improved the lipid profile by lowering the LDL-cholesterol and TAG levels, and increasing the HDL-cholesterol (Marnewick *et al.*, 2011). In addition, fermented rooibos reduced lipid peroxidation, by decreasing conjugated dienes and thiobarbituric acid reactive substances (TBARS). Furthermore, 0.1% aspalathin administered for 5 weeks (effective aspalathin dose 100mg/kg/day/mouse) reduced hypertriglyceridemia, serum TBARS and adiponectin levels in *ob/ob* mice (Son *et al.*, 2013). In these mice, aspalathin also suppressed gene expression of enzymes related to lipogenesis leading to reduced serum triglyceride levels. In a study done by Najafian and colleagues (2016) they found in STZ-induced diabetic rats receiving 5 – 40 mg/kg aspalathin for 21 days had dose-dependent improvement in dyslipidemia (and blood glucose levels). Aspalathin also induced weight loss and reduced food intake, while also reducing diabetic-induced fluid loss through urine.

MOTIVATION FOR RESEARCH

OBESITY AND INSULIN RESISTANCE PREVALENT IN CARDIOVASCULAR DISEASE

CVD's are the leading cause of death worldwide, constituting 31% of all annual global deaths (17.5 million people) ("WHO | Cardiovascular diseases (CVDs)", 2018). This figure is in part aggravated by the presence of individual risk factors such as obesity and insulin resistance. Furthermore, the risk of cancer, IHD, ischemic stroke and T2D also increase as the severity of obesity increases (Abdelaal *et al.*, 2017). Recently, there has been a shift towards research into the therapeutic properties of natural products, including plant extracts (concentration of active compounds in plants), phytochemicals (isolation of active compounds in plants) and microbial metabolites (isolation of microbes present in plants) (Lahlou, 2013). These products are increasingly recognized for their potential in treating and preventing the metabolic syndrome, and subsequent T2D and CVD.

ROOIBOS BENEFICIAL FOR CARDIOVASCULAR HEALTH

Aspalathus linearis (commonly known as rooibos) is a plant indigenous to South Africa's fynbos area. Rooibos has shown to improve antioxidant status, CVD health, lower blood glucose and improve lipid profile (Muller *et al.*, 2018). Rooibos contains various bioactive phenolic compounds such as aspalathin, a C-linked dihydrochalcone glucoside unique to rooibos, and has been implicated as one of the main contributors of therapeutic potential (Johnson *et al.*, 2018).

EXPAND OUR UNDERSTANDING OF ISCHEMIA-REPERFUSION INJURY

In view of the significant role of anaerobic glycolysis in the survival of the ischemic myocardium (Opie, 2004), GRT could possibly be cardioprotective by contributing to myocardial glucose uptake and metabolism. Therefore, the effects of long-term GRT treatment on myocardial glucose metabolism in insulin-resistant, obese animals might aid in resensitising metabolism and protecting against I/R-I. In previous studies, rats treated with an aqueous unfermented rooibos extract for 7 weeks displayed improved cardiac aortic output recovery after I/R-I (Pantsi *et al.*, 2011). However, the role of rooibos in protecting against elevated CVD risk is uncertain. Furthermore, investigating the cellular signaling in both early reperfusion (5 mins of reperfusion) and late reperfusion (30 mins of reperfusion) will elaborate our understanding of pre- and post-treatment intervention feasibility.

EFFECT OF ROOIBOS ON MITOCHONDRIA

In view of mitochondria being the major producer of ROS leading to cell death, the importance of mitophagy in myocardial I/R-I may lay in sequestering dysfunctional mitochondria to prevent extensive ROS-induced damage. Aspalathin-rich rooibos extracts and purified aspalathin have been shown to inhibit the activity of xanthine oxidase, an enzyme responsible for generating ROS (Chen *et al.*, 2013). Unfermented rooibos has also been shown to protect against mitochondrial dysfunction (Mazibuko *et al.*, 2013). Thus, using GRT as a ROS scavenger may have a profound effect on mitophagic processes. This remains unclear as the effect of GRT on the mitochondria has not yet been studied in any setting. Experimental studies provided compelling evidence for rooibos extracts as a potential therapeutic tool against obesity and related metabolic abnormalities, contributing to the health of South Africans, and the rest of the world.

PURPOSE OF RESEARCH

Thus, the primary aim of the research was to investigate the effect of 6-week Afriplex Green Rooibos Extract (GRT), which is good-laboratory-practice certified product containing 12.36% aspalathin (See Certificate in **Appendix A3**) in treating cardiometabolic disease risk factors induced by a 16-week high-fat, high-caloric diet (HCD) feeding in rats. Specific focus was placed on GRT's effect on insulin resistance, obesity, I/R-I cardioprotection and oxidative phosphorylation. The secondary aim was to elaborate our understanding of the mechanism of action of rooibos polyphenols, and to ensure its effectiveness and safety using rat models. This study investigated the signaling molecules possibly involved in Afriplex GRT's beneficial effects by determining the expression and activation of proteins known to be involved in cardioprotection as well as mitophagy.

HYPOTHESES

- **Alternate hypotheses**

We hypothesize that treating obese, insulin resistant rats with GRT, an aspalathin-rich rooibos extract, for 6 weeks can protect against cardiac I/R-I and mitochondrial dysfunction potentially through cardioprotective, anti-inflammatory and anti-oxidant mechanisms.

- **Null hypothesis**

Treating obese, insulin resistant rats with GRT, an aspalathin-rich rooibos extract, for 6 weeks is insufficient to protect against cardiac I/R-I and mitochondrial dysfunction.

RESEARCH AIMS AND OBJECTIVES

Aim 1: To determine the effects of a 6-week treatment period with GRT on the functional performance of the heart by subjecting the isolated heart to a period of ischemia followed by reperfusion.

(i) Hearts from control (n=50) and HCD (n=50) animals, with half of each group receiving GRT treatment, stabilized for 30 min in *ex vivo* Working Heart Perfusion System followed by 20 min global ischemia and 30 min reperfusion for functional recovery determination. These hearts are freeze-clamped at the end of reperfusion to be analyzed for cellular signaling proteins in objective (ii).

(ii) In order to analyse the signaling pathways involved, the previously mentioned hearts, along with additional C (n=30) and HCD (n=30) hearts, of which half GRT treated, freeze clamped in groups of 5, after either 30 min stabilization period, 20 min ischemic period or 5 min into reperfusion.

(iii) All freeze-clamped hearts analysed for expression and activation of a battery of proteins known to play a role in cardioprotection or known for their detrimental role to the heart if activated. This included the following: PKB/Akt, ERK, AMPK, ATM, GSK3β, P38MAPK, JNK and AS160.

Aim 2: To determine the effects of a 6-week treatment period with GRT on infarct size induced by regional ischemia followed by reperfusion

(i) Hearts from control (n=20) and HCD (n=20), with half of each group GRT treated, to determine infarct size as the golden standard of cardioprotection. Isolated working hearts subjected to 30 min stabilization, followed by 35 min regional ischemia by occluding the left anterior descending coronary artery followed by 1 h of reperfusion. As these hearts are stained with Evan's Blue after the perfusion period to demarcate live, area at risk and dead tissue, they cannot be used for any additional measurements. Infarcted tissue vs live tissue determined using tetrazolium chloride (TTC) staining.

Aim 3: To determine the effects of a 6-week treatment period with GRT on mitochondrial OxPhos potential of the heart, before and after ischemia.

(i) Control (n=50) and HCD (n=50) animals with half of each group on GRT treatment. Mitochondrial isolations prepared from hearts stabilized for 30 min in *ex vivo* Working Heart System, after 20 min global ischemia and after 30 min reperfusion. Mitochondrial OxPhos potential measured using oxygraph.

(ii) Lysates prepared from mitochondrial fractions to determine accumulation of mitophagy induced proteins PINK1, Parkin, p62/SQSTM1, BNIP3L and LC-3.

Chapter 4

MATERIALS AND METHODS

4.1 MATERIALS

Abcam Plc., United Kingdom

Total-(PINK1, Parkin, p62, BNIP3L, LC3I/II) primary antibodies

Afriplex (Pty) Ltd., South Africa

Green rooibos extract

Amersham Biosciences Corp. (GE Healthcare Ltd.), United States

Enhanced chemiluminescence (ECL™) western blotting detection reagents

Bayer HealthCare Animal Health, South Africa

Eutha-naze (sodium pentobarbital)

BDH Chemical Ltd., United Kingdom

Glycerol, Sodium dithionite

Bio-Rad Laboratories, Inc., United States

Bovine Serum Albumin, Clarity™ Western ECL Substrate, Millipore Immobilon-p Polyvinylidene Fluoride (PVDF) microporous membrane, Criterion™ Tris-Tricine Precast Gels, Criterion™ TGX Stain-Free™ Precast gradient (4-15%) Gels

CAB Foods (Pty) Ltd., South Africa

Gelatine powder

Cell Signaling Technology®, United States

Anti-rabbit and anti-mouse IgG HRP-linked secondary antibody, Total-(AMPKα, PKB, AS160, ATM, ERK1/2, GSK3β, p38, JNK1/2) primary antibodies, Phospho-(AMPKα (Thr^{172}), PKB (Ser^{473}), AS160 (Thr^{642}), ATM (Ser^{1981}), ERK1/2 (Thr^{202}, Tyr^{204}), GSK3β (Ser^{9}), p38 (Thr^{180}/Tyr^{182}), JNK1/2 (Thr^{183}/Tyr^{185})) primary antibodies

Clover S.A. (Pty) Ltd., South Africa

Elite fat-free milk powder, Way Better™ condensed milk

GlucoPlus Inc., Canada

Blood glucose meter strips

Greiner Bio-One International, Germany

PLAIN serum clot activator vacuettes, pyrogen free Cryo.STm cryotubes

Hanna Instruments (Pty) Ltd., South Africa

HI 70300L pH Electrode Storage Solution, HI 7004 and HI 7007 pH Buffer Solution

Hansatech Instruments (Pty) Ltd., United Kingdom

Oxygen-permeable membrane

Hudson & Knight (Pty) Ltd, South Africa

Holsum™

Johnson and Johnson Medical (Pty) Ltd, South Africa

Ethicon silk suture

Lasec SA (Pty) Ltd, South Africa

Parafilm

Merck (Pty) Ltd., South Africa

$Na_2S_2O_4$, HCl, KCl, KH2PO4, $MgSO_4$, Na_2HPO_4, Na_2SO_4, NaCl, NaH_2PO_4, $NaHCO_3$, Na^+K^+-Tartrate, NaOH, tetra-Na^+-pyrophosphate, tris (hydroxymethyl) aminomethane, dimethyl sulfoxide (DMSO), butanol, Folin-Ciocalteu's phenol reagent

Next Advance, Inc., United States

stainless-steel 1.66 mm diameter beads

NuChek Prep Inc., United States

Standard FAME mixture

Pioneer Foods (Pty) Ltd., South Africa

Moir's strawberry jelly

RayBiotech Inc., United States

Rat Insulin ELISA Kit

Roche Products (Pty) Ltd. - Diagnostics, South Africa

BSA fraction V - fatty acid free, BSA fraction V

Safeline Pharmaceuticals (Pty) Ltd., South Africa

Isofor (isoflurane)

Sigma-Aldrich Life Science, United States

2-mercaptoethanol (solution), aprotonin, $CaCl_2$, EDTA, EGTA, leupeptin, $MgCl_2$, SDS, TEMED, trypsin-EDTA solution, Tween-20, β-glycerophosphate, β-mercaptoethanol, ammonium persulfate (APS), Triton® X-100, 2-mercaptoethanol, phenylmethylsulfonyl fluoride (PMSF), Coomassie Brilliant Blue G, sodium orthovanadate, Calbiochem® SignalBoost™ Immunoreaction Enhancer Kit, Ponceau S

Thermo Fisher Scientific Inc., South Africa

Fetal Bovine Serum, PageRuler™ Prestained Protein Ladder (Fermentas Life Sciences), 15/50mL Falcon™ Conical Centrifuge Tubes, 15/50mL Sorvall™ tubes, HiMark™ Pre-Stained Protein Standard

4.2 EQUIPMENT

Amersham Biosciences Corp. (GE Healthcare Ltd.), United States

Electrophoresis Power Supply (EPS) 301

Bante Instruments Ltd., China

PHS-3BW Digital pH Meter

Benchmark Scientific Inc., United States

Incu-Shaker Mini

Bio-Rad Laboratories, Inc., United States

ChemiDoc™ MP System, Image Lab Version 5.0, Mini-PROTEAN® Tetra System, PowerPac™ Basic

BioTek Instruments Inc., United States

ELx800 Absorbance Reader

Corning Inc., United States

Telfon® pestle, PYREX® Potter-Elvehjem tissue grinder

GlucoPlus Inc., Canada

Blood glucose meter

Grant Instruments Ltd., United Kingdom

Water Bath

GraphPad Software Inc., United States

GraphPad Prism 7

Hamilton Company, United States

Air-tight syringe

Hansatech Instruments (Pty) Ltd., United Kingdom

Clark-type oxygen electrode oxygraph, Oxygraph+ software

Heidolph Instruments (Pty) Ltd., Germany

Silent Crusher M Polytron

Lasec SA (Pty) Ltd., South Africa

Sigma 1-14K Refrigerated Microfuge

Microsoft Inc., United States

Powerpoint 365

Next Advance, Inc., United States

Bullet Blender®

Orto Alresa, Spain

Digicen 20 Centrifuge

Oxford University, United Kingdom

HOMA2 Calculator 2.2.3

PZ HTL S.A., Poland

Discovery Comfort multi-pipette

Sensor Scientific Inc., United States

Temperature probe

SGE International Pty, Australia

30m capillary column of 0.32 mm internal diameter; BPX70 0.25 um

Sigma-Aldrich Life Science, United States

Eppendorff® Minispin®plus

Thermo Fisher Scientific Inc., South Africa

Spectronic® 20 Genesys™ Spectrophotometer, Heraeus™ Megafuge™ 16 Centrifuge Series

Thermon Electron Corporation, United States

Finnigan Focus Gas Chromatograph

4.3 METHODS

4.3.1 Introduction

This section elaborates on the methods and techniques used to conduct the research set out in the study aims. Briefly, the research activities will be discussed according to the specific performing work-station as follows:

- Animal House
    - Animal Care
    - Study Design
    - Feeding
    - Treatment
    - Oral Glucose Tolerance Tests
    - Blood Collection
- Heart Laboratory
    - Sacrificing and Heart Procurement
    - Isolated Cardiac Perfusions
    - Mitochondrial Isolation
    - Oxygraph
- Protein Laboratory
    - Lowry Protein Determination
    - Bradford Protein Determination
    - Insulin Assays
    - Western Blot Analysis
- External Analysis
    - Total Lipid Fatty Acid Composition
- Statistical Analysis

4.3.2 Animal House

Laboratory animals were bred, housed and supplied by the Central Research Facility, Faculty of Medicine and Health Sciences, Stellenbosch University.

4.3.2.1 Animal Care

Age and weight matched male Wistar rats were used in the present study. Four weeks after birth, rats were weaned and then allowed free access to standard rat chow and water. Rats were housed in cages (maximum 5 per cage) in a stable environment of 22 °C, 40% humidity and a 12-hour artificial day/night cycle (light from 06:00 to 18:00) at the Central Research Facility, Stellenbosch University. The experimental procedure was revised and approved by the Committee for Ethical Animal Research for the Faculty of Health Sciences, University of Stellenbosch (**Ethical Clearance: SU-ACUM16-00080**). The revised South African National Standard for the care and use of laboratory animals for scientific purpose was followed (**SABS, SANS 10386, 2008**).

4.3.2.2 Study design

Male Wistar rats (*Rattus norvegicuss*) at 6-8 weeks of age and weighing 190±10 g were randomly allocated into two groups for 16 weeks feeding with either standard rat chow (1,272 kJ/100 g) or a high-caloric diet (HCD) (1,354 kJ/100 g) consisting of standard chow, supplemented with sucrose, condensed milk and holsum

cooking fat. Each group were further subdivided into 2 groups receiving either gelatine-fortified strawberry jelly or Afriplex GRT (60 mg/kg body weight (BW)/day, dissolved in gelatine-fortified strawberry jelly) for the last 6 weeks of the experimental program. Jelly was administered individually to each rat and observation was made until the treatment finished – ~20 sec per rat to finish a 1 cm x 1 cm cube of jelly which they were quite fond of. All 4 groups had access to *ad libitum* drinking water. The food and water intake of selected cages were monitored daily throughout the study and the animal body weight on a weekly basis. An oral glucose tolerance test was performed on selected groups of animals before the onset of the 6 weeks GRT treatment and again 1 week before sacrifice. This cycle was repeated 4 times over 3 years, consisting of 80 rats twice (to address Aim 1), 40 in the 3rd cycle (Aim 2) and finally 100 rats in the final cycle (Aim 3). Additionally, young control rats on a standard commercial rat chow diet weighing between 220-300 g were used throughout the study as positive controls to verify the validity of experimental protocols. The present investigation was divided into 3 sub-studies according to their specific aim (**Figure 4.1**).

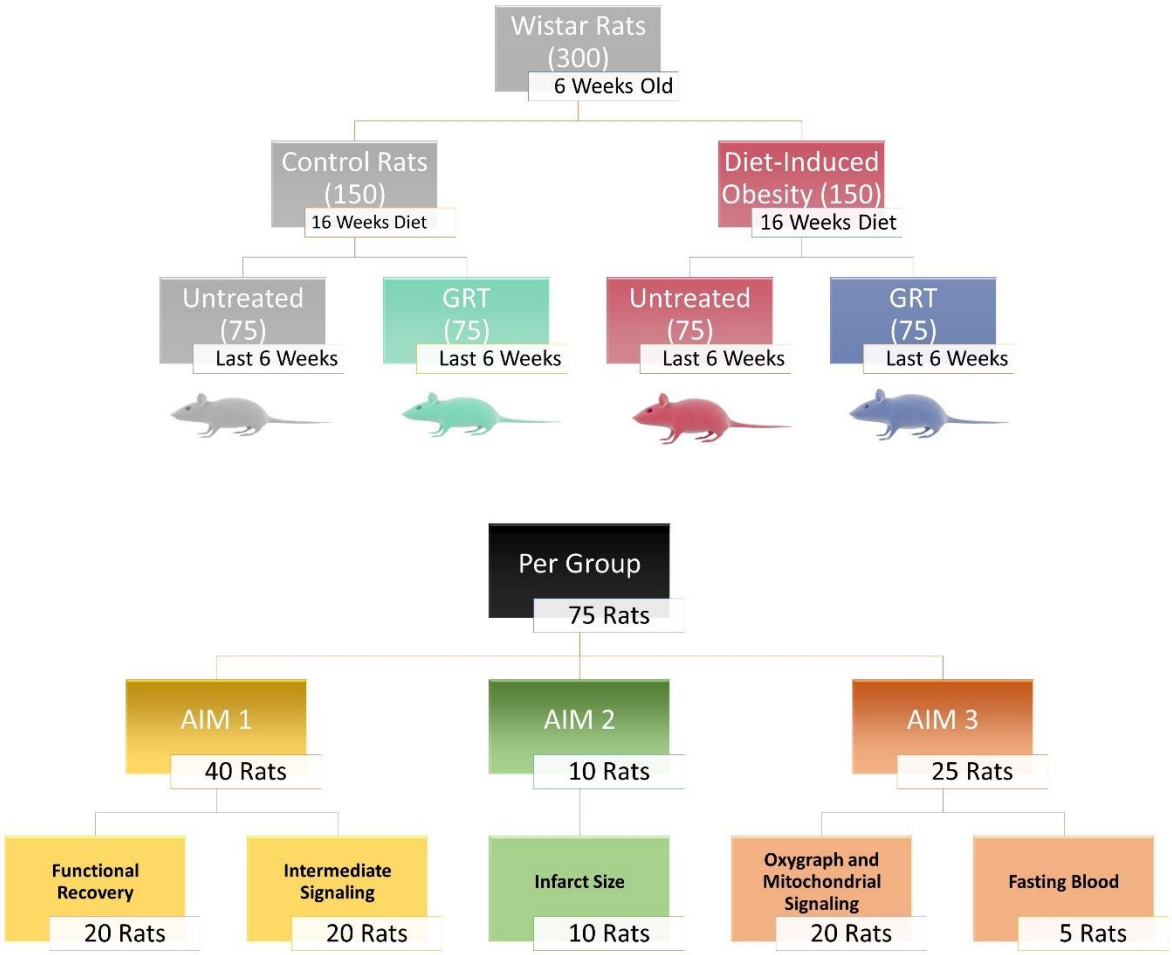

Figure 4.1 Study design according to the number of animals per aim

4.3.2.3 Feeding

After random allocation into cages, rats received either *ad libitum* standard rat chow (C) or *ad libitum* standard rat chow with a high-caloric diet (HCD). The diet compositions are given in **Table 4.1** as determined by Microchem specialized laboratory services, Cape Town, South Africa (see **Appendix A4** and **A5** for Diet

Analysis Certificates, Microchem Lab Services (Pty) Ltd., RSA). The HCD porridge was prepared weekly from standard rat chow softened with sucrose dissolved in boiling water, addition of melted cooking fat, consisting of Holsum™ (Hudson & Knight (Pty) Ltd., RSA) and Way Better™ condensed milk (Clover (Pty) Ltd., RSA), supplied to the rats in excess by allocation in bowls and replaced daily.

Table 4.1 Diet Composition of Control and High-Caloric Diet

Diet	Control	HCD
Protein (%)	17.1	8.3
Carbohydrates (%)	34.6	42
Sugar (g/100 g)	6.6	24.4
Fat (%)	4.8	11.6
Saturated Fat (g/100 g)	0.9	7.6
Mono-unsatured Fat (g/100 g)	1.5	2.9
Poly-unsaturated Fat (g/100 g)	2.4	1.1
ω-3 Polyunsaturated Fat (g/100 g)	0.2	0.1
ω-6 Polyunsaturated Fat (g/100 g)	2.2	1.0
Cholesterol (mg/100 g)	3	13
Energy (kJ/100 g)	1272	1354
Average Energy Intake Daily (kJ)	~255	~320

HCD: High-Caloric Diet

As given by Andreollo and colleagues (2012), the first 6 weeks of a rat (42.4 days) equates to one human year and is referred to as the nursing period. This is followed by the brief prepubescent period at 4.3 days for each human year, followed by adolescence 'years' every 10.5 days, and the adult years occurring similarly every 11.8 days. Considering these growth curves, the breakdown of our rat age is rationaled as follows: recruited for treatment at 6 weeks old (42 days nursing = 1 human year), and then receiving diet for 10 weeks (8 days prepubescent = 2 human years and 62 days adolescent = 6 human years), before receiving treatment for 6 weeks (42 days adolescent/adult = 4 human years), equating roughly to 13 years at age of sacrifice. This age was intentionally chosen as previous research interventions using this setting has been successful (Huisamen *et al.*, 2013; Smit *et al.*, 2018), and for the convenience of doing a large scale animal study (300 rats) without the added cost of feeding well into late adulthood.

4.3.2.4 Treatment

In this research project, the effect of Afriplex Green Rooibos Extract (GRT™) was investigated for its cardioprotective properties when used as a supplement for 6 weeks in a Wistar rat model of diet-induced obesity and insulin resistance. The treatment was administered at a dose of 60 mg GRT/kg BW/rat per day. The composition of GRT is given by **Table 4.2** as determined by the Medical Research Council of South Africa. The extract also contained neglible amounts of heavy metals and microbes as was determined by Afriplex Pharmaceuticals (See **Appendix A3** for Certificate).

Table 4.2 Compounds present in Afriplex GRT

Compound	g compound/100 g SS
Aspalathin	12.78
Nothofagin	1.97
Isoorientin	1.43
Orientin	1.26
Q-3-ROB	1.04
Isoquercitrin	0.57
Rutin	0.50
PPAG	0.42
Hyperoside	0.40
Vitexin	0.39
Isovitexin	0.30

SS: Soluble solids

Various considerations were made before elucidating the method of administration, such as ease of administration, together with retaining the stability of rooibos flavonoids which are prone to denature in response to light exposure, temperature, pH and storage time.

- *Preparation of Treatment*

The standard recipe for a batch of 35 Jelly cubes (35 daily dosages) contained

- 5.6 g Moir's Strawberry Jelly (consisting of sugar, gelatine (bovine), acidity regulators (E296, E450), ascorbic acid (E300), flavouring, salt, colourants (E122, E124))
- 5.6g Gelatine (gelatine (bovine), preserved with sulphur dioxide)
- 35ml boiling distilled water
- ~735 mg GRT (for rats averaging 350 g).

For example, to prepare weekly dosages for 5 rats/cage: 60 mg GRT/kg BW per day was divided by average rat weight per cage and multiplied by 35 cubes (7 days treatment x 5 rats). This amount of GRT powder was added to 5.6 g of Moir's Strawberry-flavoured Jelly and 5.6 g Gelatin, together with 35 ml boiling water and gently stirred at low heat until dissolved. 1mL was then aliquoted into an ice-tray containing 35 molds and stored overnight at 4°C covered with foil. The next day, each jelly cube was gently removed with a micro-spatula, paying attention to time handled at room temperature, before transported for weekly storage at 4°C and protected from light, in the animal facility. The nutritional composition of the jelly is given in **Table 4.3** and the ~2 kJ jelly cube administration is deemed neglible on overall caloric intake (compared to the average daily food intake of these rats from **Table 4.1**).

Table 4.3 Composition of Jelly

Diet	Per 100g	Per Jelly Cube
Protein (g)	17.1	26.9 mg
Carbohydrates (g)	34.6	54.4 mg
Sugar (g)	6.6	10.4 mg
Total Fat (g)	4.8	7.5 mg
Sodium (mg)	26	40.9 ug
Energy (kJ)	1272	2 kJ

- *Dosage*

Safe GRT dosage was determined according to the following rationale:

In a recent study by Son and colleagues (2013), *ob/ob* mice were gavaged an aspalathin dose of 100 mg/kg BW after fasting for 15 h, and furthermore given aspalathin supplementation for 5 weeks at a dose of 100 mg/kg BW per day. In another study done by Kawano and colleagues (2009), they gavaged an aspalathin dose of 18-110 mg/kg BW once. Given that the metabolic rate of a mouse is twice as fast as a rat, a dose of 100 mg/kg BW for a mouse would extrapolate to 50 mg/kg BW for a rat (Nair & Jacob, 2016). As the GRT product contains 12.8% aspalathin, a GRT dose of 60 mg/kg Rat BW, contains an effective aspalathin concentration of 7.7 mg/kg BW per rat - far below the safe dosages indicated in mice.

Given that the metabolism of a rat is 6 times as 'quick' or efficient as a human, this dose equated to 10 mg GRT/kg BW of a human, effectively meaning 700 mg GRT for a 70 kg person, resulting in a dose equivalent of 89.6 mg aspalathin. From Bramati and colleagues (2002) - one tea bag (2 g of leaf material) steeped for 10 min in boiling water would contain on average 1.234 mg aspalathin/g and therefore in one tea bag (2g) = 2.468 mg aspalathin. Thus, the 89.6 mg aspalathin within a single dose of GRT would contain the equivalent amount of aspalathin in ~36 cups of tea. This content within a cup of tea is corroborated by a paper by Joubert & de Beer (2012), however they indicated the aspalathin content in 6 cups of tea and, when reduced to one cup, the aspalathin content is found to be 1.22 mg aspalathin (which more roughly equates to 1g tea bags – the researchers only indicated tea bags were prepared according to standard practice), and therefore a single GRT dose would equate to the aspalathin content of ~73 Cups of tea. Regardless of the exact amount of 'tea cups' the dose equated to, it is safe to say it is not feasible to consume this concentration of aspalathin through drinking herbal infusions alone.

- *Light sensitivity*

Phytochemical oxidation experiments performed by Koeppen and Roux (1966) showed that aspalathin exposed to direct sun light can denature readily within 3 days of exposure with longer exposure time being more detrimental. To prevent oxidation from occurring to the set jelly cubes, the batches were prepared in low-light and left to set in 1cm x 1cm cube moulds and completely covered with foil until administration.

- *Temperature*

Work done by both Joubert and colleagues (2010) and also De Beer and colleagues (2015) showed that 30 min pasteurization (96°C) of GRE dissolved in water had little to no effect on flavonoid content. Furthermore, Koch and colleagues (2013) also demonstrated that steam pasteurization of fermented rooibos leaves for 60 sec had little effect on the stability of flavonoids, albeit a minor reduction <5% in aspalathin attritubed to an

acceleration in oxidation. This inferred that rapid addition of boiling water during the preparation of the jelly cubes would prevent a significant detrimental effect on GRT flavonoid content.

- *pH*

Aspalathin was also found to be most stable at decreasing pH, including pH = 4 and 5 (De Beer *et al.*, 2012). We determined the pH of strawberry jelly together with added gelatine to be acidic at 4.54 with the addition of GRT not causing a significant fluctuation in this pH level.

- *Storage*

In research done by De Beer and colleagues (2012) aspalathin in the presence of sugar can result in decreased stability occurring after 1 week of storage. Furthermore, the addition of ascorbic acid together with citric acid can help in improving stability – both components present in Moir's Strawberry Jelly. Jelly cubes were made weekly as an added measure of preventing oxidation induced over time. The cubes were stored at 4°C covered in foil for the duration of the week and administered to the rats daily. During this time, no compositional changes were noted in the consistency of the jelly.

4.3.2.5 Oral Glucose Tolerance Test

OGTT was used to determine fasting whole-body glucose homeostasis – the efficacy of rats to clear blood glucose following oral ingestion of sucrose. At both 10 weeks and 16 weeks of diet (**Figure 4.2**), a subgroup of animals were fasted overnight (with access to drinking water), and the body weights of the animals taken prior to moving the animals to a separate theatre within the animal unit. Fasting blood glucose levels were established from a tail prick using a standard glucometer (GlucoPlus Inc., Canada), before sedating the rats by intraperitoneal injection with a very low dose of sodium pentobarbital (15 mg/kg BW) using a sterile 26-gauge hypodermic needle. The site of injection was at the lower right quadrant of the abdomen to ensure that no damage is done to the urinary bladder, cecum, liver and other abdominal tissues (Zatroch *et al.*, 2016). Thereafter, a solution of 50% sucrose, containing a disaccharide bond of glucose and fructose, at a dose of 1 mg/g BW, was administered by oral gavage and blood glucose levels monitored by a drop of blood obtained from a tail prick and subsequent glucometer readings at various time points (3, 5, 10, 15, 20, 25, 30, 45, 60, 90 and 120 min). After the OGTT, animals recovered for one week from this metabolic insult before being sacrificed in other experiments. Relative glucose tolerance was determined by comparing the difference in blood glucose for each time point between groups, and by comparing the area under curve (AUC) of each individual rat tolerance test between groups.

4.3.2.6 Blood Collection

At 10 weeks and 16 weeks of diet (**Figure 4.2**), a subgroup of rats was fasted overnight, anaesthetized with 2% (v/v) isoflurane (Isofor, Safeline Pharmaceuticals (Pty) Ltd., RSA) and approximately 2 ml of blood collected via the carotid artery and allocated to eppendorf tubes. The blood was kept on ice for 30 min and then spun down at 3,000 rpms and the supernatant serum collected.

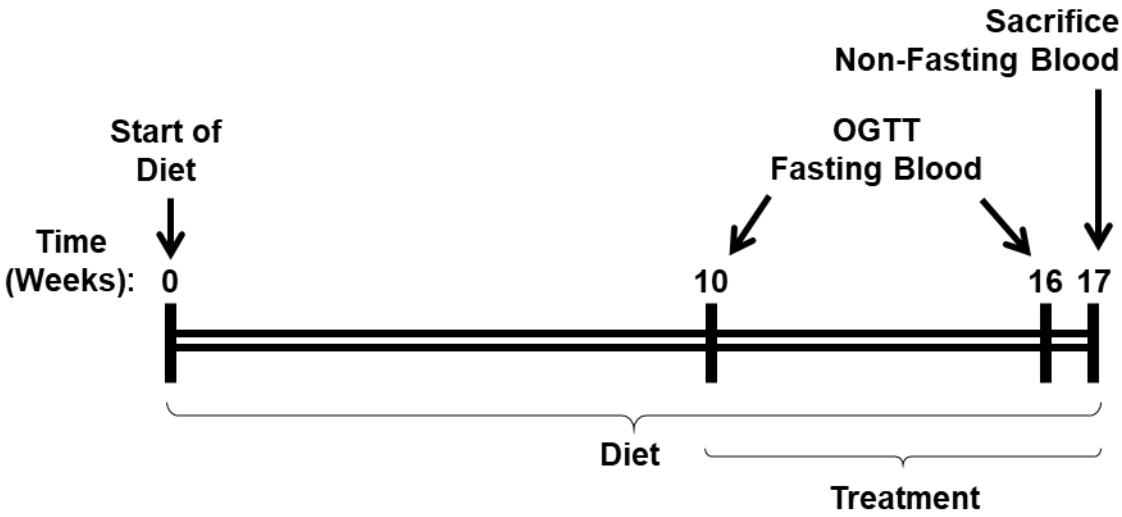

Figure 4.2 Timeline of blood-collection procedures performed on diet rats. OGTT: Oral glucose tolerance test.

4.3.3 Heart Laboratory

The cardiovascular research experiments were conducted in the Division of Medical Physiology, Faculty of Medicine and Health Sciences, Stellenbosch University.

4.3.3.1 Sacrificing and Heart Procurement

Rats were collected from the animal house a week prior to being used in experiments to reduce the stress of handling on the day of experimentation. Rats were anaesthetized with sodium pentobarbital (160 mg/kg BW). The rats were weighed and the non-fasting blood glucose (or random blood glucose test) value of the animals were determined from a tail prick using a standard glucometer (**Figure 4.2**). After determining deep anaesthesia via an unresponsive foot pinch (pedal reflex) and unresponsive eye reflex on touch (attained <5 min in most animals), hearts were quickly excised (<1 min after first incision) and arrested in ice cold Krebs-Henseleit (KH) buffer (**Table 4.2**).

- *Heart Weight*

Just prior to mounting of the heart onto the perfusion rig, the heart was trimmed of excess fat and tissue potentially obstructing the view of the important landmarks needed for cannulation. The heart was also drained of residual blood by gently squeezing and rinsing the heart in ice-cold Krebs buffer. The heart was then submerged in a weighing boat containing ice-cold Krebs buffer and the weight determined by weight displacement using a SF-700 digital Jewelry Scale. This entire procedure happened within 1-2 min after isolating the heart and just prior to cannulation of the aorta on the perfusion rig.

- *Blood Collection*

Directly after heart excision, blood was quickly collected from the chest cavity using a pipette and placed into plain serum clot activator vacuettes and kept on ice for 30 min, followed by centrifugation at 3,000 rpm for 20 min at 4°C (Heraeus™ Megafuge™ 16 Centrifuge Series). Thereafter, the supernatant (serum) was carefully aspirated and aliquoted into pyrogen free cryotubes and stored at -80 °C for future serum analyses.

- *Intraperitoneal Fat*

The intra-peritoneal fat of the control and HCD animals were dissected out and weighed at an opportune time after sacrifice and mounting of the heart onto the perfusion rig. These fat deposits include the visceral adipose

tissue surrounding the inner organs and can be clustered into the retroperitoneal, the fat surrounding the kidneys and the gonadal or fat attached to the epididymis and testes.

4.3.3.2 Isolated Cardiac Perfusions

The perfusion rig, also known as the Neely-Morgan perfusion system (Neely *et al.*, 1967) was set up in advance with reservoirs filled with filtered Krebs-Henseleit bicarbonate (KH) Buffer (**Table 4.4**) receiving permanent oxygenation (95%) and carbon dioxynation (5%), to maintain a pH of 7.4 at a temperature of 40°C to account for the temperature drop between the reservoirs and the mounted heart as a result of the lower ambient room temperature (**Figure 4.3**). The aorta (at least 5 mm of visible white aortic tissue) was mounted using surgical forceps, onto the aortic cannula (**Figure 4.4**) and retrogradely perfused (Langendorff mode) for 10 min, initially at lower pressure, and gradually increased to 100 cm H_2O hydrostatic pressure. During this time, the coronary sinus was pierced to release pressure build-up (a technique known as thebesian drainage) and to insert a temperature probe. Furthermore, the pulmonary vein bridging into the left atrium was also cannulated and tied down using surgical thread (<4 min of mounting the heart) (**Figure 4.4**). The water jacket around the heart was closed and the coronary temperature kept constant between 36.7°C and 37.0°C, especially in response to fluctuating coronary flows from different experiments. At the end of stabilization, the flow was changed to antegrade perfusion (working heart mode), with a preload of 15 cm H_2O hydrostatic pressure and a left ventricle ejection fraction against an afterload of 100 cm H_2O and continued for 20 min. Functional measurements were obtained. At 30 min of total perfusion time, two different ischemic protocols were followed as described below.

- *Global Ischemia-Reperfusion Protocol*

During global ischemia, all blood supply (substitution buffer) to the heart was ceased to start the ischemic protocol. Myocardial temperature was kept constant at 36.5°C for 20 min. After ischemia, reperfusion was initiated by Langendorff perfusion for 10 min followed by working heart for 20 min. During this protocol, following stabilization, ischemia, 5 min into reperfusion and after 30 min of reperfusion, hearts were either freeze-clamped (for subsequent Western Blot analysis of cardiac signaling proteins – described in **Section 4.3.4.5**) or homogenized and mitochondrial isolations made (for subsequent mitochondrial oxidative phosphorylation analysis and Western Blot analysis of mitophagy signaling proteins).

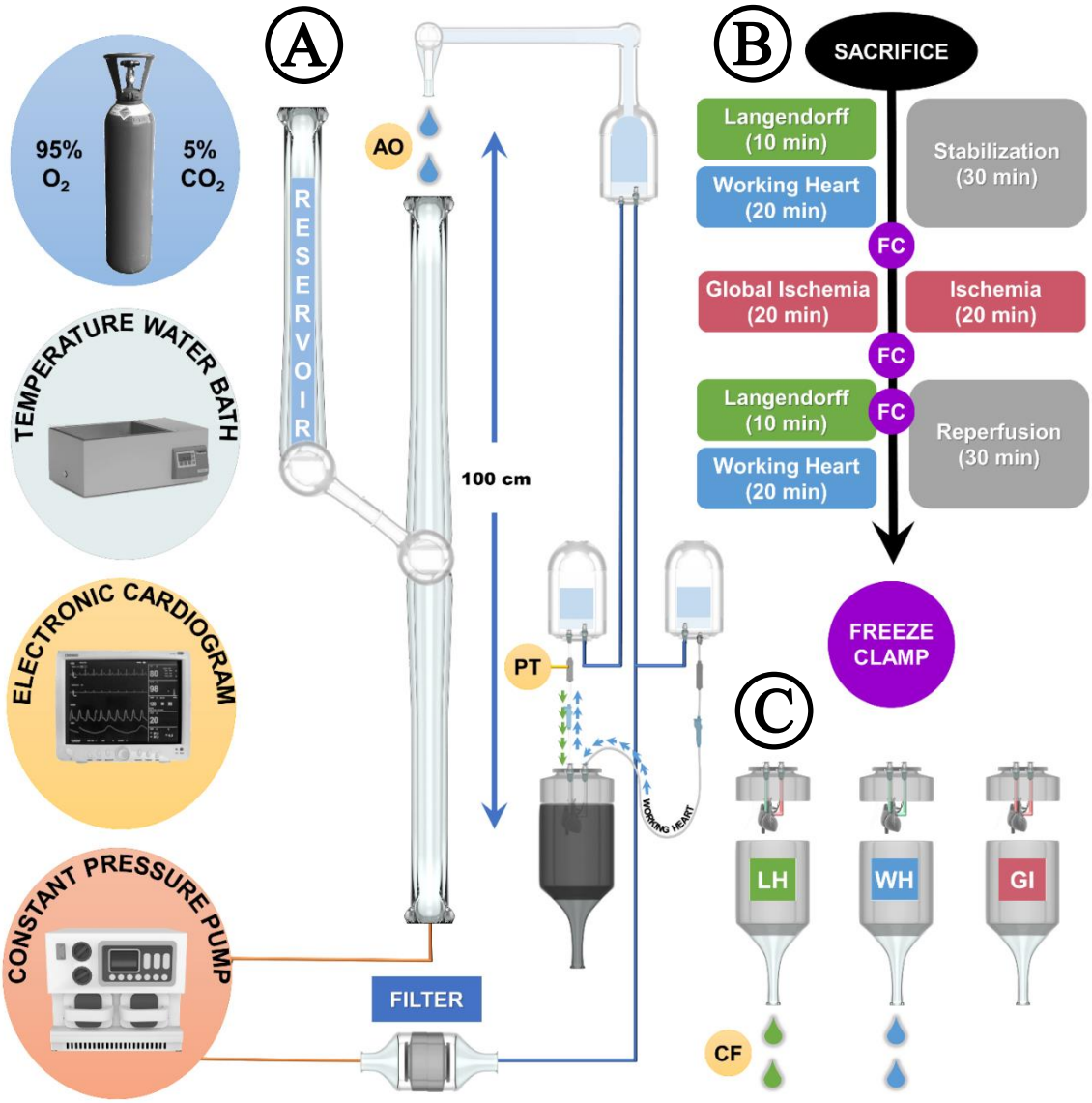

Figure 4.3 Perfusion system setup (A), protocol (B) and perfusion states (C). AO: Aortic output, PT: Pressure transducer, CF: Coronary flow, FC: Freeze-clamp heart, LH: Langendorff perfusion, WH: Working heart perfusion, GI: Global ischemia.

- *Regional Ischemia-Reperfusion Protocol*

During regional ischemia, the left anterior descending artery was ligated using a silk surgical suture (**Figure 4.4**), while temperature was kept constant at 36.5 °C for 35 min. This ligation effectively reduced coronary flow rate to one third of pre-ischemic flow. After ischemia, the suture was loosened and the hearts perfused in Langendorff for 10 min followed by working heart perfusion for 20 min and switched back to Langendorff for a final 30 min (Bell *et al.*, 2011). This was followed by infarct size determination described below.

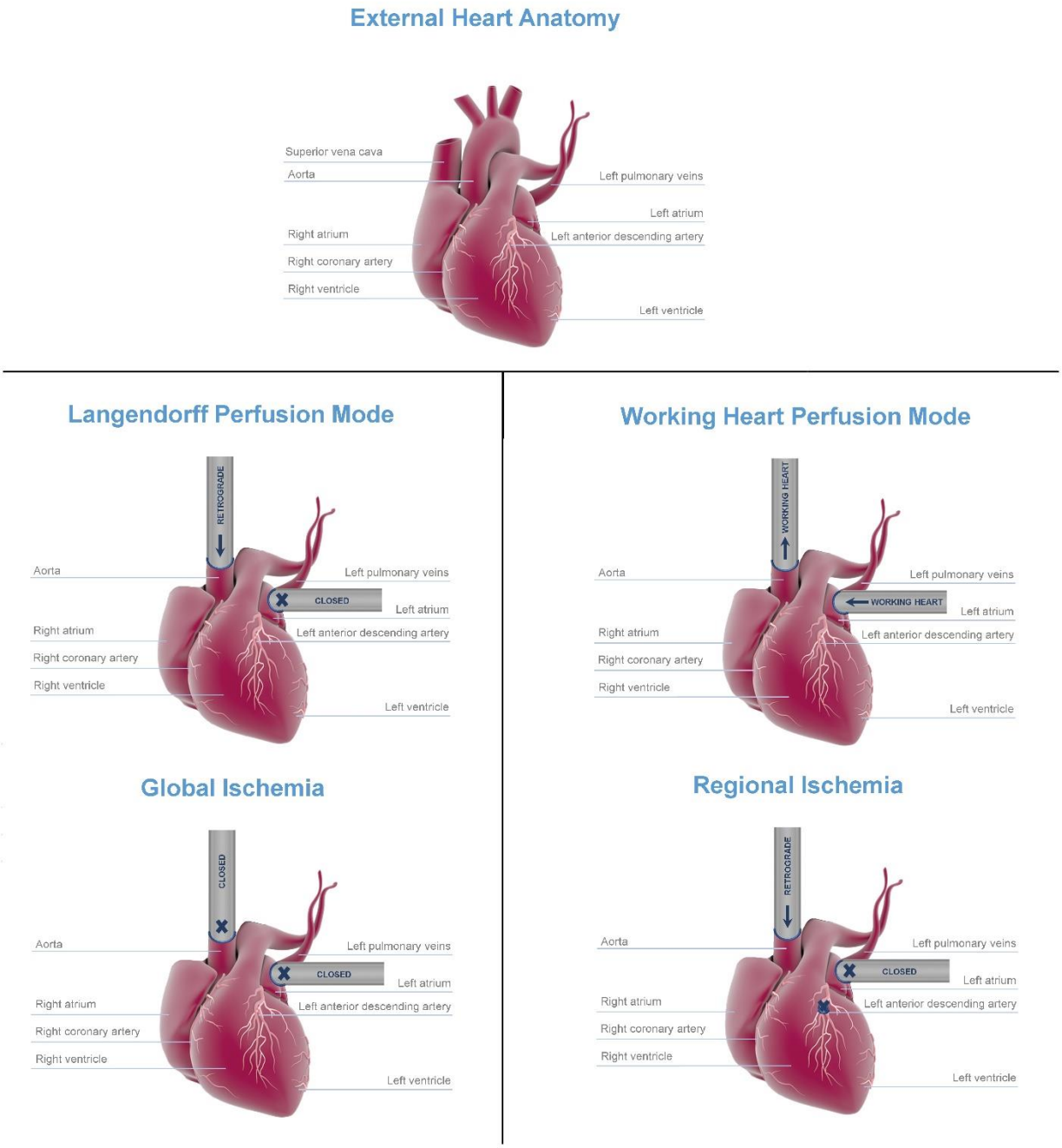

Figure 4.4 Different configurations used between the global- and regional-ischemia protocol.

- *Myocardial Functional Parameters*

Figure 4.3 contains a graphical illustration of different endpoints that were measured during the perfusion protocols. The aortic output (AO) and coronary flow (CF) rates were determined by periodic 10 sec interval fluid collections and multiplied by 6 to attain the rate per minute. Cardiac output (CO) was determined as a measure of AO and CF. The aortic systolic pressure (SysP) and diastolic pressure (DiaP) in mmHg, and heart rate (HR), in beats per minute (bpm), were measured with a Viggo-Spectramed pressure transducer and recorded on a computer running PhysiTutor® software. The total work performance indice (W_T), a measure of the strength of the heart derived from pressure and kinetic power, was determined according to the principles set out by Kannengiesser and colleagues (1979) – simplified, it is calculated multiplying CO with SysP and

then multiplying this total by 0.002222 to get the total power per gram (W/g) of heart tissue. All measurements were performed pre- and post-ischemia at various intervals, and the average of these values used in calculations. Functional recovery was expressed as the post-ischemic value's percentage of the pre-ischemic value.

- *Infarct Size Determination*

Myocardial infarct size was determined as previously demonstrated in our laboratory (Huisamen *et al.*, 2013; Salie *et al.*, 2014; Webster *et al.*, 2017). After the 60 min of reperfusion described above in the regional ischemia protocol, the silk suture was fastened again and 1mL of Evans blue suspension (0.5%) was slowly injected through the aortic cannula. The heart was then removed from the perfusion rig and frozen overnight at -20ºC. At the end of each week, after all perfusions had been performed, the hearts were cut into 2 mm thick slices and stained with 1% w/v triphenyl tetrazolium chloride (TTC) in phosphate buffer (pH 7.4 at 37ºC) for 15 min. To increase the contrast between viable and unstained necrotic regions, the tissue was fixed in 10% v/v formaldehyde solution at ambient temperature. From each heart, 5 ventricular tissue slices were mounted on a double transparent mould and scanned into a computer.

Briefly, the work-flow for infarct size graphical analysis is described in **Figure 4.6** according to the following logic: First, the background was removed from the original image using a magic wand tool from the freeware software paint.net 4.1.1, which enable the selective removal of a colour (or colour shade) as required. This image was then contrast enhanced to more easily define the colour differences. Next, using ImageJ 1.51n, navigating through Image -> Adjust -> Color Theshhold was selected. Colour space was changed to the YUV spectra, where Y is luminance, and U and V are arbitrary abbreviations used denote the x and y axes of chromaticity space. For instance, U-V planes in a range of [-1, 1] will be the following colour ranges for Y-values of 0, 0.5 and 1 respectively shown in **Figure 4.5**.

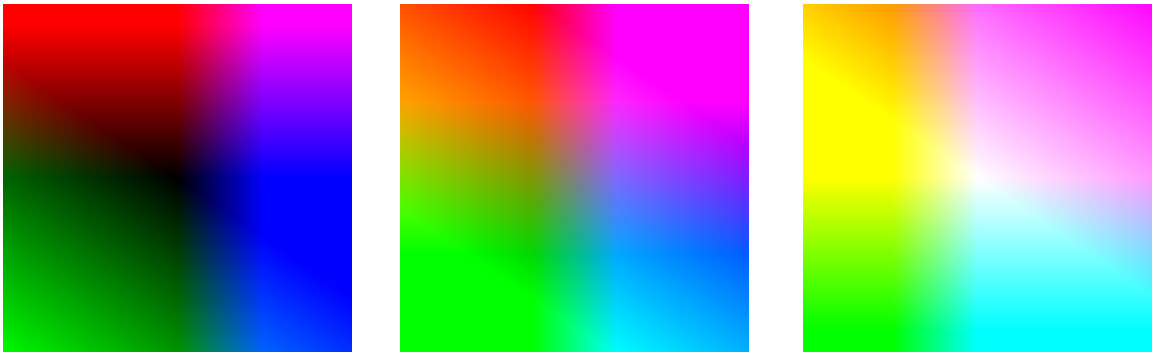

Figure 4.5 Luminance spectra illustration for varying Y = 0, 0.5 and 1.

Using this threshold system, we can select very specific colour ranges and consequently summate each colour group. Black was chosen as the colour threshold indicator (**Figure 4.6**) and the sum of all black pixels counted separately using the image software. These colour ranges were divided into i) viable tissue (blue-ranges), ii) live cells in the area at risk (TTC positive, prominent red-ranges) and iii) non-viable tissue (TTC negative, white, yellow, light-red ranges). The total Area at risk (AAR) constitute of both the infarcted area (non-viable tissue) as well as the surrounding viable red area and are expressed as a % of the total left ventricular volume. The infarct size was calculated as the percentage non-viable tissue to the area at risk.

1) IMAGE AFTER BACKGROUND REMOVAL:

2) IMAGE CONTRAST ENHANCED:

3) THRESHOLD SELECT ("BLACK") FOR VIABLE TISSUE ("BLUE"):

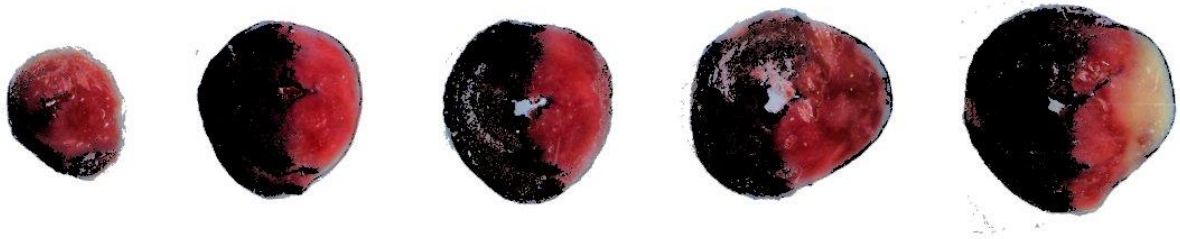

4) THRESHOLD SELECT ("BLACK") FOR VIABLE TISSUE IN AREA AT RISK ("RED"):

5) THRESHOLD SELECT ("BLACK") FOR NON-VIABLE TISSUE ("WHITE"):

Figure 4.6 Infarct size determination work-flow

Table 4. 4 Buffer compositions used in perfusion and isolation protocols

Solution	Composition
KH Buffer (pH = 7.4)	119 mM NaCl, 24.9 mM $NaHCO_3$, 4.7 mM KCl, 1.2 mM KH_2PO_4, 0.59 mM $MgSO_4.7H_2O$, 0.59 mM Na_2SO_4, 1.25 mM $CaCl_2.H_2O$, 10 mM glucose
KE Buffer (pH = 7.4)	180 mM KCl, 10 mM EDTA, pH set with 2M Tris
Lysis Buffer	20 mM Tris-HCL EGTA, 1 mM EDTA, 150 mM NaCl, 1 mM β-glycerophosphate, 2.5 mM tetra-Na^+-pirophosphate, 1 mM Na_3VO_4, 1% Triton X-100, 10 ug/mL leupeptin, 10 ug/mL aprotonin, 50 ug/mL PMSF
Glutamate Media (pH = 7.4)	250 mM sucrose, 10 mM Tris-HCL, 8.5 mM KH_2PO_4, 2 mM malate, 5 mM glutamate
Palmitate Media (pH = 7.4)	250 mM sucrose, 10 mM Tris-HCL, 8.5 mM KH_2PO_4, 2 mM malate, 0.45 mM palmitoyl-L-carnitine

Abbreviations: KH: Krebs-Henseleit bicarbonate, EGTA: ethylene glycol tetraacetic acid, EDTA: ethylenediamine tetraacetic acid, PMSF: phenylmethylsulphonyl fluoride

4.3.3.3 Mitochondrial Function

Mitochondria are dynamic and constantly fusing or dividing, even when isolated (Lackner, 2014; Meeusen *et al.*, 2004). Normally, they form tubular networks (See **Appendix A1**), but once isolated from cells they break up into pieces which will reseal again (Kühlbrandt, 2015). Isolated mitochondria maintain their membrane structure and membrane potential, and thus retain their ability to undergo OxPhos and synthesize ATP (Alexandre *et al.*, 1978). This enable us to investigate mitochondria's functional integrity in isolated mitochondrial fractions obtained from perfused rat hearts.

- *Mitochondrial Isolation*

Following the perfusion protocol described in **Section 4.3.3.2**, hearts were allocated for mitochondrial isolation after 30 min stabilization, 20 min global ischemia, 5 min into reperfusion and after 30 min of reperfusion. The isolation protocol was adapted from the methodology outlined by Lanza & Nair (2009). The hearts were cut just above the atrium using surgical scissors and placed into a 50 mL Sorvall™ tube containing ice-cold KE buffer (**Table 4.4**). The hearts were then further snipped for approximately 20 sec to achieve a size small enough <5mm as to not get stuck in the homogenizer. The supernatant was decanted (with the heavier heart tissue remaining at the bottom of the Sorvall™ tube) and rinsed twice with fresh ice-cold KE buffer. The hearts were then transferred to a 15 mL Sorvall™ tube, half-filled with KE-buffer and homogenized in five 2 sec bursts at 15,000 rpm (Silent Crusher M Polytron, Heidolph Instruments, Germany). The homogenate was transferred to a 50 mL Sorvall™ tube, topped up with KE-buffer, placed in a Sorvall™ SS34 Rotor and centrifuged for 10 min at 2,500 rpm (755g) at 4°C (Sorvall™ RC 6 Plus, Thermofisher Scientific, RSA). The supernatant was then gently decanted into a new 50 mL Sorvall™ tube, and split halfway into another 50 mL Sorvall™ tube, and both centrifuged for 10 min at 12,500 rpm (18,800g) at 4°C. The supernatant from both tubes were discarded and 250 uL KE-buffer added to the pellet of Tube 1 and 200 uL Lysis buffer added to the pellet of Tube 2. The contents of both tubes were separately resuspended using a manual Teflon® pestle and PYREX® Potter-Elvehjem tissue grinder (Corning Inc., USA) and the resuspensions transferred to Epperdorf tubes. 50 uL of resuspension 1 was precipitated in 1 mL 10% trichloroacetic acid (TCA) and refrigerated for subsequent protein

determination using the Lowry assay (described in **Section 4.3.4.6**), while the remaining 200 uL was used to determine mitochondrial OxPhos described below. The contents of resuspension 2 was stored at -80°C till Bradford protein determination (described in **Section 4.3.4.3**) and subsequent Western Blot analysis of mitophagy associated proteins (described in **Section 4.3.4.5**).

- *Mitochondrial Oxidative Phosphorylation*

In a healthy heart, the rate of OxPhos is exclusively linked to the rate of ATP hydrolysis to ensure constant ATP levels even when with varying cardiac power output (Balaban *et al.*, 1986). Mitochondrial OxPhos produces ATP via electrons transferred from NADH and $FADH_2$ generated by dehydrogenation of carbon substrates primarily in FA-β-oxidation, CAC and least of all pyruvate dehydrogenase and glycosis (See **Section 2.2, Figure 2.1**) (Stanley *et al.*, 2005). When measuring OxPhos, mitochondrial O_2 consumption is related to the rate of ATP production and can be inferred in the presence of both ADP-independent and ADP-dependent respiration. Addition of the mitochondria to the FA- or carbohydrate substrate results in baseline respiration independent of ADP called State 2 respiration (S2) (**Figure 4.8**). Addition of ADP to mitochondria causes a rapid increase in O_2 consumption, known as State 3 respiration (S3), and transcribed as a measure of ATP production, known as oxidative phosphorylation rate of State 3 (OxPhos S3) (Lesnefsky *et al.*, 2001). OxPhos S3 is primarily a function of ATP turnover and substrate oxidation, dependent on substrate metabolism, processing and ETC enzymes, whereas inhibiting any of these steps result in attenuated OxPhos S3. As the ATP/ADP ratio equilibrates (ADP depletes), proton re-entry through ATP synthase stops which raises the proton motive force (proton gradient responsible for passively driving ATP synthase) across the inner mitochondrial membrane, in effect slowing down respiration (Brand & Nicholls, 2011). This is known as State 4 respiration (S4), and can also be transcribed to indicate oxidative phosphorylation rate of State 4 (OxPhos S4) (Lesnefsky *et al.*, 2001). The ratio of S4/S3 describes a measure of mitochondrial function known as respiratory control index (RCI). A high RCI indicates a strong capacity of mitrochondria to oxidize substrates and produce ATP with low proton leakage. RCI values are usually dependent on the type of substrates used and the type of mitochondria isolated and therefore no standard range has been defined to indicate mitochondrial dysfunction, however it still remains a valuable to tool to infer relative mitochondrial dysfunction (Brand & Nicholls, 2011). The maximum amount of ATP synthesized per atom of oxygen is given by the parameter ADP/O, or the proton/oxygen ratio. A decrease in this value indicates mitochondrial uncoupling, and therefore a dissipation of the proton gradient driving ATP synthesis, which is also a measure of OxPhos efficiency (Brand & Nicholls, 2011).

To determine the OxPhos potential of mitochondria, a polarographic measure of mitochondrial respiration was carried out using a Clark-type oxygen electrode oxygraph (Hansatech Instruments Ltd., UK) set up in advance (**Figure 4.7**), as previously described (Boudina *et al.*, 2005). A drop of 50% KCl was placed on the electrodes and a small oxygen-permeable membrane fitted into place on top of it and secured with a rubber O-ring by means of an applicator shaft. A slightly bigger rubber O-ring was used to seal the electrode disk into the oxygen electrode chamber and the entire assembly fastened with a lockring. The oxygraph system was continuously temperature regulated at 25 °C using an external water bath, and all the electrode readings relayed to a computer running Oxygraph+ software (Hansatech Instruments Ltd., UK). In the current study two oxygraph systems were ran simultaneously to compare the mitochondrial OxPhos rates of carbohydrate substrate utilization vs FA substrate utilization. The first chamber represented a carbohydrate-rich environment and

made use of a Glutamate Medium and the second chamber a FA-rich environment consisting of a Palmitate Medium (See **Table 4.4** for compositions). First, both chambers were filled with distilled H_2O (25 °C) and a magnetic stirrer (Speed: 100) and calibrated to ambient oxygen (100%) and 0% oxygen by addition of sodium dithionite (BDH Chemicals (Pty) Ltd., UK) to allow the software to be zeroed when oxygen levels dropped to levels where insignificant fluctuations were recorded. The chambers were then rinsed with distilled H_2O 5 times and filled with either 650 uL Glutamate Medium or Palmitate Medium and given sufficient time to reach 100% ambient oxygen levels and the set temperature before commencing with experimentation. 100 uL of isolated mitochondria suspension in KE-buffer was added to each incubation medium and the chamber sealed with a plunger adaptor. Once a steady-state respiration rate was obtained (in presence of substrate but absence of ADP), 50 uL ADP (0.35 uM ADP) was injected into the chamber using an air-tight syringe (Hamilton Company, USA) to commence S3 (**Figure 4.8**). Once all the ADP was converted to ATP, S4 respiration commenced which is characterized by a slow-down in respiration (in the presence of substrate and ATP). Following a steady-state S4 period of approximately 30 sec, 50 uL of 10X ADP concentration (3.5 uM ADP) was injected into the chamber to saturate ATP production using oxygen as substrate – leading to a gradual depletion of all O_2 levels. Once a steady-state zero oxygen was reached, a 20-min anoxia period was ushered in. After this, oxygen was manually reintroduced into the chambers by using a plastic Pasteur pipette, and S5 attained. From the oxygraph data, together with the protein concentration determined for each sample, we can determine the parameters set out in **Figure 4.8.**

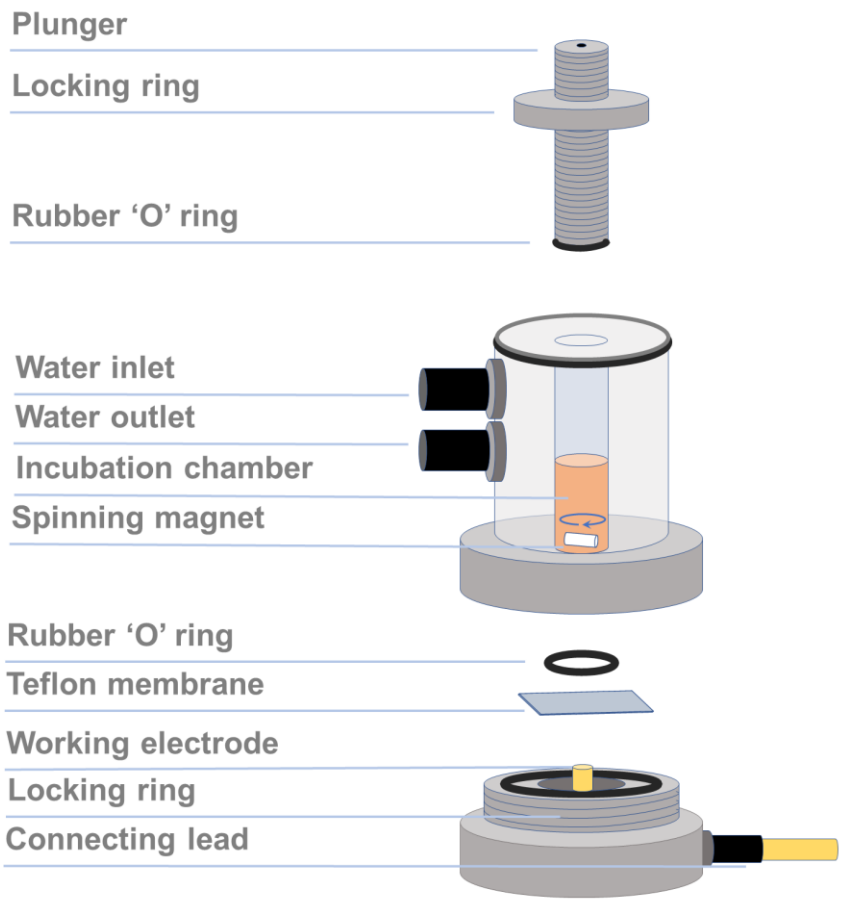

Figure 4.7 Oxygraph assembly

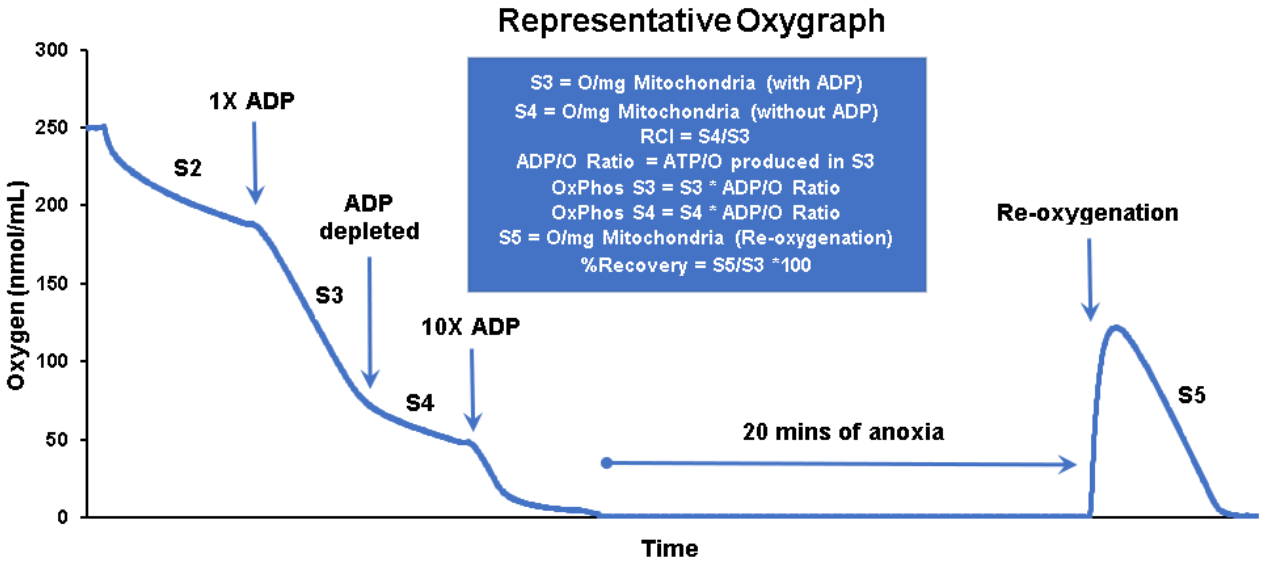

Figure 4.8 Representative oxygraph

4.3.4 Protein Laboratory

Insulin ELISA and Westerm blot analysis were conducted under the auspices of the Cardiovascular Research Group housed in the Protein Laboratory, Division of Medical Physiology, Faculty of Medicine and Health Sciences, Stellenbosch University.

4.3.4.1 Insulin assay

Insulin levels were determined in the fasting state and the homeostasis model assessment for insulin resistance (HOMA-IR) values calculated as index of glucose homeostasis, insulin resistance and β cell function (Antunes *et al.*, 2016). Rat insulin was determined from fasting blood using a rat insulin ELISA kit (RayBiotech Inc., USA). This assay consisted of a 96-well microplate coated with rat insulin-specific antibody, a wash buffer, rat insulin used in establishing a standard curve, biotinylated anti-rat insulin, HRP-conjugated streptavidin (secondary antibody), 3,3,5,5'-tetramethylbenzidine (TMB), 0.2 M sulfuric acid and diluent buffer.

All reagents and blood serum samples were used at room temperature (18 – 25°C), while all standards and samples were analyzed in duplicate. Standards were diluted in series to obtain the following concentrations: 4.69 µIU/mL, 9.38 µIU/mL, 18.75 µIU/mL, 37.5 µIU/mL, 75 µIU/mL, 150 µIU/mL, 300 µIU/mL and 1400 µIU/mL. Diluent buffer from the kit (composition unknown – usually a combination of phosphosaline, EDTA, sodium-(Na)-azide and BSA) was simply used as a blank. All samples were diluted 2-fold with the diluent buffer. First, 100 µL of each sample, standard and blank was loaded in duplicate into the 96-well plate and then slowly agitated at room temperature for 2.5 h. The solution was discarded and each well washed 4X with 300 µL Wash buffer using a multi-channel pipette (Discovery Comfort, PZ HTL S.A., Poland). The remaining liquid in each well was carefully aspirated using a glass Pasteur pipette coupled to a vacuum. The plate was then inverted and blotted dry on paper towel. Next, 100 µL of biotinylated antibody was added to each well, to act as a precursor for the secondary antibody to bind to, and gently agitated for 1 h at room temperature. The solution was once again discarded and washed 4X with wash buffer and blotted dry. Afterwards, 100 µL of HRP-conjugated streptavidin was added to each well and gently agitated for 45 min at room temperature, followed by discarding the solution, washing 4X with wash buffer and then blotting dry. Subsequently, 100 uL

TMB One-Step Substrate Reagent was added to each well and incubated for 30 min at room temperature at 30 rpms in a darkened Incu-Shaker Mini (Benchmark Scientific Inc., USA). Finally, 50 µL Stop Solution was pipetted into each well. This sulphuric acid solution changed the blue colour to a yellow colour. The intensity of the colour was immediately measured within 5 min on the microplate reader at 450 nm. A standard curve was set up by plotting the Y-absorbance at 450 nm with standard rat insulin concentrations on the X-axis and used to determine the insulin concentrations of unknown serum samples. The homeostasis model assessment for insulin resistance (HOMA-IR) index was calculated using the HOMA2 Calculator 2.2.3 software (Oxford University, UK), which calculates the product of fasting glucose concentration (mmol/L) multiplied by the fasting insulin concentration (µIU/mL) divided by 22.5 (HOMA-IR = [fasting glucose concentration X fasting insulin concentration]/22.5), as well as the product of 20 times insulin concentration divided by 3.5 units less than the fasting glucose concentration (HOMA-%B = [20 × fasting insulin concentration]/[fasting glucose concentration − 3.5]), which corrects for beta cell function (Levy *et al.*, 1998).

4.3.4.2 Tissue Homogenisation

Small sections of freeze-clamped heart ventricular tissue (~5x5 mm) were chipped off and pulverized using a liquid nitrogen pre-cooled mortar and pestle. Next, 70 mg of pulverized powder was homogenized and lysed in Lysis buffer (**Table 4.5**) containing 6 stainless-steel 1.66 mm diameter beads, using a Bullet Blender® (Next Advance Inc., USA) at 4 °C for three one-minute cycles at Speed 8, and 5 min of rest inbetween each cycle. The homogenized samples were rested for an additional 20 min at 4 °C, followed by centrifugation at 15,000 rpm (12,074g) for 20 min at 4 °C (Sigma 1-14K Refrigerated Microfuge, Lasec SA (Pty) Ltd., RSA). The supernatant was then used in subsequent Bradford protein determination.

4.3.4.3 Bradford Protein Determination

The Bradford protein determination method was used to determine the protein content of heart tissue and mitochondrial lysates (Bradford, 1976). Just prior to protein determination, the BSA stock (5 mg/mL) was diluted 1:5 times with dH_2O and then serially diluted into duplicate test tubes to generate concentrations between 1 and 30 µg in a volume of 100 µL. 5 µL supernatant of the samples generated in the above experiments, was diluted 1:10 with dH_2O to dilute all detergents that may interfere with the assay. The diluted samples were then further diluted 1:20 in test tubes to reach a volume of 100 uL. All standards and samples received 900 µL of double filtered Bradford reagent (diluted 1:5 with H_2O) (**Table 4.5**), vortexed and incubated for 30 min at room temperature. The absorbance values were measured using a spectrophotometer (Spectronic® 20 Genesys™ Spectrophotometer, Thermo Fisher Scientific Inc., RSA) at 595 nm and the protein content of the samples determined from the standard curve plotted. Hereafter, the protein concentration for each sample was calculated and proceeded to lysate preparation.

4.3.4.4 Lysate Preparation for Western Blotting

Lysis buffer was added to the appropriate amount of supernatant to obtain protein concentrations of 50 µg/12 µl final solution. Finally, a mix of 850 µl 1:2 Laemmli sample buffer (**Table 4.5**) with 150 µl mercaptoethanol was made and added to the samples in a volume equal to half of the lysis buffer and sample buffer. The samples were boiled for 5 min at 100°C and stored at -80 °C for future analysis by Western blotting.

Table 4.5 Buffer and gel compositions used in western blot protocol

Solution	Composition
Lysis Buffer	20 mM Tris-HCl, 1 mM EGTA, 1 mM EDTA, 150 mM NaCl, 1 mM β-glycerophosphate, 2.5 mM tetra-Na^+-pirophosphate, 1 mM Na_3VO_4, 1% Triton X-100, 10 μg/ml Leupeptin, 10 μg/ml Aprotinin, 50 μg/ml PMSF
Laemmli Sample Buffer	62.5 mM Tris-HCl (pH 6.8), 4% SDS, 10% glycerol, 0.03% bromophenol blue, 5% β-mercaptoethanol
Bradford Reagent	100 mg Coomassie Brilliant Blue G-250, 50 ml 95% Ethanol, 100 ml 85% (w/v) Phosphoric Acid, 850 ml dH_2O
Running Buffer	25 mM Tris-HCl,192mM Glycine, 0.1% SDS (made up with dH_2O)
Transfer Buffer	25 mM Tris, 192 mM glycine and 20% (v/v) methanol
Transfer Buffer (ATM)	25 mM Tris, 192 mM glycine and 10% (v/v) methanol
TBS-Tween Buffer (pH 7.6)	20 mM Tris-HCl, 137 mM NaCl, 0.1% Tween-20 (diluted with dH_2O)
Ponceau Red	5 mL acetic acid, 0.5 g ponceau S/ 100 mL dH_2O

4.3.4.5 Western Blot Analysis

Loading and separation of proteins

In the present study, we made use of either 26-well Criterion™ Tris-Tricine Precast gradient (4-15%) Gels or 26-well Criterion™ TGX Stain-Free™ Precast gradient (4-15%) Gels (Bio-Rad Laboratories Inc., USA). The gels were placed in a Mini-PROTEAN® Tetra System (Bio-Rad Laboratories Inc., USA) and filled with Running Buffer (**Table 4.5**). After boiling the lysates for 5 min, 12 μL (50 μg) of each sample was loaded onto the gel. The first and last lane position on each gel was loaded with 5μL PageRuler™ Prestained Protein Ladder (Fermentas Life Sciences, RSA) for proteins of interest smaller than 100 kDa, whereas 7.5 μL HiMark™ Pre-Stained Protein Standard (Thermo Fisher Scientific Inc., RSA) for proteins of interest larger than 100 kDa, to aid with determination of molecular weights of specific bands. The second and third lane was loaded with 30 min stabilized young controls hearts (for interest sake), the fourth and fifth 30 min stabilized control samples, and subsequent lanes contained treated groups. Proteins were then separated using the principle of sodiumdodecyl sulphate polyacrylamide gel electrophoresis (SDS-PAGE). Gels were run for 10 min at 200 V and set current, followed by 50-80 min (depending on definition required) at set 140 V and set current, in Running Buffer (**Table 4.5**).

Protein transfer and visualization

Following SDS-PAGE, proteins of interest <100 kDa were electrotransfered to polyvinylidene fluoride (PVDF) membranes, using a Mini Trans-Blot® Cell Transfer System (Bio-Rad Laboratories Inc., USA) for 60 min at 200 mA and set volts, or proteins >100 kDa for 90 min at 200 mA and set volts and packing the Transfer System with icepacks to prevent overheating of the transfer sandwich and denaturing of proteins. The membranes were then Stain-Free activated and visualized with the ChemiDoc™ MP System using ImageLab Software 5.0 (Bio-Rad Laboratories Inc., USA), and images stored for later use in normalization of samples.

Membranes transferred from the 26-well Criterion™ Tris-Tricine Precast Gels were first reversibly stained with Ponceau Red (**Table 4.5**) and then imaged for later normalization. After washing of the membranes with TBS-Tween Buffer (**Table 4.5**), the membranes were blocked in TBS-Tween Buffer with 5% (w/v) fat-free dry milk, while gently agitating for 2 hours at room temprature. The membranes were then 3 times washed with TBS-Tween Buffer for 5 min, followed by incubation overnight at 4°C with primary antibody, according to dilutions set out in **Table 4.6**. The membranes were again washed 3 times with TBS-Tween Buffer for 5 min, followed by agitation for 1 hour with secondary anti rabbit immunoglobulin G (IgG) horseradish peroxidase (HRP) linked whole antibody (Amersham Biosciences, UK, and Dako Cytomation, Denmark) diluted either in 7.5mL TBS-Tween Buffer, 7.5 mL 5% Milk-TBS-Tween or 7.5 mL SignalBoost™ Immunoreaction Enhancer Kit (Calbiochem®) (**Table 4.6**) at room temperature. Following secondary antibody incubation, membranes were washed again with TBS-Tween Buffer and then visualized using Clarity Western ECL Substrate for 5 min and exposed with the Bio-Rad Chemidoc MP Imager for a specific time depending on the antibody used (**Table 4.6**). The optical density readings of each band was expressed relative to the average of the two stabilized controls present in lane 4 and 5 (as the first proteins are notorious for becoming smudged due to the lack of integrity/support from the open lane used for the ladder). **Appendix A6, Figure A3** contains a western blot work-flow illustrating protein content on the stain-free gels/membrane and how they were used to normalize. All visualizations and quantification of protein bands on membranes were analyzed using Image Lab 5.0 (Bio-Rad Laboratories).

4.3.4.6 Lowry Protein determination

The refrigerated tubes containing 50 uL of resuspension 1 precipitated in 1 mL 10% (TCA) (described in **Section 4.3.3.3**) were centrifuged at 3,000 rpm for 10 min at 4 °C (Heraeus™ Megafuge™ 16 Centrifuge Series) and the supernatant decanted. Tubes were set to dry out upside down (pellet precipitated at the bottom of the tube) on a paper towel for 30 min and excess TCA still present removed with a cotton swab. 500 uL 1N NaOH was aliquoted into each tube and the protein dissolved at 45 °C in warm bath for 5 min. Once dissolved, 500 uL dH2O was added to each tube, leaving a protein concentration suspended in 0.5 N NaOH effectively and the tube vortexed. To determine the protein concentration of mitochondrial samples, 50 µl protein sample, 3 BSA concentrations (0.161, 0.322 and 0.644 mg/ml 0.5 N NaOH), used as standards and 0.5 N NaOH (used as blank) was pipetted into Lucham tubes in triplicates. 1ml reaction buffer, containing 2% Na_2CO_3, 1% $CuSO_4 \bullet 5H_20$ and 2% Na^+K^+-Tartrate, was added to each tube, vortexed and incubated at room temperature for 10 min. Hereafter, 0.1 ml of a 1:3 dH_20 diluted Folin Ciocalteus reagent was added to each tube, vortexed and incubated for 30 min after which OD values were determined using a spectrophotometer (Spectronic® 20 Genesys™ Spectrophotometer, Thermo Fisher Scientific Inc., RSA) at 750 nm. A standard curve was produced and the protein content of the samples determined.

Under alkaline conditions, cupric ions (Cu^{2+}) chelate with the peptide bonds of a protein resulting in a reduction of cupric ions (Cu^{2+}) to cuprous ions (Cu^+). Addition of reagents such as Folin Ciocalteu (phosphomolybdic-phosphotungstic acid) with the Cu^+ creates chromogens that give a colour reaction resulting in an increased absorbance between 550 nm and 750 nm. Absorbance at the peak wavelength of 750 nm quantitate protein concentrations between 1-100 mg/ml, whereas 550 nm is more suitable for quantifying higher protein concentrations (Sengupta & Chattopadhyay, 1993). The amount of colour produced can be readily detected and is proportional to the amount of peptide bonds, and thus an indication of the amount of protein.

Table 4.6 Optimized protocol for each primary and secondary antibody

Proteins	MW (kDa)	Protein Loaded (ug)	1st Antibody Preparation		2nd Antibody Preparation		Time Exposed
			Dilution Factor	% Milk	Dilution Factor	% Milk	
Cytocolic Proteins							
Insulin-dependent Metabolic Regulator							
PKB	60	50	1:1000	0%	1:4000	0%	20s
Insulin-Independent Metabolic Regulator							
AMPKα	62	50	1:1000	0%	1:4000	0%	40s
AS160	160	50	1:1000	0%	1:4000	0%	70s
RISK Pathway							
ERK1	44	50	1:1000	0%	1:4000	0%	20s
ERK2	42	50	1:1000	0%	1:4000	0%	20s
Stress-Marker							
JNK1	46	50	1:1000	0%	1:4000	0%	20s
JNK2	54	50	1:1000	0%	1:4000	0%	20s
Inflammation							
p38	43	50	1:1000	0%	1:4000	0%	20s
Autophagy Marker							
LC3-I	18	50	1:1000	0%	1:4000	0%	10s
LC3-II	16	50	1:1000	0%	1:4000	0%	10s
Auxiliary Metabolic Regulation							
GSK3β	46	50	1:1000	0%	1:4000	0%	20s
ATM	350	50	1:1000	Signal Boost™	1:4000	Signal Boost™	80s
Mitochondrial Proteins							
Mitophagy							
PINK1	63	50	1:1000	0%	1:4000	5%	300s
Parkin	52	50	1:1000	0%	1:4000	5%	180s
p62	62	50	1:1000	0%	1:4000	0%	160s
BNIP3	30	50	1:1000	0%	1:4000	0%	300s
LC3-II	62	50	1:1000	0%	1:4000	0%	10s

Calbiochem® SignalBoost™ Immunoreaction Enhancer Kit (Sigma-Aldrich Life Sciences, USA)

4.3.5 External Analysis

4.3.5.1 Total Lipid Fatty Acid Composition

The rat serum total lipid fatty acid composition was determined by means of gas-liquid chromatograpgy (GC) performed under supervision of Prof. Paul van Jaarsveld at the Non-Communicable Diseases Research Unit of the South African Medical Research Council.

Briefly, total lipids were extracted from serum obtained from the fasted rats, described in **Section 4.3.2.6**, using chloroform:methanol (2:1, vol:vol, containing 0.01% butylated hydroxytoluene) extraction in a modified Folch *et al.* (1957) method as described by Hon and colleagues (2009). Lipid extracts were concentrated till dry and the fatty acid of the lipids transesterefied using trans-methylation with methanol: sulphuric acid (95:5, vol:vol) at 70 °C for 2 hours to yield fatty acid methyl esters (FAMEs). The FAMES were then extracted with water and hexane, and the hexane layer evaporated until dry, before resuspended in a small volume of hexane and analysed by GC on a Finnigan Focus Gas Chromatograph equipped with flame ionisation detection (Thermo Electron Corporation, USA) and a 30m capillary column of 0.32 mm internal diameter; BPX70 0.25 um (SGE International Pty, Australia) as described by (Chimhashu *et al.*, 2018). The sample FAMEs were identified according to retention times compared to the standard FAME mixture (27 FAMEs, NuChek Prep Inc., USA). Relative percentages of FAs were calculated by taking the AUC of a given FAME as percentage of the total area count of all FAs identified in the sample.

4.3.6 Graphical Illustrations

All of the figures used in this dissertation were self-illustrated in Powerpoint 365 (Microsoft Inc., USA) with the help of stock images obtained from http://www.somersault1824.com/resources/. These images are freeware and no copyrights are attached to the use thereof.

4.3.7 Statistical Analysis

Unless stated otherwise, all results are presented as the means ± standard error of the mean (SEM). For comparative studies, statistical analysis was done with a one-way analysis of variance (ANOVA) for multiple comparisons followed by Bonferroni post-hoc test (for $p<0.05$) (marked in black on all graphs) or as an additional test, Student's t-test (unpaired) (for $p<0.05$ taken as significant, and $p<0.10$ indicated as points of interest for potential future research) (indicated in grey on all graphs) using GraphPad Prism 7 (Graphpad Software Inc., USA). $P<0.05$ was considered as significant.

CHAPTER 5

RESULTS

5.1 CHARACTERISTICS OF DIET MODEL WITH AFRIPLEX GREEN ROOIBOS EXTRACT

5.1.1 Body Weight

Figure 5.1 shows the average increase in body weight over the 16 weeks of feeding, with week 17 being the week of sacrifice. At the start of the treatment in week 11, HCD rats did not weigh significantly more than control rats (335.8±6.3 g; n=147 vs. 326.2±4.7 g; n=146). However, at the end of the study (week 17), control rats averaged 373.6±4.8 g (n=74) and HCD animals 403.9±5.1 g (n=74), having gained 65.63±2.97 g (n=74) vs. the 45.22±2.80 g (n=74) in the treatment span of 6 weeks, equating to a 45.1% increase in weight gain for the same duration. HCD resulted in an average higher body weight of 30.3 g or 8.1% ($p < 0.001$). From **Figure 5.2 (**and **Table 5.1)**, GRT supplementation did not significantly influence weight gain in the control rats (382.7±5.5 g; n=72), however the final weight of HCD animals supplemented with GRT was significantly increased (423.9±6.0 g; n=73), equating to an average gain of 20 g or 5.0% body weight ($p<0.05$).

- ***Average Weekly Body Weight Per Rat***

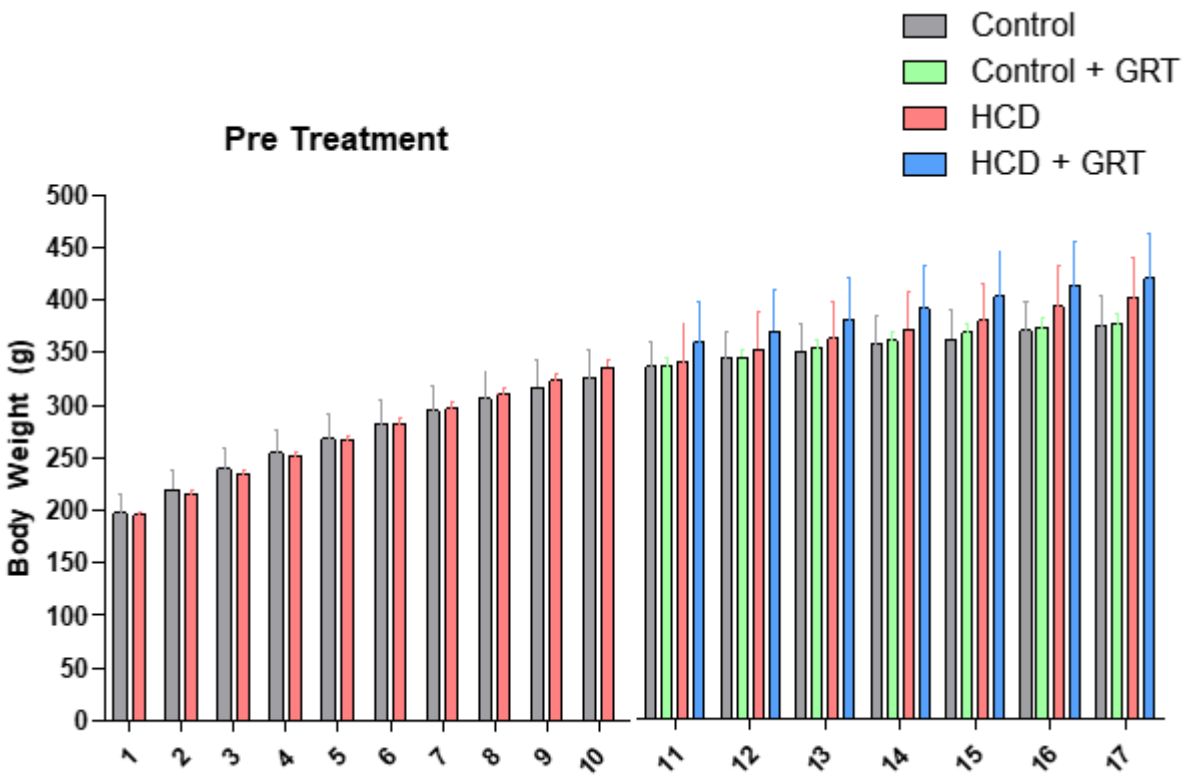

Figure 5.1 Average body weight per week before-, during treatment and at the time of sacrifice

- ***Body Weight of Different Treatment Groups at 16 Weeks***

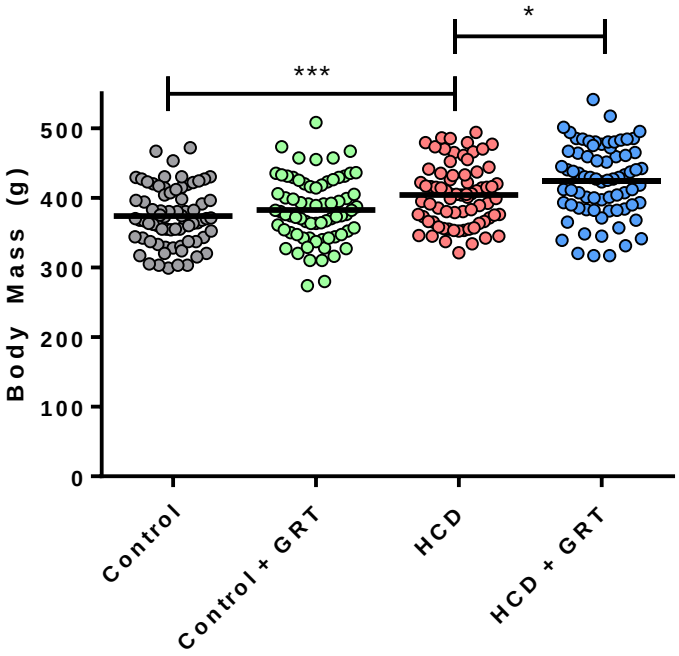

Figure 5.2 Scatterplot of body weight for each rat at the time of sacrifice (17th week of diet). ***p<0.001 (Control vs HCD), *p<0.05 (HCD vs HCD + GRT).

5.1.2 Intraperitoneal Fat

Intraperitoneal fat was dissected at the time of sacrifice. From **Figure 5.3** (and **Table 5.1**), HCD rats had significantly more intraperitoneal fat, 23.69±0.89 g or 5.79±0.18% of BW (n=73), compared to controls, 13.98±0.43 g or 3.74±0.10% of BW (n=73), equating to a 41.0% increase in intraperitoneal fat. Supplementation with GRT did not significantly increase intraperitoneal fat in controls (13.71±0.55 g or 3.54±0.12% of BW; n=72) but did approach a significant increase in HCD (26.50±1.19 g or 6.11±0.21% of BW; n=73; p=0.0595).

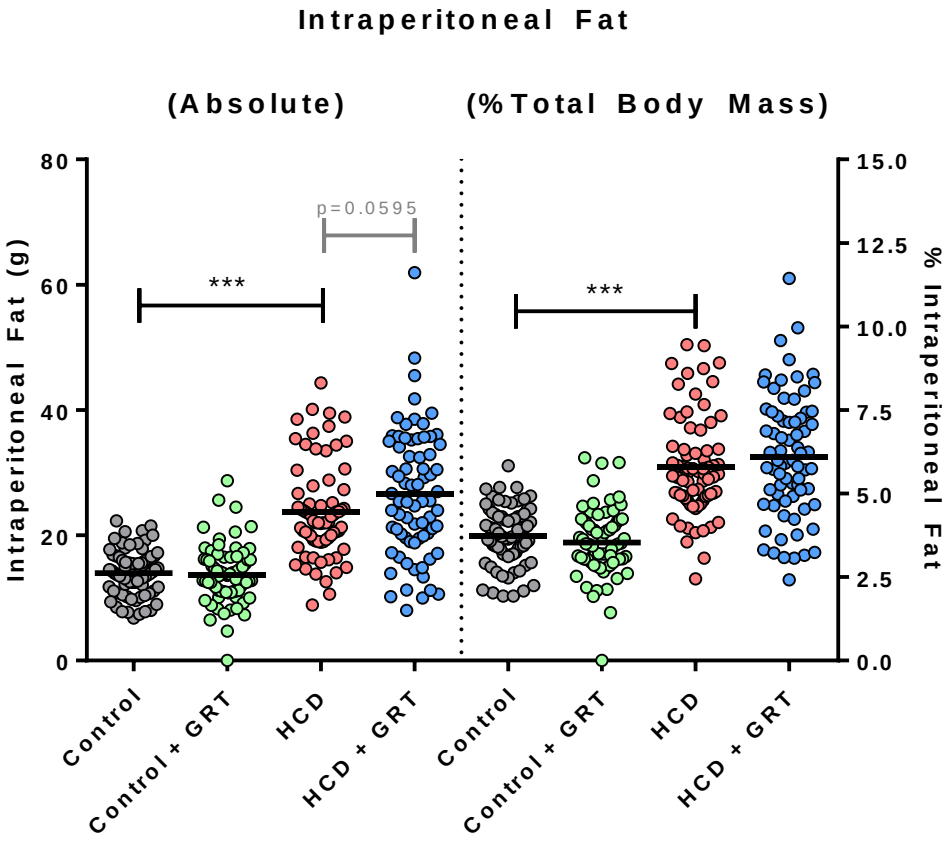

Figure 5.3 Absolute intraperitoneal fat and percentage intraperitoneal fat of total body weight

5.1.3 Food Consumption

Food intake of selected groups of animals was monitored daily (and divided by the number of rats per cage to obtain individual food consumption) from the start of the diet until the week of sacrifice. **Figure 5.4** shows a scatterplot of the average derived food consumption per rat for selected cages monitored. HCD animals consistently ate more food daily (23.41±0.52 g; n=40) than the control chow diet animals (17.62±0.36 g; n=40) in the first 10 weeks (**Figure 5.5, Table 5.1**). Furthermore, during the 6-week treatment period, the HCD animals still ate significantly more food daily (21.10±0.92 g; n=20) compared to the control group (17.76±0.44 g; n=20). The addition of GRT did not significantly influence daily food intake compared to their untreated groups in either the control rats (17.10±0.47 g; n=20) or the HCD counterparts (23.80±0.96 g; n=20).

- ***Average Daily Food Consumption Per Rat***

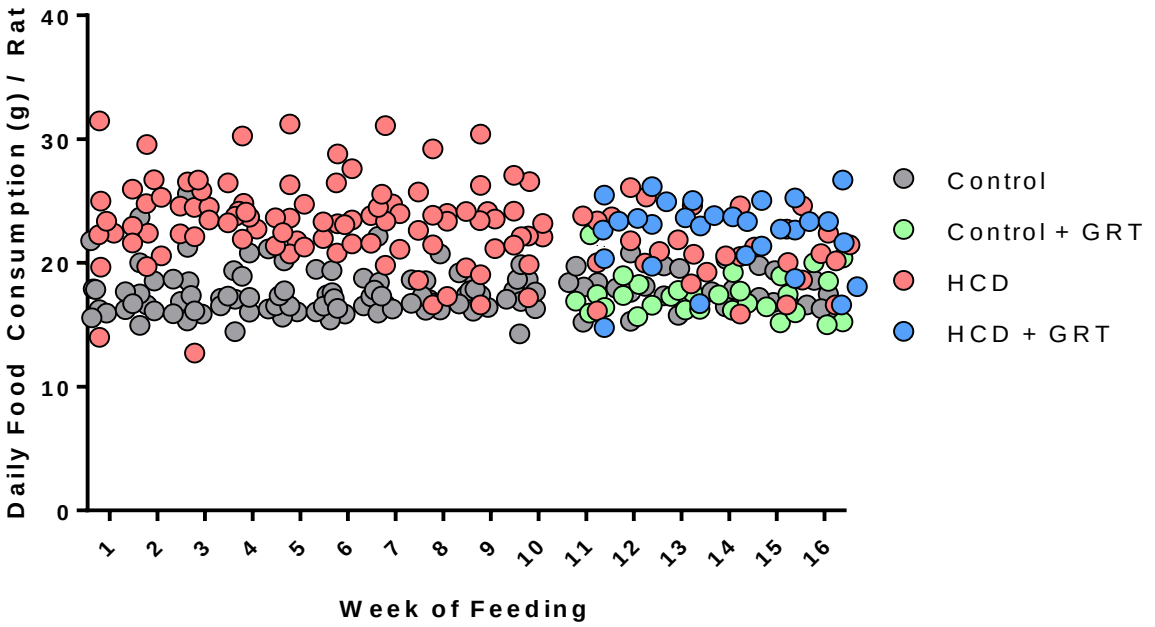

Figure 5.4 Scatterplot showing the distribution of average daily food intake per rat for each cage monitored.

- ***Average Daily Food Consumption Before and After Treatment***

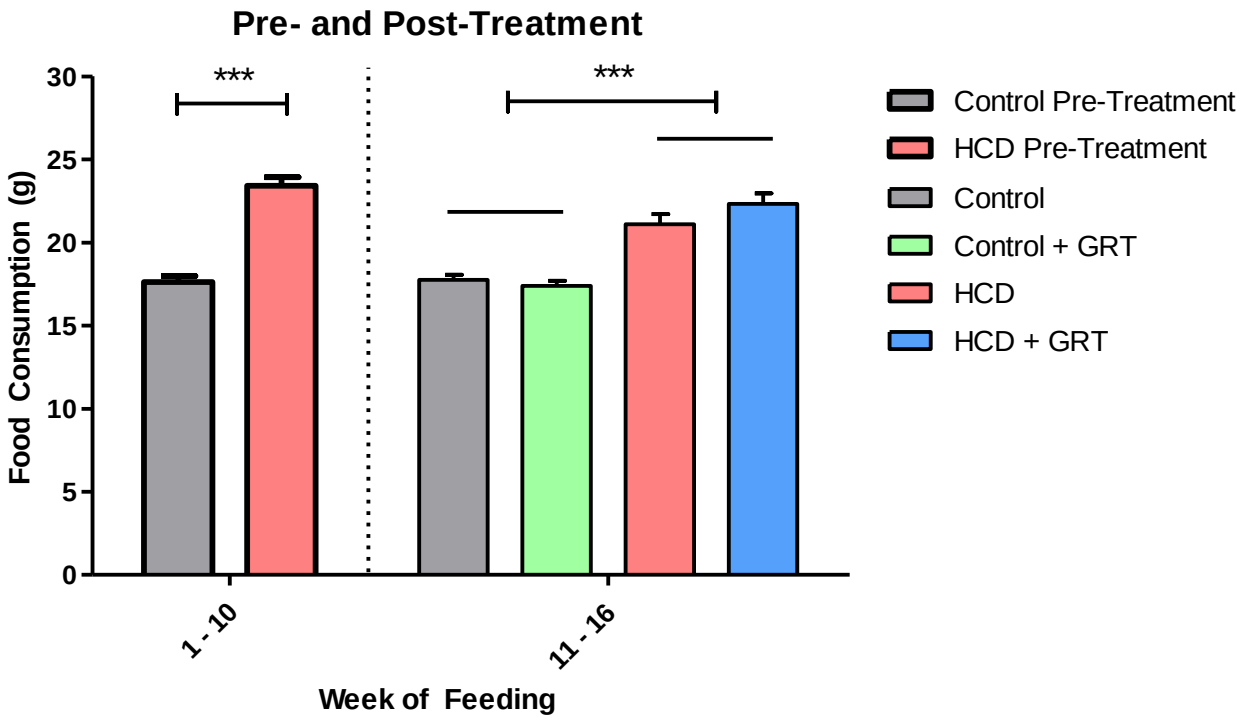

Figure 5.5 Average Daily Food Consumption Per Rat Grouped into Pre-Treatment (Week 1 – 10) and With-Treatment (Week 11-16). ***p<0.001 (Control vs HCD at 10 Weeks; Control +/- GRT vs HCD +/- GRT at 16 weeks).

5.1.4 Water Consumption

Water intake of selected cages was monitored daily (and divided by the number of rats per cage to obtain individual water consumption) from the start of the diet until the week of sacrifice. **Figure 5.6** shows a scatterplot of the average derived water intake per rat for each individual cage monitored. HCD animals consistently drank less water daily (19.85±0.64 mL; n=40) compared to control animals (29.09±0.90 mL; n=40) in the first 10 weeks (**Figure 5.7, Table 5.1**). During the 6-week treatment period, the HCD animals still drank significantly less water daily (20.25±0.76 mL; n=20) compared to the control group (29.76±0.88 mL; n=20). The addition of GRT did not influence daily water intake compared to their untreated counterparts in either the control rats (28.76±0.48 mL; n=20) or the HCD treated groups (19.60±0.60 mL; n=20).

- ***Average Daily Water Consumption Per Rat***

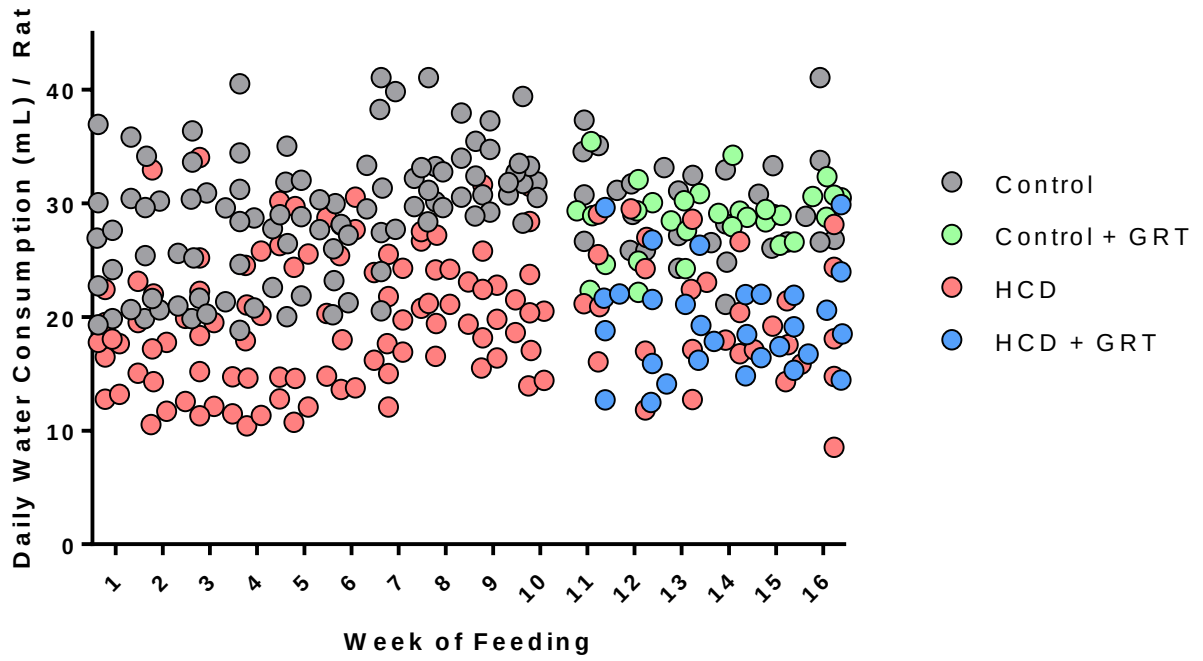

Figure 5.6 Scatterplot showing the average daily water intake per rat for each cage monitored

- ***Average Daily Water Consumption Before and After Treatment***

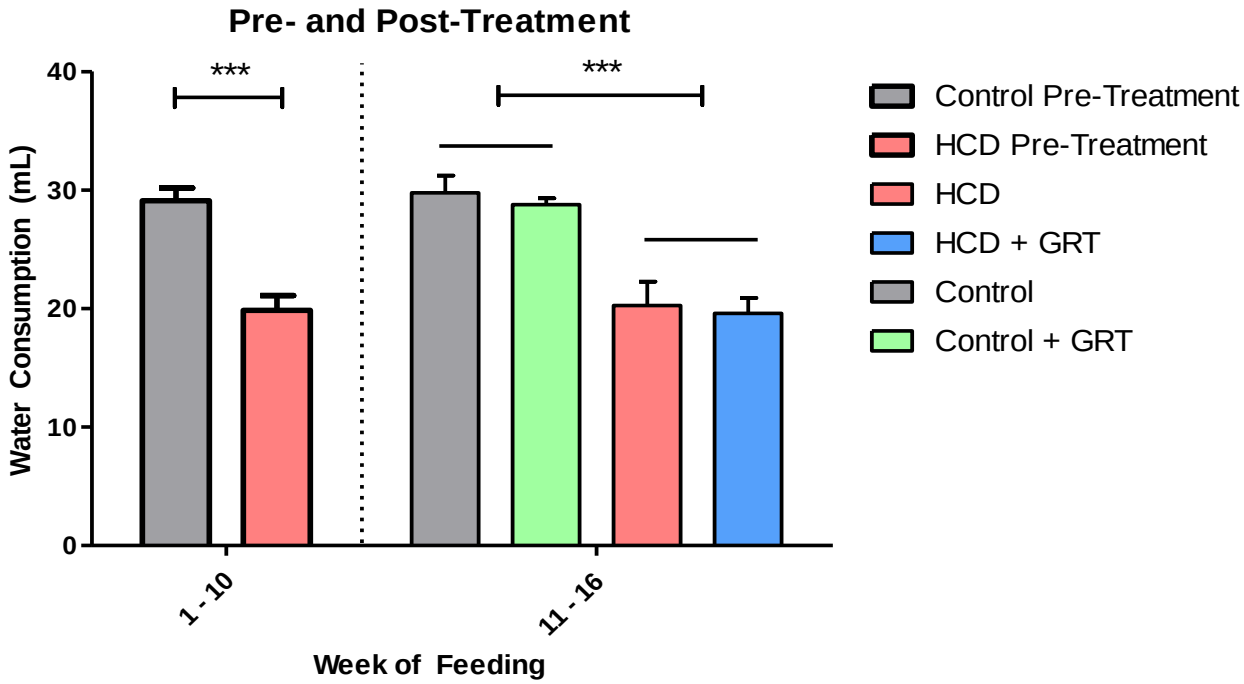

Figure 5.7 Average daily water consumption grouped into pre-treatment (week 1 – 10) and with-treatment (week 11-16). ***p<0.001 (Control vs HCD at 10 Weeks; Control vs HCD, Control +/- GRT vs HCD +/- GRT at 16 weeks).

5.1.5 Non-Fasting Blood Glucose Levels

Non-fasting blood glucose levels were obtained just prior to sacrificing rats. Control rats had an average blood glucose level of 6.88±0.11 mmol/L (n=63), control with GRT 6.78±0.12 mmol/L (n=62), HCD rats 7.78±0.14 mmol/L (n=65), and HCD with GRT 7.54±0.13 mmol/L (n=64). Non-fasting blood glucose levels were 13.1% higher in HCD rats compared to control rats ($p<0.001$), and supplementation with GRT did not significantly reduce the 11.2% higher blood glucose levels of HCD rats receiving GRT compared to their control counterparts. (**Figure 5.8, Table 5.1**).

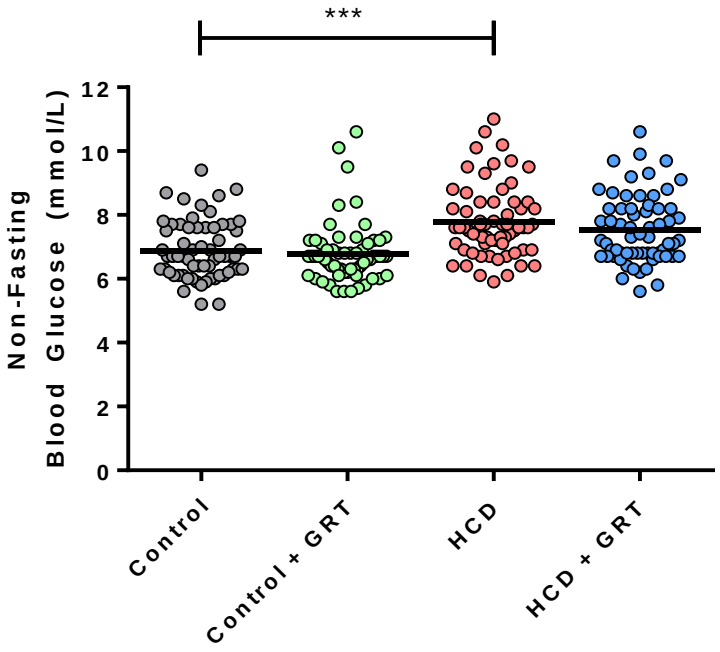

Figure 5.8 Non-Fasting blood glucose levels taken at time of sacrifice (Week 17)

5.1.6 Fasting Blood Glucose and Oral Glucose Tolerance Test

To test for initial whole-body insulin resistance after 10 weeks of HCD, an OGTT was performed (**Figure 5.9**). Following overnight fasting, HCD rats had elevated basal blood glucose levels compared to the controls (5.63±0.15 (n=26) vs 5.16±0.10 mM (n=26); $p<0.05$) (**Table 5.1**). After an oral gavage, the blood glucose levels of HCD rats remained significantly elevated for up to 45 min (6.89±0.14 (n=26) compared to controls (6.37±0.14 (n=26) mM; $p<0.05$). AUC analysis of each individual OGTT for both groups also revealed significantly increased AUC in HCD compared to the control counterparts (771.8±13.6 (n=26) vs. 715.1±10.6 (n=26; $p<0.01$). At 16 weeks, fasting blood glucose levels remained elevated in HCD rats compared to controls (5.75±0.16 (n=12) vs 5.21±0.16 mM (n=12); $p<0.05$) (**Table 5.1**). After an oral gavage, the blood glucose levels of HCD rats remained significantly elevated for up to 60 min (6.81±0.32 (n=12) vs controls, 5.92±0.18 (n=12) mM; $p<0.05$) (**Figure 5.10**). Furthermore, AUC analysis of each individual OGTT for each group, revealed significantly increased AUC in HCD and HCD with GRT compared to the control counterparts ($p<0.05$ for both) (793.3±19.20; n=12 and 849.0±24.90; n=12 respectively for HCD, vs. 732.2±12.38; n=12 and 722.9±13.89; n=12 respectively for controls).

- ***Oral Glucose Tolerance at 10 Weeks***

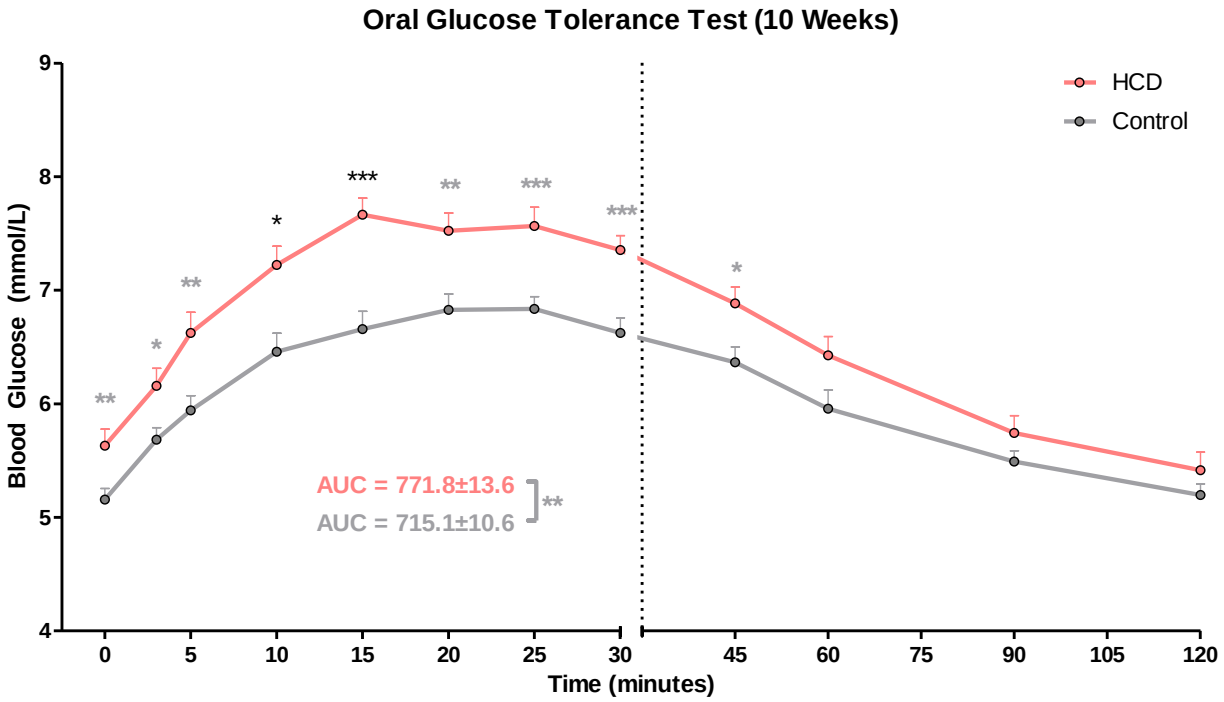

Figure 5.9 Oral glucose tolerance test performed at 10 weeks (Prior to Treatment). At 60 min, HCD vs Control non-significant at p=0.05.

- ***Oral Glucose Tolerance Test at 16 Weeks***

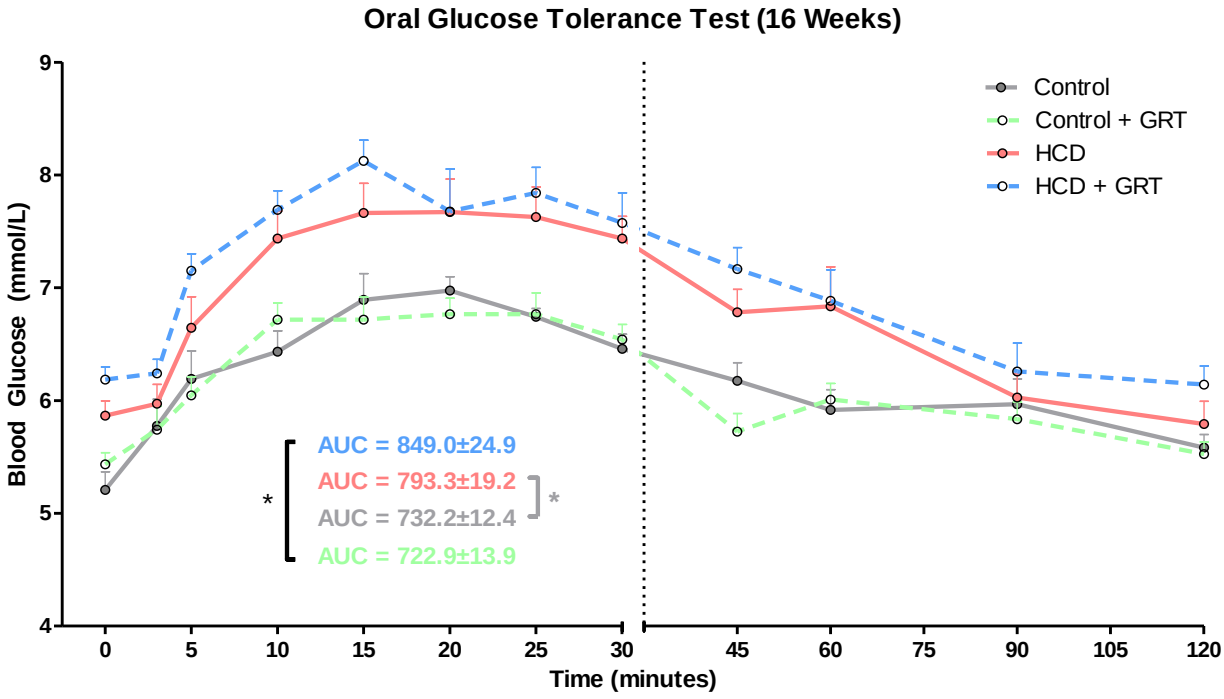

Figure 5.10 Oral glucose tolerance test performed at 16 weeks (After 6 weeks of Treatment). HCD: high-caloric diet; AUC: area under curve.

5.1.7 Fasting Serum Insulin Levels

Fasting insulin levels were obtained from blood collected directly from the carotid artery under anaesthesia. From **Figure 5.11**, 16 Weeks of diet significantly elevated serum insulin compared to 10 Weeks in both diet models (4.31±0.54 ng/mL (n=5) vs 2.47±0.27 ng/mL (n=10); p<0.001 for control, and 6.20±0.33 ng/mL (n=5) vs 3.10±0.33 ng/mL (n=10); p<0.001 for HCD) (**Table 5.1**). Furthermore, at 16 weeks HCD rats had signifcantly higher fasting serum insulin levels compared to controls rats (6.20±0.33 ng/mL (n=5) vs 4.31±0.54 ng/mL (n=5); p<0.05), constituting an increase in serum insulin levels of 43.9%. Supplementation with GRT for 6 weeks had no significant effect on serum insulin levels in both control and HCD models.

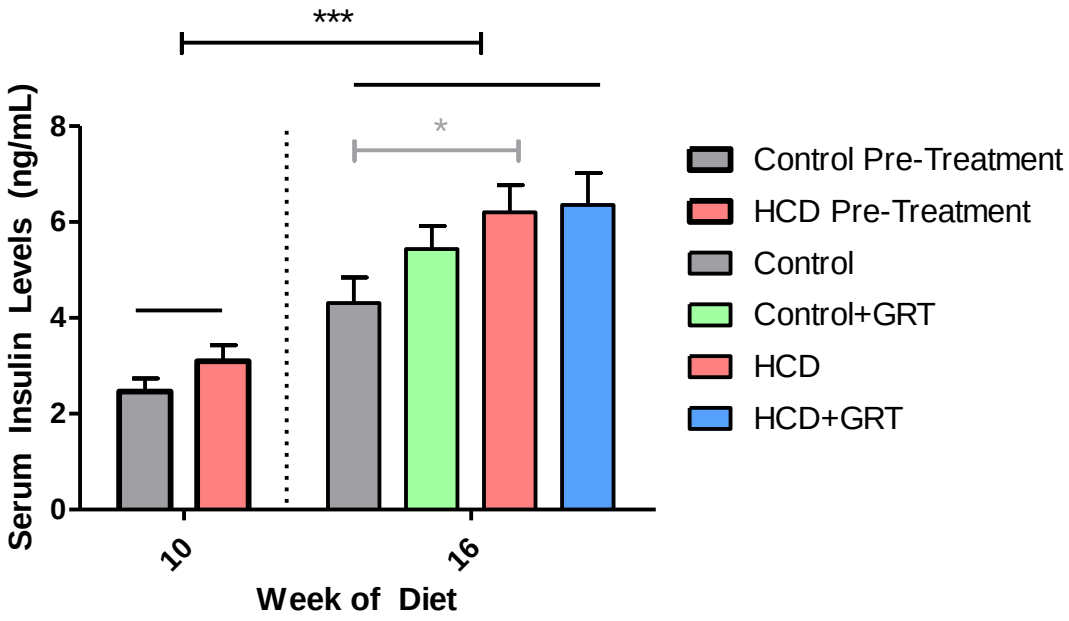

Figure 5.11 Fasting serum insulin at 10 weeks (pre-treatment) and 16 weeks (6 weeks of treatment). HCD: High-caloric diet, GRT: Afriplex green rooibos extract; *p<0.05 (Control vs HCD at 16 weeks), ***p<0.001 (Fasting serum insulin levels at 10 weeks vs 16 weeks of diet).

5.1.8 Major summary of biometric parameters

Table 5.1 Characteristics of the diet models with GRT treatment

Parameter	Unit	Control		Control + GRT		HCD		HCD + GRT	
		MEAN±SEM	n	MEAN±SEM	n	MEAN±SEM	n	MEAN±SEM	n
BODY WEIGHT									
Week 10	g	326.2±4.7	146			335.8±6.3 (♣n.s.)	147		
Week 16	g	373.6±4.8	74	382.7±5.5	72	403.9±5.1 (♣***)	74	423.9±6.0 (♥*)	73
Weight Gain during Treatment	g	45.22±2.80	74	51.51±3.32	72	65.63±2.97 (♣***)	74	76.35±4.77 (♥p=0.067)	73
INTRAPERITONEAL FAT									
Absolute Values	g	13.98±0.43	73	13.71±0.55	72	23.69±0.89 (♣***)	73	26.50±1.19 (♥p=0.060)	73
Percentage of BW	%	3.74±0.10	73	3.54±0.12	72	5.79±0.18 (♣***)	73	6.11±0.21	73
FOOD per rat/day									
Week 1-10	g	17.62±0.36	40			23.41±0.52 (♣***)	40		
Week 11-16	g	17.76±0.44	20	17.10±0.47	20	21.10±0.92 (♣***)	20	23.80±0.96	20
Week 1-16	g	18.00±0.54	20	17.21±0.43	20	22.30±1.27 (♣***)	20	23.24±1.40	20
WATER per rat/day									
Week 1-10	mL	29.09±0.90	40			19.85±0.64 (♣***)	40		
Week 11-16	mL	29.76±0.88	20	28.76±0.48	20	20.25±0.76 (♣***)	20	19.60±0.60	20
Week 1-16	mL	29.74±0.74	20	28.56±0.68	20	19.55±0.58 (♣***)	20	20.21±0.51	20
NON-FASTING BLOOD GLUCOSE									
Week 16	mM	6.88±0.11	63	6.78±0.12	62	7.78±0.14 (♣***)	65	7.54±0.13	64
FASTING BLOOD GLUCOSE									
Week 10	mM	5.16±0.10	26			5.63±0.15 (♣**)	26		
Week 16	mM	5.21±0.16	12	5.43±0.10	12	5.75±0.16 (♣*)	12	6.23±0.13 (♥p=0.073)	12
FASTING SERUM INSULIN									
Week 10	ng/mL	2.47±0.27	10			3.10±0.33	10		
Week 16	ng/mL	4.31±0.54	5	5.43±0.48	5	6.20±0.57 (♣*)	5	6.36±0.66	5
HOMA-IR INDEX									
Week 10	AU	1.31±0.14	10			1.62±0.18	10		
Week 16	AU	2.30±0.28	5	2.89±0.25	5	3.52±0.35 (♣*)	5	3.48±0.34	5

GRT: Afriplex green rooibos extract, HCD: high-caloric diet, HOMA-IR: homeostasis model assessment of insulin resistance, AU: arbitrary units, n.s.: no significance, *p<0.05, **p<0.01, ***p<0.001 (♣HCD vs Control; ♥HCD + GRT vs HCD).

5.2 PERFUSION PARAMETERS OF 20 MIN GLOBAL ISCHEMIA PROTOCOL

5.2.1 Heart Weight

Heart weight was measured just prior to mounting of the heart onto the perfusion rig (**Figure 5.12, Table 5.2**). The average absolute heart weight was greatest in the HCD with GRT group, 1.31±0.02 g or 0.318±0.004% of BW (n=55), followed by HCD without GRT, 1.27±0.02 g or 0.322±0.003% of BW (n=61), both of which were significantly greater than their control counterparts, with GRT, 1.23±0.02 g or 0.326±0.003% of BW (n=55), and without GRT, 1.18±0.01 g or 0.324±0.003% of BW (n=61), respectively. However, when taken as a percentage of total body weight, the significance was lost. Thus, heart weight was found to be directly proportional to total body weight.

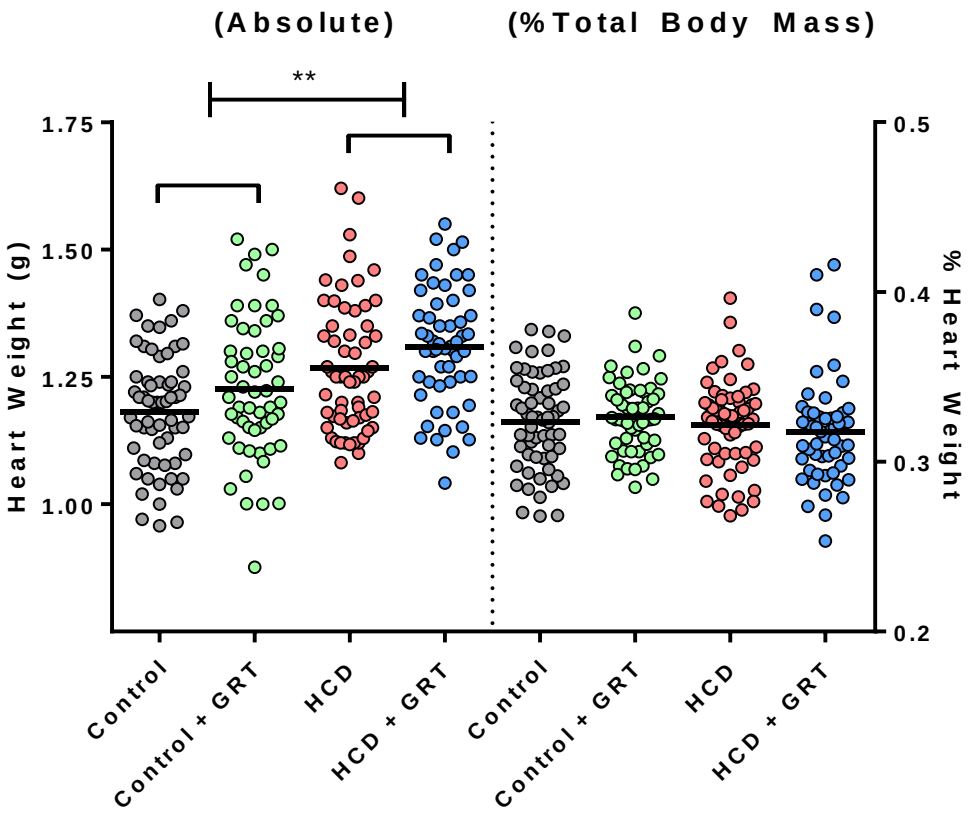

Figure 5.12 Absolute heart weight and percentage heart weight of total body weight

5.2.2 Heart Rate

Pre-ischemia (**Figure. 5.13**), GRT supplementation significantly decreased the heart rate of both controls (266.7±3.32 beats/min; n=55, vs. 275.5±3.18 beats/min; n=55; $p<0.05$) and HCD hearts (260.3±2.80 beats/min; n=60, vs. 270.6±3.05 beats/min; n=61; $p<0.05$). Heart rate was also signicantly lower in all groups post-global ischemia vs. pre-ischemia (**Table 5.2**), however there was no significant differences between groups in percentage heart rate recovery post-ischemia.

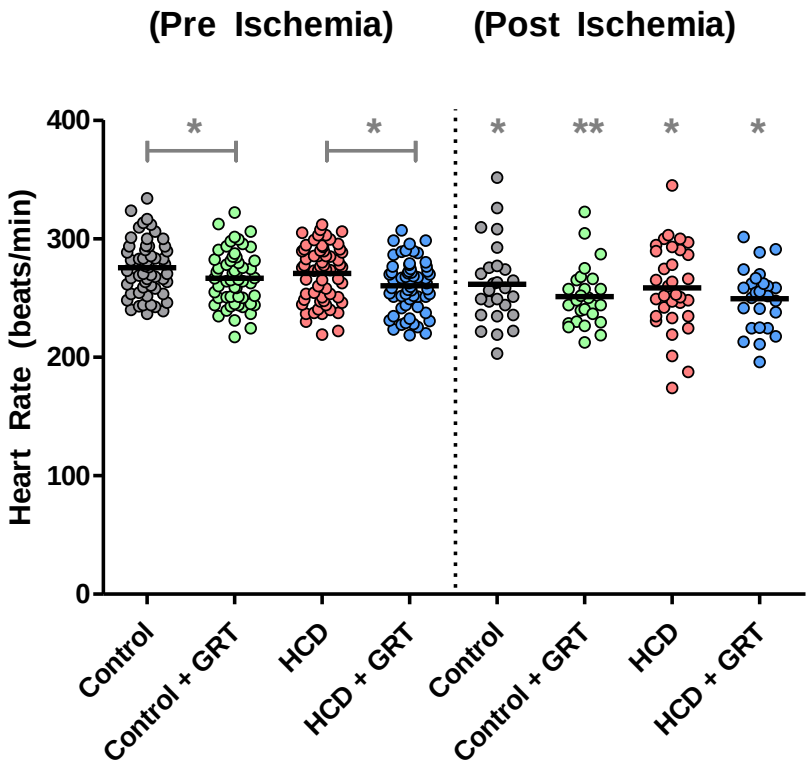

Figure 5.13 Average heart rate rate recorded pre- and post-global ischemia. HCD: High-caloric diet, GRT: Afriplex green rooibos extract; *p<0.05 (Control vs Control + GRT, HCD vs HCD + GRT Pre-Ischemia; Control-, HCD- and HCD + GRT Post-Ischemia vs Pre-Ischemia), **p<0.01 (Control + GRT Post-Ischemia vs Pre-Ischemia).

5.2.3 Coronary Flow

Pre-ischemia, there was no significant differences in coronary flow between the 4 groups (**Figure 5.14, Table 5.2**). However, post ischemia, coronary flow was significantly lower in hearts from HCD rats compared to hearts from control rats (16.22±0.59 mL/min; n=33 vs. 18.67±0.63; n=27, p<0.01), which equated to a 96.9±2.60% and 105.6±2.63% recovery, respectively; p<0.05).

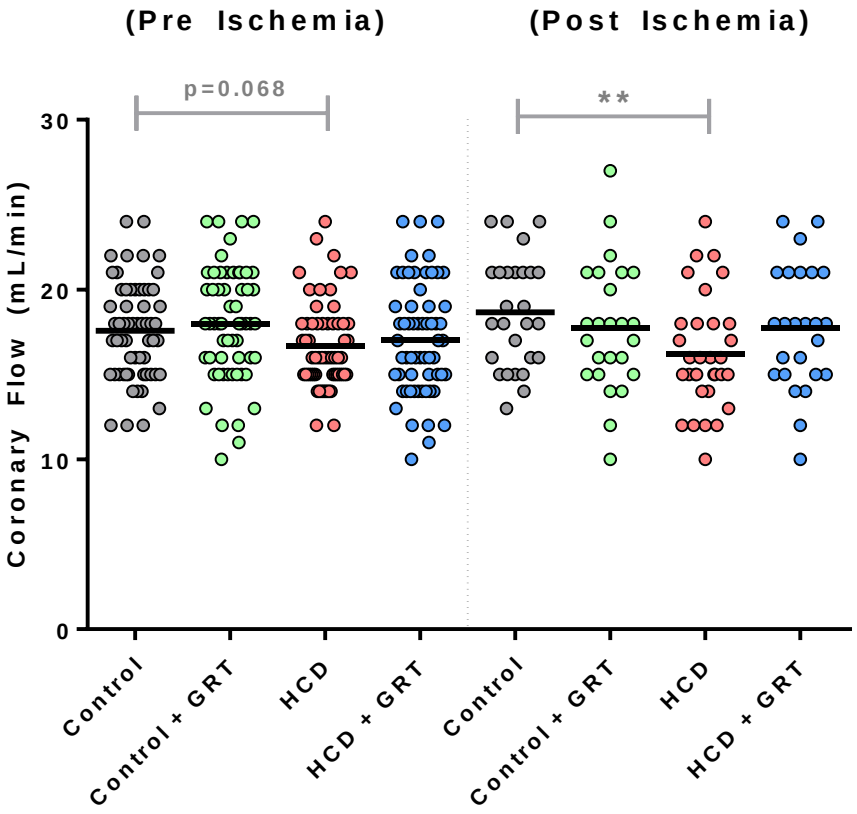

Figure 5.14 Coronary flow pre- and post-global ischemia. HCD: High-caloric diet, GRT: Afriplex green rooibos extract; **p<0.01 (Control vs HCD Post-Ischemia).

5.2.4 Diastolic Pressure

Pre-ischemia, diastolic pressure was significantly lower in the HCD group compared to controls (72.67±0.48 mmHg; n=56 vs. 74.27±0.37 mmgHg; n=55; p<0.01) (**Figure 5.15, Table 5.2**). Furthermore, supplementation with GRT increased diastolic pressure in both controls (75.68±0.49 mmHg; n=56; p<0.05) and HCD (74.11±0.43 mmHg; n=61; p<0.05) compared to their untreated counterparts. Post-ischemia, diastolic pressure was significantly lower in Control (71.74±0.59 mmHg; n=27; p<0.05), Control + GRT (72.37±0.47 mmHg; n=27; p<0.001) and HCD + GRT (70.54±0.55 mmHg; n=26; p<0.001) compared to pre-ischemia, while HCD did not decrease significantly. These decreases, however, did not result in a significantly different percentage diastolic pressure recovery between any of the 4 groups.

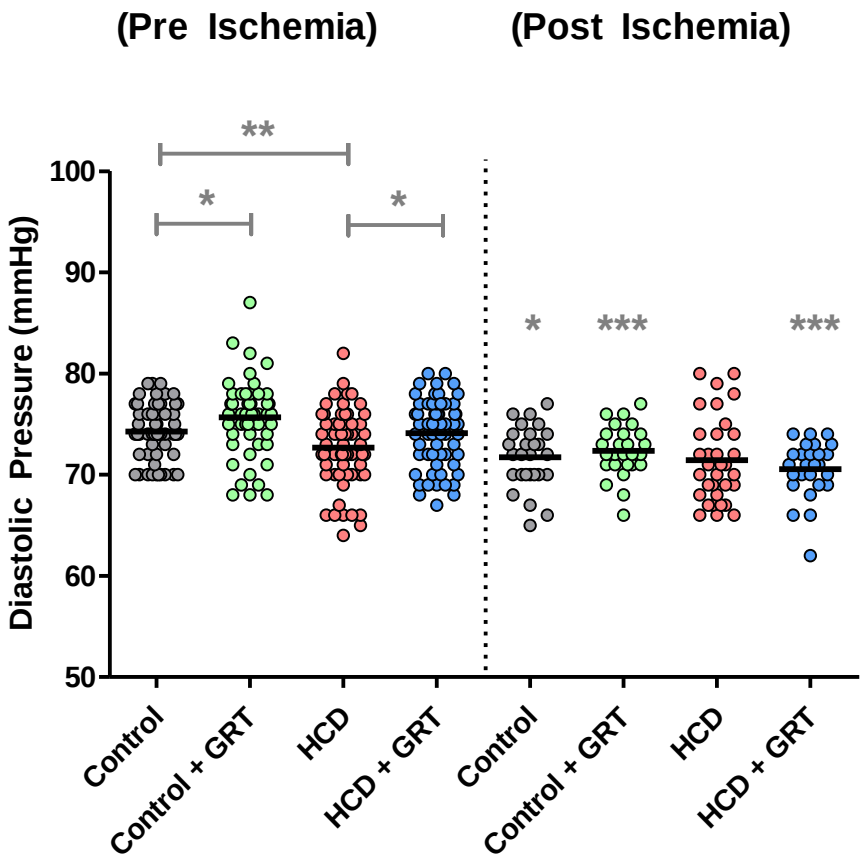

Figure 5.15 Diastolic pressure pre- and post-global ischemia. HCD: High-caloric diet, GRT: Afriplex green rooibos extract; *p<0.05 (Control vs Control + GRT Pre-Ischemia; HCD vs HCD + GRT Pre-Ischemia; Control Pre-ischemia vs Post-ischemia), **p<0.01 (Control vs HCD Pre-Ischemia), ***p<0.001 (Control + GRT and HCD + GRT Pre- vs Post-ischemia).

5.2.5 Systolic Pressure

Pre-ischemia, systolic pressure was significantly lower in the HCD group compared to controls (92.01±0.28 mmHg; n=61 vs. 94.24±0.36 mmHg; n=55; p<0.0001) (**Figure 5.16, Table 5.2**). Supplementation with GRT increased systolic pressure in both controls (95.98±0.36 mmHg; n=56; p<0.001) and HCD (94.22±0.36 mmHg; n=61; p<0.0001) compared to their untreated counterparts. Post-ischemia, systolic pressure was significantly lower in all groups. However, this did not result in a significantly different percentage systolic pressure recovery between any of the 4 groups.

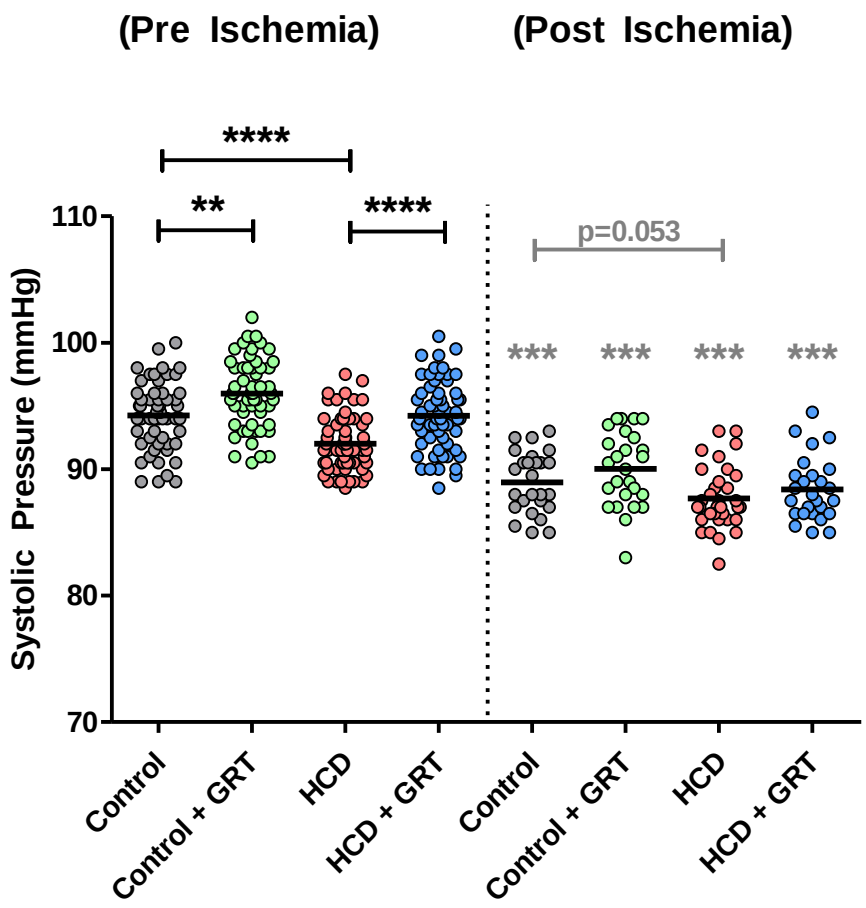

Figure 5.16 Systolic pressure pre- and post-global ischemia. HCD: High-caloric diet, GRT: Afriplex green rooibos extract; **p<0.01 (Control vs Control + GRT Pre-Ischemia), ***p<0.001 (Pre- vs Post-ischemia), ****p<0.0001 (Control vs HCD Pre-Ischemia, HCD vs HCD + GRT Pre-Ischemia).

5.2.6 Aortic Output

Pre-ischemia, aortic output (AO) was significantly lower in the HCD group compared to controls (34.76±0.45 mL/min; n=61 vs. 41.79±0.47 mL/min; n=55, p<0.0001) (**Figure 5.17**). Furthermore, supplementation with GRT improved AO in both controls (44.38±0.56 mL/min; n=56; p<0.001) and HCD (37.78±0.58 mL/min; n=60; p<0.0001) compared to their untreated counterparts. Post-ischemia, AO was still significantly lower in HCD compared to controls (13.07±0.95 mL/min; n=33 vs. 20.33±0.97 mL/min; n=27, p<0.0001), equating to a percentage AO recovery of 38.04±2.76% and 51.03±2.29%, p<0.001 respectively (**Table 5.2**). Supplementation with GRT improved post-ischemic AO in HCD hearts (18.15±0.90 mL/min; n=26; p<0.001, percentage AO recovery of 49.04±2.20%, p<0.01), equating to a 28.9% improvement in AO recovery compared to the untreated HCD hearts.

.

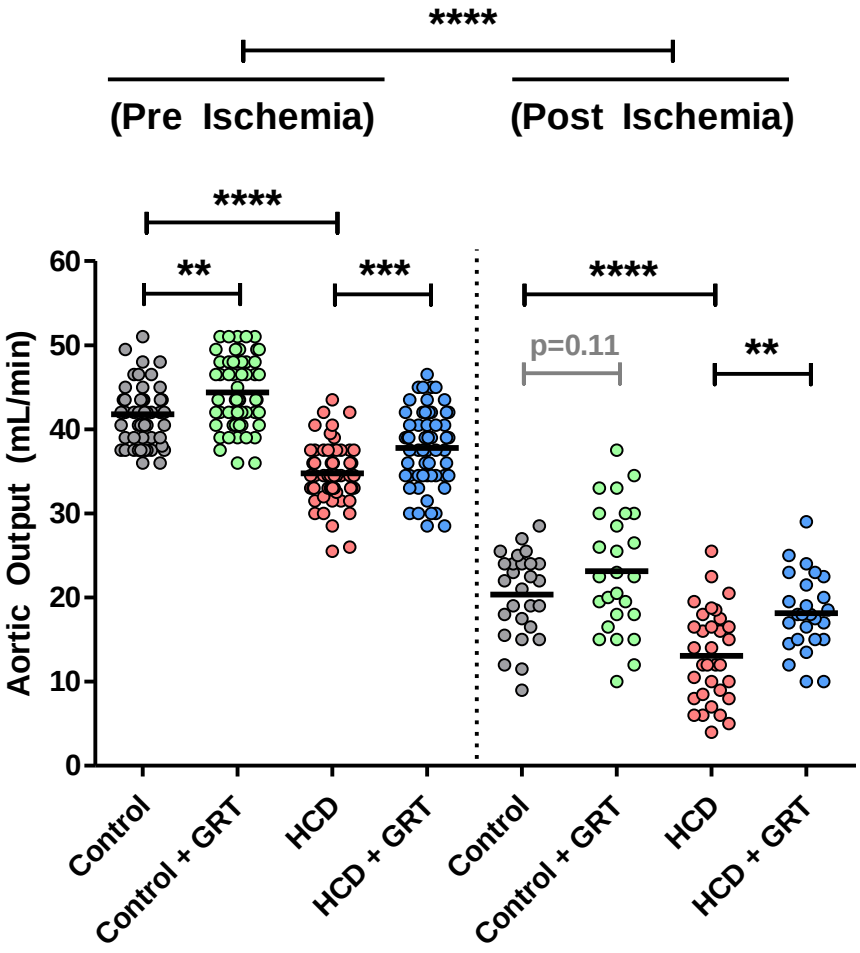

Figure 5.17 Aortic output pre- and post-global ischemia. HCD: High-caloric diet, GRT: Afriplex green rooibos extract; **p<0.01 (Control vs Control + GRT Pre-Ischemia; HCD vs HCD + GRT Post-Ischemia), ***p<0.001 (HCD vs HCD + GRT Pre-Ischemia), ****p<0.0001 (Control vs HCD Pre- and Post-Ischemia; Pre- vs Post-ischemia).

5.2.7 Cardiac Output

Pre-ischemia, cardiac output (CO) was significantly lower in the HCD group compared to controls (52.07±0.58 mL/min; n=61 vs. 59.97±0.69; n=55, p<0.0001) (**Figure 5.18**). Furthermore, supplementation with GRT improved CO in both controls (63.3±0.85 mL/min; n=56; p<0.01) and HCD (55.88±0.81 mL/min; n=60; p<0.001) compared to their untreated counterparts. Post-ischemia, CO was still significantly lower in HCD compared to controls (30.2±1.16 mL/min; n=33 vs. 38.84±1.40 mL/min; n=28, p<0.0001), equating to a percentage CO recovery of 58.34±2.25% and 68.36±1.87%, p<0.01 respectively (**Table 5.2**). Supplementation with GRT improved post-ischemic CO in hearts from HCD rats (36.38±1.354 mL/min; n=26; p<0.001 percentage CO recovery of 66.49±2.32%, p<0.05), equating to a 14.0% improvement in CO recovery compared to the hearts from untreated HCD rats.

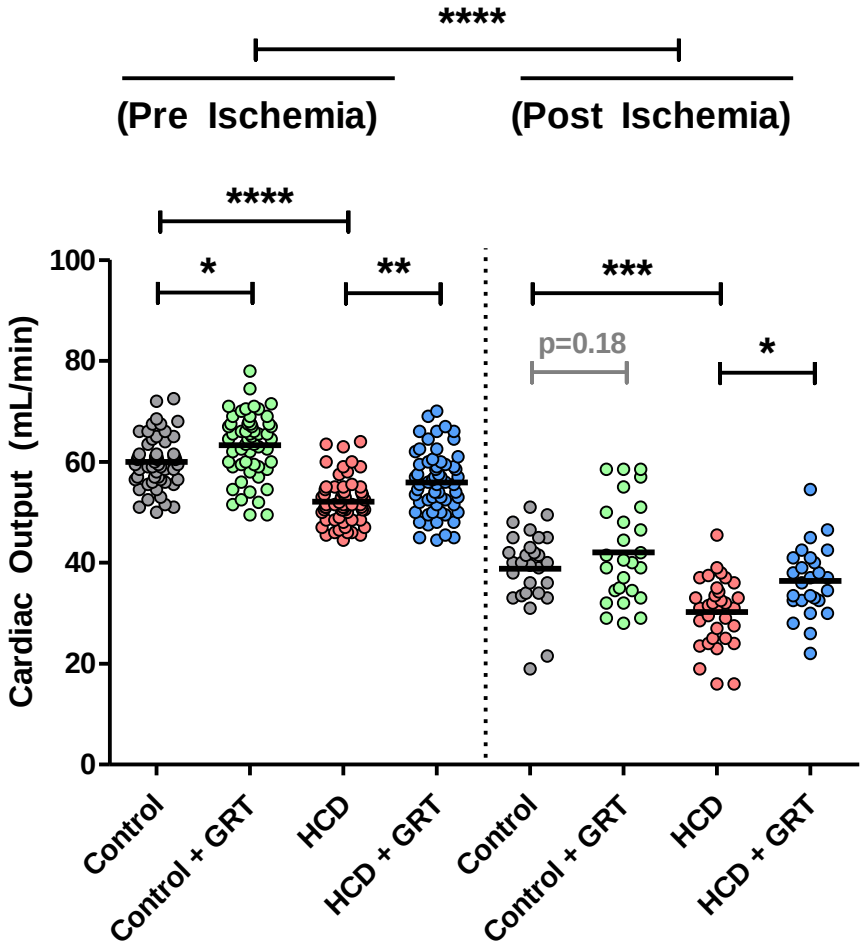

Figure 5.18 Cardiac output pre- and post-global ischemia. HCD: High-caloric diet, GRT: Afriplex green rooibos extract; *p<0.05 (Control vs Control + GRT Pre-Ischemia; HCD vs HCD + GRT Post-Ischemia), **p<0.01 (HCD vs HCD + GRT Pre-Ischemia), ***p<0.001 (Control vs HCD Post-Ischemia), ****p<0.0001 (Control vs HCD Pre-Ischemia, Pre-ischemia vs Post-ischemia).

5.2.8 Total Work

Pre-ischemia, total work (W_T) was significantly lower in the HCD group compared to controls (10.69±0.14 mW; n=61 vs. 12.6±0.19 mW; n=55, p<0.0001) (**Figure 5.19**). Furthermore, supplementation with GRT improved W_T in both controls (13.91±0.23 mW; n=56; p<0.0001) and HCD (11.98±0.20 mW; n=60; p<0.0001) compared to their untreated counterparts. Post-ischemia, W_T was still significantly lower in HCD compared to controls (5.91±0.24 mW; n=33 vs. 8.01±0.24 mW; n=26, p<0.0001), equating to a percentage W_T recovery of 64.80±2.04% and 55.51±2.28%, p<0.01 respectively (**Figure 5.20**). Supplementation with GRT improved post-ischemic W_T in hearts from HCD rats (7.29±0.30 mW; n=26; p<0.001, percentage W_T recovery of 63.35±2.49%, p<0.05), equating to a 14.1% improvement in W_T recovery compared to the untreated HCD hearts.

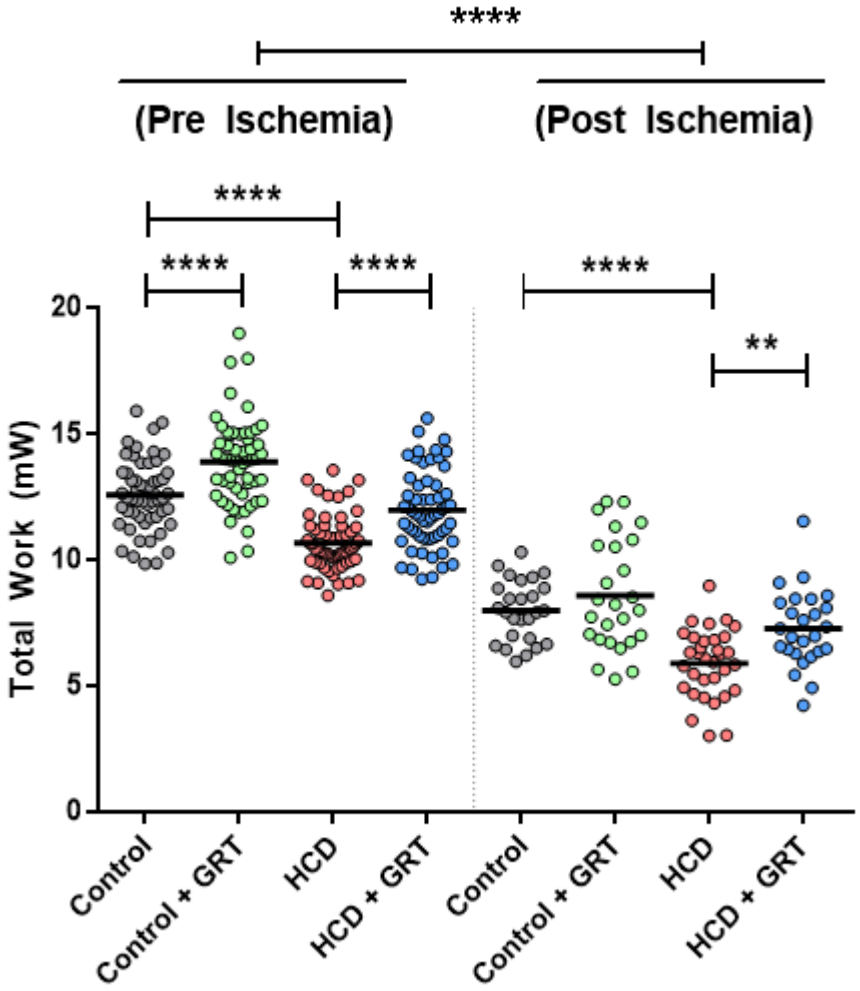

Figure 5.19 Total work pre- and post-global ischemia. HCD: High-caloric diet, GRT: Afriplex green rooibos extract; **p<0.01 (HCD vs HCD + GRT Post-Ischemia), ****p<0.0001 (Control vs HCD Pre- and Post-Ischemia; Control vs Control + GRT Pre-Ischemia; HCD vs HCD + GRT Pre-Ischemia; Pre- vs Post-ischemia).

- ***Total Work Recovery***

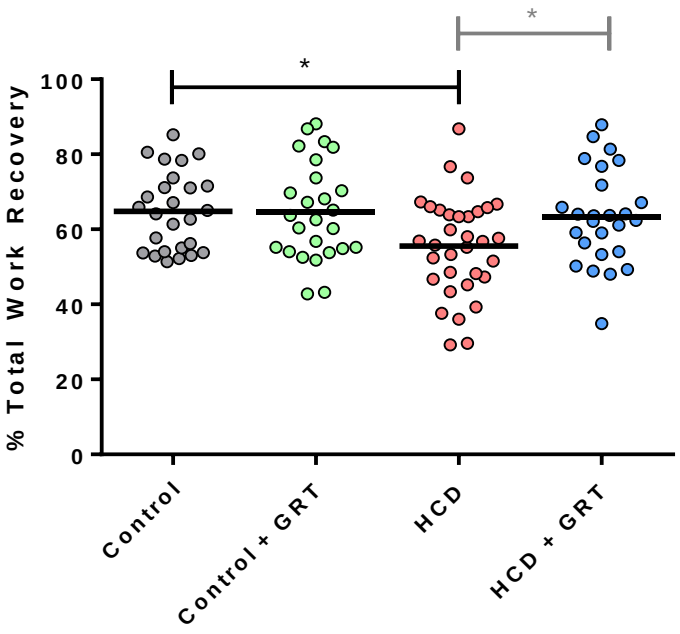

Figure 5.20 Percentage total work recovery post-global ischemia. HCD: High-caloric diet, GRT: Afriplex green rooibos extract; *p<0.05 (Control vs HCD; HCD vs HCD + GRT).

5.2.9 Summary of functional heart parameters

Table 5.2 Summary of functional heart parameters in global ischemia protocol

Parameter		CONTROL MEAN±SEM	n	CONTROL+GRT MEAN±SEM	n	HCD MEAN±SEM	n	HCD+GRT MEAN±SEM	n
Heart Weight	Absolute Values (g)	1.18±0.01	61	1.23±0.02	55	1.27±0.02 (♣**)	61	1.31±0.02	55
	% of BW	0.324±0.003	61	0.326±0.003	55	0.322±0.003	61	0.318±0.004	55
Heart Rate (beats/min)	Pre-Ischemia	275.5±3.18	55	266.7±3.32 (♠*)	55	270.6±3.05	61	260.3±2.80 (♥*)	60
	Post-Ischemia	261.5±6.78 (♦*)	26	251.2±5.04 (♦**)	26	255.±5.89 (♦*)	33	249.4±5.07 (♦*)	26
	% Recovery	96.15±1.73	26	96.08±1.74	26	96.53±1.70	33	95.73±1.75	26
Coronary Flow (mL/min)	Pre-Ischemia	17.57±0.37	60	17.98±0.44	58	16.66±0.33	61	17.05±0.42	61
	Post-Ischemia	18.67±0.63	27	17.76±0.76	26	16.22±0.59 (♣**)	33	17.72±0.73	26
	% Recovery	105.6±2.63	25	97.02±2.96 (♠*)	25	96.9±2.60 (*)	32	98.89±3.17	24
Diastolic Pressure (mmHg)	Pre-Ischemia	74.27±0.37	55	75.68±0.49 (♠*)	56	72.67±0.48 (♣**)	61	74.11±0.43 (♥*)	61
	Post-Ischemia	71.74±0.59 (♦*)	27	72.37±0.47 (♦***)	27	71.42±0.73	33	70.54±0.55 (♦***)	26
	% Recovery	96.95±0.77	26	96.15±0.90	26	96.35±074	33	96.87±0.99	26
Systolic Pressure (mmHg)	Pre-Ischemia	94.24±0.36	55	95.98±0.36 (♠***)	56	92.01±0.28 (♣****)	61	94.22±0.36 (♥****)	60
	Post-Ischemia	88.96±0.47 (♦***)	26	90.02±0.58 (♦***)	26	87.7±0.43 (♦***)	33	88.4±0.49 (♦***)	26
	% Recovery	94.82±0.50	26	94.8±0.53	26	95.48±0.43	32	94.6±0.53	26
Aortic Output (mL/min)	Pre-Ischemia	41.79±0.47	55	44.38±0.56 (♠***)	56	34.76±0.45 (♣****)	61	37.78±0.58 (♥****)	60
	Post-Ischemia	20.33±0.97 (♦****)	27	23.13±1.45 (♦****)	26	13.07±0.95 (♦,♣****)	33	18.15±0.90 (♥****)	26
	% Recovery	51.03±2.29	27	53.52±2.98	26	38.04±2.76 (♣***)	33	49.04±2.20 (♥**)	26
Cardiac Output (mL/min)	Pre-Ischemia	59.97±0.69	55	63.3±0.85 (♠**)	56	52.07±0.58 (♣****)	61	55.88±0.81 (♥***)	60
	Post-Ischemia	38.84±1.40 (♦****)	28	42.06±1.94 (♦****)	26	30.2±1.16 (♦,♣****)	33	36.38±1.35 (♦****, ♥***)	26
	% Recovery	68.36±1.87	26	67.52±2.46	26	58.34±2.25 (♣**)	33	66.49±2.32 (♥*)	26
Total Work (mW)	Pre-Ischemia	12.6±0.19	55	13.91±0.23 (♠****)	56	10.69±0.14 (♣****)	61	11.98±0.20 (♥****)	60
	Post-Ischemia	8.01±0.24 (♦****)	26	8.61±0.43 (♦****)	26	5.91±0.24 (♦****, ♣****)	33	7.29±0.30 (♦****, ♥***)	26
	% Recovery	64.8±2.04	26	64.69±2.54	26	55.51±2.28 (♣**)	33	63.35±2.49 (♥*)	26

HCD: High-caloric diet, GRT: Afriplex green rooibos extract; *p<0.05, **p<0.01, ***p<0.001, ****p<0.0001 (♠Control + GRT vs Control; ♣HCD vs Control; ♥HCD + GRT vs HCD; ♦post-ischemia vs pre-ischemia).

5.3 PERFUSION PARAMETERS OF 35 MIN REGIONAL ISCHEMIA PROTOCOL

5.3.1 Heart Rate

There were no significant differences in heart rate pre- or post-ischemia for either of the groups during the regional ischemia protocol (**Table 5.3**).

5.3.2 Coronary Flow Rate

Pre-ischemia there were no significant differences in coronary flow between the 4 groups, however supplementation with GRT did initially increase coronary flow in control groups, albeit non-significantly due the low n-value (p=0.063) (19.30±0.51 mL/min; n=10 vs. 17.67±0.64 mL/min; n=9) (**Table 5.3**). Post regional ischemia, there were no major differences in coronary flow rate and with only minor decreases (p=0.056) in the percentage coronary flow recovery observed in the GRT supplemented controls (96.92±6.07%; n=10 vs. 114.3±5.55%; n=9).

5.3.3 Diastolic and Systolic Pressure

There were no significant differences in either diastolic or systolic pressure pre- or post-ischemia for either of the groups during the regional ischemia protocol (**Table 5.3**).

5.3.4 Aortic Output

Pre-ischemia, AO was significantly lower in the HCD group compared to controls (33.67±1.15 mL/min; n=9 vs. 39.00±0.85 mL/min; n=9, p<0.05) (**Table 5.3**). Furthermore, supplementation with GRT improved AO in both controls (43.80±1.28 mL/min; n=10; p<0.05) and HCD (37.33±1.21 mL/min; n=9; p<0.05) compared to their untreated counterparts. Post-ischemia, AO was lower in HCD compared to controls (13.06±2.34 mL/min; n=9 vs. 19.13±2.05 mL/min; n=9, p=0.0712), equating to a percentage AO recovery of 32.36±4.93% and 49.09±5.31%, p<0.05 respectively. Supplementation with GRT improved post-ischemic AO in HCD hearts (17.89±1.36 mL/min; n=9; p=0.0865, percentage AO recovery of 47.48±2.38%, p<0.05), equating to a 26.4% improvement in AO recovery compared to the untreated HCD heart.

5.3.5 Cardiac Output

Pre-ischemia, CO was significantly lower in the HCD group compared to controls (51.39±1.07 mL/min; n=9 vs. 56.63±1.51; n=9, p<0.05) (**Table 5.3**). Furthermore, supplementation with GRT improved CO in controls (63.10±1.55 mL/min; n=10; p<0.01), but not significantly in HCD (54.89±1.56 mL/min; n=9) compared to their untreated counterparts. Post-ischemia, CO was still significantly lower in HCD compared to controls (30.44±2.33 mL/min; n=9 vs. 38.19±2.31 mL/min; n=9, p<0.05), equating to a percentage CO recovery of 58.22±4.39% and 67.39±3.55%, respectively. Supplementation with GRT did not have a significant effect on coronary output post-regional ischemia.

5.3.6 Total Work

Pre-ischemia, W_T was significantly lower in the HCD group compared to controls (10.42±0.27 mW; n=9 vs. 11.63±0.33 mW; n=9, p<0.05) (**Figure 5.21**). Furthermore, supplementation with GRT improved W_T in controls (13.28±0.40 mW; n=10; p<0.01), but not significantly in HCD (11.38±0.38 mW; n=9; p=0.057) compared to their untreated counterparts. Post-ischemia, W_T was still significantly lower in HCD compared to controls (5.70±0.43 mW; n=9 vs. 7.49±0.45 mW; n=9, p<0.05), equating to a percentage total work recovery of 53.55±4.22% and 64.42±3.51%, respectively (p=0.067) (**Figure 5.22**). Supplementation with GRT improved post-ischemic W_T in HCD hearts (7.00±0.35 mW; n=9; p<0.05, percentage total work recovery of 61.46±2.09%, p=0.093), equating to a 14.8% improvement in W_T recovery compared to the untreated HCD hearts.

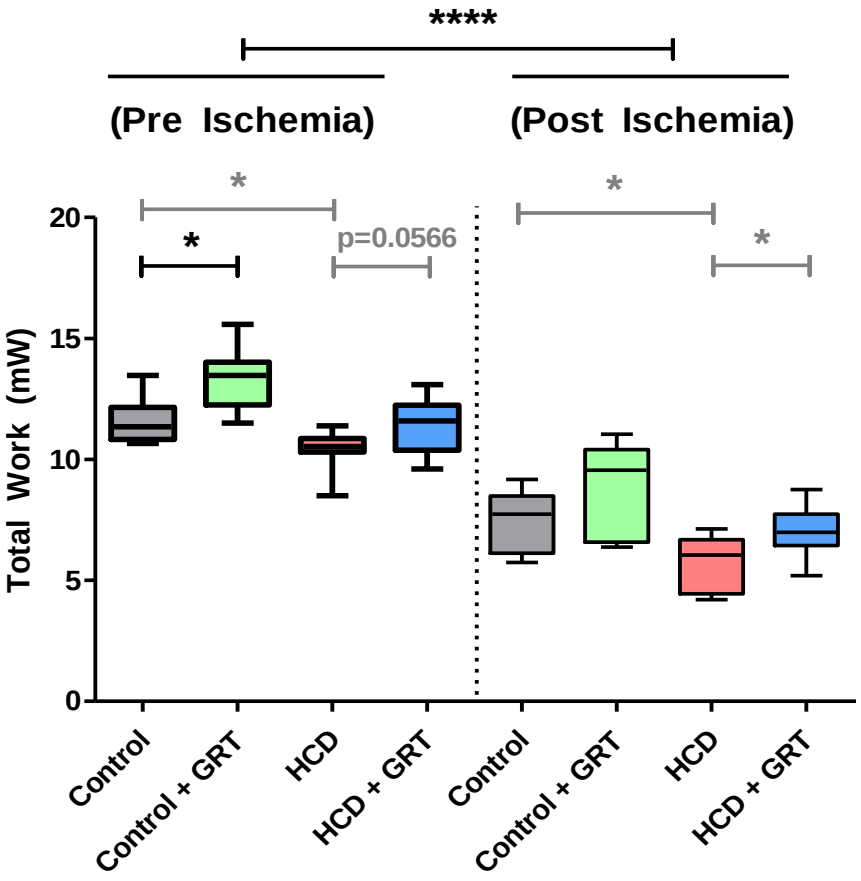

Figure 5.21 Total work pre- and post-regional ischemia. HCD: High-caloric diet, GRT: Afriplex green rooibos extract; *p<0.05 (Control vs Control + GRT and HCD Pre-Ischemia, Control vs HCD Post-Ischemia, HCD vs HCD + GRT Post-Ischemia), ♦p<0.001 (Pre- vs Post-ischemia).

- ***Total Work Recovery***

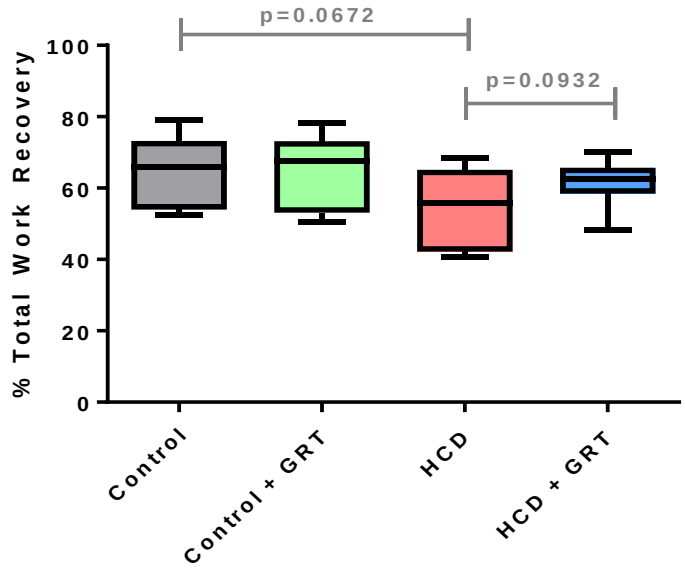

Figure 5.22 Percentage total work recovery post-regional ischemia. HCD: High-caloric diet, GRT: Afriplex green rooibos extract.

5.3.7 Infarct Size

%AAR did not differ between the groups (**Table 5.3**). HCD had the greatest infarct size (34.99±11.56%; n=9 compared to controls: 16:42±8.71%; n=9; p<0.01), while GRT supplementation completely reversed the infarct size (13.22±6.66%; n=9; p<0.001) (**Figure 5.23, Figure 5.24**).

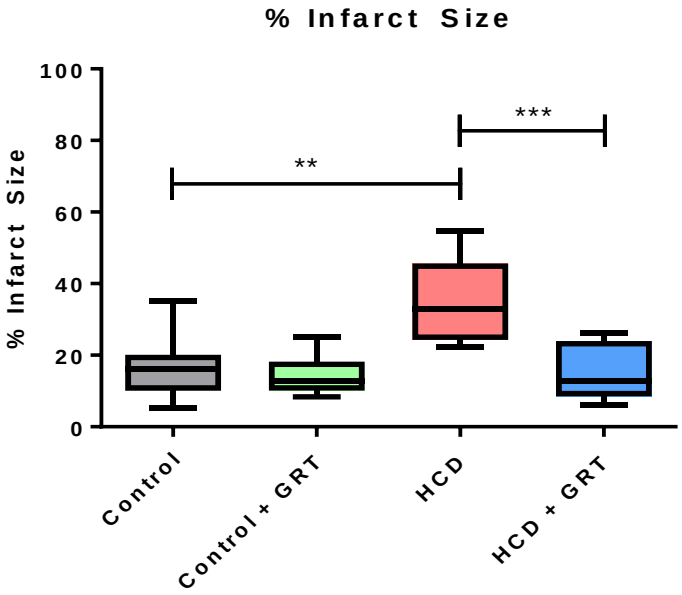

Figure 5.23 Percentage infarct size following regional ischemia and reperfusion. HCD: High-caloric diet, GRT: Afriplex green rooibos extract; **p<0.01 (HCD vs Control), ***p<0.001 (HCD + GRT vs HCD).

- ***Representative slices of 4 different groups after staining***

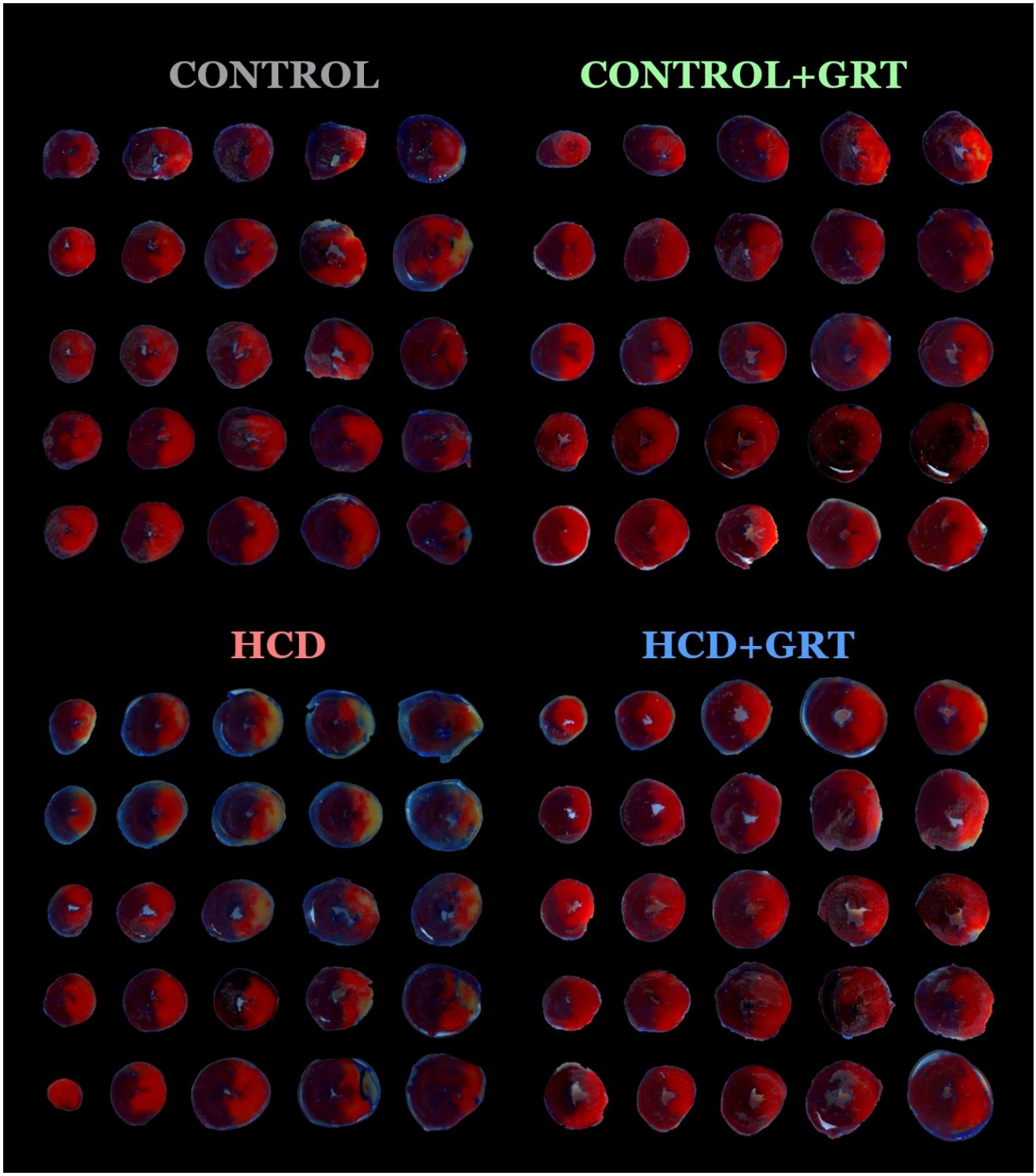

Figure 5.24 Representative stained heart slices after ischemia and reperfusion. HCD: High-caloric diet, GRT: Afriplex green rooibos extract. Viable area (stained by Evans blue), area at risk (AAR, i.e. area not stained by Evans Blue), live cells (TTC positive, i.e. red) and infarcted area (TTC negative, i.e. white).

5.3.8 Summary of functional heart parameters

Table 5.3 Summary of functional heart parameters in regional ischemia protocol

Parameter		CONTROL (n = 9) MEAN±SEM	CONTROL+GRT (n = 10) MEAN±SEM	HCD (n = 9) MEAN±SEM	HCD+GRT (n = 9) MEAN±SEM
Heart Rate (beats/min)	Pre-Ischemia	249.4±6.6	261.8±8.31	262.4±7.2	259.1±5.2
	Post-Ischemia	243.6±10.4	247.9±5.3	252.3±10.22	258.9±9.0
	% Recovery	96.81±3.00	95.15±1.95	96.92±3.08	100.10±3.67
Coronary Flow (mL/min)	Pre-Ischemia	17.67±0.64	19.30±0.51	17.72±0.31	17.56±0.72
	Post-Ischemia	19.06±0.99	17.70±0.71	17.38±0.66	18.22±0.98
	% Recovery	114.3±5.55	96.92±6.07	99.25 ± 4.61	105.90±5.60
Diastolic Pressure (mmHg)	Pre-Ischemia	73.55±1.00	75.10±1.18	72.83±1.25	73.44±0.91
	Post-Ischemia	72.75±0.51	72.85±0.87	71.13±0.99	71.89±0.53
	% Recovery	99.10±1.32	97.15±1.54	96.96±1.38	98.00±1.58
Systolic Pressure (mmHg)	Pre-Ischemia	92.85±1.07	94.6±1.02	91.22±0.84	93.22±0.98
	Post-Ischemia	88.31±0.60	89.90±0.98	88.00±1.10	87.17±0.61
	% Recovery	95.59±1.08	95.05±0.69	95.78±0.98	93.54±0.56
Aortic Output (mL/min)	Pre-Ischemia	39.00±0.85	43.80±1.28 (♠**)	33.67±1.15 (♣**)	37.33±1.21 (♥*)
	Post-Ischemia	19.13±2.05 (♦****)	23.65±2.95 (♦****)	13.06±2.34 (♦****)	17.89±1.36 (♦****)
	% Recovery	49.09±5.31	56.12±5.12	32.36±4.93 (♣*)	47.48±2.38 (♥*)
Cardiac Output (mL/min)	Pre-Ischemia	56.63±1.51	63.10±1.55 (♠**)	51.39±1.07 (♣*)	54.89±1.56
	Post-Ischemia	38.19±2.31 (♦****)	41.35±3.26 (♦****)	30.44±2.33 (♦****, ♣*)	36.11±1.73 (♦****)
	% Recovery	67.39±3.55	65.00±4.11	58.22±4.39	65.69±2.16
Total Work (mW)	Pre-Ischemia	11.63±0.33	13.28±0.40 (♠**)	10.42±0.27 (♣*)	11.38±0.38
	Post-Ischemia	7.49±0.45 (♦****)	8.71±0.64 (♦****)	5.70±0.43 (♦****, ♣*)	7.00±0.35 (♦****, ♥*)
	% Recovery	64.42±3.51	64.23±3.51	53.55±4.22	61.46±2.09
Infarct size	% Area at Risk	50.65±1.71	50.46±1.22	51.29±2.26	49.75±0.72
	% Infarct Size	16.42±8.71	14.58±5.43	34.99±11.56 (♣**)	13.22±6.66 (♥***)

HCD: High-caloric diet, GRT: Afriplex green rooibos extract; *p<0.05, **p<0.01, ***p<0.001 (♠Control + GRT vs Control; ♣HCD vs Control; ♥HCD + GRT vs HCD; ♦post-ischemia vs pre-ischemia).

5.4 CARDIAC PROTEIN SIGNALING

In order to describe the protein signaling as possible mechanistic explanation for the observed changes, we investigated the change in total protein (expression) and phosphorylated protein (referred to as activation) relative to the basal control (referred to as C1 - 30 min stabilized control marker) in isolated perfused cardiac ventricular tissue freeze-clamped at the following time points (n=5): Stabilization (30 min total perfusion time), Ischemia (20 min global-ischemia and 50 min total perfusion time), Early Reperfusion (5 min into reperfusion and 55 min total perfusion time) and Late Reperfusion (30 min into reperfusion and 80 min total perfusion time). Additionally, a young control marker (YC) was also placed on the first two lanes to serve as an additional positive control and out of interest for future comparative studies.

5.4.1 PKB

PKB plays a primary role in insulin-dependent metabolism and is well-recognized to be cardioprotective as part of the RISK pathway when activated in early reperfusion (Rossello & Yellon, 2018).

- ***Stabilization***

GRT supplementation in controls significantly increased PKB activation compared to untreated controls ($p<0.05$), and decreased activation and expression in HCD compared to untreated HCD ($p<0.01$ for both) (**Figure 5.25, Table 5.4**).

- ***Ischemia***

HCD significantly decreased PKB activation ($p<0.05$) and PKB activation/expression ratio ($p=0.072$) compared to controls. GRT supplementation increased PKB expression ($p=0.060$) and consequently decreased PKB activation/expression ratio ($p=0.063$) in controls.

- ***Early Reperfusion***

HCD significantly increased PKB expression ($p<0.01$) but decreased PKB activation ($p<0.05$), resulting in a decreased PKB activation/expression ratio ($p=0.075$). GRT supplementation in HCD significantly increased PKB expression ($p<0.001$) but not the activation/expression ratio.

- ***Late Reperfusion***

HCD significantly decreased PKB expression ($p<0.001$), resulting in an increased PKB activation/expression ratio ($p<0.001$). GRT supplementation increased PKB expression ($p=0.051$) in HCD, whilst decreasing PKB expression in controls ($p<0.05$). However, GRT supplementation decreased PKB activation in both controls ($p<0.001$) and HCD ($p<0.05$), simultaneously also decreasing the PKB activation/expression ratio ($p<0.01$) in HCD.

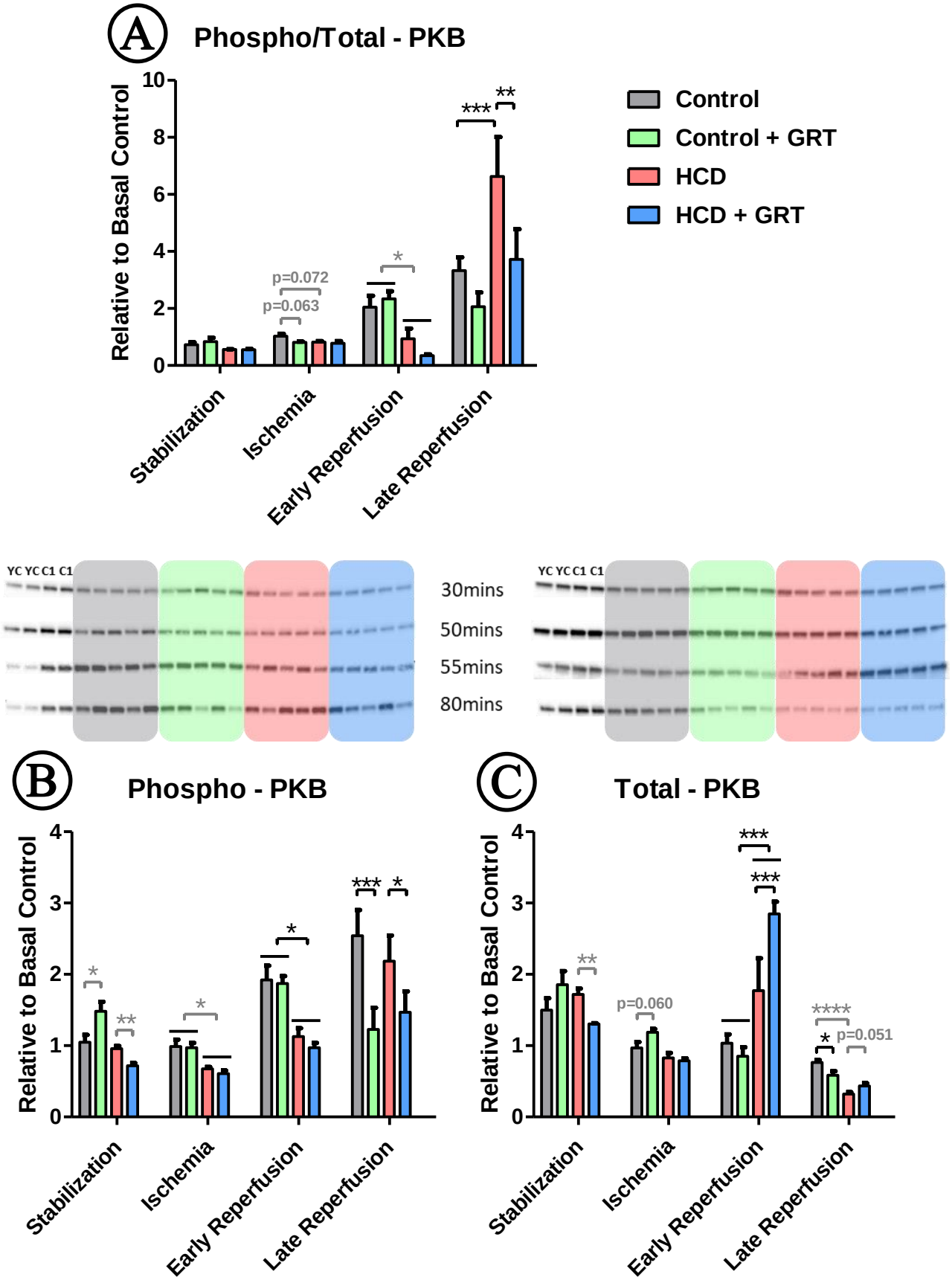

Figure 5.25 PKB Ratio (A) of Activation (B) to Expression (C) between the different groups and time points (n=5). HCD: High-caloric diet, GRT: Afriplex green rooibos extract.

5.4.2 AMPK

AMPK is considered an insulin-independent metabolic regulator (Xu *et al.*, 2014).

- ***Stabilization***

HCD significantly increased AMPK expression ($p<0.01$) and consequently decreased the AMPK activation/expression ratio ($p<0.05$) compared to controls. GRT supplementation increased AMPK activation in controls ($p<0.001$), whilst consequently decreasing the AMPK activation/expression ratio ($p=0.060$) (**Figure 5.26, Table 5.4**).

- ***Ischemia***

HCD significantly increased AMPK activation ($p<0.05$) and activation/expression ratio ($p<0.05$) compared to controls. GRT supplementation increased AMPK activation in controls ($p<0.05$), resulting in increased activation/expression ratio ($p=0.09$), whilst contrastingly decreasing AMPK activation in HCD ($p=0.075$).

- ***Early Reperfusion***

GRT supplementation significantly decreased AMPK expression in HCD ($p<0.05$), whilst significantly increasing AMPK activation ($p<0.001$) and consequently increasing the AMPK activation/expression ratio ($p<0.001$).

- ***Late Reperfusion***

HCD significantly decreased AMPK expression ($p<001$), resulting in an increased AMPK activation/expression ratio ($p<0.05$). GRT supplementation in controls decreased AMPK expression ($p=0.01$) resulting in an increased AMPK activation/expression ratio ($p<0.05$). In contrast, GRT supplementation in HCD significantly increased AMPK expression ($p<0.001$).

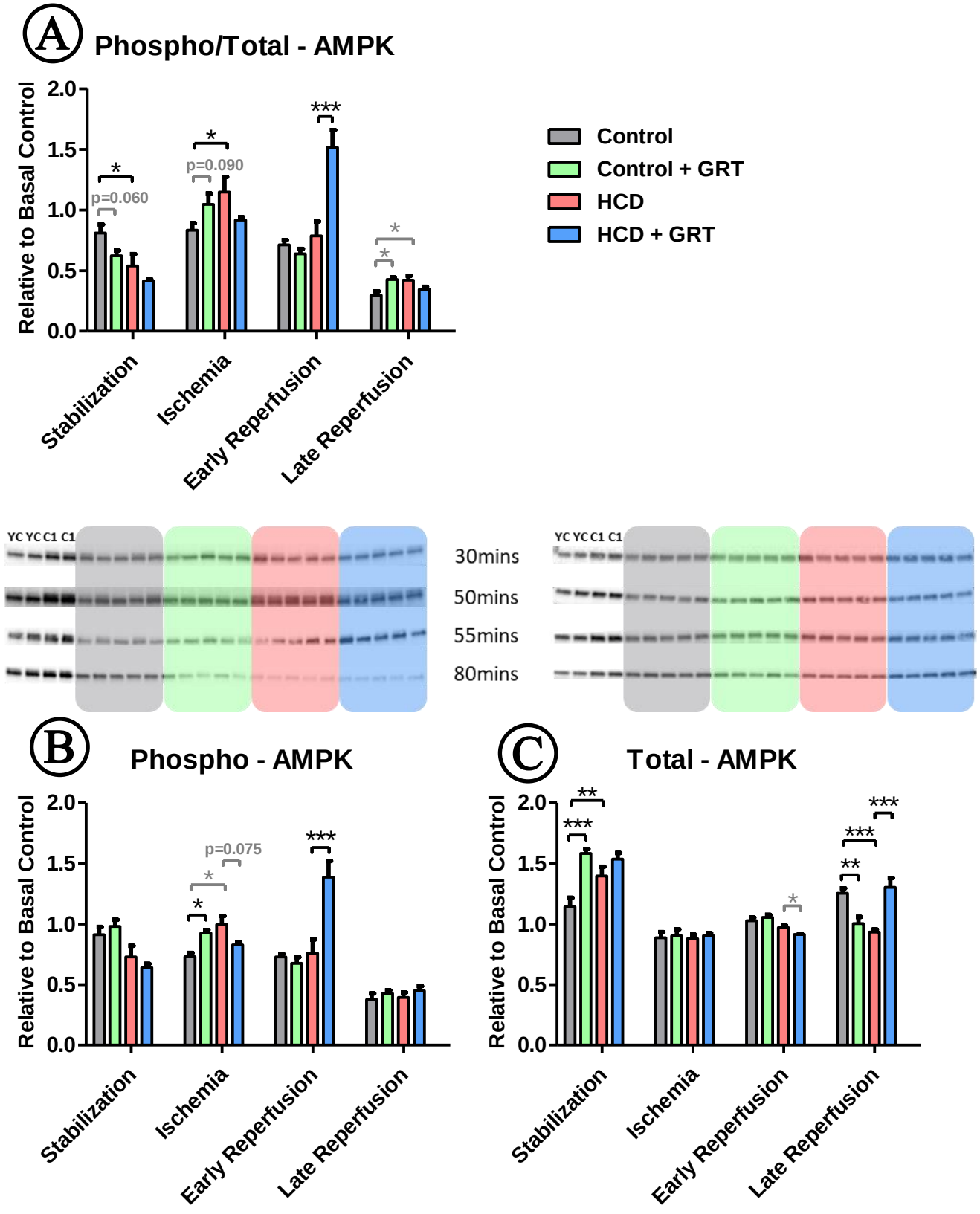

Figure 5.26 AMPK Ratio (A) of Activation (B) to Expression (C) between the different groups and time points (n=5). HCD: High-caloric diet, GRT: Afriplex green rooibos extract.

5.4.3 AS160

AS160 serve as a precursor to GLUT4 mediated glucose uptake into cells (Mîinea *et al.*, 2005).

- ***Stabilization***

HCD increased AS160 expression ($p=0.065$) compared to controls (**Figure 5.27, Table 5.4**). GRT supplementation significantly increased AS160 expression in both controls ($p<0.05$) and HCD ($p<0.01$), while decreasing AS160 activation in both controls ($p<0.01$) and HCD ($p<0.05$) and resulting in decreased AS160 activation/expression ratio ($p=0.097$ and $p=0.087$ respectively).

- ***Ischemia***

GRT supplementation decreased AS160 expression in both controls ($p<0.05$) and HCD ($p=0.079$), and significantly increasing the AS160 activation/expression ratio in controls ($p<0.001$) but not in HCD.

- ***Early Reperfusion***

HCD significantly decreased the AS160 activation/expression ratio compared to controls ($p<0.05$).

- ***Late Reperfusion***

GRT supplementation decreased the AS160 activation/expression ratio in HCD ($p=0.086$).

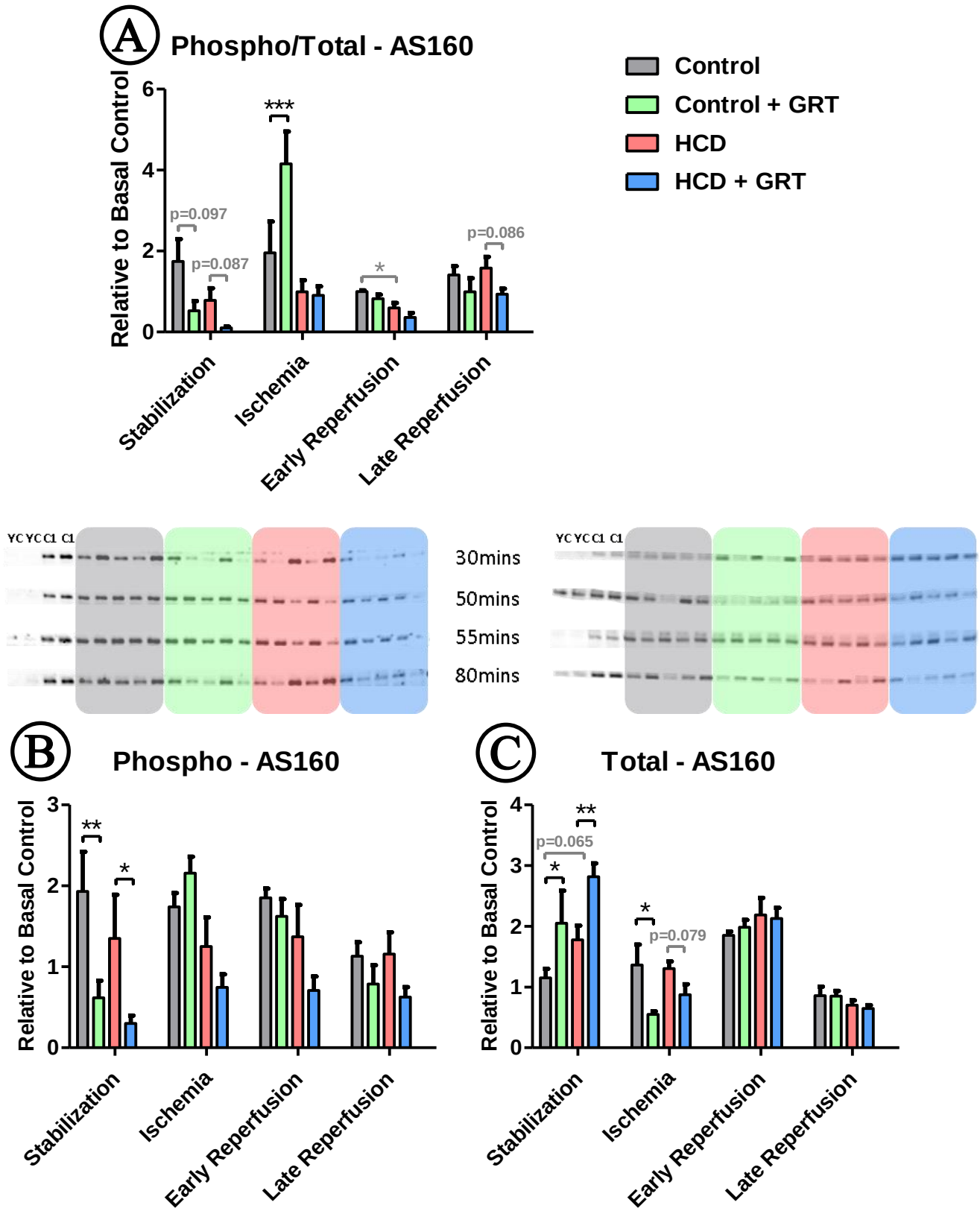

Figure 5.27 AS160 Ratio (A) of Activation (B) to Expression (C) between the different groups and time points (n=5). HCD: High-caloric diet, GRT: Afriplex green rooibos extract.

5.4.4 ERK1

ERK cascade plays a crucial role in multiple cellular processes such as cell proliferation, differentiation, adhesion, migration and survival. Therefore, it is essential for many physiological events including development, immunity, metabolism, and memory formation (Buscà *et al.*, 2016). Activation of ERK during reperfusion is associated with cardioprotection (RISK pathway).

- ***Stabilization***

GRT supplementation significantly increased ERK1 expression in controls ($p<0.05$), but not HCD (**Figure 5.28, Table 5.5**).

- ***Ischemia***

GRT supplementation resulted in significant decreased ERK1 expression and in effect increased ERK1 activation/expression ratio ($p<0.05$ and $p=0.068$) compared to HCD. No significant differences were observed in controls.

- ***Early Reperfusion***

GRT supplementation led to a significant decrease in ERK1 activation and in effect decreased ERK1 activation/expression ratio ($p<0.01$ for both) compared to HCD. No significant differences were recorded in controls.

- ***Late Reperfusion***

HCD significantly decreased ERK1 activation and expression compared to controls ($p<0.05$ and $p<0.01$ respectively). Likewise, GRT supplementation also decreased ERK1 activation and expression compared to controls ($p<0.001$ for both). There were no significant differences observed in the ERK1 activation/expression ratio between the 4 groups.

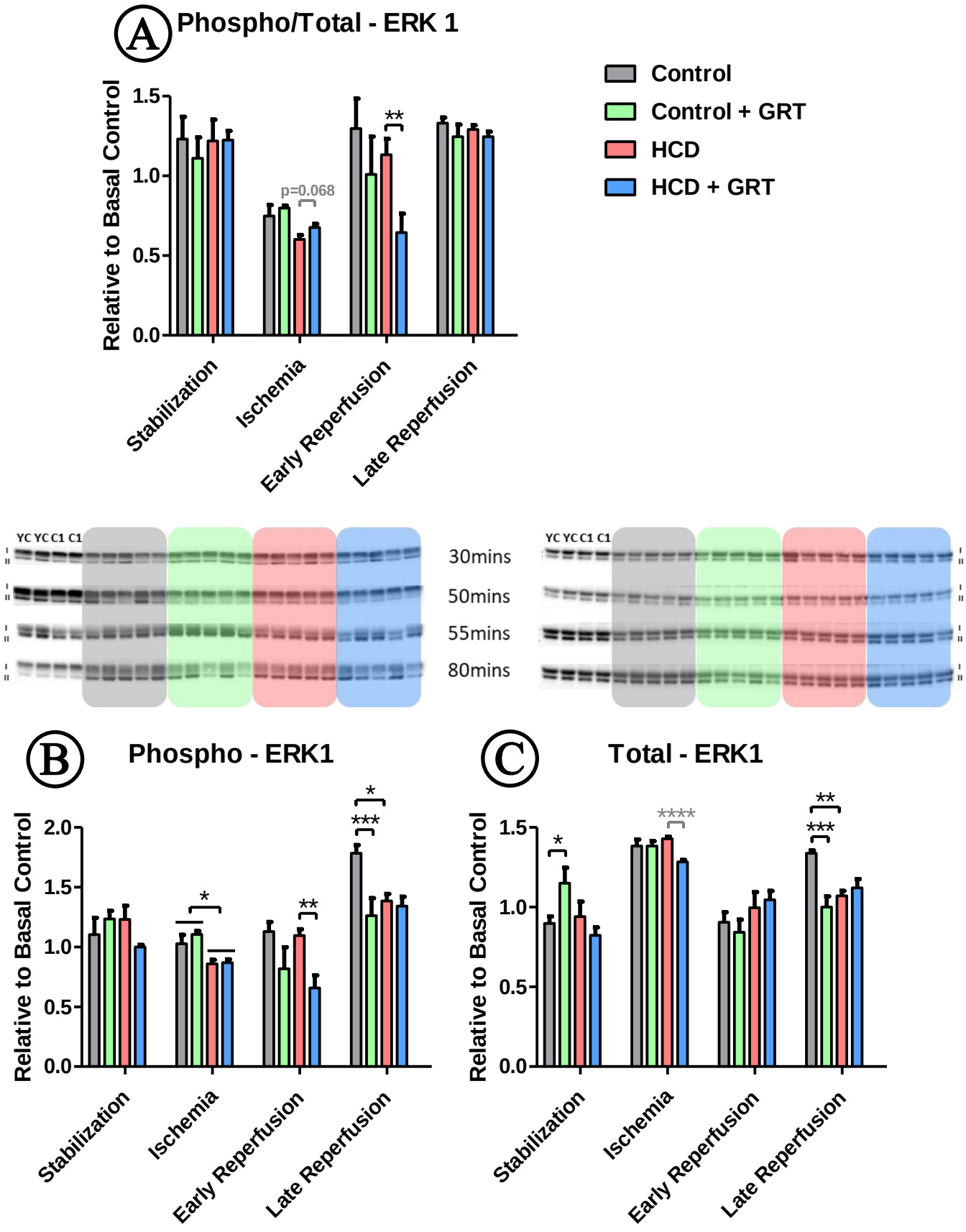

Figure 5.28 ERK1 Ratio (A) of Activation (B) to Expression (C) between the different groups and time points (n=5). HCD: High-caloric diet, GRT: Afriplex green rooibos extract.

5.4.5 ERK2

Whether ERK1 and ERK2 specify functional differences or are in contrast functionally redundant, constitutes an ongoing debate despite the huge amount of studies performed to date (Buscà *et al.*, 2016). However, for the sake of investigating both isoforms were considered for analysis.

- ***Stabilization***

GRT supplementation significantly increased ERK2 expression in controls ($p<0.05$), but not HCD (**Figure 5.29, Table 5.5**).

- ***Ischemia***

GRT supplementation resulted in a significant decreased ERK2 expression and activation ($p<0.01$ for both) and increased ERK2 activation/expression ratio ($p=0.075$) compared to HCD. No significant differences were observed in controls.

- ***Early Reperfusion***

GRT supplementation significantly increased ERK2 activation and activation/expression ratio in controls ($p<0.0001$ and $p<0.001$ respectively). GRT supplementation also decreased the ERK2 activation/expression ratio ($p<0.01$) in HCD.

- ***Late Reperfusion***

HCD had significantly increased ERK2 expression ($p<0.05$), resulting in increased ERK2 activation/expression ratio ($p<0.05$) compared to controls. GRT supplementation decreased ERK2 expression in controls ($p<0.01$) and decreased the ERK2 activation/expression ratio in HCD ($p<0.01$).

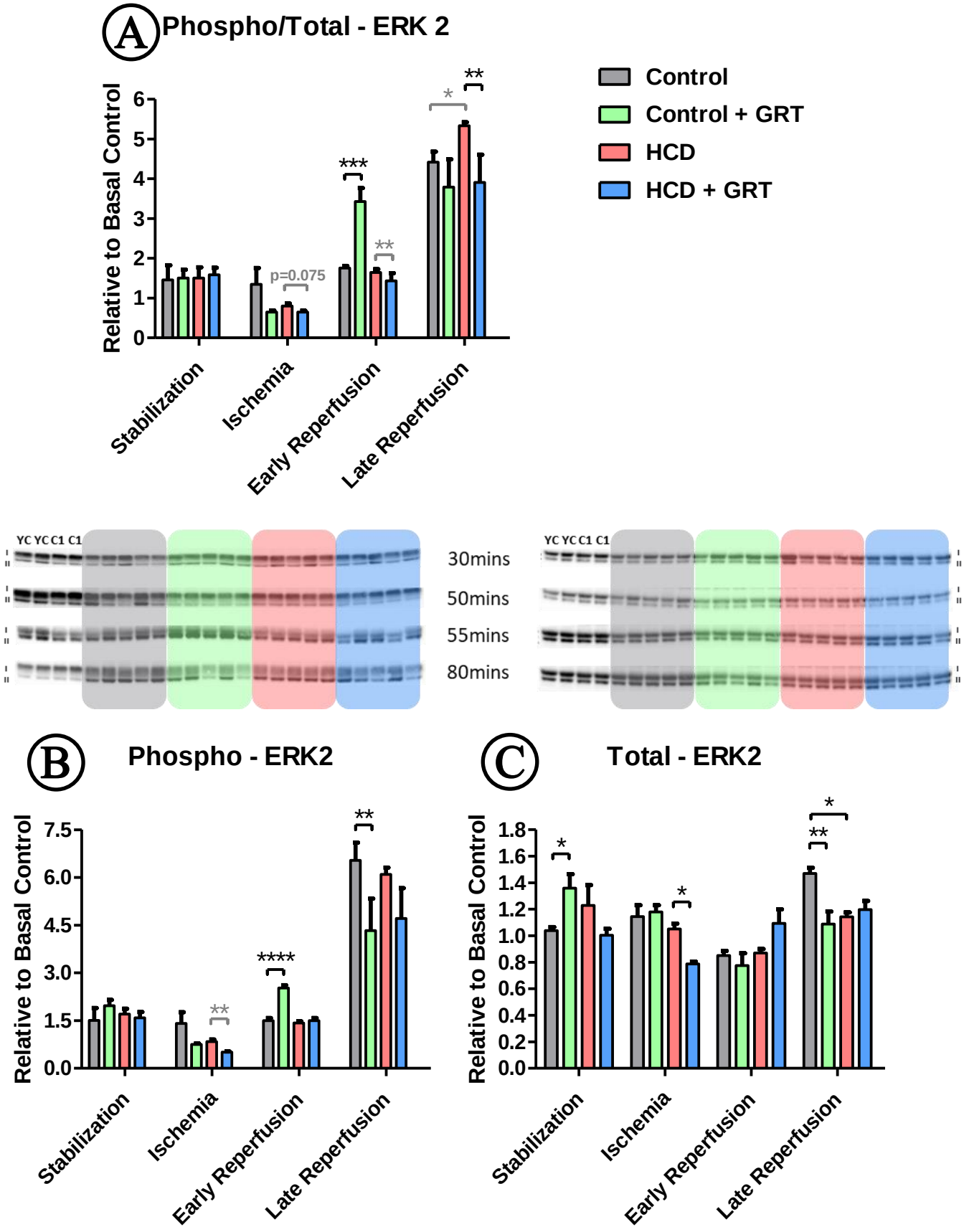

Figure 5.29 ERK2 Ratio (A) of Activation (B) to Expression (C) between the different groups and time points (n=5). HCD: High-caloric diet, GRT: Afriplex green rooibos extract.

5.4.6 ERK1/ERK2

ERK1 and ERK2 seem to be expressed ubiquitously and there are no obvious regulatory differences inferred from their protein sequences, their regulation or their sub-cellular localization (Buscà *et al.*, 2016).

- ***Stabilization***

There were no significant differences in ERK1/ERK2 expression or activation ratios for any of the 4 groups (**Figure 5.30, Table 5.5**).

- ***Ischemia***

GRT supplementation resulted in significantly increased ERK1/ERK2 activation ratio in both control and HCD ($p<0.001$ for both) and increased ERK1/ERK2 expression ratio in HCD ($p<0.001$).

- ***Early Reperfusion***

GRT supplementation resulted in significantly decreased ERK1/ERK2 activation ratio in both control and HCD ($p<0.001$ and $p<0.05$ respectively) and decreased ERK1/ERK2 expression ratio in HCD ($p<0.05$).

- ***Late Reperfusion***

There were no significant differences in ERK1/ERK2 expression or activation ratios for any of the 4 groups.

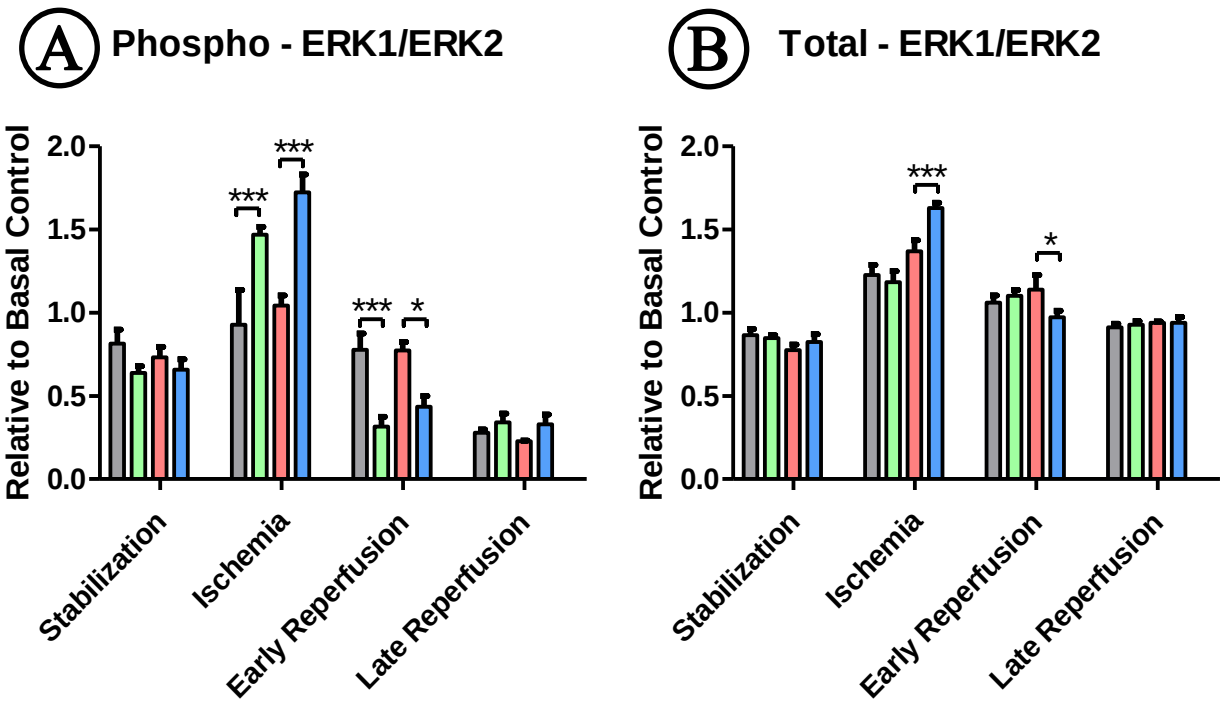

Figure 5.30 Ratio between ERK1 and ERK2 Activation (A) and Expression (B) between the different groups and time points (n=5). HCD: High-caloric diet, GRT: Afriplex green rooibos extract.

5.4.7 JNK1

JNK's are activated in response to inflammatory cytokines and cellular stress but early activation of JNK in reperfusion is known to be a pre-requisite for the activation of PKB (Fan, 2017). The latter occurrence is recognized as cardioprotective as part of the RISK pathway.

- ***Stabilization and Ischemia***

JNK1 activation was detectable in either of the groups prior to reperfusion, while expression was also faint in comparison to JNK2 (**Figure 5.31, Table 5.5**).

- ***Early Reperfusion***

HCD resulted in significantly decreased JNK1 expression and activation ($p<0.001$ for both), and increased JNK1 activation/expression ratio ($p<0.001$) compared to controls. GRT supplementation resulted in increased JNK1 activation, and subsequently JNK1 activation/expression ratio in controls but not in the HCD ($p<0.05$ and $p<0.001$ respectively).

- ***Late Reperfusion***

HCD had significantly increased JNK1 activation ($p<0.001$) and increased JNK1 activation/expression ratio ($p<0.001$) compared to controls. GRT supplementation resulted in increased JNK1 activation, and subsequently JNK1 activation/expression ratio in controls ($p<0.001$ for both) but not in the HCD.

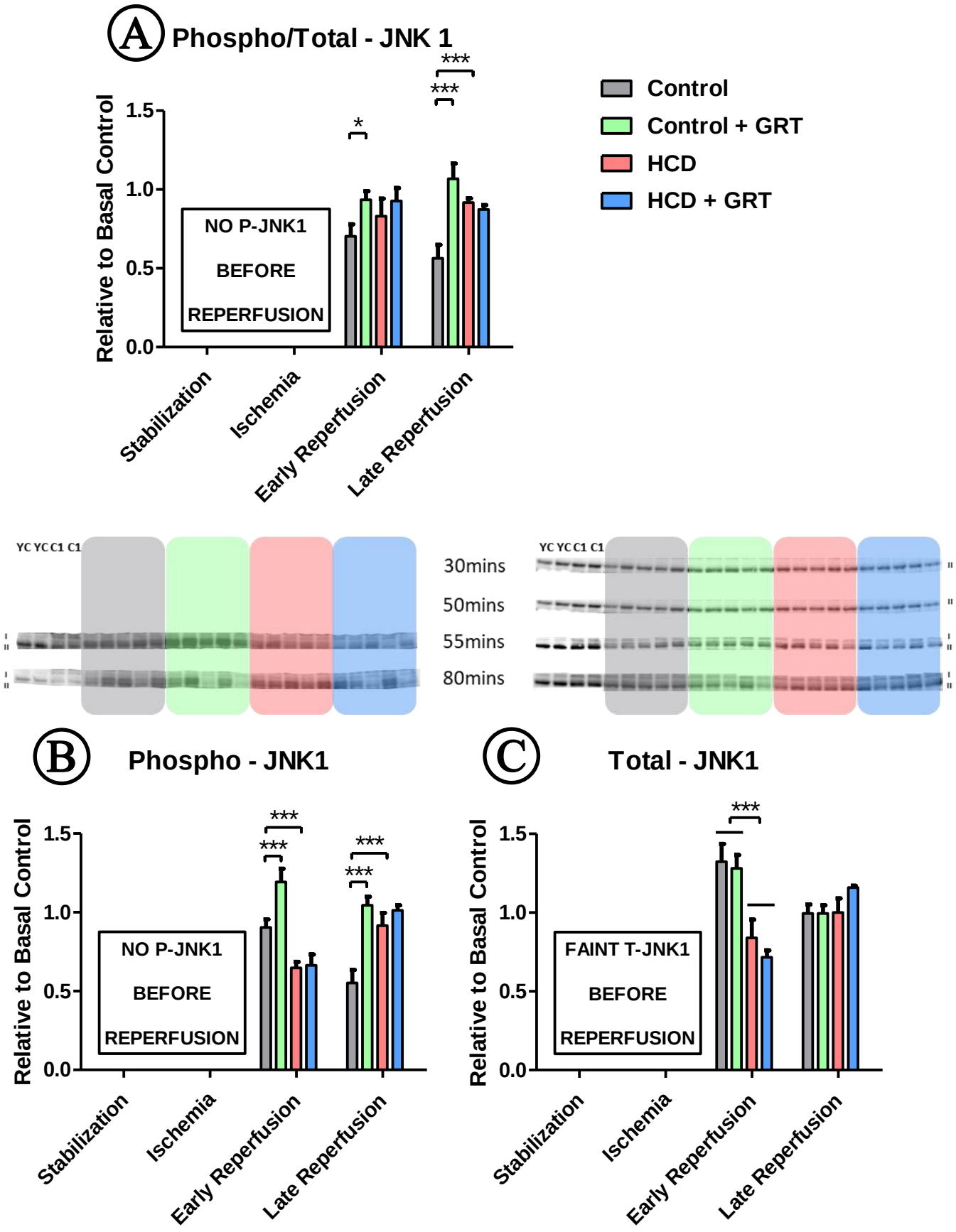

Figure 5.31 JNK1 Ratio (A) of Activation (B) to Expression (C) between the different groups and time points (n=5). HCD: High-caloric diet, GRT: Afriplex green rooibos extract.

5.4.8 JNK2

- ***Stabilization***

GRT supplementation increased JNK2 expression in controls ($p<0.05$), but not HCD. No JNK2 activation detected prior to reperfusion.

- ***Ischemia***

No significant differences were observed in JNK2 expression during ischemia, and no JNK2 activation detected prior to reperfusion (**Figure 5.32, Table 5.5**).

- ***Early Reperfusion***

HCD increased JNK2 expression ($p<0.05$), but decreased JNK2 activation ($p<0.01$), resulting in a decrease of JNK2 activation/expression vs controls ($p<0.001$). GRT supplementation significantly increased JNK2 expression ($p<0.05$) and activation ($p<0.01$) in controls. In HCD, GRT supplementation decreased JNK2 activation and consequently decreased the JNK2 activation/expression ratio ($p<0.05$ for both).

- ***Late Reperfusion***

HCD had significantly increased JNK2 activation ($p<0.001$), resulting in increased JNK2 activation/expression ratio ($p<0.05$) compared to controls. Subsequently, GRT supplementation decreased JNK2 activation ($p<0.05$) in HCD.

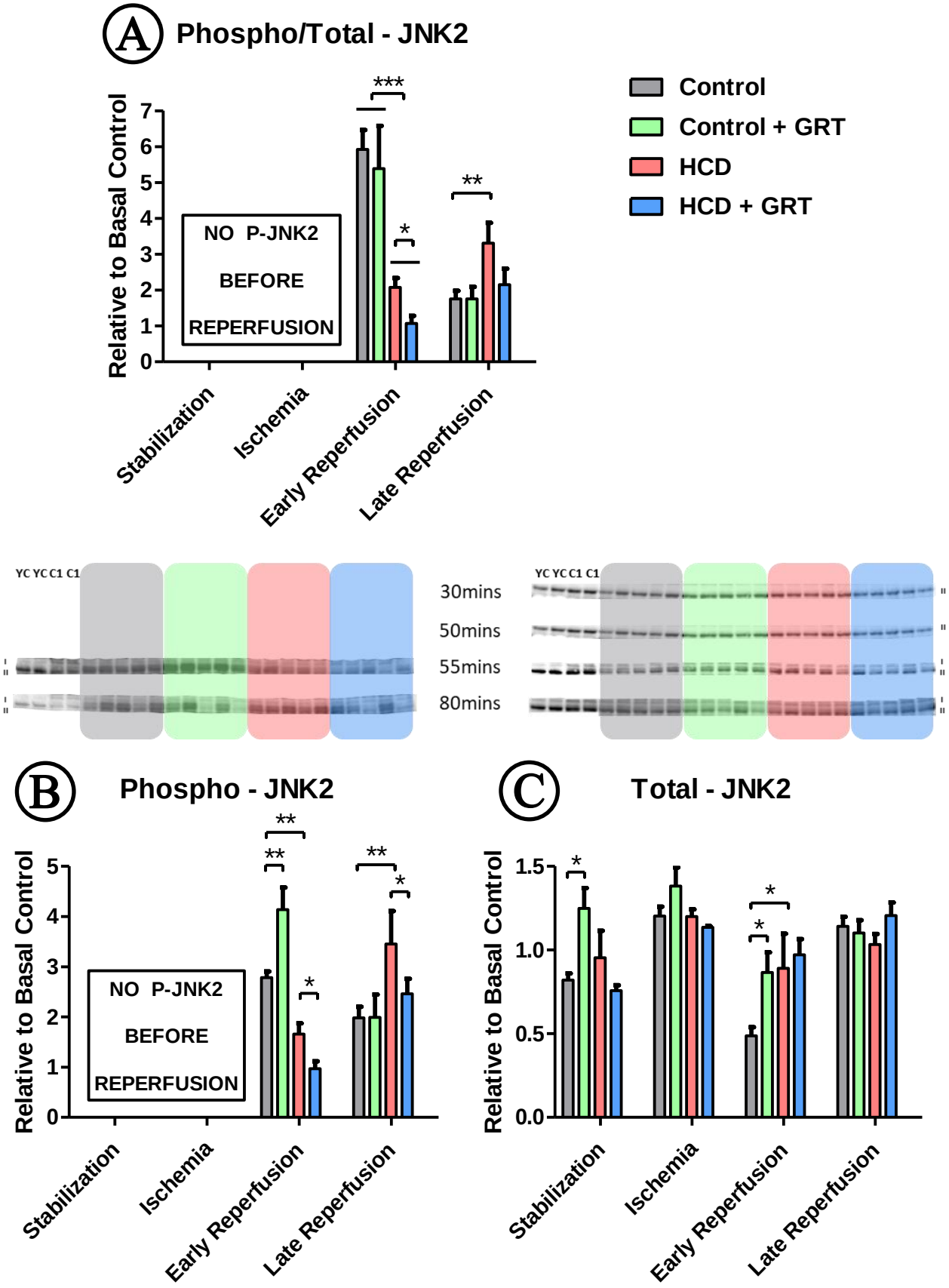

Figure 5.32 JNK2 Ratio (A) of Activation (B) to Expression (C) between the different groups and time points (n=5). HCD: High-caloric diet, GRT: Afriplex green rooibos extract.

5.4.9 p38

p38 MAPK is predominately expressed and activated in response to inflammation but is also known to be activated during reperfusion where elevated levels are associated with apoptotic cell death (Surinkaew *et al.*, 2013).

- ***Stabilization***

P38 activation was significantly increased in HCD compared to controls ($p<0.001$), which also led to an increased p38 activation/expression ratio ($p<0.001$) (**Figure 5.33, Table 5.6**). GRT supplementation in controls also led to significantly higher p38 activation ($p<0.001$) and p38 activation/expression ratio ($p<0.01$). GRT supplementation in HCD decreased p38 activation and expression ($p<0.01$), but increased p38 activation/expression ratio compared to untreated HCD ($p<0.05$).

- ***Ischemia***

GRT supplementation resulted in increased p38 expression and activation ($p<0.01$ and $p=0.078$) in controls, but not in HCD.

- ***Early Reperfusion***

GRT supplementation led to a significant increase in p38 activation in controls ($p<0.01$) and decrease in p38 expression in HCD ($p<0.05$). No significant differences between untreated controls and HCD were recorded.

- ***Late Reperfusion***

P38 expression and activation was decreased in HCD compared to controls ($p<0.01$ and 0.074 respectively).

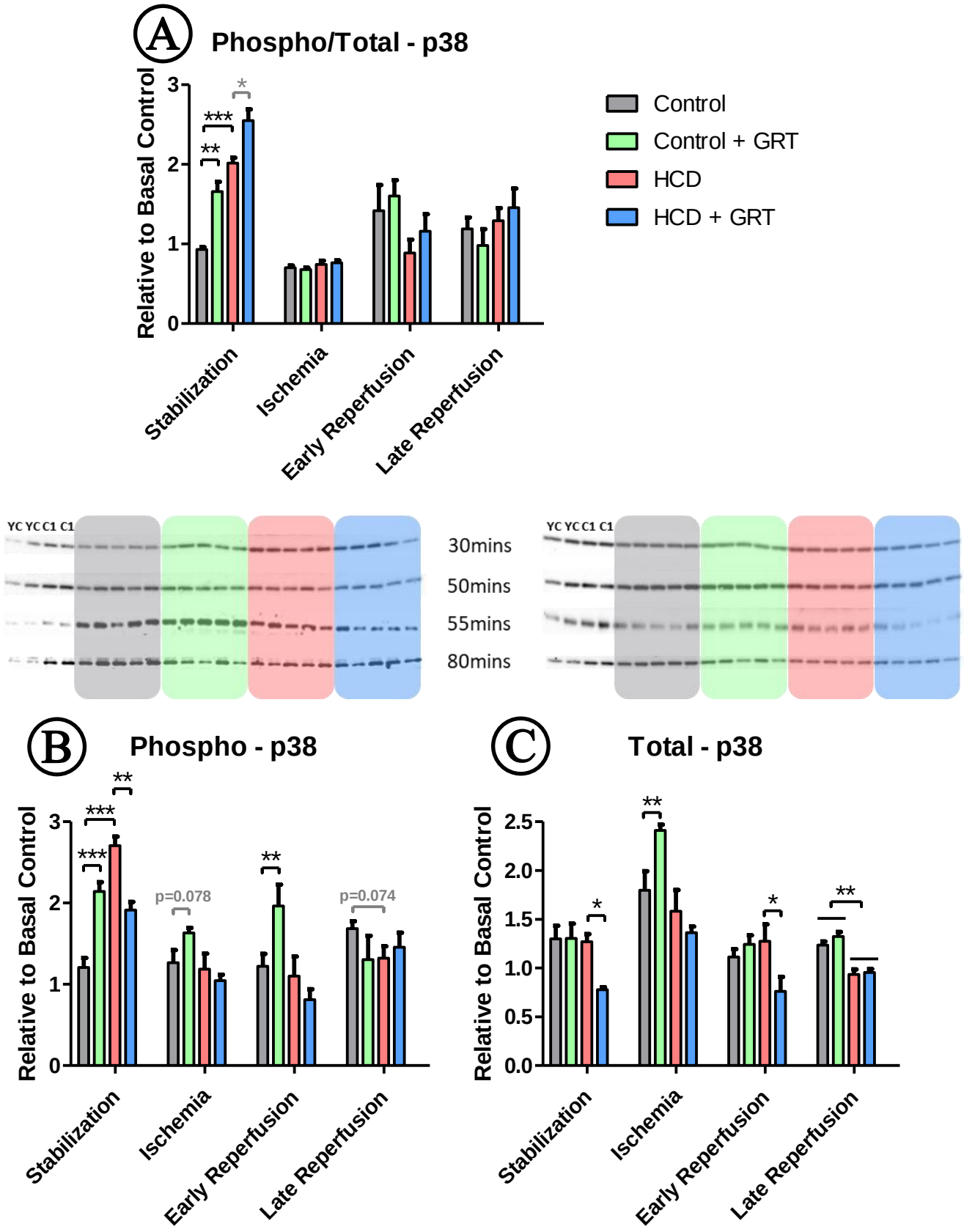

Figure 5.33 p38 Ratio (A) of Activation (B) to Expression (C) between the different groups and time points (n=5). HCD: High-caloric diet, GRT: Afriplex green rooibos extract.

5.4.10 LC3-I and -II

LC3-A and LC3-B are referred to as LC3-I and LC3-II, respectively. During the activation of autophagy, the cytosolic LC3-I (substrate) is converted into the phagophore-bound LC-II (product) – a process termed LC3 conversion. The LC-II/LC-I ratio thus shows the degree of conversion, and to a certain degree the flux of autophagy (Oh *et al.*, 2017).

- ***Stabilization***

LC3-I and II was significantly elevated in HCD compared to controls ($p<0.05$ and $p<0.01$ respectively). LC3-II was also significantly elevated in controls supplemented with GRT ($p<0.001$), which also resulted in an elevated LC3-II/LC3-I ratio ($p<0.05$). No significant differences were noted in HCD supplemented with GRT (**Figure 5.34, Table 5.6**).

- ***Ischemia***

HCD increased LC3-I ($p=0.086$), while GRT supplementation in HCD resulted in a significant decrease in LC3-I ($p<0.05$). LC3-II/LC3-I ratio was significantly decreased in controls with GRT and HCD compared to stabilization ($p<0.05$ for both).

- ***Early Reperfusion***

LC3-I and II were significantly increased in HCD groups compared to controls ($p<0.01$ and $p<0.05$ respectively), while GRT supplementation resulted in decreased LC3-I ($p<0.01$) and therefore increased LC3-II/I ratio ($p<0.05$). In controls, GRT supplementation decreased the LC3-II/I ratio ($p<0.05$).

- ***Late Reperfusion***

LC3- II was decreased in HCD ($p<0.01$), thereby decreasing the LC3-II/I ratio ($p<0.05$). GRT supplementation resulted in a decrease in LC3-I ($p<0.01$) and LC3-II ($p<0.05$) in control animals, but no effect in HCD animals. LC3-II/LC3-I ratio was significantly increased in controls compared to stabilization ($p<0.05$), in controls, controls with GRT and HCD with GRT compared to ischemia ($p<0.05$ for all), and controls with and without GRT compared to early reperfusion ($p<0.05$ for both).

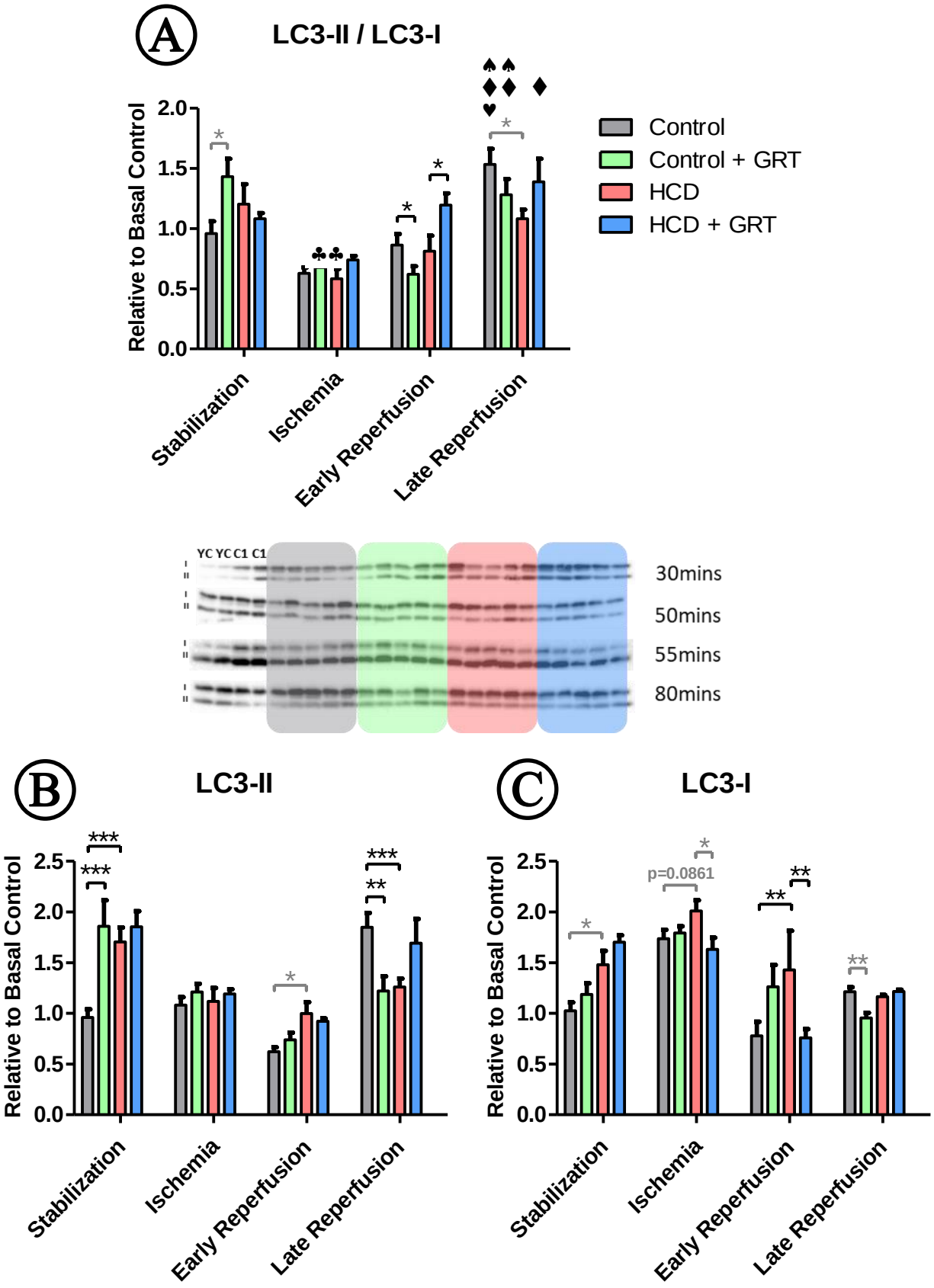

Figure 5.34 LC3-I (C) and II (B) Expression Ratio (A) between the different groups and time points (n=5). HCD: High-caloric diet, GRT: Afriplex green rooibos extract. ♣p<0.05 (Stabilization vs Ischemia), ♥p<0.05 (Stabilization vs Late Reperfusion), ♦p<0.05 (Late Reperfusion vs Ischemia), ♠ p<0.05 (Late Reperfusion vs Early Reperfusion).

5.4.11 GSK3β

GSK3β plays a prominent role within glucose homeostasis, cardioprotection and the RISK pathway where it is seen as the end-effector in the closure of the mPTP (Ghaderi *et al.*, 2017a).

- ***Stabilization***

HCD elevated the GSK3β phosphorylation/expression ratio ($p=0.053$) compared to controls. GRT supplementation in HCD decreased GSK3β expression ($p<0.05$) and phosphorylation ($p<0.01$) compared to untreated HCD (**Figure 5.35, Table 5.6**).

- ***Ischemia***

HCD significantly decreased GSK3β phosphorylation ($p<0.05$) and subsequently decreased the GSK3β phosphorylation/expression ratio ($p<0.05$) compared to controls. GRT supplementation had no significant effect on GSK3β signaling.

- ***Early Reperfusion***

HCD significantly decreased GSK3β phosphorylation ($p<0.001$) and subsequently the GSK3β phosphorylation/expression ratio ($p<0.001$) compared to controls. GRT supplementation had no significant effect on GSK3β signaling.

- ***Late Reperfusion***

No significant differences were recorded in GSK3β signaling for either diet or GRT supplementation.

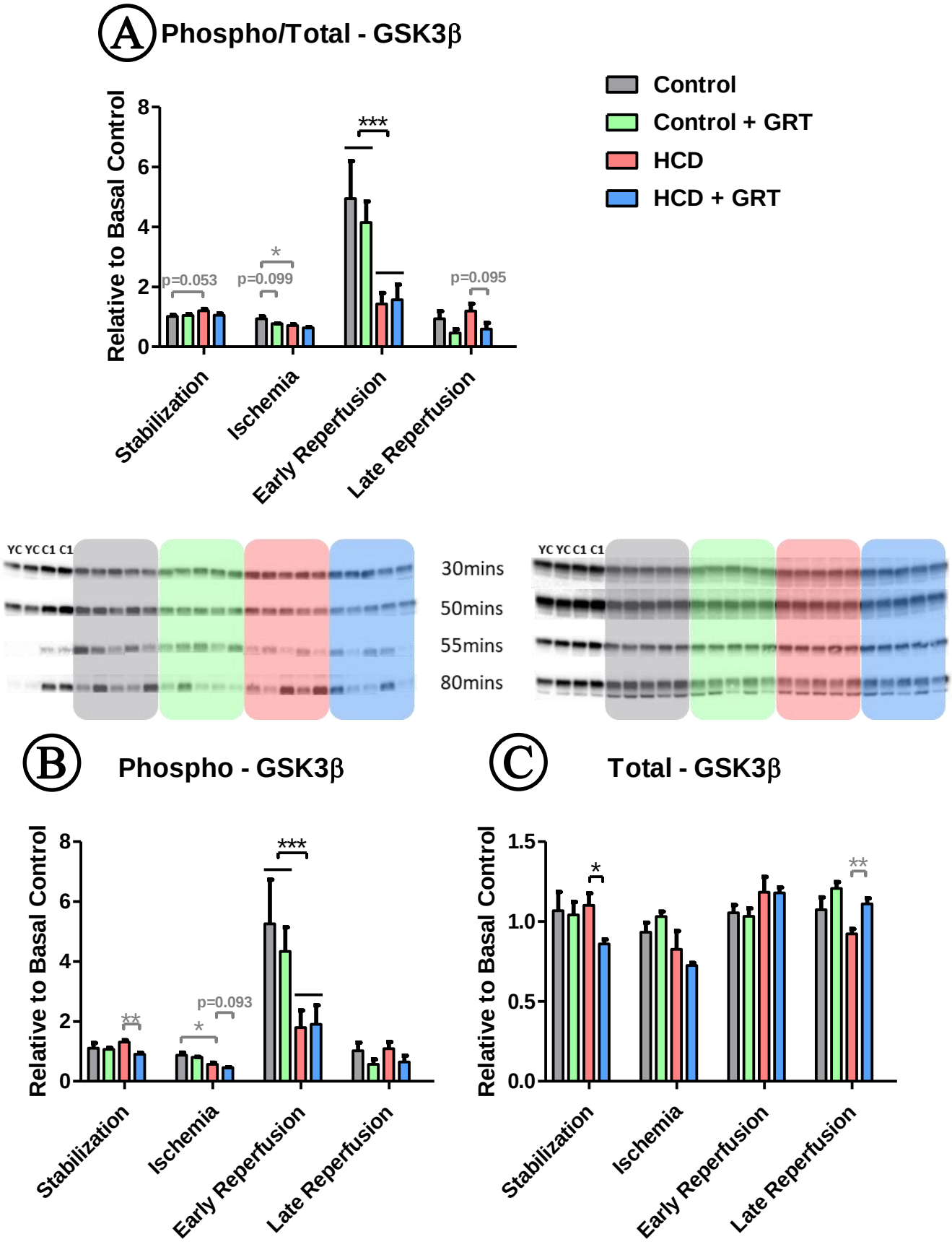

Figure 5.35 GSK3β Ratio (A) of Activation (B) to Expression (C) between the different groups and time points (n=5). HCD: High-caloric diet, GRT: Afriplex green rooibos extract.

5.4.12 ATM

ATM is an important cell signaling kinase in response to cell damage. Its activation is postulated to be a prerequisite for the activation of both PKB and AMPK (Li, Luo, *et al.*, 2017; Viniegra *et al.*, 2005).

.

- ***Stabilization***

There were no significant differences in ATM expression or activation between the groups (**Figure 5.36, Table 5.6**).

- ***Ischemia***

HCD significantly increased ATM activation ($p<0.05$) compared to controls. GRT supplementation in controls but not HCD led to increased ATM expression ($p=0.081$) and activation ($p<0.05$).

- ***Early Reperfusion***

HCD decreased ATM activation ($p<0.05$) compared to controls. GRT supplementation in controls led to decreased ATM expression ($p<0.05$) and ATM activation ($p<0.05$).

- ***Late Reperfusion***

HCD decreased ATM expression ($p<0.05$) and activation ($p<0.001$), whilst GRT supplementation in controls similarly decreased ATM expression ($p<0.05$) and activation ($p<0.001$) compared to controls. GRT supplementation in HCD had no significant effect.

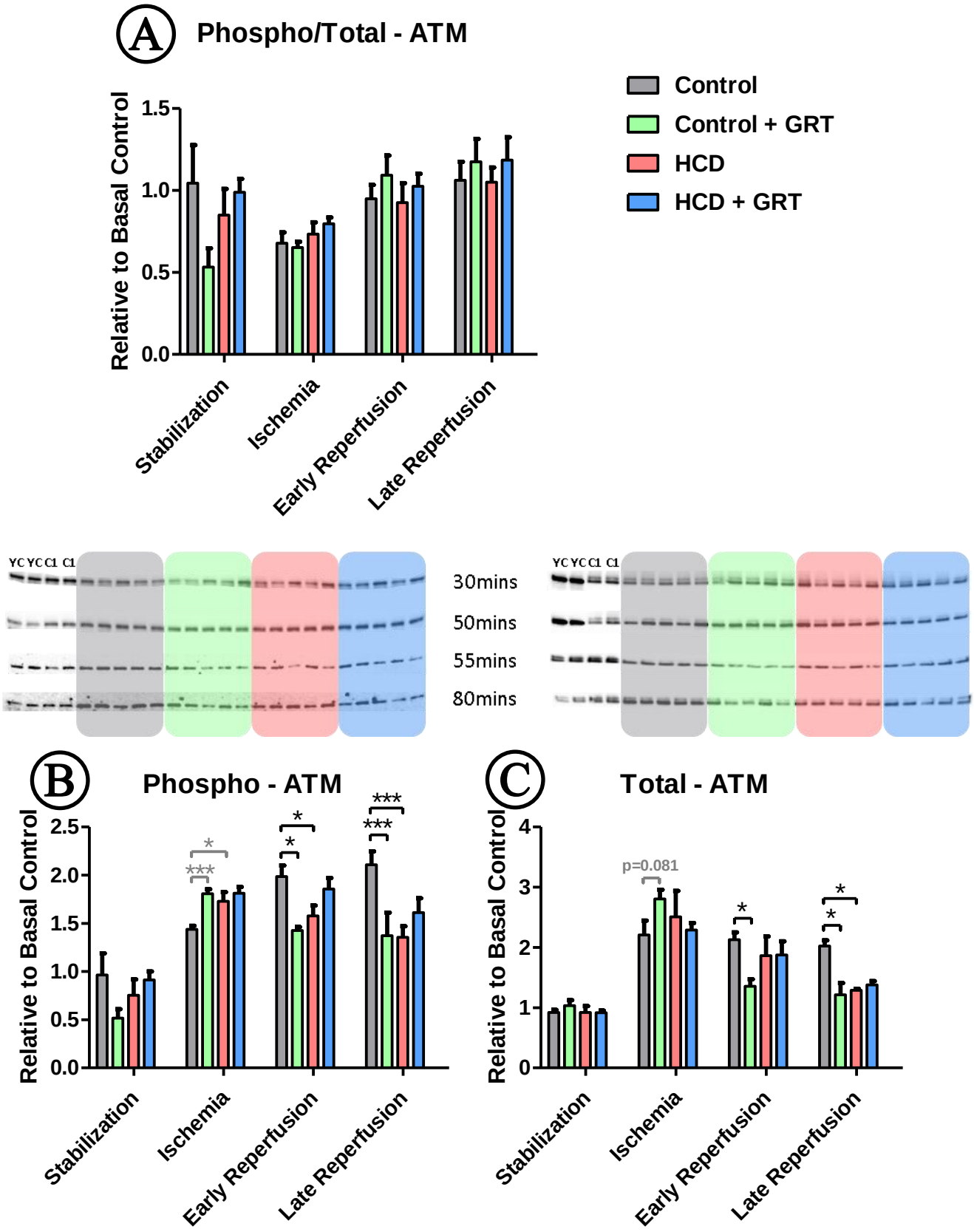

Figure 5.36 ATM Ratio (A) of Activation (B) to Expression (C) between the different groups and time points (n=5). HCD: High-caloric diet, GRT: Afriplex green rooibos extract.

5.4.13 Summary of western blot parameters

Table 5.4 Summary of all cardiac western blot parameters

Parameter	Time Point	CONTROL MEAN±SEM	CONTROL + GRT MEAN±SEM		HCD MEAN±SEM		HCD + GRT MEAN±SEM	
Insulin-dependent Signaling								
T-PKB	Stabilization	1.49±0.16	1.85±0.18		1.71±0.08		1.30±0.07 (♥**)	↓
	Ischemia	0.96±0.08	1.18±0.04(p=0.06)	↑	0.83±0.06		0.79±0.03	
	Early Reperfusion	1.03±0.12	0.85±0.12		1.77±0.45 (♣**)	↑	2.84±0.17 (♥***)	↑
	Late Reperfusion	0.76±0.03	0.58±0.05 (♠*)	↓	0.32±0.02 (♣****)	↓	0.43±0.04(p=0.05)	↑
P-PKB	Stabilization	1.04±0.10	1.48±0.13 (♠*)	↑	0.95±0.03		0.72±0.03 (♥**)	↓
	Ischemia	0.98±0.09	0.97±0.06		0.67±0.02 (♣*)	↓	0.60±0.04	
	Early Reperfusion	1.92±0.20	1.87±0.10		1.12±0.11 (♣*)	↓	0.97±0.06	
	Late Reperfusion	2.54±0.35	1.22±0.30 (♠***)	↓	2.18±0.35		1.46±0.29 (♥*)	↓
P/T-PKB	Stabilization	0.72±0.08	0.84±0.13		0.56±0.01		0.55±0.02	
	Ischemia	1.02±0.08	0.81±0.02(p=0.06)	↓	0.82±0.03 (p=0.07)	↓	0.77±0.07	
	Early Reperfusion	2.04±0.40	2.33±0.27		0.93±0.36 (p=0.08)	↓	0.34±0.04	
	Late Reperfusion	3.33±0.46	2.06±0.49		6.63±1.38 (♣***)	↑	3.72±1.05 (♥**)	↓
Insulin-independent Signaling								
T-AMPK	Stabilization	1.14±0.07	1.58±0.03 (♠***)	↑	1.39±0.07 (♣**)	↑	1.53±0.05	
	Ischemia	0.88±0.04	0.90±0.05		0.87±0.03		0.90±0.02	
	Early Reperfusion	1.02±0.02	1.05±0.02		0.97±0.01		0.91±0.00 (♥*)	↓
	Late Reperfusion	1.25±0.04	1.00±0.05 (♠**)	↓	0.93±0.02 (♣***)	↓	1.30±0.07 (♥***)	↑
P-AMPK	Stabilization	0.91±0.06	0.98±0.05		0.72±0.09		0.63±0.03	
	Ischemia	0.73±0.03	0.92±0.02 (♠*)	↑	0.99±0.07 (♣*)	↑	0.82±0.01(p=0.08)	↓
	Early Reperfusion	0.72±0.02	0.67±0.05		0.76±0.11		1.38±0.13 (♥***)	↑
	Late Reperfusion	0.37±0.05	0.42±0.02		0.39±0.04		0.44±0.03	
P/T-AMPK	Stabilization	0.81±0.07	0.62±0.04(p=0.06)	↓	0.53±0.09 (♣*)	↓	0.41±0.01	
	Ischemia	0.83±0.05	1.04±0.09(p=0.09)	↑	1.14±0.12 (♣*)	↑	0.91±0.02	
	Early Reperfusion	0.71±0.03	0.63±0.04		0.78±0.12		1.51±0.14 (♥***)	↑
	Late Reperfusion	0.29±0.03	0.42±0.01 (♠*)	↑	0.42±0.03 (♣*)	↑	0.34±0.02	
T-AS160	Stabilization	1.15±0.14	2.05±0.53 (♠*)	↑	1.77±0.23 (p=0.07)	↑	2.81±0.21 (♥**)	↑
	Ischemia	1.36±0.33	0.55±0.04 (♠*)	↓	1.30±0.11		0.87±0.17(p=0.08)	↓
	Early Reperfusion	1.85±0.06	1.98±0.12		2.18±0.27		2.13±0.17	
	Late Reperfusion	0.85±0.14	0.85±0.08		0.70±0.07		0.64±0.05	
P-AS160	Stabilization	1.93±0.49	0.61±0.21 (♠**)	↓	1.35±0.54		0.30±0.09 (♥*)	↓
	Ischemia	1.74±0.17	2.15±0.20		1.25±0.35		0.74±0.16	
	Early Reperfusion	1.85±0.11	1.62±0.21		1.37±0.39		0.70±0.17	
	Late Reperfusion	1.13±0.17	0.78±0.23		1.15±0.27		0.62±0.12	
P/T-AS160	Stabilization	1.74±0.54	0.52±0.24(p=0.10)	↓	0.78±0.29		0.10±0.03(p=0.09)	↓
	Ischemia	1.95±0.77	4.15±0.79 (♠***)	↑	0.99±0.28		0.90±0.22	
	Early Reperfusion	0.99±0.03	0.82±0.10		0.59±0.12 (♣*)	↓	0.36±0.11	
	Late Reperfusion	1.41±0.21	0.99±0.33		1.58±0.27		0.93±0.13(p=0.09)	↓

HCD: High-caloric diet, GRT: Afriplex green rooibos extract; Control + GRT significance and arrow direction compared to Control, HCD significance and arrow direction compared to Control, HCD + GRT significance and arrow direction compared to HCD; *p<0.05, **p<0.01, ***p<0.001, ****p<0.0001 (♠Control + GRT vs Control; ♣HCD vs Control; ♥HCD + GRT vs HCD); n=5 for all groups.

Table 5.5 Summary of all cardiac western blot parameters (continued)

Parameter	Time Point	CONTROL MEAN±SEM	CONTROL + GRT MEAN±SEM		HCD MEAN±SEM		HCD + GRT MEAN±SEM	
RISK Pathway								
T-ERK1	Stabilization	0.89±0.04	1.15±0.09 (♠*)	↑	0.94±0.09		0.82±0.05	
	Ischemia	1.38±0.04	1.38±0.03		1.42±0.01		1.28±0.01 (♥****)	↓
	Early Reperfusion	0.90±0.06	0.84±0.07		0.99±0.09		1.04±0.05	
	Late Reperfusion	1.33±0.01	1.00±0.06 (♠***)	↓	1.07±0.03 (♣**)	↓	1.12±0.05	
P-ERK1	Stabilization	1.10±0.14	1.23±0.06		1.23±0.11		1.00±0.01	
	Ischemia	1.02±0.07	1.10±0.02		0.86±0.03 (p=0.09)	↓	0.86±0.02	
	Early Reperfusion	1.13±0.08	0.81±0.18		1.09±0.05		0.65±0.10 (♥**)	↓
	Late Reperfusion	1.78±0.06	1.26±0.14 (♠***)	↓	1.38±0.05 (♣*)	↓	1.34±0.07	
P/T-ERK1	Stabilization	1.23±0.13	1.11±0.13		1.22±0.13		1.22±0.05	
	Ischemia	0.74±0.06	0.79±0.01		0.60±0.02		0.67±0.02(p=0.07)	↑
	Early Reperfusion	1.29±0.18	1.01±0.23		1.13±0.09		0.64±0.11 (♥**)	↓
	Late Reperfusion	1.33±0.03	1.24±0.07		1.29±0.02		1.24±0.03	
T-ERK2	Stabilization	1.03±0.02	1.35±0.10 (♠*)	↑	1.22±0.15		1.00±0.05	
	Ischemia	1.14±0.08	1.18±0.05		1.05±0.04		0.78±0.01 (♥**)	↓
	Early Reperfusion	0.85±0.03	0.77±0.09		0.87±0.02		1.09±0.10	
	Late Reperfusion	1.47±0.04	1.08±0.09 (♠**)	↓	1.14±0.03 (*)	↑	1.19±0.06	
P-ERK2	Stabilization	1.50±0.39	1.97±0.18		1.70±0.16		1.59±0.45	
	Ischemia	1.41±0.35	0.75±0.02		0.83±0.06		0.50±0.02 (♥**)	↓
	Early Reperfusion	1.49±0.08	2.52±0.08 (♠****)	↑	1.42±0.05		1.49±0.08	
	Late Reperfusion	6.53±0.55	4.33±1.00 (♠**)	↓	6.09±0.20		4.71±0.95	
P/T-ERK2	Stabilization	1.45±0.37	1.50±0.21		1.50±0.26		1.58±0.17	
	Ischemia	1.34±0.40	0.64±0.04		0.80±0.06		0.64±0.03(p=0.08)	↓
	Early Reperfusion	1.35±0.15	3.43±0.34 (♠***)	↑	1.25±0.03		0.64±0.13 (♥**)	↓
	Late Reperfusion	4.41±0.26	3.79±0.69		5.33±0.08 (♣*)	↑	3.90±0.69 (♥**)	↓
T-ERK1/2	Stabilization	0.86±0.03	0.84±0.01		0.77±0.03		0.82±0.04	
	Ischemia	1.22±0.06	1.18±0.06		1.37±0.06		1.63±0.03 (♥***)	↑
	Early Reperfusion	1.06±0.04	1.10±0.03		1.13±0.08		0.97±0.04 (♥*)	↓
	Late Reperfusion	0.91±0.02	0.92±0.02		0.93±0.00		0.94±0.03	
P-ERK1/2	Stabilization	0.81±0.08	0.63±0.04		0.73±0.06		0.65±0.06	
	Ischemia	0.92±0.20	1.46±0.04 (♠***)	↑	1.04±0.06		1.72±0.10 (♥***)	↑
	Early Reperfusion	0.77±0.09	0.31±0.05 (♠***)	↓	0.77±0.09		0.43±0.06 (♥*)	↓
	Late Reperfusion	0.27±0.02	0.34±0.05		0.22±0.00		0.32±0.05	
Stress-Signaling								
T-JNK1	Early Reperfusion	1.32±0.11	1.28±0.08		0.83±0.11 (♣***)	↓	0.71±0.04	
	Late Reperfusion	0.99±0.05	0.99±0.05		1.00±0.08		1.15±0.01	
P-JNK1	Early Reperfusion	0.90±0.05	1.19±0.08 (♠***)	↑	0.64±0.03 (♣***)	↓	0.66±0.06	
	Late Reperfusion	0.56±0.08	1.06±0.09 (♠***)	↑	0.91±0.02 (♣***)	↑	0.87±0.02	
P/T-JNK1	Early Reperfusion	0.70±0.07	0.93±0.05 (♠*)	↑	0.83±0.11		0.92±0.08	
	Late Reperfusion	0.56±0.08	1.06±0.09 (♠***)	↑	0.91±0.02 (♣***)	↑	0.87±0.02	
T-JNK2	Stabilization	0.82±0.03	1.24±0.12 (♠*)	↑	0.95±0.16		0.75±0.03	
	Ischemia	1.20±0.05	1.38±0.11		1.20±0.04		1.13±0.00	
	Early Reperfusion	0.48±0.05	0.86±0.12 (♠*)	↑	0.89±0.20 (♣*)	↑	0.97±0.09	
	Late Reperfusion	1.14±0.05	1.10±0.07		1.03±0.06		1.20±0.07	
P-JNK2	Early Reperfusion	2.78±0.11	4.13±0.44 (♠**)	↑	1.66±0.21 (♣**)	↓	0.96±0.15 (♥*)	↓
	Late Reperfusion	1.98±0.21	1.99±0.45		3.45±0.65 (♣***)	↑	2.46±0.29 (♥*)	↓
P/T-JNK2	Early Reperfusion	5.92±0.53	5.38±1.19		2.07±0.25 (♣***)	↓	1.06±0.21 (♥*)	↓
	Late Reperfusion	1.75±0.22	1.75±0.33		3.30±0.56 (♣*)	↑	2.15±0.44	

HCD: High-caloric diet, GRT: Afriplex green rooibos extract; Control + GRT significance and arrow direction compared to Control, HCD significance and arrow direction compared to Control, HCD + GRT significance and arrow direction compared to HCD; *p<0.05, **p<0.01, ***p<0.001, ****p<0.0001 (♠Control + GRT vs Control; ♣HCD vs Control; ♥HCD + GRT vs HCD); n=5 for all groups.

Table 5.6 Summary of all cardiac western blot parameters (continued)

Parameter	Time Point	CONTROL	CONTROL + GRT		HCD		HCD + GRT	
		MEAN±SEM	MEAN±SEM		MEAN±SEM		MEAN±SEM	
Inflammation								
T-p38	Stabilization	1.30±0.13	1.30±0.15		1.27±0.07		0.77±0.25 (♥**)	↓
	Ischemia	1.79±0.19	2.41±0.06 (♠**)	↑	1.58±0.21		1.36±0.06	
	Early Reperfusion	1.11±0.08	1.24±0.09		1.27±0.17		0.76±0.14 (♥*)	↓
	Late Reperfusion	1.23±0.03	1.32±0.04		0.93±0.05 (♣**)	↓	0.95±0.03	
P-p38	Stabilization	1.20±0.11	2.14±0.11 (♠***)	↑	2.70±0.11 (♣***)	↑	1.91±0.10 (♥**)	↓
	Ischemia	1.26±0.15	1.63±0.06(p=0.08)	↑	1.18±0.18		1.04±0.07	
	Early Reperfusion	1.22±0.15	1.96±0.26 (♠**)	↑	1.10±0.24		0.81±0.12	
	Late Reperfusion	1.68±0.09	1.30±0.29		1.32±0.14 (p=0.07)	↓	1.45±0.17	
P/T-p38	Stabilization	0.93±0.03	1.66±0.12 (♠**)	↑	2.01±0.06 (♣***)	↑	2.55±0.13 (♥*)	↑
	Ischemia	0.70±0.02	0.67±0.02		0.74±0.04		0.76±0.02	
	Early Reperfusion	1.41±0.32	1.60±0.19		0.88±0.17		1.16±0.21	
	Late Reperfusion	1.18±0.14	0.98±0.20		1.29±0.15		1.45±0.24	
Autophagy								
LC3-I	Stabilization	1.02±0.08	1.18±0.11		1.48±0.13 (♣*)	↑	1.70±0.06	
	Ischemia	1.73±0.08	1.79±0.06		2.01±0.10 (p=0.09)	↑	1.63±0.11 (♥*)	↓
	Early Reperfusion	0.77±0.14	1.26±0.21		1.42±0.38 (♣**)	↑	0.76±0.08 (♥**)	↓
	Late Reperfusion	1.21±0.04	0.95±0.05 (♠**)	↓	1.16±0.01		1.21±0.01	
LC3-II	Stabilization	0.96±0.07	1.85±0.25 (♠***)	↑	1.70±0.14 (♣**)	↑	1.85±0.15	
	Ischemia	1.08±0.07	1.21±0.08		1.11±0.13		1.19±0.14	
	Early Reperfusion	0.62±0.04	0.73±0.07		0.99±0.11 (♣*)	↑	0.92±0.02	
	Late Reperfusion	1.84±0.14	1.22±0.14 (♠***)	↓	1.25±0.08 (♣**)	↓	1.69±0.24	
LC3-II/I	Stabilization	0.95±0.10	1.43±0.14 (♠*)	↑	1.20±0.16		1.08±0.04	
	Ischemia	0.62±0.05	0.67±0.03		0.58±0.08		0.73±0.03	
	Early Reperfusion	0.86±0.09	0.62±0.06 (♠*)	↓	0.81±0.12		1.19±0.09 (♥*)	↑
	Late Reperfusion	1.53±0.12	1.28±0.13		1.08±0.07 (♣*)	↓	1.39±0.19	
Auxiliary Metabolic Regulation								
T-GSK3β	Stabilization	1.06±0.11	1.04±0.08		1.10±0.07		0.86±0.02 (♥*)	↓
	Ischemia	0.93±0.06	1.03±0.03		0.82±0.11		0.72±0.01	
	Early Reperfusion	1.05±0.04	1.03±0.05		1.18±0.09		1.18±0.03	
	Late Reperfusion	1.07±0.07	1.20±0.03		0.92±0.03		1.11±0.03 (♥**)	↑
P-GSK3β	Stabilization	1.10±0.17	1.06±0.04		1.30±0.06		0.90±0.04 (♥**)	↓
	Ischemia	0.87±0.08	0.79±0.02		0.56±0.05 (♣*)	↓	0.45±0.01(p=0.09)	↓
	Early Reperfusion	5.26±1.47	4.33±0.81		1.79±0.57 (♣***)	↓	1.90±0.63	
	Late Reperfusion	1.02±0.27	0.56±0.16		1.09±0.21		0.64±0.21	
P/T-GSK3β	Stabilization	1.01±0.04	1.04±0.05		1.20±0.06 (p=0.05)	↑	1.05±0.05	
	Ischemia	0.93±0.07	0.77±0.00(p=0.10)	↓	0.70±0.04 (♣*)	↓	0.63±0.02	
	Early Reperfusion	4.94±1.25	4.15±0.69		1.42±0.36 (♣***)	↓	1.57±0.50	
	Late Reperfusion	0.93±0.24	0.45±0.12		1.19±0.24		0.59±0.20(p=0.10)	↓
T-ATM	Stabilization	0.92±0.04	1.03±0.08		0.92±0.10		0.91±0.03	
	Ischemia	2.20±0.24	2.80±0.15(p=0.08)	↑	2.50±0.43		2.28±0.11	
	Early Reperfusion	2.12±0.12	1.35±0.11 (♠*)	↓	1.86±0.31		1.87±0.22	
	Late Reperfusion	2.02±0.09	1.21±0.19 (♠*)	↓	1.29±0.02 (♣*)	↓	1.37±0.06	
P-ATM	Stabilization	0.96±0.22	0.51±0.09		0.75±0.16		0.91±0.08	
	Ischemia	1.43±0.03	1.80±0.04 (♠***)	↑	1.72±0.09 (♣*)	↑	1.81±0.06	
	Early Reperfusion	1.98±0.11	1.42±0.03 (♠*)	↓	1.57±0.10 (♣*)	↓	1.85±0.11	
	Late Reperfusion	2.10±0.14	1.37±0.23 (♠***)	↓	1.35±0.11 (♣***)	↓	1.61±0.15	
P/T-ATM	Stabilization	1.04±0.23	0.53±0.11		0.85±0.16		0.98±0.08	
	Ischemia	0.67±0.06	0.65±0.03		0.73±0.07		0.79±0.03	
	Early Reperfusion	0.95±0.08	1.09±0.12		0.92±0.12		1.02±0.07	
	Late Reperfusion	1.06±0.11	1.17±0.14		1.05±0.08		1.18±0.13	

HCD: High-caloric diet, GRT: Afriplex green rooibos extract; Control + GRT significance and arrow direction compared to Control, HCD significance and arrow direction compared to Control, HCD + GRT significance and arrow direction compared to HCD; *p<0.05, **p<0.01, ***p<0.001, ****p<0.0001 (♠Control + GRT vs Control; ♣HCD vs Control; ♥HCD + GRT vs HCD); n=5 for all groups.

5.5 MITOCHONDRIAL OXPHOS

5.5.1 ADP/O Ratio

The ADP/O Ratio, also referred to as the OxPhos efficiency, gives the ratio of ATP production to total oxygen utilization during state 3 (nmoles ATP/nAtom of oxygen consumed). The ADP/O ratio is calculated as follows: nmoles ADP phosphorylated/nAtoms oxygen utilization during state 3.

- ***Stabilization***

HCD did not significantly influence the ADP/O ratio in either the glutamate or palmitate medium compared to controls. In the glutamate/malate medium, GRT supplementation decreased the ADP/O ratio in controls (2.17±0.11 vs 2.53±0.08; $p<0.05$) and HCD (1.97±0.13 vs 2.33±0.12; $p=0.066$) compared to their untreated counterparts. In the palmitate/malate medium, GRT supplementation also significantly decreased the ADP/O ratio in controls (2.37±0.05 vs 2.76±0.01; $p<0.001$), but not in HCD. (**Figure 5.37, Table 5.7, Appendix A7**).

- ***Ischemia***

In the palmitate medium, GRT supplementation decreased the ADP/O ratio in HCD (2.46±0.07 vs 2.78±0.26; $p=0.065$), but not in controls.

- ***Early Reperfusion***

GRT supplementation in HCD resulted in a greater ADP/O ratio of mitochondria in palmitate medium, compared to glutamate medium (3.05±0.09 vs 2.32±0.05; $p<0.05$) – a statistical significance not found in the other groups.

- ***Late Reperfusion***

Mitochondria from HCD hearts had a significantly increased ADP/O ratio in palmitate medium compared to glutamate medium (2.75±0.18 vs 2.19±0.16; $p<0.05$).

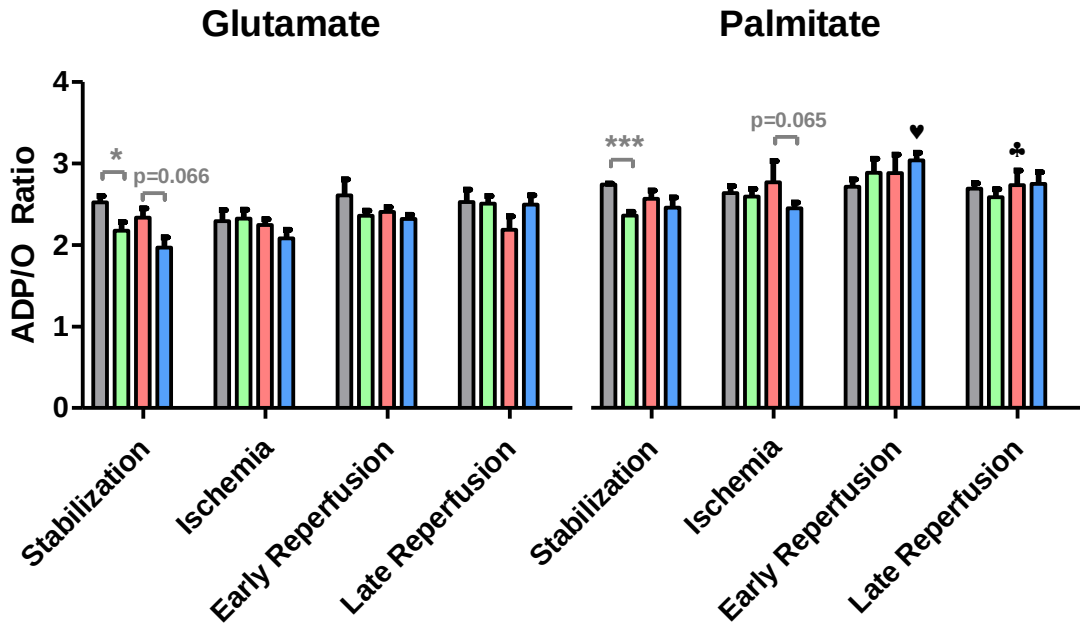

Figure 5.37 ADP/O ratio in glutamate and palmitate medium between different groups and time points (n=5). ♣$p<0.05$ (Palmitate vs Glutamate in HCD), ♥$p<0.05$ (Palmitate vs Glutamate in HCD + GRT).

5.5.2 State 3 Respiration

State 3 respiration (S3) is defined as the mitochondrial respiration in the presence of conversion of ADP to ATP. It is a measure of the number of oxygen atoms utilized in the presence of ADP/mg mitochondrial protein/ min.

- ***Stabilization***

There were no significant differences recorded in mitochondrial S3 attributed to diet prior to ischemia (**Figure 5.38, Table 5.7, Appendix A7**). GRT supplementation in controls did significantly increase mitochondrial S3 in controls only (358.92±12.71 O-atoms/mg/min vs 313.35±13.09 O-atoms/mg/min; $p<0.05$).

- ***Ischemia***

In the glutamate medium, HCD significantly increased mitochondrial S3 compared to controls (272.81±25.6 O-atoms/mg/min vs 177.82±21.37 O-atoms/mg/min; $p<0.05$). In both the glutamate/malate and palmitate/malate medium, GRT supplementation resulted in a significant increase in S3 of mitochondria from controls (280.45±17.34 O-atoms/mg/min vs 177.82±21.37 O-atoms/mg/min; $p<0.01$ and 318.09±5 O-atoms/mg/min vs 245.96±26.73 O-atoms/mg/min, $p=0.053$ respectively), while no effect was found in the HCD group.

- ***Early Reperfusion***

In the palmitate/malate medium, HCD resulted in a significant increase in mitochondrial S3 ($p<0.05$) compared to controls (446.68±26.38 O-atoms/mg/min vs 368.84±10.77 O-atoms/mg/min; $p<0.05$), while GRT supplementation significantly decreased mitochondrial S3 in both glutamate medium (275.61±37.77 O-atoms/mg/min vs 392.34±10.44 O-atoms/mg/min; $p<0.05$) and palmitate medium (297.88±26.53 O-atoms/mg/min vs 446.68±26.38 O-atoms/mg/min; $p<0.01$).

- ***Late Reperfusion***

GRT supplementation resulted in a significant decrease in S3 in mitochondria from controls in both glutamate medium (227.09±14.49 O-atoms/mg/min vs 305.2±19.03 O-atoms/mg/min; $p<0.05$) and palmitate medium (259.76±6.34 O-atoms/mg/min vs 314.9±6.5 O-atoms/mg/min; $p<0.001$).

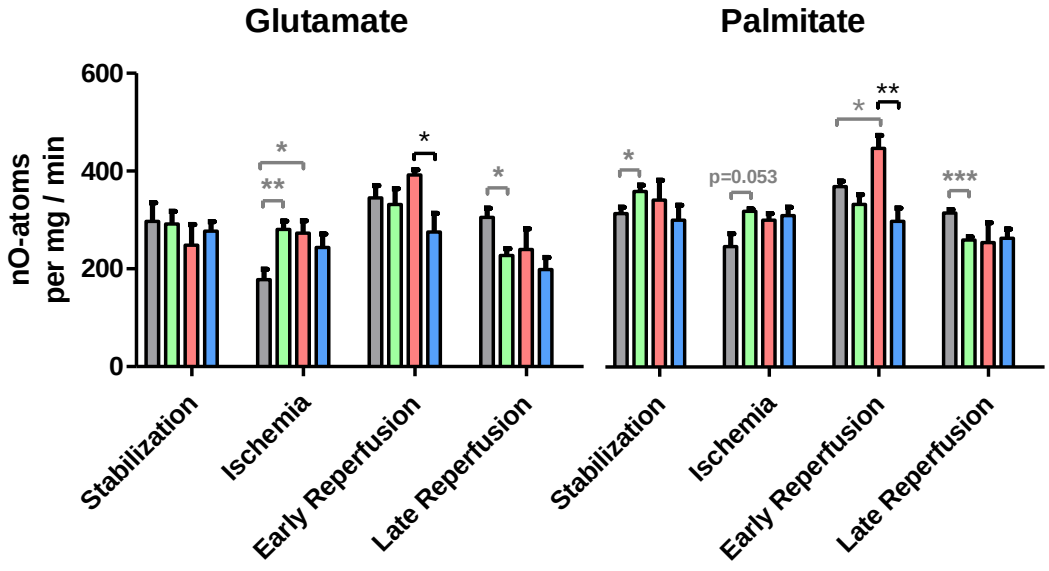

Figure 5.38 State 3 respiration in glutamate and palmitate medium between different groups and time points (n=5).

5.5.3 Oxphos S3

Oxidative phosphorylation rate of State 3 (OxPhos S3) indicates the rate at which ATP is produced during State 3 and is calculated as State 3 X ADP/O ratio (nmoles ATP produced/mg mitochondrial protein/min).

- ***Stabilization***

In the palmitate medium, HCD significantly increased mitochondrial OxPhos S3 compared to glutamate medium (879.23±101.5 moles ATP/mg/min vs 579.11±106.35 moles ATP/mg/min; p<0.05) (**Figure 5.39, Table 5.8, Appendix A7**).

- ***Ischemia***

In the palmitate medium, GRT supplementation in HCD increased mitochondrial OxPhos S3 compared to glutamate medium (724.49±41.41 moles ATP/mg/min vs 441.14±38.77 moles ATP/mg/min; p<0.05). In the glutamate/malate medium, GRT supplementation in controls resulted in a significant increase in OxPhos S3 (653.83±58.72 moles ATP/mg/min vs 355±37.38 moles ATP/mg/min; p<0.05), while non-signifantly increasing OxPhos S3 in Palmitate medium (830.26±36.8 moles ATP/mg/min vs 578.04±106.03 moles ATP/mg/min; p=0.075).

- ***Early Reperfusion***

In both the glutamate/malate and palmitate/malate medium, GRT supplementation in HCD decreased mitochondrial OxPhos S3 (641.21±92.55 moles ATP/mg/min vs 943.19±28.14 moles ATP/mg/min; p<0.05 and 913.69±92.23 moles ATP/mg/min vs 1276.93±70.55 moles ATP/mg/min; p<0.05 respectively), while no effect was observed in the controls. In palmitate medium, HCD had significantly increased mitochondrial OxPhos S3 compared to controls (1276.93±70.55 moles ATP/mg/min vs 1007.01±51.39 moles ATP/mg/min; p<0.05) and compared to glutamate medium (943.19±28.14 moles ATP/mg/min; p<0.05).

- ***Late Reperfusion***

In the glutamate/malate medium, HCD had a decreased mitochondrial OxPhos S3 compared to controls (511.31±73.96 moles ATP/mg/min vs 760.98±24.93 moles ATP/mg/min; p<0.05). In the palmitate medium, GRT supplementation in controls resulted in a borderline non-signifant decrease in OxPhos S3 (717.37±47.61 moles ATP/mg/min vs 853.09±38.38 moles ATP/mg/min; p=0.059).

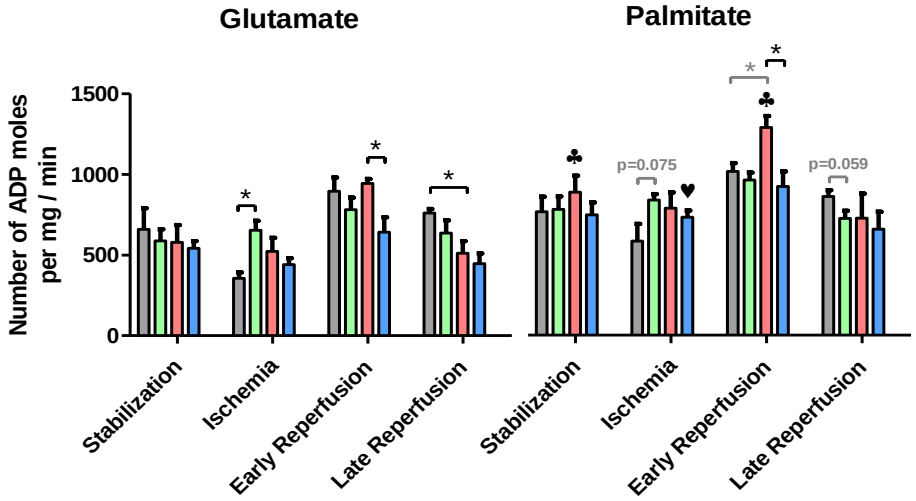

Figure 5.39 Oxidative phosphorylation rate of State 3 in glutamate and palmitate medium between different groups and time points (n=5). ♣p<0.05 (Palmitate vs Glutamate in HCD), ♥p<0.05 (Palmitate vs Glutamate in HCD + GRT).

5.5.4 State 4 Respiration

State 4 respiration (S4) follows State 3 respiration and describes the mitochondrial respiration after all ADP was converted to ATP as nAtoms oxygen utilized in the absence of ADP/mg mitochondrial protein/min.

- ***Stabilization***

In the glutamate medium, HCD significantly decreased S4 compared to controls (64.53±8.99 vs 92.81±8.4 O-atoms/mg/min; p<0.05). In the palmitate medium, GRT supplementation resulted in a significant decrease in S4 in HCD (66.67±2.76 O-atoms/mg/min vs 89.38±11.59 O-atoms/mg/min; p<0.05) (**Figure 5.40, Table 5.7, Appendix A7**).

- ***Ischemia***

In the glutamate medium, HCD significantly increased S4 compared to controls (64.44±3.64 O-atoms/mg/min vs 46.31±5.19 O-atoms/mg/min; p<0.05). In both the glutamate/malate and palmitate/malate medium, GRT supplementation resulted in a significant increase in S4 in controls (69.51±5.36 O-atoms/mg/min vs 46.31±5.19 O-atoms/mg/min; p<0.05 and 87.77±5.69 O-atoms/mg/min vs 65.76±4.98 O-atoms/mg/min; p<0.05 respectively), while no effect was found in the HCD group.

- ***Early Reperfusion***

In the palmitate/malate medium, HCD resulted in an increase in S4 compared to controls (107.27±8.86 O-atoms/mg/min vs 87.31±3.49 O-atoms/mg/min; p=0.088), while GRT supplementation decreased S4 in both glutamate medium (63.46±6.32 O-atoms/mg/min vs 78.31±3.32 O-atoms/mg/min; p=0.083) and palmitate medium (76.16±3.37 O-atoms/mg/min vs 107.27±8.86 O-atoms/mg/min; p<0.01). Furthermore, HCD had a significantly increased S4 in palmitate compared to glutamate (107.27±8.86 O-atoms/mg/min vs 78.31±3.32 O-atoms/mg/min; p<0.05).

- ***Late Reperfusion***

There were no significant differences recorded in S4 during late reperfusion between either of the 4 groups.

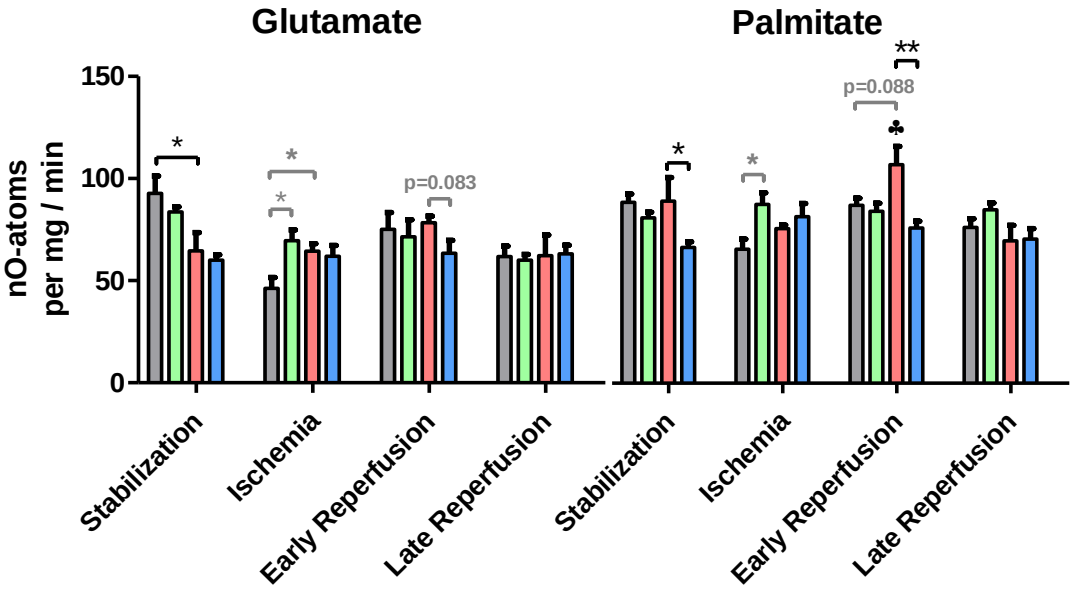

Figure 5.40 State 4 respiration in glutamate and palmitate medium between different groups and time points (n=5). ♣p<0.05 (Palmitate vs Glutamate in HCD).

5.5.5 Oxphos S4

Oxidative phosphorylation rate of State 4 (OxPhos S4): Calculated as State 4 X ADP/O ratio (nmoles ATP produced/mg mitochondrial protein/min).

- ***Stabilization***

HCD has a significantly increased mitochondrial OxPhos S4 in palmitate medium compared to glutamate medium (230.25±29.53 moles ATP/mg/min vs 149.51±20.53 moles ATP/mg/min; p<0.05), while GRT supplementation in HCD decreased OxPhos S4 in palmitate medium (163.9±8.02 moles ATP/mg/min vs 230.25±29.53 moles ATP/mg/min; p=0.088) (**Figure 5.41, Table 5.8, Appendix A7**).

- ***Ischemia***

In both glutamate/malate and palmitate/malate medium, GRT supplementation resulted in an increase in OxPhos S4 in controls (163.28±18.76 moles ATP/mg/min vs 112.19±10.48 moles ATP/mg/min; p=0.053 and 229.65±19.02 moles ATP/mg/min vs 169.86±19.33 moles ATP/mg/min; p=0.059 respectively), while no effect was found in the HCD group. In the palmitate medium compared to glutamate medium, OxPhos S4 was significantly increased in both HCD (202.41±26.53 moles ATP/mg/min vs 130.03±12.66 moles ATP/mg/min; p<0.05) and HCD supplemented with GRT (196.59±20.07 moles ATP/mg/min vs 124.43±7.34 moles ATP/mg/min; p<0.05).

- ***Early Reperfusion***

In the palmitate/malate medium, OxPhos S4 was significantly increased in HCD compared to control (306.79±23.57 moles ATP/mg/min vs 238.03±12.52 moles ATP/mg/min; p<0.05), whereas GRT supplementation in HCD resulted in a decreased OxPhos S4 in both palmitate medium (231.53±6.43 moles ATP/mg/min vs 306.79±23.57 moles ATP/mg/min; p<0.05) and glutamate medium (147.76±16.14 moles ATP/mg/min vs 189.11±12.17 moles ATP/mg/min; p=0.078). Furthermore, both HCD and HCD supplemented with GRT had increased OxPhos S4 in palmitate medium compared to glutamate medium (306.79±23.57 moles ATP/mg/min vs 189.11±12.17 moles ATP/mg/min; p<0.05 and 231.53±6.43 moles ATP/mg/min vs 147.76±16.14 moles ATP/mg/min; p<0.05 respectively).

- ***Late Reperfusion***

No significant differences were noted in OxPhos S4 between either of the groups during late reperfusion.

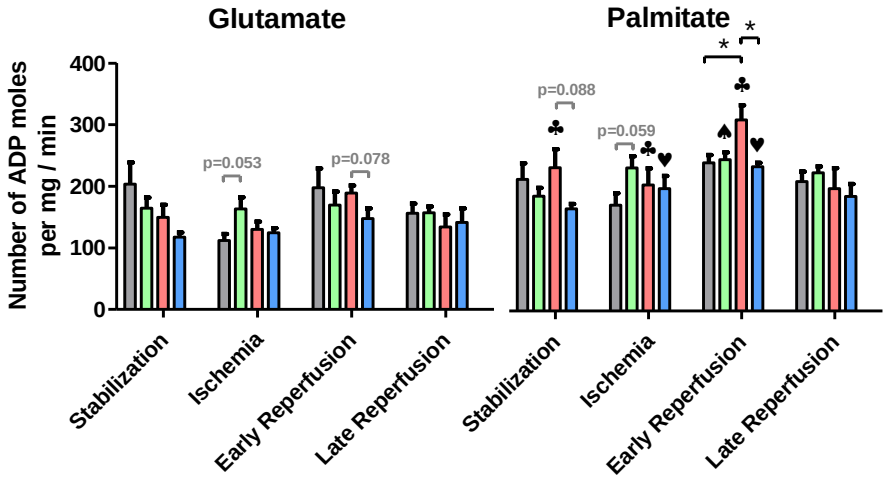

Figure 5.41 Oxidative phosphorylation rate of State 4 in glutamate and palmitate medium between different groups and time points (n=5). ♠p<0.05 (Palmitate vs Glutamate in Control + GRT), ♣p<0.05 (Palmitate vs Glutamate in HCD), ♥p<0.05 (Palmitate vs Glutamate in HCD + GRT).

5.5.6 RCI

Respiratory control index (RCI) is given by S3/S4 (an indicator of the tightness of coupling between respiration and phosphorylation).

- ***Stabilization***

HCD did not significantly alter RCI compared to controls. In the palmitate medium, GRT supplementation in controls significantly increased RCI (4.46±0.28 vs 3.55±0.19; p<0.05) (**Figure 5.42, Table 5.8, Appendix A7**).

- ***Ischemia***

There were no significant differences between either of the groups in RCI.

- ***Early Reperfusion***

There were no significant differences between either of the groups in RCI.

- ***Late Reperfusion***

In both the glutamate and palmitate medium, GRT supplementation in controls significantly decreased RCI (3.84±0.34 vs 5.05±0.45; p=0.065 and 3.06±0.07 vs 4.16±0.17; p<0.05 respectively).

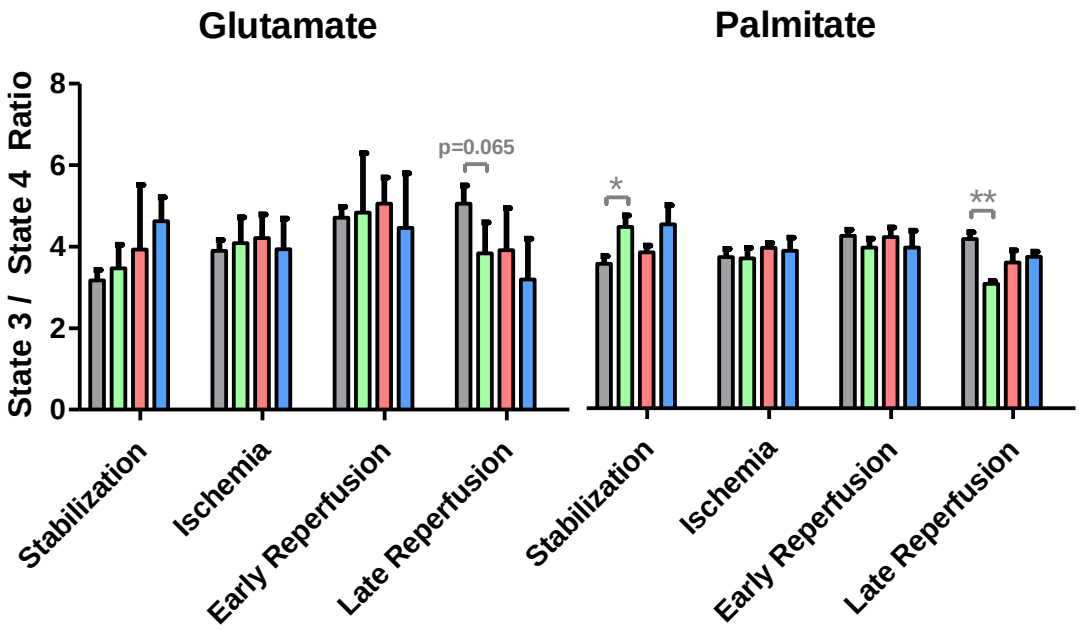

Figure 5.42 Respiratory control index in glutamate and palmitate medium between different groups and time points (n=5).

5.5.7 State 5 Respiration

State 5 respiration (S5) describes the mitochondrial respiration after a 20 min period of anoxia when oxygen is reintroduced into the system (re-oxygenation). It is also a measure of nAtoms oxygen utilized in the presence of ADP/mg mitochondrial protein/min.

- ***Stabilization***

In the palmitate medium, mitochondria from HCD rats had a significant decrease in S5 compared to controls (274.1±44 O-atoms/mg/min vs 419.64±22.56 O-atoms/mg/min; p<0.05) and GRT supplementation increased S5 in HCD (392.13±17.28 O-atoms/mg/min vs 274.1±44 O-atoms/mg/min; p=0.053). Furthermore, mitochondria from controls had higher S5 in palmitate compared to glutamate medium (419.64±22.56 O-atoms/mg/min vs 255.55±41.43 O-atoms/mg/min; p<0.05) (**Figure 5.43, Table 5.7, Appendix A7**).

- ***Ischemia***

In the glutamate/malate medium, HCD had significantly elevated S5 compared to controls (311.04±31.57 O-atoms/mg/min vs 200.52±33.7 O-atoms/mg/min; p<0.05). Also, GRT supplementation resulted in a significant increase in S5 in controls (314.7±26.3 O-atoms/mg/min vs 200.52±33.7 O-atoms/mg/min; p<0.05).

- ***Early Reperfusion***

In the palmitate/malate medium, GRT supplementation in HCD decreased S5 (352.65±26.72 O-atoms/mg/min vs 468.71±9.8 O-atoms/mg/min; p<0.01), while no effect was observed in the controls.

- ***Late Reperfusion***

In both the glutamate and palmitate medium, GRT supplementation resulted in a decrease in S5 in controls (277.88±26.39 O-atoms/mg/min vs 383.46±35.35 O-atoms/mg/min; p<0.05 and 356.74±5.42 O-atoms/mg/min vs 416.2±9.56 O-atoms/mg/min; p<0.01 respectively).

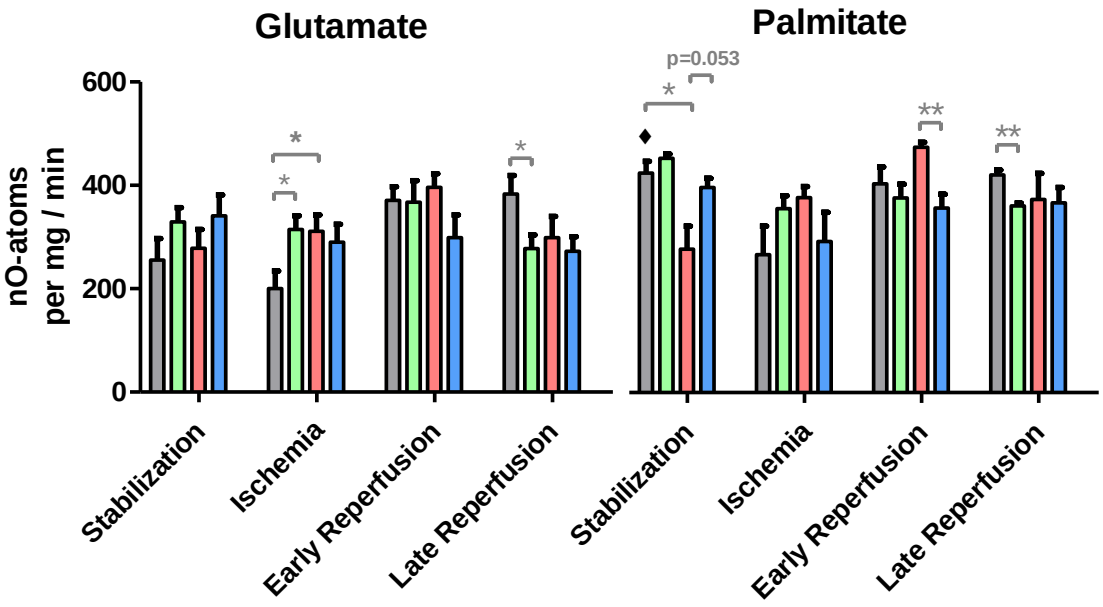

Figure 5.43 State 5 respiration in glutamate and palmitate medium between different groups and time points (n=5). ♦p<0.05 (Palmitate vs Glutamate in Stabilization).

5.5.8 %Respiration Recovery

The percentage respiration recovery (%RR) following reoxygenation was also determined to indicate the mitochondrial susceptibility to anoxia/reoxygenation. The calculation is simply taken as S5/S3 x 100 to get percentage.

- ***Stabilization***

In the glutamate medium, mitochondria from HCD rats had increased %RR compared to controls (118.4±11.59% vs 86.07±5.92%; p<0.05), whereas in the palmitate medium, HCD decreased %RR compared to controls 89.14±21.44% vs 133.45±2.06%; p<0.05), an effect that was reversed by GRT supplementation (134.67±10.32%; p<0.05). GRT supplementation of control rats also resulted in an increase in %RR in mitochondria incubated in a glutamate medium (115.6±10.26% vs 86.07±5.92%; p<0.05). Furthermore, %RR in mitochondria from controls was significantly greater in the palmitate medium compared to the glutamate medium (133.45±2.06% vs 86.07±5.92%; p<0.01) (**Figure 5.44, Table 5.8, Appendix A7**).

- ***Ischemia***

There were no other significant differences recorded in %RR during ischemia between either of the 4 groups.

- ***Early and Late Reperfusion***

There were no other significant differences recorded in %RR during either early or late rerperfusion between either of the 4 groups.

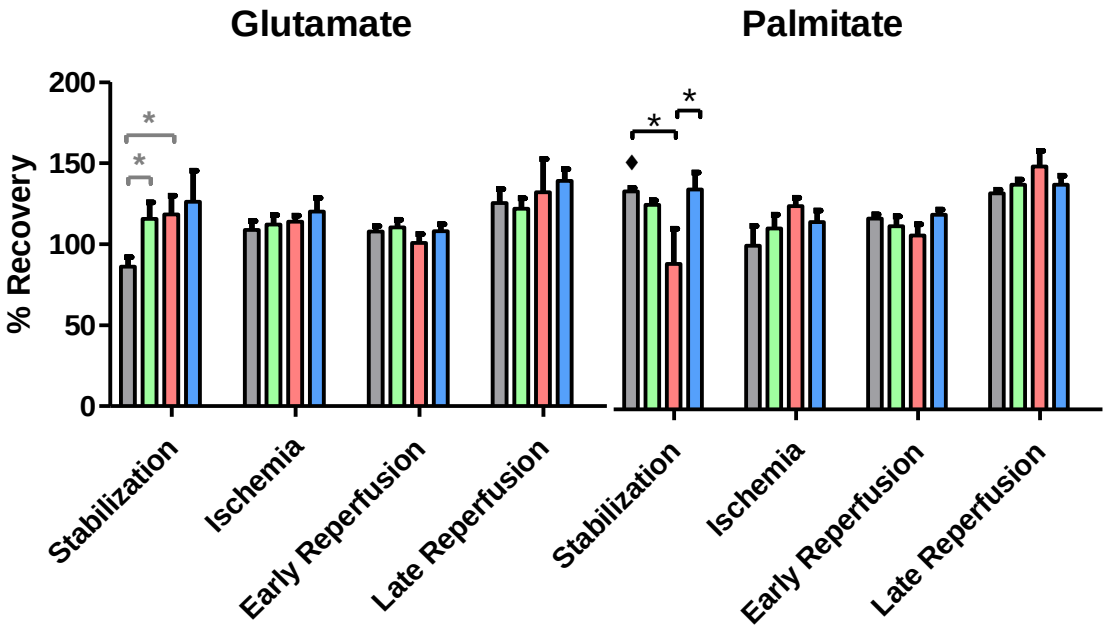

Figure 5.44 %Respiratory recovery in glutamate and palmitate medium between different groups and time points (n=5). ♦p<0.05 (Palmitate vs Glutamate in Stabilization).

5.5.9 Summary of OxPhos parameters in glutmate and palmitate

- ***Stabilization***

- *Carbohydrate Medium*

Prior to ischemia, cardiac mitochondria from rats on both diets presented with a similar S3 (**Table 5.7**). However, in the glutamate/malate medium, GRT supplementation in animals from both control and HCD decreased the mitochondrial ADP/O ratio. Once ADP was depleted, mitochondria from rats on the HCD had a significantly decreased S4 compared to animals on the control diet when incubated in the glutamate medium. After 20 min of anoxia, mitochondria from animals on the HCD had increased %RR compared to mitochondria from controls, while GRT supplementation in controls also resulted in an increase in %RR of the mitochondria.

- *Fatty Acid Medium*

GRT supplementation significantly decreased the ADP/O ratio in palmitate medium in cardiac mitochondria prepared from control rats, while having no effect in mitochondria from the HCD rats (**Table 5.7**). GRT supplementation in control animals also increased the mitochondrial OxPhos S3 but resulted in increased RCI. HCD resulted in a significantly increased mitochondrial OxPhos S3 and OxPhos S4 in palmitate medium compared to glutamate medium, while GRT supplementation significantly decreased mitochondrial S4 in hearts from HCD rats. After subjecting the mitochondria to 20 min of anoxia, mitochondria from HCD animals had a decrease in S5 in palmitate medium, whereas GRT was able to enhance the %RR. Furthermore, mitochondria from the control groups had higher S5 and %RR in the palmitate medium compared to the glutamate medium.

Table 5.7 Summary of OxPhos parameters in stabilization

Parameter	Time Point	GLUTAMATE				PALMITATE			
		C	C+ GRT	HCD	HCD+ GRT	C	C+ GRT	HCD	HCD+ GRT
ADP/O Ratio	S		↓		↓		↓		
S3	S						↑		
Oxphos S3	S						↑	(♣↑)	
S4	S			↓					↓
Oxphos S4	S							(♣↑)	
RCI	S						↑		
S5	S					(♦↑)		↓	↑
%RR	S		↑	↑		(♦↑)		↓	↑

S: Stabilization; HCD: High-caloric diet, GRT: Afriplex green rooibos extract; Control + GRT significance compared to Control, HCD significance compared to Control, HCD + GRT significance compared to HCD; ♦p<0.05 (Palmitate vs Glutamate in Control), ♣p<0.05 (Palmitate vs Glutamate in HCD); n=5 for all groups.

- ***Ischemia***

  - *Carbohydrate Medium*

After 20 min of global ischemia, ingestion of the HCD significantly increased mitochondrial S3 compared to controls (**Table 5.8**). GRT supplementation also increased mitochondrial S3 and OxPhos S3 in controls, while having no effect in HCD – possibly due to the already elevated ATP production and respiration. Once supplemented ADP was depleted, mitochondria from rats on the HCD also presented with increased S4, while again GRT supplementation resulted in increased S4 and OxPhos S4 in controls, while having no effect in mitochondria from HCD rats. Post 20 min of anoxia, HCD again had elevated S5, while GRT supplementation increased S5 in controls.

  - *Fatty Acid Medium*

After 20 min of global ischemia, cardiac mitochondria from GRT supplemented rats had significantly increased S3 and OxPhos S3 in controls in palmitate medium (**Table 5.8**). Furthermore, GRT supplemented HCD groups had increased OxPhos S3 in palmitate compared to glutamate. In low presence of ADP, both GRT treated and untreated HCD had elevated S4 OxPhos in FA compared to carbohydrates. Furthermore, mitochondria from control rats supplemented with GRT presented with improved S4 and OxPhos S4, while having no effect in animals on the HCD. After 20 additional minutes of anoxia, there were no more significant differences between the 4 groups in the palmitate medium.

Table 5.8 Summary of OxPhos parameters in ischemia

Parameter	Time Point	GLUTAMATE				PALMITATE			
		C	C+ GRT	HCD	HCD+ GRT	C	C+ GRT	HCD	HCD+ GRT
ADP/O Ratio	I								
S3	I		↑	↑			↑		
Oxphos S3	I		↑				↑		(♥↑)
S4	I		↑	↑			↑		
Oxphos S4	I		↑				↑	(♣↑)	(♥↑)
RCI	I								
S5	I		↑	↑					
%RR	I								

I: Ischemia; HCD: High-caloric diet, GRT: Afriplex green rooibos extract; Control + GRT significance compared to Control, HCD significance compared to Control; ♣p<0.05 (Palmitate vs Glutamate in HCD), ♥p<0.05 (Palmitate vs Glutamate in HCD + GRT); n=5 for all groups.

- ***Early Reperfusion***

- *Carbohydrate Medium*

GRT supplementation decreased S3 and OxPhos S3 in mitochondria from HCD rats, while having no effect in controls (**Table 5.9**). Following depletion of supplemented ADP, mitochondria from HCD rats supplemented with GRT also presented with decreased OxPhos S4.

- *Fatty Acid Medium*

OxPhos S3 was elevated in HCD in FA compared to carbohydrates (**Table 5.9**). Furthermore, HCD also had significantly increased cardiac mitochondrial S3 and OxPhos S3 compared to controls, an effect that was reversible by GRT supplementation which had improved ADP/O ratio in FA compared to carbohydrates. OxPhos S4 was elevated in HCD, and GRT supplemented control and HCD mitochondria in FA compared to carbohydrates. HCD also increased mitochondrial S4 and OxPhos S4 compared to controls, while GRT supplementation on the animals decreased mitochondrial S4 and OxPhos S4. After anoxia, GRT supplementation in HCD also decreased S5, while having no effect in controls.

Table 5.9 Summary of OxPhos parameters in early reperfusion

Parameter	Time Point	GLUTAMATE				PALMITATE			
		C	C+ GRT	HCD	HCD+ GRT	C	C+ GRT	HCD	HCD+ GRT
ADP/O Ratio	ER								(♥↑)
S3	ER				↓			↑	↓
Oxphos S3	ER				↓			↑(♣↑)	↓
S4	ER							(♣↑)	↓
Oxphos S4	ER				↓		(♠↑)	↑(♣↑)	↓(♥↑)
RCI	ER								
S5	ER								↓
%RR	ER								

ER: Early Reperfusion; HCD: High-caloric diet, GRT: Afriplex green rooibos extract; HCD significance compared to Control, HCD + GRT significance compared to HCD; ♠p<0.05 (Palmitate vs Glutamate in Control + GRT), ♣p<0.05 (Palmitate vs Glutamate in HCD), ♥p<0.05 (Palmitate vs Glutamate in HCD + GRT); n=5 for all groups.

- ***Late Reperfusion***

- *Carbohydrate Medium*

In late reperfusion, HCD decreased OxPhos S3 in cardiac mitochondria compared to the controls (**Table 5.10**). GRT supplementation of the animals resulted in a significant decrease in cardiac mitochondrial S3 and decreased the RCI in controls. GRT supplementation in controls decreased mitochondrial S5 after anoxia.

- *Fatty Acid Medium*

HCD had significantly elevated mitochondrial ADP/O ratio in FA medium compared to carbohydrates (**Table 5.10**). GRT supplementation in control rats resulted in mitochondria obtained from the hearts to have decreased OxPhos S3 and decreased RCI. GRT supplementation in controls decreased S5 after anoxia.

Table 5.10 Summary of OxPhos parameters in late reperfusion

Parameter	Time Point	GLUTAMATE				PALMITATE			
		C	C+ GRT	HCD	HCD+ GRT	C	C+ GRT	HCD	HCD+ GRT
ADP/O Ratio	LR							(♣↑)	
S3	LR		↓				↓		
Oxphos S3	LR			↓			↓		
S4	LR								
Oxphos S4	LR								
RCI	LR		↓				↓		
S5	LR		↓				↓		
%RR	LR								

LR: Late Reperfusion; HCD: High-caloric diet, GRT: Afriplex green rooibos extract; Control + GRT significance compared to Control, HCD significance compared to Control); ♣p<0.05 (Palmitate vs Glutamate in HCD); n=5 for all groups.

5.6 *Mitophagy SIGNALING*

5.6.1 PINK1

PINK1 accumulates on the outer membrane of damaged mitochondria.

- ***Stabilization***

No significant differences were recorded in PINK1 levels between either of the 4 groups (**Figure 5.45, Table 5.11**).

- ***Ischemia***

HCD significantly increased mitochondrial PINK1 levels ($p<0.05$), while supplementing controls with GRT also significantly increased PINK1 levels ($p<0.05$). GRT supplementation in HCD had no significant effect.

- ***Early and Late Reperfusion***

No significant differences were recorded in PINK1 levels between either of the 4 groups.

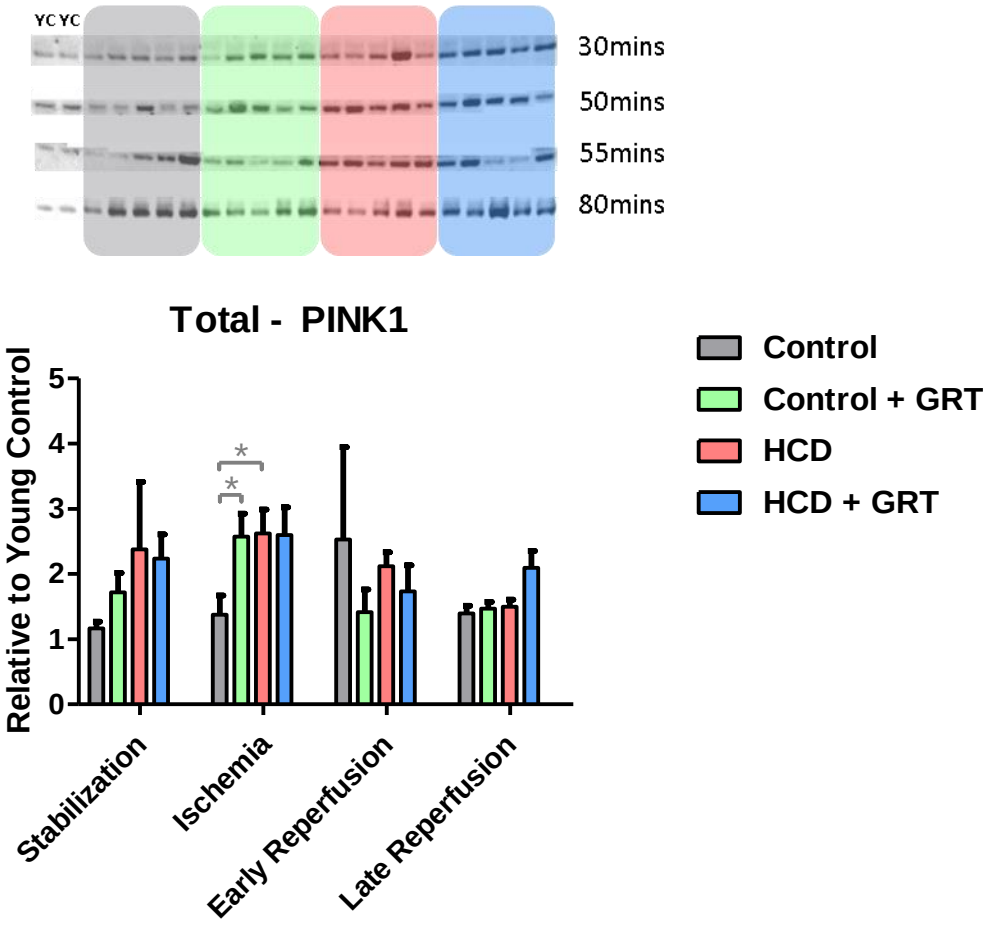

Figure 5.45 Mitochondrial PINK1 levels between the different groups and time points (n=5). HCD: High-caloric diet, GRT: Afriplex green rooibos extract.

5.6.2 Parkin

Parkin ubiquitinates outer mitochondrial membrane proteins to trigger selective autophagy.

- ***Stabilization***

HCD significantly increased Parkin levels ($p<0.01$), while supplementing controls with GRT also increased Parkin levels ($p<0.05$). GRT supplementation in HCD had no significant effect (**Figure 5.46, Table 5.11**).

- ***Ischemia***

No significant differences were recorded in Parkin levels between either of the 4 groups.

- ***Early Reperfusion***

Parkin levels were significantly increased in early reperfusion in all 4 groups. GRT supplementation in HCD also led to a significant increase in Parkin levels ($p<0.01$).

- ***Late Reperfusion***

Parkin was significantly reduced towards late reperfusion. GRT supplementation significantly decreased Parkin levels in controls ($p<0.05$), but not in HCD.

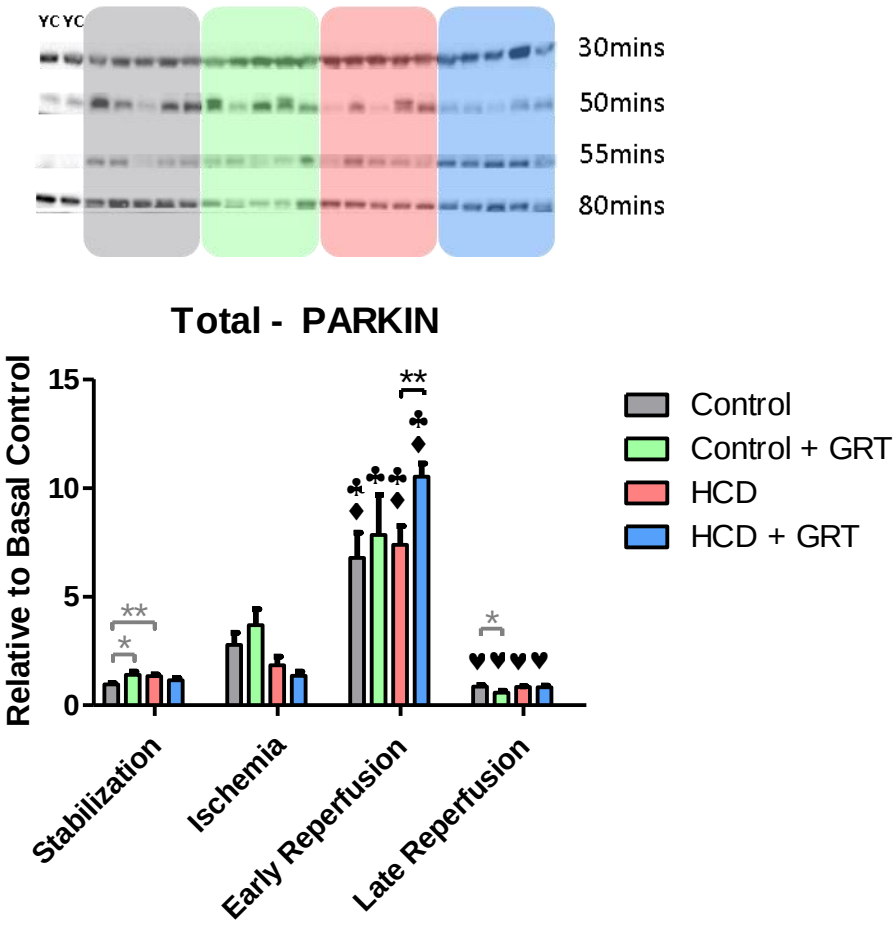

Figure 5.46 Mitochondrial Parkin levels between the different groups and time points (n=5). HCD: High-caloric diet, GRT: Afriplex green rooibos extract. ♣p<0.05 (Compared to Stabilization), ♦p<0.05 (Compared to Ischemia), ♥p<0.05 (Compared to Early Reperfusion).

5.6.3 p62

p62 serve as the link between the damaged mitochondria and LC3 to initiate autophagolysosomal degradation.

- ***Stabilization***

GRT supplementation significantly reduced p62 levels in controls (p=0.083), but not in HCD (**Figure 5.47, Table 5.11**).

- ***Ischemia***

p62 was significantly increased in ischemia compared to stabilization in all groups except GRT supplemented HCD. GRT supplementation significantly increased p62 levels in controls (p<0.001) and decreased p62 levels in HCD (p=0.058). Untreated HCD had the same p62 levels as untreated controls.

- ***Early Reperfusion***

p62 levels were significantly reduced compared to ischemia in GRT supplemented controls and untreated HCD. No significant differences were recorded in p62 levels between either of the 4 groups.

- ***Late Reperfusion***

Towards late reperfusion, p62 levels were still elevated compared to stabilization in HCD groups. HCD also had significantly increased p62 levels (p<0.05) compared to controls, while supplementing controls with GRT also significantly increased p62 levels (p<0.05). GRT supplementation in HCD had no significant effect.

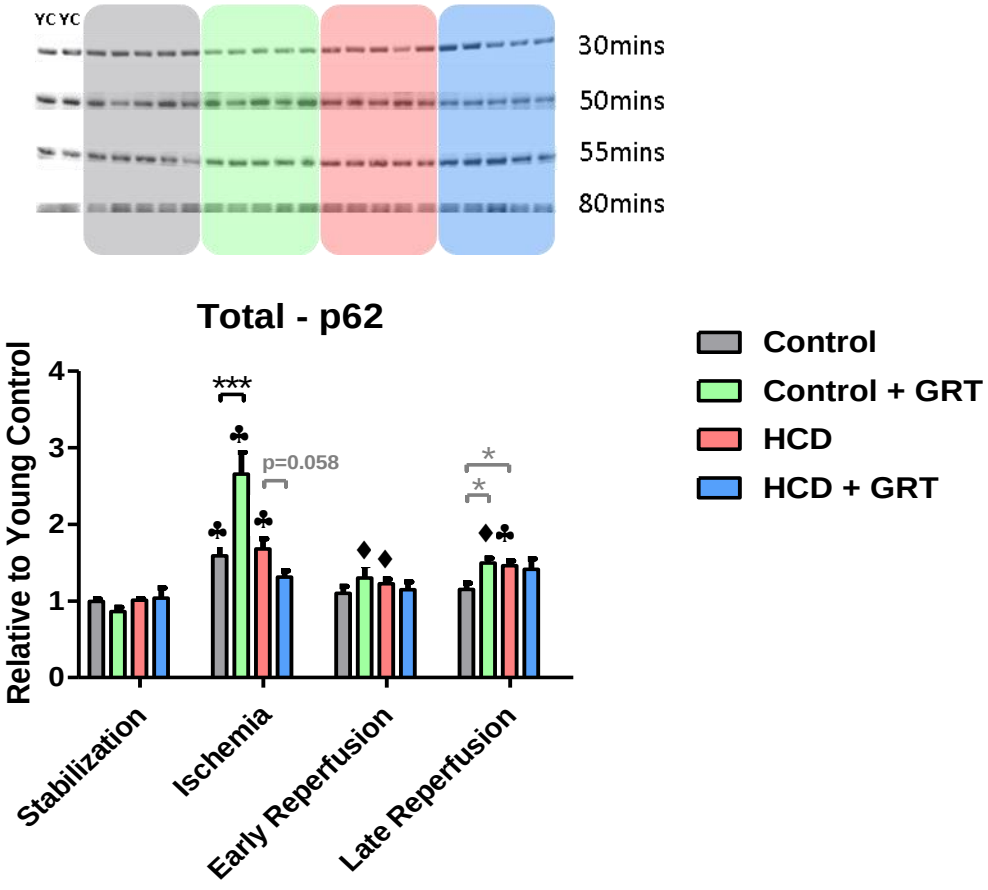

Figure 5.47 Mitochondrial p62 levels between the different groups and time points (n=5). HCD: High-caloric diet, GRT: Afriplex green rooibos extract. ♣p<0.05 (Compared to Stabilization), ♦p<0.05 (Compared to Ischemia).

5.6.4 BNIP3L

BNIP3L serves as an autophagy receptor which recruits mitochondria to the autophagosome.

- ***Stabilization***

HCD significantly reduced mitochondrial BNIP3L levels ($p<0.01$), while supplementing controls with GRT also reduced BNIP3L levels ($p<0.05$). GRT supplementation in HCD had no significant effect (**Figure 5.48, Table 5.11**).

- ***Ischemia***

HCD significantly increased mitochondrial BNIP3L levels ($p=0.085$), while supplementing controls with GRT also significantly increased BNIP3L levels ($p<0.001$). GRT supplementation in HCD had no significant effect.

- ***Early Reperfusion***

No significant differences were recorded in BNIP3L levels between either of the 4 groups. However, HCD, together with GRT supplemented controls and HCD maintained elevated BNIP3L levels compared to stabilization.

- ***Late Reperfusion***

HCD significantly increased BNIP3L levels ($p<0.001$), while supplementing controls with GRT also significantly increased BNIP3L levels ($p<0.001$) – these two groups remained elevated since ischemia, whereas untreated controls saw a significant reduction in BNIP3L content during later reperfusion. GRT supplementation in HCD had no significant effect.

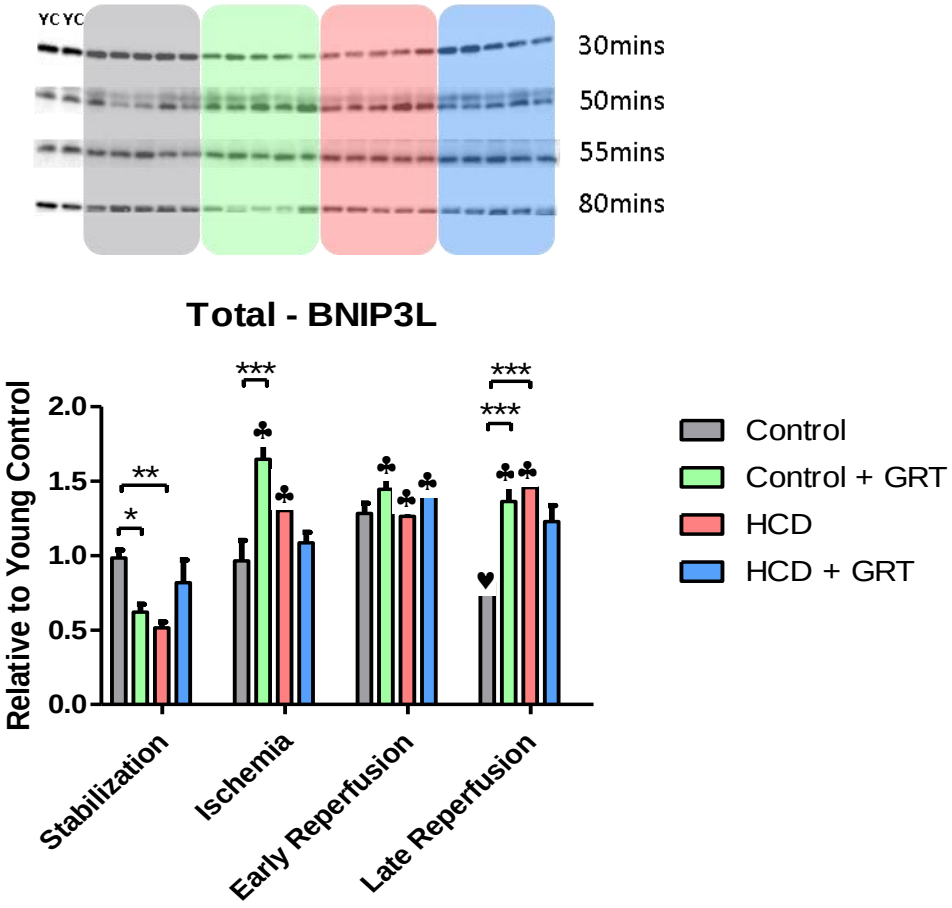

Figure 5.48 Mitochondrial BNIP3L levels between the different groups and time points (n=5). HCD: High-caloric diet, GRT: Afriplex green rooibos extract. ♣$p<0.05$ (Compared to Stabilization), ♥$p<0.05$ (Compared to Early Reperfusion).

5.6.5 LC3-II

Mitochondria-bound LC3-II is present on the forming phagophore and targets the mitochondria for autophagy. It can used as a steady state indicator for mitophagy levels (Oh *et al.*, 2017).

- ***Stabilization***

No significant differences were recorded in LC3-II levels between either of the 4 groups (**Figure 5.49, Table 5.11**).

- ***Ischemia***

HCD significantly decreased LC3-II levels ($p<0.01$). No other significant differences were noted.

- ***Early Reperfusion***

Both treated and untreated HCD animals presented with increased mitochondrial LC3-II levels compared to stabilization ($p<0.05$ for both) and mitochondrial LC3-II level in GRT treated HCD was also significantly elevated compared to ischemia ($p<0.05$).

- ***Late Reperfusion***

GRT supplementation significantly increased LC3-II levels in HCD ($p<0.05$), which also remained elevated since ischemia.

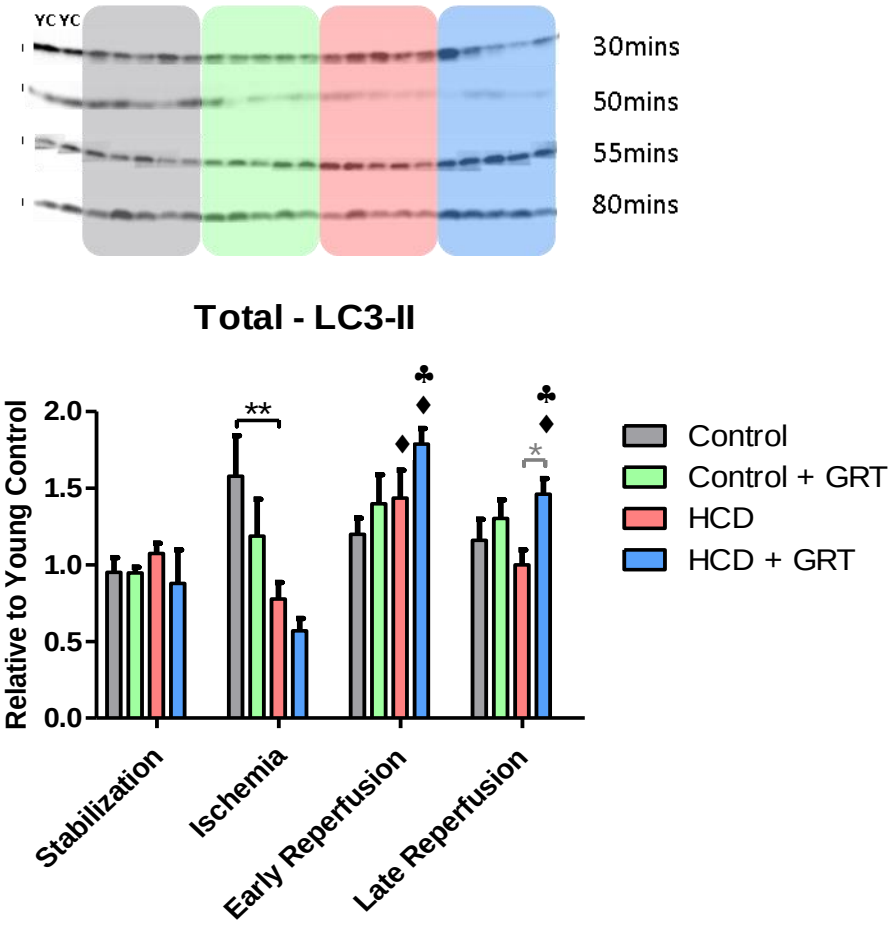

Figure 5.49 Mitochondrial LC3-II levels between the different groups and time points (n=5). HCD: High-caloric diet, GRT: Afriplex green rooibos extract. ♣$p<0.05$ (Compared to Stabilization), ♦$p<0.05$ (Compared to Ischemia).

5.6.6 Summary of mitophagy associated proteins

Table 5.11 Summary of mitophagy associated proteins

Parameter	Time Point	CONTROL	CONTROL+GRT		HCD		HCD+GRT	
		MEAN±SEM	MEAN±SEM		MEAN±SEM		MEAN±SEM	
LC3 II	Stabilization	0.95±0.09	0.94±0.03		1.07±0.06		0.87±0.21	
	Ischemia	1.57±0.26	1.18±0.24		0.77±0.10 (♣**)	↓	0.56±0.08	
	Early Reperfusion	1.19±0.01	1.40±0.19		1.43±0.18		1.78±0.10	
	Late Reperfusion	1.15±0.13	1.30±0.12		1.00±0.09		1.46±0.10 (♥*)	↑
BNIP3L	Stabilization	0.98±0.05	0.62±0.05 (♠*)	↓	0.51±0.03 (♣**)	↓	0.81±0.15	
	Ischemia	0.96±0.13	1.64±0.13 (♠***)	↑	1.30±0.09 (p=0085)	↑	1.08±0.07	
	Early Reperfusion	1.28±0.06	1.44±0.11		1.26±0.06		1.40±0.04	
	Late Reperfusion	0.81±0.03	1.36±0.14 (♠***)	↑	1.45±0.05 (♣***)	↑	1.22±0.10	
PARKIN	Stabilization	0.96±0.05	1.40±0.14 (♠*)	↑	1.33±0.07 (♣**)	↑	1.15±0.09	
	Ischemia	2.77±0.55	3.68±0.73		1.84±0.38		1.35±0.19	
	Early Reperfusion	6.78±1.15	7.84±1.84		7.37±0.87		10.50±0.53 (♥**)	↑
	Late Reperfusion	0.85±0.06	0.57±0.09 (♠*)	↓	0.83±0.03		0.82±0.07	
p62	Stabilization	0.99±0.03	0.86±0.05 (p=0.083)	↓	1.01±0.01		1.03±0.13	
	Ischemia	1.58±0.21	2.65±0.28 (♠***)	↑	1.67±0.13		1.31±0.08(p=0.058)	↓
	Early Reperfusion	1.09±0.09	1.29±0.16		1.22±0.06		1.14±0.10	
	Late Reperfusion	1.15±0.08	1.49±0.06 (♠*)	↑	1.45±0.06 (♣*)	↑	1.41±0.13	
PINK1	Stabilization	1.16±0.10	1.71±0.30		2.37±1.03		2.23±0.36	
	Ischemia	1.37±0.29	2.57±0.35 (♠*)	↑	2.62±0.36 (♣*)	↑	2.59±0.42	
	Early Reperfusion	2.52±1.42	1.41±0.34		2.11±0.21		1.73±0.40	
	Late Reperfusion	1.39±0.11	1.46±0.10		1.49±0.10		2.09±0.25(p=0.084)	↑

HCD: High-caloric diet, GRT: Afriplex green rooibos extract; Control + GRT significance and arrow direction compared to Control, HCD significance and arrow direction compared to Control, HCD + GRT significance and arrow direction compared to HCD; *p<0.05, **p<0.01, ***p<0.001, ****p<0.0001 (♠Control + GRT vs Control; ♣HCD vs Control; ♥HCD + GRT vs HCD); n=5 for all groups.

CHAPTER 6
DISCUSSION

6.1 INTRODUCTION

The primary aim of this study was to characterise the effect of 6 weeks Afriplex green rooibos extract treatment (aspalathin-rich equating to a daily aspalathin dose of 2 “cups-of-tea” in a rat or 70 “cups-of-tea” in a human) on functional heart recovery and infarct size following ischemia reperfusion injury in a pre-diabetic rat model with established obesity and insulin resistance vs controls. The secondary objective was to elaborate our understanding of the role of Afriplex GRT on cell signaling mechanisms pertaining to cardioprotection, inflammation and cardiac stress. The secondary aim was to investigate the mitochondrial oxidative phosphorylation potential of these hearts and relate how Afriplex GRT influenced bio-energetics, and to correlate these parameters with the mitochondrial mitophagy process.

Our results showed that the pre-diabetic heart had lower mechanical function prior to ischemia, presented with impaired mechanical recovery post reperfusion and had increased infarct size. Furthermore, mitochondria isolated from these hearts showed elevated beta-oxidation throughout the protocol and elevated OxPhos post-ischemia, culminating in increased ROS production and, while mitophagy was increased, without added antioxidant defence, cell death was inevitable. Administration of GRT treatment improved mechanical heart function before and after ischemia, resulting in better heart recovery and decreased infarct size. GRT treatment resulted in lessor inflammation signaling and GSK3b inhibition prior to reperfusion, while also increasing mitochondrial uncoupling, resulting in a decreased metabolic rate connected to less ROS production. In early reperfusion, GRT treated pre-diabetic rats had lower stress and inflammatory signaling, while furthermore inhibiting mitochondrial OxPhos, and thereby contributing to less ROS production, without really affecting mitophagy. These effects proved to be cardiotonic in the present study, implicating Afriplex GRT’s potential in being cardioprotective in a high-caloric diet-induced pre-diabetic rat model.

6.2 BIOMETRIC PARAMETERS

Our research made use of two animal models induced by two different diets: a normal rat chow diet (referred to as control diet) and a high calorie diet (referred to as the HCD diet). Both these diets were supplied *ad libitum* for a period of 16 weeks to male Wistar rats (aged approximately 6 weeks and weighing approximately 180 g at baseline) (Pickavance *et al.*, 1999; Salie *et al.*, 2014; Webster *et al.*, 2017).

6.2.1 Weight gain

The impact of obesity and its comorbidities are well established to impair quality of life and diminish life expectancy (Boden, 2011). It is defined as excessive and abnormal body fat accumulation leading to adverse health effects. Obesity poses a threat to an individual’s health and unnecessarily places a financial burden on society through diverted capital and increased health care expenditure (Abdelaal *et al.*, 2017). Furthermore, obesity is associated with co-morbidities such as T2D and dyslipidemia, which further increases mortality. Staying obese should thus be considered as a high-risk lifestyle, or more colloquially ‘living on the edge’. The pathology of obesity arises from the inability to control appetite which arises from both environmental factors and a genetic susceptibility (Abdelaal *et al.*, 2017). Obesity is underlined by consuming more energy than one

expends and is most commonly induced by hyperphagia through hormonal cues either increasing hunger, decreasing satiety or both. The first essential hormone in appetite control is ghrelin, secreted by the gut, which plays a central role in inducing food intake (increasing hunger) (Klok *et al.*, 2007). Conversely, adipose tissue secretes leptin which mediates long-term energy balance by suppressing food intake (increasing satiety) resulting in weight loss (Klok *et al.*, 2007). However, consistently overriding leptin signaling by consuming food when satisfied, gives rise to a phenomenon called leptin resistance, resulting in decreased satiety from average portion meals causing chronic overconsumption and weight gain (Hagan & Niswender, 2012).

Monitoring body weight is an essential diagnostic technique to describe the quality of health in both humans and animals. As obesity is a serious risk indicator and narrowly tied to increased energy intake and total body weight, the weight of animals was continually monitored from the onset of the study until the time of sacrifice (**Figure 5.1 and 5.2**) Before the onset of treatment, HCD animals did not weigh significantly more than controls (**Table 5.1**). However, 6 more weeks of HCD diet resulted in a significant increase in weight gain for both untreated (↑8%) and GRT treated (↑11%) rats compared to their respective controls (**Figure 5.2**). Increased weight gain induced by high-caloric diets compared to control diets have been established previously (Kamau, 2018; Nduhirabandi *et al.*, 2017; Salie *et al.*, 2014). These studies also reflected similar differences in body weight between high-caloric diets and controls following 16 weeks of diet (↑18%, ↑19%, ↑12% respectively). GRT supplementation in HCD also led to a 5% increase in body weight compared to the untreated HCD (**Figure 5.2**), albeit having no significant increase in weight gain *per se*. Interpreting the weekly body weight totals of rats from week 11 onwards (**Figure 5.1**), it is noted that HCD with GRT had an increased average body weight since the start of the treatment term. Thus, this elevation in body weight at the time of sacrifice could be the effect of random allocation, as these animals were allocated for either GRT treatment or placebo since week 1. It is therefore uncertain whether the observed increase in body weight is due to the effect of the GRT or random allocation and would require further investigation.

6.2.2 Visceral fat

Obesity can also be defined as enlargement of the adipose tissue to store excess energy intake. This expansion occurs through both adipocyte hypertrophy (cell size increase) and adipocyte hyperplasia (cell number increase) (Jo *et al.*, 2009). Distinction must be made between visceral fat, which wraps around internal organs – and is associated with increased risk for metabolic disorders and mortality (Merlotti *et al.*, 2017) - and subcutaneous fat, which lies under the skin around the belly, thighs and rear – and carries less risk, and have even been associated with cardioprotection in T2D (Golan *et al.*, 2012). Body weight and the inferences made through BMI alone are not enough to make a diagnosis of obesity – additional measurements such as body adiposity index or the waist to hip circumference ratio is required. This ratio can be used to measure abdominal obesity and is an independent risk factor for metabolic disorders such as T2D (Li *et al.*, 2014). As there are no such indices for rats, we harvested and weighed the IP fat (or visceral fat) after sacrifice and expressed this fat mass as a percentage of total body mass. It must be mentioned that it is possible to distinguish between visceral and subcutaneous fat stores, however this requires determining total fat content by DEXA and then subtracting the excised IP fat to obtain subcutaneous fat content (Donner *et al.*, 2015). In the present study, HCD had significantly higher IP fat and IP fat percentage compared to controls (**Table 5.3, Figure 5.7**). GRT treatment in the present study had no significant effect on body fat accumulation in the control animals but did indicate a higher propensity to increasing total intraperitoneal fat in HCD groups. This was surprising as rooibos

has recently drawn attention for its potential weight loss effects (Sanderson *et al.*, 2014). The researchers used both hot water extracts from infused fermented rooibos and the soluble solids (at a “cup of tea”-strength) to treat differentiated 3T3-L1 adipocytes. They found that rooibos significantly inhibited lipid accumulation, decreased PPARγ, PPARα, SREBF1 and FASN messenger RNA, impeded glycerol release and decreased leptin secretion. Taken together, these results indicated that rooibos can inhibit adipogenesis and thereby affect adipocyte metabolism, potentially preventing obesity. In our present study, a dose of roughly 12 times this amount of aspalathin had no significant effect on fat accumulation in controls but did show higher propensity for IP fat accumulation in HCD animals. However, since weight gain was not significantly different between GRT treated and untreated HCD at the time of sacrifice (**Table 5.1**), the perceived increased in IP fat could be due to random chance as these animals were allocated for GRT treatment at 10 weeks without discretion given to initial body weight. This phenomenon warrants further investigation.

6.2.3 Food intake

Considering the effect of higher energy intake, dietary monitoring was essential in this present study to determine its potential contribution on weight gain. HCD animals consistently ate more food than the control counterparts before (↑33%) and after the onset of treatment (↑19%) (**Table 5.1, Figure 5.4 and 5.5**). The present findings were in accord with previous studies which also established increased food consumption by HCD animals (Kamau, 2018; Nduhirabandi *et al.*, 2017; Pickavance *et al.*, 1999). In all three these studies, increased food consumption by HCD Wistar rats compared to standard control-chow fed Wistar rats resulted in increased weight gain, elevated serum insulin and blood lipids. As such, the present study can also be considered a hyperphagia diet model which can be translated to human conditions with the same underlining pathology. Interestingly, food consumption was significantly decreased after introducing the jelly, which was not due to a significant effect on calorie intake as the jelly contributed a ~2kJ extra calories (**Table 4.3**) compared to 255 – 320 kJ intake from food (**Table 4.1**). The HCD animals could have potentially had lower activity from week 10 resulting in lower energy expenditure and therefore a lowered energy consumption. This phenomena has been found in human children, whereby there is an increase in sedentary downtime from age 9 to 12 (Janssen *et al.*, 2015). However, to verify such an progression occurring into later rat adolescence daily activity measures during the 10 to 16-week period will need to be performed.

GRT supplementation did not influence food intake in the present study. The claim that rooibos can increase appetite has long been maintained by individuals (Morton, 1983). However, no direct mechanism has been established to confirm this. To the contrary, rooibos is implicated in curbing appetite through indirect measures. For instance, in a study performed by Schloms *et al.* (2014), 80 mg GRE/rat (±0.96 mg aspalathin/day) for 10 days resulted in decreased glucocorticoid (stress hormone) levels. This mechanism has been implicated as a means for rooibos to contribute to decreasing appetite and induce weight loss –stemming from curbing stress-eating and stress-induced hyperphagia (Yau & Potenza, 2013). However, in the present study this mechanism had no effect on food intake.

6.2.4 Water consumption

Water is deemed to be physiologically essential to regulate body temperature, lubricate and preserve joints, protect your spinal cord and other sensitive tissues, and aid in waste removal through improving urination, perspiration and bowel movements (Popkin *et al.*, 2010). Water consumption was significantly decreased in HCD compared to controls, both before (↓32%) and after (↓32%) treatment (**Table 5.1, Figure 5.6 and 5.7**).

This decrease in water consumption can partly be attributed to the higher moisture content within the HCD diet, as food was prepared to have a runny porridge consistency, while the standard rat-chow pellets were served dry. However, it cannot be excluded that this might be the effect of an unhealthy diet such as HCD leading to worse hydration as well (Popkin *et al.*, 2010). In the present study, GRT treatment had no significant effect on water consumption in either control or HCD diets, and GRT thus had no significant influence on dehydration or induction of increased fluid loss through symptoms such as nausea or diarrhea.

6.2.5 Summary

Taken together, animals on a high-caloric diet had increased energy intake (of a diet more energy dense) (**Table 4.1**) without increased energy expenditure (inferred by similar housing arrangements) resulted in increased energy storage (in the form of IP fat – both absolute and as percentage of total body mass), which gave rise to increased body mass compared to control diet animals. In a clinical setting, these elevated parameters result in a syndrome called metabolic syndrome. As the HCD did not differ significantly in micronutrient composition (see **Appendix A4** vs **A5**) compared to the standard rat chow diet, the perceived effect can solely be attributed to the increased caloric intake of fat and carbohydrates.

6.3 SERUM ANALYSES

The effect of both diet and GRT treatment on blood and serum biochemistry were investigated. These are important considerations as alterations in biochemical markers can be early indications for organ dysfunction.

6.3.1 Hyperglycemia

One of the first clinical consequences of insulin resistance is a dysregulation in glucose homeostasis - the maintenance of blood glucose concentration within very narrow physiological limits (Norris & Rich, 2012). This abnormality can be determined by measuring the fasting blood glucose concentration. Fasting blood glucose is closely regulated by endogenous glucose production (hepatic glycogenolysis, gluconeogenesis) and glucose utilization by insulin-sensitive tissues. In the present study both non-fasting and fasting blood glucose levels were measured. HCD animals presented with elevated non-fasting blood glucose levels (or random blood glucose levels taken just prior to sacrificing of rats) compared to controls (**Table 5.1, Figure 5.8**). Fasting blood glucose was also elevated in HCD animals before the onset of treatment and one week prior to sacrifice (**Table 5.1**). Furthermore, OGTTs performed on these animals showed that HCD animals had poorer glucose tolerance for the first 45 min of the OGTT before treatment (**Figure 5.9**) and this extended to 60 min after 6 additional weeks of receiving the HCD diet (**Figure 5.10**). In both instances blood glucose returned to baseline levels at the clinically relevant 2-hour time point. Considering that these rats are only the equivalent of about 13 years old in human years (**See Section 4.3.2.3**) the severity of this profile is expected to increase as these rats get older. These results replicate previous studies using a similar diet (George *et al.*, 2011; Kamau, 2018; Pickavance *et al.*, 1999).

In the present study, GRT supplementation had no effect on fasting blood glucose or glucose tolerance. This was unexpected, as various *in vitro* and *in vivo* studies have indicated that rooibos has hypoglycemic effects. Aspalathin and GRE dose-dependently increased glucose uptake in rat L6 skeletal myotubes (Kamakura *et al.*, 2015; Kawano *et al.*, 2009; Son *et al.*, 2013) and cardiomyocytes isolated from both control and HCD rats (Smit *et al.*, 2018), while FRE and GRE enhanced glucose uptake in palmitate-induced insulin-resistant C2C12 skeletal muscle cells (Mazibuko *et al.*, 2013). Furthermore, *in vivo*, aspalathin suppressed elevated fasting blood glucose and improved impaired glucose tolerance in *ob/ob* mice (Son *et al.*, 2013) and *db/db* mice

(Kawano *et al.*, 2009), while also suppressing gene expression of enzymes related to gluconeogenesis and glycogenolysis, and upregulating glycogenesis in the liver of *ob/ob* mice, resulting in a reduced blood glucose levels (Son *et al.*, 2013).

Two potential reasons will be addressed to explain GRT's lack of effect on glucose homeostasis: Kamakura and colleagues (2015) reported on the hypoglycemic effect of GRE in type 2 diabetic KK-Ay mice fed a control diet supplemented with 0.3% GRE (initial 3 weeks) – containing 6.6g aspalathin / 100g GRE. The authors however did not disclose the amount of food intake by the mice, and it is therefore uncertain what the exact daily dose of rooibos compounds were. The authors showed that 0.3% GRE did not elicit any effect in decreasing blood glucose, whilst increasing the dose to 0.6% GRE for an additional two weeks showed a significant hypoglycemic effect – an effect that was dissipated once again in the final week. The authors attributed the loss in hypoglycemic effect to a 'chance' decrease in the diabetic controls, which dissipated the statistical significance. The study was subsequently ended, and the authors concluded that a hypoglycemic effect had been established. Due to this 'unfortunate' termination it is uncertain whether the hypoglycemic effect induced by GRE can be sustained for an extended time, or whether it was only effective for one week in a mouse model, before it was reversed for unknown limitations used in the model. However, in the present study, it could also be possible that GRT induced an initial hypoglycemic effect, which dissipated over time, and through hyperphagia by the HCD animals, was overturned. This is in line with a study done by Mikami and colleagues (2015), which found that GRE supplementation in mice receiving glucose, maltose and starch had a significant post-prandial blood glucose lowering effect through surpressing intestinal α-glucosidase, an enzyme involved in the breakdown of glucose. This α-glucosidase inhibitory effect by rooibos was also corroborated in a recent study published by Miller and colleagues (2018). Thus, the glucose lowering of rooibos might be a direct consequence of inhibiting glucose metabolism.

Considering the dosage variances between studies, Muller and colleagues (2012) showed that pre-treating for 1 hour with aspalathin-rich fractions were most effective at surpressing increases in blood glucose at a dose of 25 mg GRE/kg BW (equal to 4.61mg aspalathin//kg BW compared to the 7.7 mg aspalathin/kg BW in the present study) in STZ-induced T1D Wistar rats, and the combination of aspalathin and rutin also significantly suppressed blood glucose for up to 6 hours. They also showed a dose-dependent decrease in efficacy at higher doses of rooibos (300mg GRE/kg BW, equal to 55.32 mg aspalathin/kg BW and effectively 16 "cup-of-tea"-strengths for a 300 g rat) which were not able to surpress glucose beyond 4 hours. Taken together, in the present study, *ad libitum* feeding of HCD animals and only receiving one daily dose of GRT could have contributed to the lack of effect on improving glucose homeostasis. To investigate this phenomenon in more detail, multiple smaller doses of GRT would have to be administered throughout the day, and OGTTs would need to be done one and two weeks after introducing the GRT treatment to confirm that the glucose lowering effect can be sustained beyond 3 weeks. This would be an interesting approach for future studies.

6.3.2 Insulin resistance

HOMA-IR can be used to measure insulin resistance and β cell function from serum insulin levels and fasting blood glucose and has been validated for inference in Wistar rats (Antunes *et al.*, 2016). Furthermore, hyperinsulinemia has been independently associated with increased risk for CVD (Libman *et al.*, 2010). Prior to the treatment period, there were no significant differences in serum insulin concentrations. However,

following 6 additional weeks on diet, serum insulin was significantly elevated in HCD compared to controls (**Figure 5.11**). This, together with the raised fasting blood glucose levels and worse tolerance discussed in the previous section, also equated to a significant increase in HOMA-IR in HCD compared to controls (**Table 5.1**), indicating that the HCD animals were insulin resistant – or at least more so than the controls. Previous studies using the same diet also reported on increased serum insulin and HOMA-IR (Huisamen *et al.*, 2011; Nduhirabandi *et al.*, 2017; Smit *et al.*, 2018). The cardiovascular effects of a 16-week high-sucrose diet without high-fat has been well characterised by Huisamen and colleagues (2011). These rats also presented with whole-body insulin resistance, as well as myocardial insulin resistance. In an additional study, Nunes and colleagues (2013) administered a high-sucrose diet to 16-week old Wistar rats for 9 weeks and found left ventricle hypertrophy with no differences in fasting blood glucose between their diet group and controls (~5.6 mM), but these rats presented with raised fasting blood insulin of 10.83±1.00 ng/mL compared to the 3.74±1.84 ng/mL of controls. Thus, in establishing a pre-diabetic model, even in the absence of significantly raised fasting blood glucose, hyperinsulinemia can be a prominent indicator of CVD risk. GRT supplementation had no significant effect on insulin serum levels or insulin resistance. Again, this was surprising as both rooibos and its polyphenols have been implicated to play a role in insulin sensitization. Aspalathin has shown to upregulate insulin secretion at concentration of 100 μM in RIN-5F pancreatic β-cells (Kawano *et al.*, 2009). Furthermore, treating insulin-resistant C2C12 skeletal muscle cells with either FRE or GRE enhanced glucose uptake, an effect attributed to a resensitization of P-PKB activity, suggesting improvement in insulin signaling (Mazibuko *et al.*, 2013). Similarly, in our previous publication (Smit *et al.*, 2018) we found aspalathin action in isolated cardiomyocytes to be significantly enhanced when co-treated with insulin. It could thus be that unless β-cell function is also improved by an additional treatment (which would result in elevated insulin) that the glucose uptake effect of rooibos is dissipated. Thus, supplementary insulin in conjunction with rooibos might be needed to improve glucose homeostasis.

6.3.3 Toxicity

Currently, the only known studies that showed toxic effects of rooibos were isolated case studies (Engels *et al.*, 2013; Sinisalo *et al.*, 2010). In the first instance a 42-year-old woman, receiving treatment for low-grade B-cell malignancy drank 1 L of rooibos infusions per day and presented with signs of liver toxicity, which stopped upon cessation of rooibos. In the second instance, a 52-year old man having a history of hyperlipidemia and stage III chronic kidney disease, using daily oral steroids and long-term statins to manage the disease, also presented with liver toxicity when consuming daily servings of buchu and rooibos. In the present study, at a daily aspalathin dose as found in 60 mg/kg GRT showed that GRT had no toxic effect on biometric parameters and did not induce morphological changes in the heart (**Table 5.2, Section 6.4.1**). Visual inspection of organs (liver, kidneys, intestines), also showed no obvious discolouration and rats did not present with any 'increased' irritation or aggression. **Appendix A8 (Table A3)** shows the fasting serum lipid markers indicating no adverse changes in lipid composition in either the control or HCD diet. From this we can at least deduce that lipid profile had not deteriorated in response to GRT treatment, and rooibos is known to improve in lipid profiles in rats (Canda *et al.*, 2014) and humans (Marnewick *et al.*, 2011). The safety of the dosage was predetermined and compared with previous studies performed on mice which showed no toxic effects (**Section 4.3.2.4**). One such study showed that *ob/ob* mice gavaged daily with 100 mg/kg BW aspalathin for 5 weeks (compared to the 7.8 mg/kg BW aspalathin in the present study) presented with decreased hepatic gene expression of gluconeogenesis and lipogenesis, considered to be anti-diabetic without toxic side-effects (Son *et al.*, 2013).

Granted, contraindications between related polyphenols in the GRT could have had a pro-oxidant effect (Goszcz *et al.*, 2015). Thus, the potential toxic effects of daily GRT administration for a period of 6 weeks in a control and pre-diabetic Wistar rat model remains to be determined as the current study did not measure liver enzymes.

6.3.4 Summary

We speculate that the mechanism for insulin resistance development following a high-fat, high-caloric diet is due to an increase in adipose tissue which causes elevated circulating FFA levels, altering adipose tissue derived factors, such as increasing leptin (responsible for inhibiting appetite) and TNFα (known to induce peripheral insulin resistance) and decreasing adiponectin (sensitize insulin action) (Yadav *et al.*, 2013), followed by the eventual visceral fat accumulation (Ding *et al.*, 2015; Grundy, 2012). In this regard, an increase in plasma FFA may have contributed to the elevated glucose levels as follows: i) inhibition of insulin action leading to increased lipolysis in fat cells, (ii) induction of insulin resistance by altering glucose transport, phosphorylation of relevant proteins or both (inhibition of insulin-mediated glucose uptake pathways) in cardiac muscle and possibly skeletal muscle and adipose tissue, (iii) increasing endogenous glucose production by increasing hepatic glucose output (Boden, 2011), (iv) and increased FFA-induced insulin secretion exacerbated by the FFA-induced insulin resistance (Boden, 1999).

Taken together, increased fasting blood glucose, fasting serum insulin and HOMA-IR, along with increased body weight and IP fat, confirm that the HCD diet was successful in establishing a model of pre-diabetes. However, in the present study, GRT supplementation had no significant effect on the biometric parameters in either control or pre-diabetic animals.

6.4 Effect of GRT on Ischemia/Reperfusion Injury

The basis of all experimentation in this study hinged on the working rat heart model, which generates haemodynamic endpoints used to indicate myocardial function. Subsequently these hearts can also be stained with TTC to determine the infarcted area present after regional ischemia (35 min of occluded blood supply) or the mitochondria can be isolated from ventricular heart tissue after global ischemia (20 min of zero blood supply) and mitochondrial function determined by measuring OxPhos. The effects of different protocols of ischemia and reperfusion on mechanical recovery post ischemia have been established previously in our laboratories, with 20 min global ischemia protocol resulting in partial contractile dysfunction short of complete heart failure during reperfusion (Nduhirabandi, 2014), while 35 min regional ischemia has been shown to result in significant infarcted areas without completely dissipating contractile function (Webster *et al.*, 2017).

6.4.1 Heart mass

Cardiac remodeling are molecular, cellular and interstitial variations that present in altered mass, size, shape and function of the heart (Azevedo *et al.*, 2016). This process is narrowly associated with ventricular dysfunction and malignant arrhythmias and therefore a strong indicator of a poor prognosis. Thus, it is important to investigate the effect of new treatments on these parameters of the heart. In the present study we measured the heart mass just prior to mounting the heart. The absolute cardiac mass was significantly increased by 8% in HCD compared to controls (**Table 5.2**, **Figure 5.12**), however when taken as a percentage of total body weight, this significance dissipated. Heart weight is associated with body weight, gender and age, (Kumar *et al.*, 2014), but can also be associated with hypertrophy - an independent indicator of CVD (Okwuosa *et al.*, 2015), which is also evident by the detrimental function of HCD hearts discussed in **Section 6.4.4**. In

the present study GRT supplementation had no significant effect on heart mass in either the controls or the HCD animals. Elevated heart mass had not been reported previously using the same diets (Kamau, 2018; Salie *et al.*, 2014). In our study, after weighing the hearts of 232 rats, we found values ranging between 0.876 and 1.620 g from rats weighing between 271-541 g, which equated to ranges between 0.25 and 0.45% of total body mass. However, in a study done by De Carvalho & Thomazini (2014) they reported on the mass of Wistar rat hearts ranging between 1.100 and 3.456 grams from rats weighing between 150 - 770 g. This equated to a ratio of heart weight to total body mass ranging between 0.5 and 0.7%. The authors of this study stated that after dissection of the heart, it was simply weighed immediately. To explain this discrepancy, we stress that after dissection of the hearts, residual blood was first squeezed out (to prevent blood clots forming during transport) before weighing as these hearts were destined for working heart perfusions. Furthermore, it is well established that heart mass increases with body mass (Beznak, 1954). Diet can also be a factor, as showed by a study done on Wistar rats receiving low- and high-fat diets, respectively comprising 16.4% and 50.4% of total caloric intake, whereby the high-fat diet resulted in increased cardiac mass found to be associated with increased triglyceride levels within the heart which resulted in cardiac dysfunction (Ouwens *et al.*, 2005). These high-fat diets were especially high in palmitate and oleate. In the present study, no differences were observed in serum palmitate levels between controls and HCD, however, HCD did present with elevated serum oleic acid (**Appendix A8**).

6.4.2 Heart Rate

In conditions such as angina pectoris, characterized by insufficient myocardial blood supply leading to chest pain, a higher heart rate is usually counterintuitive and accelerates the discomfort induced by myocardial ischemia (Riccioni, 2009). At baseline, GRT supplementation significantly decreased heart rate in both control and HCD animals (**Table 5.2, Figure. 5. 13**) without compromising heart function (**Section 6.4.4**). Heart rate lowering drugs, such as the benzocycloalkane, Ivabradine, selectively inhibits pacemaker activity (through inhibition of I_f, hyperpolarization-activated pacemaker current, which contributes to action potential generation in the sinoatrial node) (Verkerk *et al.*, 2007). It has been shown to dose-dependently lower both resting and maximal heart rate during exercise, shown greater efficacy in patients with elevated heart rate and protects against excessive bradycardia (Borer & Heuzey, 2008). We propose that GRT could have a similar pacemaker inhibitory effect. In humans, only one study has been done on rooibos' potential heart rate lowering effect. Persson and colleagues (2010) investigated the effect of 400 ml of Green, Black and Rooibos tea ("cup-of-tea" strength) on health volunteers and found no significant differences in heart rate for up to 3 hours of administration. However, in contrast, the present study administered a daily dose of aspalathin-rich extract at 2 "cup-of -tea" strength to rats and found a significant heart rate lowering effect on baseline perfusion measurements. This is a potential avenue for future research and would need further investigation.

6.4.3 Coronary flow rate and aortic diastolic / systolic pressure

Healthy coronary circulation is a direct product of coronary blood flow and myocardial-oxygen consumption according to the energy requirements of the heart. In humans, coronary perfusion at rest is an estimated 200 mL/min and can increase up to 1000 mL/min at maximal exercise (Hirasawa *et al.*, 1974). The main parameters dictating cardiac oxygen consumption and therefore coronary blood flow are heart rate, cardiac contractility (aortic perfusion pressure), and left ventricular wall stress (or afterload – kept constant throughout our experiments) (Depre *et al.*, 2011). Interestingly, unlike most other vasculature, the myocardium is perfused

mainly during diastole and coronary flow sharply decrease during systole attributed to myocardial compression (Depre *et al.*, 2011).

Pre-ischemia there were no significant differences in coronary flow between the 4 groups (**Figure 5.14**), while diastolic and systolic pressure were significantly lower in hearts from the HCD group compared to controls (**Figure 5.15, Figure 5.16**). Post-ischemia, coronary flow was significantly lower (↓13.1%) in HCD hearts compared to control hearts (**Figure 5.14**). Ischemia also significantly lowered diastolic and systolic pressure but did not result in inter-group differences (**Figure 5.15, Figure 5.16**). It has been shown in a study done on Zucker Diabetic Fatty rats that as the severity of diabetes progresses, the damage incurred by I/R-I also increases and results in decreased coronary flow (Povlsen *et al.*, 2013). Also during myocardial ischemia, left ventricular diastolic function deteriorates, which is considered a precursor for systolic dysfunction (Stewart *et al.*, 1992). Furthermore, supplementation with GRT increased diastolic and systolic pressure in hearts from both controls and HCD rats pre-ischemia, but this effect was lost after ischemia and not significant. Similar to the heart rate lowering effect of Ivabradine described in the previous action (**Section 6.4.3**), this drug also showed to selectively induce a positve inotropic effect on cardiac contractility in both mice and humans (Boldt *et al.*, 2010).

6.4.4 Aortic output, total cardiac output and total work

Myocardial I/R-I contributes to cardiac dysfunction following myocardial ischemia, cardiac surgery or circulatory cessation (Frank *et al.*, 2012). Pre- and post-ischemia, AO, CO and W_T were significantly reduced in hearts from HCD rats compared to controls (**Figure 5.17, Figure 5.18, Figure 5.19**) and HCD hearts had poorer recovery post-ichemia for all three parameters (**Table 5.2, Figure 5.20**). These findings are characteristic of previous data obtained from diet-induced obese (Du Toit *et al.*, 2008), insulin-resistant models (Huisamen *et al.*, 2012) and interestingly, also high-fat, low-carb diets (Liu *et al.*, 2014, 2016), which resulted in the same biometric morphology as induced in our study by a high-sucrose, high-fat diet.

GRT supplementation significantly improved all three parameters measured pre-ischemia in hearts from control and HCD rats, whilst also improving all three parameters post-ischemia in the HCD group, resulting in improved aortic and coronary output recovery (**Table 5.2**) and total work recovery (**Figure 5.20**). Antioxidant pre-treatment is known to reduce myocardial I/R-I (Crouser & Parinandi, 2011). These findings corroborate previous studies showing rats treated with either GRE or FRE displayed increased myocardial total GSH content (endogenous antioxidant) and reduced oxidative stress, resulting in improved cardioprotection through increased aortic output recovery against I/R-I (Pantsi *et al.*, 2011). Furthermore, rats receiving fermented rooibos tea for 7 weeks had increased antioxidant capacity and reduced lipid peroxidation, conferring neuroprotection against I/R-I in the brain (Akinrinmade *et al.*, 2017). Based on GRT's effect on increasing heart contractility, it can be considered cardiotonic – per definition a substance that favorably effect upon the action of the heart.

6.4.5 Left ventricular infarct size

It has been illustrated that, without reperfusion, 100% of the area at risk will become an infarct, whereas through timely reperfusion about half of the lethal I/R-I can be prevented (Sattur *et al.*, 2015). The addition of therapeutic interventions in the form of pre-conditioning or post-conditioning results in salvaging another quarter of reversible infarcted area - but even considering the best cardioprotective drug known, 25% damage

of the initial theoretical untreated infarct size will remain. In general, the longer the coronary artery is occluded, the bigger the infarct size, and the worse the outcome for the patient (Heusch & Gersh, 2016). In the present study we determined the effect of GRT following 35 min of regional ischemia/reperfusion. Similar to the global ischemia protocol, coronary artery occlusion during the regional ischemia protocol also caused significant decreases in all functional heart parameters for each group (**Table 5.3**, **Figure 5.21**), signifying the detrimental effect of I/R-I on myocardial contractile function. GRT treatment once again showed improvement in functional heart recovery, albeit not as profound as for the global ischemia protocol, with some of the previous significance lost, such as improvement in both coronary flow, diastolic, systolic pressures and total work recovery (**Table 5.3, Figure 5.22**). Staining these hearts for viable tissue, we saw a significant increase in infarct size in HCD compared to controls (**Table 5.3**, **Figure 5.23**). It has been shown previously in diet-induced obese models using the same ischemic protocol that infarct sizes were grossly increased (Huisamen *et al.*, 2011; Du Toit *et al.*, 2008). Remarkably, GRT supplementation completely diminished the infarcted area in HCD (↓62.2%) to that seen in controls (**Figure 5.23**, **Figure 5.24**). This is the first time Afriplex GRT has been shown to have a cardioprotective effect on infarct size reduction *in vivo*. Thus, we speculate that the improvement in heart function can be partly attributed to the cardioprotective effect in preventing necrotic tissue damage and subsequently preventing additional ROS release and inflammation, ameliorating a necrotic chain reaction, which would have exacerbated surrounding cardiomyocyte damage.

6.5 SIGNALING PROTEINS

In view of GRT's cardioprotective effects pertaining to heart function and infarct size reduction discussed in the previous section, we aimed to investigate a broad-spectrum of various cellular signaling intermediates pertaining to cardioprotection, including the Ras–MAPK signaling pathway such as p38, ERK1/2 and JNK, which are precursors of cell stress signaling; and intermediates in the PI3K–PKB–eNOS pathway, which results in metabolic modulation and cardiovascular protection.

In aiming to understand the effect of treatment on the progression of T2D, it is essential to recognize two points: First, glucose uptake into cells (including heart muscle) can result from two distinct pathways, namely insulin-dependent (through PI3K/PKB and contraction-mediated stimulation) (Sriwijitkamol *et al.*, 2007), and insulin independent (through AMPK and hypoxia-mediated stimulation) (Jing *et al.*, 2008). Secondly, in the progression of T2D, AMPK activation remains largely intact (Jing *et al.*, 2008), whereas PKB and other proteins relating to the PI3K pathway becomes dysfunctional (Mackenzie & Elliott, 2014).

6.5.1 Insulin-Dependent Signaling

- **PKB/Akt**

PKB is a serine/threonine-specific protein kinase that plays an essential role in insulin-stimulated cellular processes, including cell growth, survival, proliferation, and metabolism (Gonzalez & McGraw, 2009). Insulin binding to insulin receptor on the cell surface results in activation of insulin receptor substrate and recruitment of PI3-Kinase and then PKB, which proceeds to activate AS160, likened to AMPK's action discussed below, which then result in GLUT4 translocation to the membrane and glucose uptake (Sakamoto & Holman, 2008). Therefore, any reduction in PI3K/PKB/AS160 activation results in suppressed glucose uptake. It has been shown that insulin resistant conditions present with downregulation of up- and downstream targets of PKB (Mackenzie & Elliott, 2014). Also, PKBβ-knockdown mice (Cho *et al.*, 2001) and PKBβ-mutations in humans (George *et al.*, 2004) result in severe insulin resistance and diabetic-like symptoms, implicating PKB as a key

role player in maintaining normal blood glucose levels. Prior to ischemia there were no significant differences between PKB expression or activation in hearts from control and HCD rats (**Figure 5.25, Table 5.4**). This was surprising as HCD had significantly poorer glucose tolerance and increased insulin resistance, which would indicate lower PKB activity. Previous studies using diet-induced obese rats and high-fat diet rats also reported no difference in baseline cardiac PKB activation (Salie *et al.*, 2014). Alternatively, it has been shown in mice with high-fat diet induced insulin resistance and obesity presenting with high circulating FA that even with established systemic insulin resistance, cardiac tissue can remain insulin sensitive (Gupte *et al.*, 2013). Similarly, in our present HCD model cardiac tissue could have remained insulin-sensitive, even while presenting with systemic insulin resistance (**Section 6.3.2**) and elevated circulating FA (**Appendix A8, Table A3**). Furthermore, GRT supplementation increased basal PKB activation in hearts from controls, but decreased activation and expression in HCD. As both GRT treated groups did not differ significantly in glucose tolerance or insulin sensitivity compared to their untreated counterparts, this was also unexpected. In our previous study, it was found that 10 μM aspalathin treatment could induce glucose uptake in isolated cardiomyocytes from insulin-sensitive rats, while the effect was lost in insulin-resistant rats without administering additional insulin (Smit *et al.*, 2018). Given that HCD had elevated serum insulin levels compared to controls, it would appear that the presence of insulin is not the determining factor in eliciting GRT's glucose uptake response, but rather downstream insulin signaling, such as GLUT4 translocation that is impaired. As a possible confounder, it has been shown before by Huisamen & Lochner (2005) that diabetic rats receiving exercise had increased cardiomyocyte glucose uptake and normative PKB activation compared to controls. If this is the case in our present study, it would point out the disparity between full body insulin resistance (as measured: **Table 5.1**) and cardiac insulin resistance, or alternatively call into question the sedentary lifestyles led by our animals, and their potential to be highly active at night (Borbély *et al.*, 1975).

- ISCHEMIA

HCD significantly decreased myocardial PKB activation during ischemia compared to controls, whereas GRT had no statistically significant effect in reversing or improving these parameters (**Figure 5.25, Table 5.4**). Surprisingly, not much is known about the role of PKB during ischemia. By definition, ischemia and the absence of blood flow means no circulating insulin, and therefore no PKB signaling. It has been shown in the isolated perfused heart that ischemia inhibits PKB activation through the lowering of pH (Beauloye *et al.*, 2001). Consequently, insulin-independent AMPK signaling becomes more important during ischemia (**Section 6.5.2 - Ischemia**) (Qi & Young, 2015).

- REPERFUSION

Upon reperfusion, PKB activation results in various protective mechanisms sequestering or inactivating pro-apoptotic proteins such as BAD, BAX and caspase 9 (Bertrand *et al.*, 2008). In early reperfusion, hearts from rats on the HCD has significantly decreased PKB activity compared to controls (**Figure 5.25A+B, Table 5.4**), correlating with the poorer heart function and increased infarct size (**Section 6.4.4-5**). Similarly, it has previously been shown in our laboratories in an obese, insulin-resistant rat model, that 15 min of myocardial ischemia followed by 10 min of reperfusion resulted in significantly decreased PKB activation in comparison to hearts from control animals, also resulting in decreased cardioprotection (Salie *et al.*, 2014). Furthermore, HCD animals had significantly elevated PKB expression, with GRT treatment resulting in even higher PKB expression (**Figure 5.25C)**. The significance thereof remains unclear as these hearts did not have elevated PKB activation. All of the previous work showing Rooibos to stimulate PKB activation occurred *in vitro* in L6

myocytes (Son *et al.* 2013) and insulin-resistant C2C12 myocytes (Mazibuko *et al.* 2013). *In vivo,* isolated hearts from a control rat model pre-treated for 7-weeks with GRE, wereubjected to I/R-I in while PKB activation remained unchanged after 10 min of reperfusion - even though these hearts also had improved infarct size and heart function (Pantsi *et al.*, 2011). Even in the absence of PKB activation, due to a lack of upstream PI3K or insulin-stimulation, these hearts are still protected against subsequent stressors. In the present study we did not use insulin in our perfusates as insulin by itself was shown to be cardioprotective in I/R-I (Ji *et al.*, 2010). During late reperfusion, hearts from rats on the HCD had significantly decreased PKB expression (**Figure 5.25C, Table 5.4**), while GRT supplementation significantly decreased PKB activation in both controls and HCD (**Figure 5.25B**), implicating GRT in switching over metabolism to non-insulin dependent mechanisms in extended reperfusion.

6.5.2 Insulin-Independent Signaling

- **AMPK**

AMPK is a protein serine/threonine kinase and the master energy regulator of cells operating independent of insulin-action. It senses the energy status of the cell and responds by restoring energy balance (Hue & Rider, 2007). As a result, therapies are often aimed at activating AMPK in managing metabolic syndrome (and associated) diseases, which include anti-diabetic drugs, such as metformin (Hawley *et al.*, 2002) and thiazolidinediones (LeBrasseur *et al.*, 2006), insulin sensitizing adipokine therapies, such as adiponectin (Zhou *et al.*, 2009), and exercise (Richter & Ruderman, 2009). The opposite is also true, in that decreased AMPK activity has been associated with increased prevalence of metabolic disorders in animals and humans (Xu, Valentine, *et al.*, 2014). In the present study, prior to ischemia, HCD decreased myocardial AMPK activity compared to controls (**Figure 5.26A, Table 5.4**) in alignment with the increased metabolic stress experienced in this model. GRT supplementation increased myocardial AMPK expression in controls, but not in HCD (**Figure 5.26B**). Rooibos has been shown in previous studies to increase AMPK activation, including *in vitro* in insulin-resistant mouse C2C12 skeletal muscle cells (Mazibuko *et al.*, 2013), and aspalathin treatment in L6 myocytes and in mice fed aspalathin for 5 weeks (Son *et al.*, 2013). In all three these instances, AMPK activation led to GLUT4 translocation, which resulted in glucose uptake. However, it has been shown by Muller and colleagues (2012) that aspalathin treatment only resulted in glucose uptake if GLUT4 was present in the cell line (C2C12 skeletal muscle cells vs Chang liver cells – a cell line absent of GLUT4). The inference is that for rooibos (aspalathin) to induce glucose uptake, altogether AMPK, AS160 and GLUT4 signaling need to be sensitized.

- ISCHEMIA

Normally, glycolysis only contributes about 5% of ATP production in a normal oxygenated heart (Abozguia *et al.*, 2009). However, during ischemia, reduced oxygen delivery results in decreased ATP formation through oxidative phosphorylation (Rosano *et al.*, 2008). This results in increased reliance on glycolysis to provide ATP production (Depre *et al.*, 1999). During ischemia, AMPK activation is associated with increased glucose utilization and ATP production, which serves a critical role in preserving ionic gradients across membranes and preserving cell function and viability (Weiss & Hiltbrand, 1985). Glucose uptake by AMPK activation is a result of AS160 activation leading to GLUT4 translocation to cell membranes (Samovski *et al.*, 2012). Additionally, AMPK upregulates glycolysis in myocardial ischemia through PFK-2 activation (an intermediate in the glycolysis pathway) increasing the glycolytic rate-limiting step, PFK-1 (Marsin *et al.*, 2000). Conversely, AMPK also suppresses the activity of glycogen synthase, resulting in less glycogen synthesis during stress,

and therefore more ATP conservation (Halse *et al.*, 2003). Presently in ischemia, HCD significantly increased myocardial AMPK activity compared to hearts from control rats (**Figure 5.26A+B, Table 5.4**). Likewise, GRT supplementation also increased myocardial AMPK activation in control rats, without a significant effect in HCD rats. The exact mechanism how an increase in AMPK during ischemia resulted in cardiodamaging outcomes in the HCD model, but improved cardioprotection induced by GRT supplementation in controls is uncertain. Given that both PKB and AMPK activation did not result in increased glucose uptake, a dysfunctional GLUT4 translocation or activation can be inferred or that downstream myocardial AMPK signaling is inhibited in the HCD animals. This may be at the level of GLUT4 translocation, which was not measured in the current study. Alternatively, the response of each model to the effect of acute vs prolonged ischemia needs to be considered. It has been found during moderate myocardial ischemia, sustaining glycolysis can be beneficial as maintaining ion gradients is potentially essential in optimal diastolic relaxation (Kusuoka & Marban, 1994). However, in sustained ischemia, should glucose oxidation not increase parallel to increased glycolysis, it results in accumulation of protons and lactate correlated with a poorer outcome in the heart (Vaughan-Jones *et al.*, 2009).

- REPERFUSION

In early reperfusion, GRT supplementation significantly increased myocardial AMPK activation in HCD rats (**Figure 5.26A+B, Table 5.4**). Accumulating research is implicating AMPK activation post-ischemia as a protective mechanism in reducing ischemic injury and reducing necrosis (Qi & Young, 2015). For instance, high dosages of metformin administration have been shown to activate cardiac AMPK through inhibition of mitochondrial complex I and thereby inhibition of mitochondrial ATP production (Hou *et al.*, 2018). This results in a protective effect to ischemic damage in both normal and diabetic mice when administered prior to ischemia and at the onset of reperfusion (Calvert *et al.*, 2008). This same effect has also been shown to protect against acute I/R-I and chronic rejection (a condition whereby antibodies injure the blood vessels and thereby restrict blood flow to the heart) following heart transplants in mice (Chin *et al.*, 2011). In late reperfusion there were no differences in the specific AMPK activation between the 4 groups. However, HCD significantly decreased myocardial AMPK expression, while GRT supplementation increased the AMPK expression (**Figure 5.26C, Table 5.4**). Conversely, in controls, GRT supplementation decreased AMPK expression. The significance of difference in AMPK expression levels at this point is considered arbitrary as the initial cardiodamaging or protective effects in response to reperfusion had already been incurred.

- **AS160**

AS160 acts as a precursor to GLUT4 mediated glucose uptake into cells. AS160 is a GTPase-activating protein, which functions to inhibit the small GTP-binding proteins in control of key intracellular vesicle movement steps (Fukuda, 2011). As an insulin-independent mechanism, AMPK-induced activation of AS160 removes the GAP inhibition on Rab GTPases triggering GLUT4 vesicle translocation to the cell membrane (Ishikura *et al.*, 2007). In insulin-sensitive tissues, insulin binding to insulin receptor initiates signaling through PKB resulting in GLUT4 translocation and subsequent glucose uptake into the cell (Thorell *et al.*, 1999). However, the activity level of intermediates in this signaling cascade, such as PKB, can remain normal under various conditions, including fasting (Vendelbo *et al.*, 2012), obesity (Bandyopadhyay *et al.*, 2005) and diabetes (Sakamoto & Holman, 2008), thereby implicating the importance of downstream signals relating to insulin action. AS160 is currently acknowledged as the most distal signaling step in insulin-mediated glucose transport (Consitt *et al.*, 2013). Insulin stimulated activation of AS160 becomes impaired in insulin-resistant

conditions (Karlsson *et al.*, 2005) and as a result decreases GLUT4 translocation and consequently decrease glucose uptake into cells. Sedentary aging decreases insulin-induced phosphorylation of AS160 in skeletal muscles - an effect that can be reversed with exercise training (Consitt *et al.*, 2013). In the present study, pre- and during ischemia there were no significant differences in AS160 activation between hearts from controls and HCD rats (**Figure 5.27B, Table 5.4**). As the hearts from the HCD rats were more insulin resistant, we expected AS160 activity to also be lower at baseline compared to controls. However, this could be the effect of 30 min of insulin-free perfusion, and the levels could potentially have been different if these hearts were investigated for AS160 levels before perfusion. Pre-ischemia, GRT supplementation significantly increased AS160 expression in hearts from both control and HCD rats (**Figure 5.27C**) while decreasing AS160 activation in both (**Figure 5.27B**). Without AS160 activation, GLUT4 would also remain indifferent and no glucose clearance would take place. AS160 appears to be the primary signal that requires resensitization in order for GRT to have any beneficial effect on glucose uptake. To date, no other study has been done on the effect of GRT on the signaling of AS160.

- ISCHEMIA

In ischemia, GRT supplementation significantly increased the myocardial AS160 activation/expression ratio in controls but not in HCD (**Figure 5.27A**). As previously mentioned, GRT supplementation also improved myocardial AMPK activation in controls, while decreasing AMPK activation in HCD. Therefore, AS160 activation is a direct consequence of an AMPK-dependent mechanism, which is not present during ischemia in HCD animals. It has been noted that FA-oxidation can be detrimental in ischemia when preferred over glucose-oxidation. In a study done by (Chang *et al.*, 2012) they treated rats for 14 days with 100 mg/kg BW/day berberine (a compound present in European barberry) and subjected the isolated hearts to 30 min ischemia followed by 120 min of reperfusion. They found that the treatment significantly decreased AMPK activation in the ischemic areas of the heart while significantly increasing AMPK activation in the non-ischemic areas. Likewise, it is possible that GRT also resulted in improving myocardial AMPK activation resulting in AS160 activation and higher glucose-oxidation within hearts from control rats and decreased myocardial AMPK activation resulting in decreased AS160 activation and decreased glucose oxidation in hearts from HCD rats at higher risk for infarct size generation.

- REPERFUSION

Upon reperfusion, hearts from HCD had significantly decreased AS160 activation/expression ratio compared to controls (**Figure 5.27A**), as a result of lower upstream myocardial PKB and AMPK activation - which would implicate lower glucose uptake and inversely, increased FA-oxidation (**Section 6.6.3**). Increased FA-oxidation rates early into reperfusion has been linked to severe cardiac dysfunction. In a study by Kudo and colleagues (1995) they found isolated rat hearts subjected to 30 min ischemia followed by 60 min reperfusion to have elevated FA-oxidation compared to pre-ischemia, but these hearts only had a 16% functional recovery. Thus, metabolic switching from glucose to FA into reperfusion can be detrimental to at risk heart tissue. Presently, GRT had no effect on AS160 expression or activation during late reperfusion (**Figure 5.27B+C, Table 5.4**).

6.5.3 RISK

- **ERK 1 / 2**

The ERK cascade has been identified as a key player in cell proliferation, differentiation, adhesion, migration and survival (Buscà *et al.*, 2016). Through proteomic screening, ERK has shown to phosphorylate at least 270 substrates to date (von Kriegsheim *et al.*, 2009). ERKs phosphorylate numerous transcription factors through

passive diffusion to the nucleus (Lenormand *et al.*, 1993). The longer and the more pronounced ERK is activated, the more substrates are phosphorylated in turn at their respective docking sites (Murphy *et al.*, 2004). It is still unclear whether ERK1 and ERK2 have functional differences despite the determination of a vast amount of studies aimed at answering this question (Buscà *et al.*, 2016). Given that ERK2 is more highly expressed than ERK1 in most mammalian cells (Frémin *et al.*, 2015), it is important to consider the relative expression and activation level of both to interpret and compare data between studies (Buscà *et al.*, 2016). Presently, the only difference in activation over expression ratio for either ERK1 or ERK2 between HCD and controls occurred 30 min into reperfusion, when HCD had significantly decreased ERK2 activation/expression ratio (**Figure 5.28A**, **Table 5.5**). It has been shown that increased ERK1/2 activation is correlated with increased cell function and survival following stress stimulation in a rat model of myocardial ischemia/reperfusion (Milano *et al.*, 2007). In the present study, GRT had varying effects on both controls and HCD, indicating that separate mechanisms are at play in response to the different cellular signaling profiles induced by two different diets. During stabilization, GRT supplementation increased ERK1 and 2 expression in controls, but not HCD (**Figure 5.28C**, **Figure 5.29C, Table 5.5**). Bueno and colleagues (2000) showed that transgenic mice over-expressing activated MEK1 (an upstream activator of ERK), resulted in improved cardiac function and increased ERK1/2 protein levels, which was presumed to be a result of improved stability and reduced endogenous ERK degradation. These mice were also more resilient to ischemia/reperfusion induced apoptosis than control mice (Lips *et al.*, 2004). Therefore, increased ERK expression during stabilization can be considered as a mechanism of preconditioning to subsequent ischemic insults.

- ISCHEMIA

At the end of a 20 min ischemic insult, GRT supplementation resulted in decreased ERK1 and 2 expression (**Figure 5.28C, Figure 5.29C)**, and decreased ERK2 activation compared to HCD (**Figure 5.29B, Table 5.5**). However, when considering the relative ERK1/ERK2 ratio, GRT supplementation significantly increased activation in both control and HCD (**Figure 5.30A)** and increased the expression ratio in HCD (**Figure 5.30B, Table 5.5**). In a study done by Yang and colleagues (2011) they investigated the effect of 30 min myocardial ischemia on isolated rat hearts at two different temperatures. The authors found infarct size to be greatly reduced at 35°C (mean infarct size of 15.6%), which had consistently higher ERK activation compared to 38.5°C (mean infarct size of 34.4%), reducing ERK activation. Therefore, ERK activation during ischemia rather than reperfusion was found to be a crucial indicator of cardioprotection. In contrast, but done in a separate organ system, another study performed by Lu and colleagues (2007) induced spinal cord ischemia for 5 min in rats before restoring blood flow. In control rats, ERK1 and 2 were activated, corresponding to the abundant microglial formation at the infarcted area and increased IL-1β expression. Whereas receiving MEK1/2 inhibitor, U0126, completely inhibited ERK1/2 activation, resulting in significantly lower microglial activation, IL-1β levels and improved neuronal survival and functional performance. Therefore, ERK1 and 2 inhibition resulted in reduced inflammatory reactions and cytokine production, which can be beneficial to post ischemia-reperfusion injury.

- REPERFUSION

During early reperfusion, GRT supplementation significantly increased ERK2 activation in controls (**Figure 5.29B**), while decreasing ERK1 activation in HCD (**Figure 5.28B, Table 5.5**). Considering the above-mentioned studies this could indicate a pro-survival response in controls and a more anti-inflammatory response in HCD. The ERK1/ERK2 activation were also significantly decreased by GRT supplementation in

both controls and HCD (**Figure 5.30A**) showing GRT's identical response on ERK signaling albeit towards producing different cellular responses. In late reperfusion, GRT supplementation furthermore decreased ERK2 expression and the ERK2 activation/expression ratio in HCD (**Figure 5.29C+A**) – indicating a reduction in stress and therefore ERK activation, while in controls also decreasing ERK1/2 expression but increasing ERK1 activation and ERK2 activation/expression ratio – indicating a sustained pro-survival effect.

6.5.4 Stress

- **JNK 1/2**

JNKs, or stress-activated protein kinase, form part of the death receptor-initiated extrinsic pathways, as well as the mitochondrial intrinsic apoptotic pathways. JNKs lead to apoptosis through upregulating pro-apoptotic genes via specific transcription factors or modulating mitochondrial pro- and anti-apoptotic proteins by kinase action (Dhanasekaran & Reddy, 2011). JNK1, and not JNK2, has been indicated as essential for tumor necrosis factor alpha (TNFα)-induced c-Jun kinase activation, c-Jun expression, and apoptosis (Liu *et al.*, 2004). TNFα activates JNK1, but not JNK2. However, JNK2 can still influence JNK1 activity through upstream kinases. JNK activation does not significantly increase during myocardial ischemia in human coronary artery bypass surgery (Talmor *et al.*, 2000) however subsequent JNK activation significantly contributes to myocardial I/R-I in heart transplantations (Vassalli *et al.*, 2012).

- ISCHEMIA

In the present study, we also found no significant changes JNK1 and JNK2 activation prior to reperfusion (**Figure 5.31**, **Figure 5.32, Table 5.5**). Interestingly, during stabilization, GRT supplementation increased JNK2 expression in controls, but not HCD (**Figure 5.32C)**. The meaning hereof is uncertain and could potentially just indicate the overall health of the cells or serve as a form of preconditioning – having the capacity to defend against potential increases in stress.

- REPERFUSION

In early reperfusion, HCD had significantly decreased JNK1 expression and activation, compared to controls (**Figure 5.31B+C, Table 5.5**). Concurringly, even though HCD increased JNK2 expression, it also significantly decreased JNK2 activation, resulting in a decrease of JNK2 activation/expression compared to controls (**Figure 5.32A, Table 5.5**). This is strange, as at face value this would infer that HCD had less inflammatory markers, such as TNFα, and less oxidative stress, through ROS, to stimulate JNK activation, and is also less prone to apoptosis. GRT supplementation, decreased JNK2 activation even further in HCD. However, during late reperfusion, HCD had significantly increased JNK1 and JNK2 activation levels (**Figure 5.31B, Figure 5.32B**) and increased JNK1 and JNK2 activation/expression compared to controls (**Figure 5.31A, Figure 5.32A**), indicative that the bulk of apoptosis would only occur later into reperfusion. Once again, GRT supplementation decreased JNK2 in this late stage (**Figure 5.32B**) and thereby potentially prevented more pro-apoptotic signaling. Taken together, it would appear as though HCD has a slower response to increasing stress brought upon by reperfusion compared to controls, and perhaps first need to express more JNK to meaningfully respond to the new stress stimulus. Considering that these hearts had worse function, it would also indicate a preoccupation with handling the new influx of stress, rather than focusing on maintaining functional parameters. Considering GRT in controls, during early reperfusion, JNK1 activation was significantly increased (**Figure 5.31B**). This was also the case for both JNK1 activation and activation/expression ratio in late reperfusion (**Figure 5.31A, Figure 5.31B**). This is difficult to explain given the prior argument that HCD delayed JNK expression and subsequent activation, whereas now, GRT resulted in elevated JNK activation –

given that these hearts performed mechanistically better, and had similar infarct sizes, I would argue that it's not reflective of apoptosis *per se*, but rather reflects on the responsiveness of control animals' susceptibility to treatment. JNK-dependent signaling results in ROS generation, mitochondrial dysfunction and cardiomyocyte apoptosis (Chambers *et al.*, 2013). Higher ROS generation would result in a greater need for endogenous antioxidant systems to maintain a positive balance of antioxidants to oxidants – and vice versa. And since GRT is abundant in polyphenols, known for their strong antioxidant capacity, 6 weeks treatment could have instilled quite a reservoir of antioxidants in membranes of the myocardium. Therefore, JNK could potentially be activated by upstream signaling to counter the high amounts of antioxidants present in the myocardium.

6.5.5 Inflammation

- **p38 MAPK**

p38 MAPKs are a class of serine/threonine protein kinases which relays extracellular stress signals to the cell nucleus and thereby induce adaptive intracellular responses. It can be thought of as an 'emergency switch' that results in activation of transcription factors, cytokines and surface receptors (Korb *et al.*, 2006). p38 activation is especially prominent step in chronic inflammation (Korb *et al.*, 2006). Therefore, p38 inhibition is regarded as a promising target to manage inflammatory diseases. Furthermore, T2D is associated with hyperglycemia, chronic inflammation, and high plasma levels of FFAs, all capable of activating p38 (Liu & Cao, 2009). This is also confirmed by our findings that p38 activation was significantly increased in HCD compared to controls prior to ischemia (**Figure 5.33B**), which also led to an increased p38 activation/expression ratio (**Figure 5.33A, Table 5.6**). This elevation in p38 activation in HCD could also be attenuated by GRT supplementation (**Figure 5.33B+C**) and would infer that GRT had an anti-inflammatory effect prior to ischemia. In a study by Ku and colleagues (2015), they showed that aspalathin and nothofagin treatment in both high-glucose induced inflammation in human umbilical vein endothelial cells and mice suppressed ROS and NFKB (a cytokine production signal and proinflammatory marker). Furthermore, it has been demonstrated that hearts from transgenic mice with a dominant-negative p38-alpha mutant were significantly protected from ischemia reperfusion injury and had smaller infarct size compared to controls (Lips *et al.*, 2004). In another study done by Chai and colleagues (2008) rats were fasted overnight and hearts investigated for 30 min regional ischemia-reperfusion injury with an insulin infusion starting 10 min prior to ischemia. Insulin had no cardioprotective effect by itself, however, when co-administered with a p38 inhibitor 10 min prior to ischemia or 5 min prior to reperfusion, a considerable decrease in infarct size was detected. Therefore, this inhibitory mechanism induced by GRT could potentially have been a form of preconditioning and thereby cardioprotective to subsequent I/R-I.

- ISCHEMIA/REPERFUSION

There were no differences between HCD and control p38 expression or activation during ischemia and early reperfusion, however upon later reperfusion, p38 expression was significantly decreased in HCD compared to controls (**Figure 5.33C, Table 5.6**). GRT supplementation in controls led to significant elevation in p38 expression during ischemia (**Figure 5.33C**), and increased p38 activation in early reperfusion (**Figure 5.33B**), while also decreasing p38 expression in HCD during early reperfusion (**Figure 5.33B**). It has been shown that non-selective p38 activation through anisomycin prior to 25 min of global ischemia can precondition the rat heart against reperfusion injury (Lochner *et al.*, 2003) while attenuation of p38 after extended reperfusion can be considered a prerequisite for improved recovery and reduced infarct size. However, these findings early into reperfusion are novel and as such hard to definitively explain the mechanism. Most studies on isolated rat

hearts subjected to 30 min ischemia and 30 min reperfusion only sampled protein signaling at the end of reperfusion, whereby significant left ventricular dysfunction, together with increased p38 and JNK activation was observed (Kumar *et al.*, 2004; Milano *et al.*, 2007). Furthermore, in a study by Surinkaew and colleagues (2013) using adult wistar rats subjected to 30 min regional ischemia followed by 120 min reperfusion, they found that p38 inhibition before or during ischemia was beneficial, however when given at the onset of reperfusion, hearts presented with decreased ventricular tachycardia/ventricular fibrillation and increased heat shock protein 27 activation. Therefore, timing of p38 inhibition and relative activation prior to ischemia is essential to confer cardioprotection. However, from the findings of the current study, it is still uncertain what the role of p38 activation is prior to ischemia.

6.5.6 Autophagy

- **LC3**

LC3 (microtubule-associated protein 1 light chain 3) is a mediator in the autophagic process. The formation of the autophagosome is initiated by PI3K, Beclin 1 and two ubiquitin-like conjugation systems resulting in Atg5-12 and LC3 formation (Yang & Klionsky, 2010). Once LC3 is converted from its cytoplasmic form, LC3-I (18 kDa), to the autophagosome-bound form, LC3-II (16 kDa), autophagy is activated (Walczak *et al.*, 2017). Therefore, the LC3-II/LC3-I ratio is considered an important indicator of autophagy (Kadowaki & Karim, 2009). During autophagy, injured protein and organelles are enzymatically digested to supply energy and provide substrates for repairing organelles important in cell homeostasis (Yang & Klionsky, 2010). However, excessive autophagy can also induce irreversible cell atrophy resulting in autophagic cell death, or by inducing apoptosis and necrosis (Maiuri *et al.*, 2007). Autophagy have been shown to be upregulated in response to I/R-I (Dai *et al.*, 2017), however the degree of upregulation and timing of autophagy remains a mystery. In the present study HCD had more LC3-I and II during stabilization compared to controls (**Figure 5.34B+C, Table 5.6**) indicating higher levels of autophagy. Furthermore, GRT supplementation increased autophagic flux in controls, but not in HCD (**Figure 5.34A**) – potentially because autophagy had already been upregulated.

- ISCHEMIA

Ischemia presented with the lowest autophagy activity in all 4 groups, with both HCD and GRT supplemented controls also experiencing a significant decrease from baseline autophagy levels (**Figure 5.34A, Table 5.6**). It has been shown in rabbit hearts exposed to 20 min of ischemia that autophagy remained fairly dormant, as though the cell was in a hibernative state (Decker & Wildenthal, 1980).

- REPERFUSION

Early into reperfusion, HCD had upregulated LC3-I and II and compared to controls (**Figure 5.34B+C**). GRT supplementation further increased autophagy in HCD, while suppressing autophagy in controls (**Figure 5.34A**). As reperfusion progressed, HCD had decreased LC3-II content compared to controls (**Figure 5.34B**). GRT supplementation also reduced autophagy in controls, but not in HCD – as these groups already had lowered autophagy (**Figure 5.34B**). In all 4 groups autophagy was gradually increased and peaked at the end of reperfusion – with HCD having an initial burst during early reperfusion, but then slowing down upregulation of autophagy (**Figure 5.34A**). Continueing with the rabbit study described above, autophagy was shown to be extensively upregulated following reperfusion, with a certain subgroup also showing signs of necrotic damage (Decker & Wildenthal, 1980). Furthermore, severe stress, such as prolonged I/R-I can result in excessive and long-term autophagic upregulation which results in cell death and digestion of essential organelles and proteins (Gustafsson & Gottlieb, 2009). Given the functional and infarct cardioprotection

conferred by GRT in this study, the pattern of gradually increasing autophagy seems most beneficial to preserving cell integrity, whereas sudden increases in autophagy can become detrimental – as was found in the HCD groups. GRT has not been investigated for its role in autophagy before. However, one of its polyphenols, quercetin has shown to extensively induce autophagy and promote cell death in cancer cells through inhibition of proteasomal activity and mTOR signaling (Klappan *et al.*, 2012). Furthermore, various other polyphenols, such as resveratrol, catechin, silibinin and curcumin (Hasima & Ozpolat, 2014; Pallauf & Rimbach, 2013) have shown to regulate autophagy through Beclin-1 dependent and independent pathways, and could implicate GRT to have similar action. These observations warrant further elucidation.

6.5.7 Auxiliary Metabolic Regulation

- **GSK3β**

GSK3β plays a key role in deactivating glycogen synthase (resulting in lower blood glucose utilization), gene regulation (inducing apoptosis) (Meares & Jope, 2007) and GSK3β inactivation significantly inhibits the mPTP opening in response to increases of ROS and calcium overload (Ghaderi *et al.*, 2017b). It is distributed throughout the cell, and once activated, translocates from the cytoplasm to the cellular membrane or mitochondria (Bijur & Jope, 2003). It can be deactivated (inhibited) through phosphorylation by various pro-survival pathways, including p38, PI3K and AMPK (Ghaderi *et al.*, 2017b), making it a central but complex role player in cell survival (Mnatsakanyan *et al.*, 2017). GSK3β expression and phosphorylation has been shown to be upregulated in skeletal muscle of T2D (Nikoulina *et al.*, 2000) and in adipose tissue of obese diabetic mice (Eldar-Finkelman *et al.*, 1999). This tendency was observed in our present study, as pre-ischemia HCD elevated the GSK3β phosphorylation/expression ratio compared to controls (**Figure 5.35A, Table 5.6**), whereas GRT supplementation in HCD reduced GSK3β activation and expression (**Figure 5.35B+C**). To date, no other study has investigated the effect of GRT or its polyphenols on GSK3β signaling. There was however one unrelated study that reported rutin to have a pro-apoptotic effect in adherent leukemic cells which was correlated with a decrease in GSK3β phosphorylation (Bourogaa *et al.*, 2011).

- ISCHEMIA/REPERFUSION

From ischemia, HCD had significantly less GSK3β activation (and therefore less inhibition) compared to controls, persisting until early reperfusion (up to 3 times less GSK3β phosphorylation), and only reached similar levels to controls towards the end of reperfusion (**Figure 5.35A+B, Table 5.6**). The determinant role of GSK3β inhibition is to suppress the mPTP opening post ischemia. Most research indicate that GSK3β inhibition leads to inhibition of apoptosis and thereby reduce the damage caused by myocardial I/R-I (Huisamen & Lochner, 2010). For instance, in a study done by Wagner and colleagues (2010) open chest rats subjected to a 30 min regional ischemia protocol and receiving post-conditioning by three 30 s cycles of reperfusion and occlusion at the start of reperfusion had significantly smaller infarct size and 2.3 times higher phosphorylation of GSK3β than controls. However, in another study done by Skyschally and colleagues (2008), performing an ischemia/reperfusion protocol on pigs, by subjecting them to 90 min of regional ischemia, followed by 120 min of reperfusion, a group receiving 6 cycles of 20/20 sec reperfusion/occlusion upon reperfusion presented with the greatest reduction infarct size without any correlating with GSK3β phosphorylation levels post-ischemia. These discrepancies point to the complex role of GSK3β in ischemia/reperfusion and how apparently animal and model specific its signaling can be. Given that HCD had less GSK3β activation compared to controls at a time when it was more critical, yet had worse functional recovery and infarct size, it would more strongly indicate the importance of GSK3β inhibition upon reperfusion. Also, during late reperfusion, GRT significantly

increased GSK3β expression, albeit having no difference in GSK3β activation (**Figure 5.35B+C, Table 5.6**). This is in accordance with our argument, that GSK3β inhibition upon reperfusion is a significant determinant of heart resilience to potential cardiac events, which would lift the inhibition on AMPK (Suzuki *et al.*, 2013) and consequently increase AS160 and GLUT4 translocation improving glucose clearance.

- **ATM**

ATM kinase is considered one of the master regulators of signaling networks, with over 490 substrates (Matsuoka *et al.*, 2007). ATM is activated in response to oxidative stress, hypoxia and insulin, giving rise to ATM-dependent activation of autophagy through AMPK (Li, Luo, *et al.*, 2017) or insulin-stimulated PKB activation leading to AS160 phosphorylation and subsequent glucose uptake (Viniegra *et al.*, 2005). These are but a few of the mechanisms of importance to choosing ATM as a potential signal to investigate in elucidating GRT action. In the present study, there were no significant differences in ATM expression or activation prior to ischemia between either of the 4 groups (**Figure 5.36**).

- ISCHEMIA

During ischemia, ATM activation was significantly increased in HCD compared to controls (**Figure 5.36B, Table 5.6**), resulting in insulin-independent mechanism preference (AMPK activation) above insulin-dependence (PKB inactivation), albeit without resulting in elevated autophagy or AS160 activation. GRT supplementation increased ATM activation in controls, but not in HCD – potentially due to the elevated mitochondrial OxPhos resulting in increased ROS production. This mechanism did however also result in increased AMPK activation and AS160 activation, potentially increasing glucose utilization during ischemia (as described in **Section 6.5.2**). It has been shown previously in our labs that ATM inhibitors given to HCD animals just prior to 30 min ischemia resulted in improved cardiac function 5 min into reperfusion, but the cardioprotection was lost after 10 min of reperfusion (Espach, 2017). It was also shown that ATM inhibition attenuated downstream insulin-signaling, but PKB activation could still be stimulated in the presence of insulin alone.

- REPERFUSION

Both during early and late reperfusion, HCD decreased ATM activation compared to controls (**Figure 5.36B**). ATM downregulation in HCD also resulted in decreased PKB and AMPK activation and ultimately a decreased AS160 activation, inferring that these hearts were significantly less dependent on glucose metabolism during reperfusion. This is also in line with our findings on HCD hearts having upregulated β-oxidation preference (discussed in **Section 6.6.3**). Given that autophagy was upregulated in these hearts as evidenced by increased LC3-II:-I ratio yet absent of increased AMPK, would furthermore implicate an AMPK-independent mechanism of autophagy at work. GRT supplementation in controls also led to decreased ATM expression and ATM activation (Figure 5.36B+C) in both early and late reperfusion, which culminated in less PKB activation and less autophagy during late reperfusion (mechanism unknown but ATM-dependent). Since these hearts performed functionally better and had better resilience to infarct size development we propose a mechanism as described by Xie and colleagues (2015): Acute and excessive ROS production has shown to activate ATM which promotes cardiomyocyte apoptosis, whereas treatment with antioxidant agents can significantly inhibit ATM activation and attenuate cardiomyocyte apoptosis and contractile dysfunction (Yoshida *et al.*, 2009). Therefore, GRT could potentially have deterred both autophagic and apoptotic cell death through strong antioxidant action alleviating increased ROS-induced cell damage. Surprisingly, we found that throughout all the perfusion time points investigated, GRT supplementation had no effect on ATM expression or activation in

HCD animals - although it has been shown previously in a study done by Espach (2017) that drugs aimed at activating or inhibiting ATM in HCD hearts had no effect on ATM expression or activation. It remains unclear why ATM signaling is so difficult to manipulate in a pre-diabetic rat heart.

6.6 Mitochondrial Function and Mitophagy in Global Ischemia - Reperfusion Injury

Obesity is known to increase myocardial infarction susceptibility and worsen the outcome following an ischemic event (Zhu *et al.*, 2014). This has also been verified in numerous animal models (Andres *et al.*, 2016; Kamau, 2018; Kleindienst *et al.*, 2016). It is still unknown whether mitochondrial dysfunction is the reason for metabolic impairment or the result thereof, however it is certain that there's an association in various tissues including pancreas, liver, skeletal muscle and adipose tissue (Bhatti *et al.*, 2017). Dysfunctional mitochondria are a common feature in metabolic diseases implicating impairment of mitochondrial quality control, which entail dysregulation of fission, fusion, mitophagy and mitochondrial biogenesis (Gottlieb & Thomas, 2017).

Our last aim was to determine the effect of 6 weeks of GRT treatment on potential myocardial mitochondrial dysfunction parameters induced by both a 16-week HCD and a 20 min global ischemia reperfusion protocol. Sub-sarcolemmal mitochondria were isolated and polarographically evaluated for respiration and ADP conversion to ATP through the activity of the ETC chain in the presence of glutamate (as a carbohydrate-rich substrate) or palmitate (as a FA-rich substrate) to determine OxPhos substrate preference and efficiency, before subjecting the isolated samples to an additional 20 min anoxia reoxygenation protocol to assess mitochondrial dysfunction and OxPhos recovery. Furthermore, we focused on the role of mitophagy which plays a critical role in degrading and recycling dysfunctional mitochondria to restore energy homeostasis. As discussed in **Section 2.3.2**, mitophagy occurs through either Parkin-dependent or independent pathways, and proceed by first recognizing damaged mitochondria, and then inducing autophagy (Ding & Yin, 2012). Following the loss of Δψm, PINK1 accumulates on the damaged mitochondria, promoting Parkin activation which then ubiquinates p62, the link between damaged mitochondria and LC3-II attached to the expanding phagophore - destined to engulf the mitochondria and fuse with a lysosome for degradation (Song *et al.*, 2015). Independent of parkin, BNIP3L located on the outer membrane of mitochondria can also link to LC3-II to initiate the same aforementioned degradation (Novak *et al.*, 2010).

6.6.1 Stabilization

OxPhos plays an important role in the supply of energy for the continuously contracting myocardium (Gnaiger, 2014). As the severity of metabolic disorders such as T2D and obesity increase, the capacity of mitochondria to retain normal functioning also decline (Bhatti *et al.*, 2017). During stabilization, OxPhos rates were not significantly different between HCD and controls (**Figure 5.39, Figure 5.41, Table 5.7**), even though HCD had worse heart function compared to controls. Previously in our laboratory it was found that hearts from obese rats harvested at baseline (prior to perfusion) and after stabilization on the perfusion rig, did not present with significantly different OxPhos rates compared to controls (Nduhirabandi, 2014) even with varying function. Furthermore, it has been shown in early obese and insulin-resistant humans that these conditions do not always present with mitochondrial dysfunction (Samocha-Bonet *et al.*, 2012). HCD did however show improved OxPhos rate 3 efficiency in a FA compared to carbohydrate medium (**Figure 5.39, Figure 5.41**). It has been shown in previous studies that high-sucrose diet fed rats presented with significantly elevated β-oxidation prior to ischemia which also resulted in poorer heart recovery post-ischemia (Gonsolin *et al.*, 2007). However, this

phenomenon can be a double-edged sword. Firstly, increased FA OxPhos as a result of high circulating FA present in conditions such as obesity and diabetes increases oxidative stress and mitochondrial alterations and functions, including mitochondrial uncoupling which increases the risk for the mPTP opening and ultimate cell death (Rial *et al.*, 2010). Paradoxically, activating uncoupling proteins are often therapeutic targets in obesity and diabetes as they also result in reducing the accumulation of FA in the mitochondria and ultimately attenuate FA-oxidation (Busiello *et al.*, 2015). As the HCD heart had worse contractile function pre-ischemia, we propose the former: that β-oxidation prior to ischemia results in worse cardiac outcome. The initial signals, PINK1 or BNIP3L accumulation on the outer membrane of damaged mitochondria initiates the first step in responding to stress. In the present study after 30 min of stabilizing hearts on a perfusion rig and isolating mitochondria, there were no significant differences in PINK1 levels between either of the 4 groups (**Figure 5.45, Table 5.11**), while HCD animals presented with increased Parkin levels (**Figure 5.46**). It has been shown in PINK1-deficient mice that Parkin can be recruited to damaged mitochondria in the absence of PINK1 (Kubli *et al.*, 2015). As LC3-II levels remained the same between the 4 groups (**Figure 5.49**) it could be possible that Parkin-activation was the initial step or priming of the HCD mitochondria to subsequent degradation to follow. Additionally, HCD also had significantly reduced mitochondrial BNIP3L levels (**Figure 5.48**), pointing towards Parkin being a more preferred method to induce degradation during low-stress. GRT supplementation in both controls and HCD rats resulted in increased mitochondrial uncoupling (evidenced by a decrease in ADP/O ratio) in the glutamate medium, and also in GRT treated controls in the FA medium. Mitochondrial OxPhos is not perfectly coupled to ATP synthesis as part of the energy liberated from the oxidation of energy substrates is lost as both heat and proton reuptake in to the matrix, called proton leak (Mookerjee *et al.*, 2010). This is postulated to account for up to 30% of the resting metabolic rate and can be induced through inducing mitochondrial uncoupling. This can be protective in conditions favouring ROS production, including obesity and diabetes (Busiello *et al.*, 2015). Furthermore, GRT supplementation resulted in a decrease in Parkin, p62 and BNIP3L in mitochondria from control rats while having no effect in HCD (**Figure 5.46, Figure 5.47, Figure 5.48**), implicating these hearts to be the least prone to mitophagy during this time point. The discrepancies seen here in the mitophagy signaling confirms the similar OxPhos rates noted and also indicates that, during stabilization, no significant mitochondrial dysfunction is present in HCD hearts. Following an anoxic insult, mitochondria from HCD rats had improved %RR in a carbohydrate medium and poorer %RR in a FA medium compared to controls, while GRT supplementation improved %RR in the FA medium (**Figure 5.44**). Interestingly, it was shown before that mitochondria obtained from T2D patient hearts presented with impairments in both FA substrate (palmitoyl-L-carnitine) and carbohydrate substrate (glutamate) respiration, together with less endogenous antioxidant (glutathione) and increased ROS production (greater H_2O_2 emission release) (Anderson *et al.*, 2009). Epidemiological studies have revealed a direct link between high dietary polyphenol intake and ameliorated cellular damage as a consequence of improved radical scavenging and combatting dysfunctional free radical producing enzymes (Hussain *et al.*, 2016; Losada-Barreiro & Bravo-Díaz, 2017; Pandey & Rizvi, 2009). Rooibos is known to have radical scavenging properties therefore GRT may also be beneficial in maintaining oxidative homeostasis during mitochondrial OxPhos. In previous studies, fermented and unfermented rooibos infusions given to rats for 10 weeks, with hydroperoxide induced oxidative stress in the final 2 weeks, showed restoration of liver antioxidant capacity without negatively impacting lipid peroxidation or liver enzymes (Canda *et al.*, 2014). It is therefore possible in the present study that GRT played a role in attenuating ROS-induced damage in anoxia-

compromised mitochondria. Also, of interest, this 20 min anoxia period used in investigating mitochondrial functional recovery proved to be more robust at inducing mitochondrial dysfunction than the global ischemia protocol discussed in the next section – which once again shows the discrepancies between investigating mitochondria in isolation compared to its *in vivo* environment.

6.6.2 Ischemia

When coronary arteries are occluded for 15-20 sec, anaerobic glycolysis takes over metabolism as the only available supplier of new high-energy phosphates (Frank *et al.*, 2012). This is good enough to take care of all basic cardiomyocyte energy demands. However, as ischemia is extended to 5 min and beyond, all reserve energy phosphates are depleted and the heart undergoes a phenomenon called rigor-contracture (heart shivering) (Stowe, 1999). Due to the high quantity of mitochondria in cardiomyocytes, the heart is extremely susceptible to hypoxic and ischemic conditions (Ghaderi *et al.*, 2017b). Mitochondria is essential in reactive oxygen homeostasis (Bratic & Trifunovic, 2010) and contains various ATP-dependent antioxidant defences which are necessary as it can produce up to 12 different types of ROS released as by-products in the ETC - and scavenge additional ROS originating from the extramitochondrial environment (Mailloux, 2018). In response to time-dependent ischemia, cardiac tissue is primed for reperfusion injury which induces free radical release from the mitochondria (Eltzschig & Eckle, 2011). In the present study, after 20 min of global ischemia, there were no difference in OxPhos rates between mitochondria isolated from hearts of control rats compared to HCD in either of the mediums (**Table 5.8**). However, mitochondria from the HCD diet rats did show elevated OxPhos S4 in FA compared to carbohydrate medium (**Figure 5.41**), potentially showing higher oxygen consumption without elevated ATP production, further implicating uncoupling and poorer OxPhos potential. It has been shown that increased cardiac FA oxidation is particularly prevalent in conditions such as ischemic heart disease and T2D, while simultaneously impairing glucose oxidation (Fillmore *et al.*, 2014). All the more, GRT supplementation in HCD also showed increased mitochondrial preference for FA-oxidation compared to carbohydrates (**Figure 5.39, Figure 5.41**). Given the possibility that GRT can scavenge against ROS-induced damage, increased OxPhos can potentially be sustained without causing adverse cell damage. For instance, in a study performed on primary leukemia cells it has been shown that upregulated OxPhos can produce anti-oxidant measures independent of upregulated ROS (Khan *et al.*, 2016). Therefore, it is plausible that supplementation with GRT increases residual antioxidant capacity capable of ameliorating high OxPhos cell damage. This argument is also strengthened by the upregulation of OxPhos S3 witnessed in GRT supplementation of control rats in mitochondria incubated in both FA and carbohydrate mediums but not in HCD (**Figure 5.39**), which could indicate a potential ceiling effect reached in the mitochondria from the HCD rats. The upregulated OxPhos rates in a carbohydrate medium in GRT treated controls is also in line with the findings that AS160 was upregulated during ischemia, thereby implying increased glucose oxidation rates. Curiously, GRT supplementation in controls significantly increased mitophagy through upregulation of mitochondrial PINK1, p62 and BNIP3L levels (potentially removing defective mitochondria, thereby decreasing ROS production and enabling nominal OxPhos rates to continue), while having no effect in HCD – which were arguably already elevated (**Figure 5.45, Figure 5.47, Figure 5.48, Table 5.11**). Myocardial mitochondria from HCD rats had significantly elevated PINK1, similar Parkin and p62 levels, and decreased LC3-II levels compared to controls (**Figure 5.45 - 5.47**). Furthermore, p62 levels were significantly elevated in all groups (except GRT treated HCD) compared to pre-ischemia (**Figure 5.48**). From these findings it is evident that mitophagy is upregulated in both HCD and after treatment with GRT. Clearance of defective mitochondria is

essential to preserve optimal function in heart cells, as the failure to do so will result in additive oxidative damage brought upon by ROS-producing mitochondria (Gottlieb *et al.*, 2011), and recall that even phagophore formation, essential in mitophagy, is an ATP-dependent process (Abounit *et al.*, 2012). This is also in accordance with the OxPhos rates described during ischemia, as both HCD and GRT treatment in controls resulted in elevated OxPhos levels – for better or worse, as persistent higher levels of OxPhos is also related to higher ROS-by-products (Zhang *et al.*, 2017). Therefore, mitochondrial ROS production and detoxification is tightly balanced. When glucose-stimulated ROS production is not matched by glucose-stimulated ROS scavenging systems, a toxic cycle ensues leading to cell death (Liemburg-Apers *et al.*, 2015). It has been shown in hyperglycemia-induced human umbilical vein endothelial cells that treatment with rooibos extracts resulted in increased catalase and SOD activity, which dose-dependently reduced intracellular ROS (Waisundara & Hoon, 2015). This substantiates the argument that GRT may also act as ROS scavenger. Furthermore, high glucose treatment in cardiac H9c2 cells caused downregulation of *Prkag1* (a gene coding for AMPK and involved in mitophagy (Ross *et al.*, 2016)) which could be reversed by aspalathin treatment (Johnson *et al.*, 2017). Thus, increasing mitochondrial OxPhos without the capacity to effectively scavenge added ROS and a growing decline in substrate availability induced by ischemia would potentially start to trigger cell death mechanisms in HCD.

Early Reperfusion

Upon reperfusion, mitochondrial OxPhos return to pre-ischemic levels within seconds, while contraction is still lagging, known as myocardial stunning (Kloner & Jennings, 2001). Stunned myocardium has more oxygen supply than the slow rate of contraction requires, and therefore decreased mechanical efficiency (Frank *et al.*, 2012). Early into cardiac reperfusion, both mitochondrial ROS production and increased Ca^{2+} concentrations in the matrix result in the mPTP opening, resulting in a major loss of nucleotides and the release of pro-apoptotic factors, such as cytochrome c (Di Lisa *et al.*, 2003) into the cytoplasm, upregulating apoptosis and further aggravating I/R-I (Zhou, Prather, *et al.*, 2018). Oxidative damage is also induced to the mitochondrial respiratory chain, mitochondrial metabolic enzymes and mitochondrial membrane structure resulting in more free radical production (Zorov *et al.*, 2014). The fate of cardiomyocytes is dictated by the amount of oxidative damage induced, particularly to mitochondria (Kurian *et al.*, 2016). Presently, in early reperfusion, mitochondria from HCD still presented with significantly elevated OxPhos rates in a FA medium and showed a preference for palmitate over glutamate in respiration (**Figure 5.38-41, Table 5.9**), which is characteristic of T2D and ischemic heart disease as described during ischemia. Alternatively, it has also been shown that high-fat diet-induced insulin resistant and obese mice presented with improved mitochondrial OxPhos (Gupte *et al.*, 2013). These mice, showing similar high circulating FA as present in our HCD rats (**Appendix A8, Table A3**) also showed improved insulin sensitivity in cardiac tissue, even though systemic insulin resistance was established. As discussed under insulin-dependent PKB signaling (**Section 6.5.1**) it is possible, that in the present study our animals also presented with insulin-sensitive cardiac tissue, even while presenting with systemic insulin resistance (**Section 6.3.2**). Considering that JNK1/2 activation was initially downregulated in early reperfusion (**Section 6.5.4**) GRT supplementation in HCD downregulated OxPhos in both mediums but retained greater OxPhos efficiency in palmitate compared to glutamate. This is also in line with the elevated AMPK levels induced by GRT supplementation in HCD during early reperfusion (**Section 6.5.2**). AMPK has been shown to accelerate FA-oxidation with the degree of activation dependent on the duration of ischemia (Zordoky *et al.*, 2014). GRT had no significant effect on OxPhos in controls during early reperfusion, potentially because

OxPhos was not dysfunctional in controls. In early reperfusion, Parkin was significantly elevated in all groups compared to pre-reperfusion (**Figure 5.46, Table 5.11**), while untreated and treated HCD animals also presented with increased LC3-II levels compared to control counterparts (**Figure 5.49**). PINK1 and p62 remained similar between all 4 groups. Taken together this would indicate an elevation in mitophagy during early reperfusion, with the highest levels recorded in both the treated and untreated HCD animals. This could potentially indicate higher oxidative stress from dysfunctional mitochondria in need of recycling in accordance with I/R-I induced ROS (Zorov *et al.*, 2014). Interestingly, both untreated HCD and GRT supplemented controls (the two groups described during ischemia to have elevated mitophagy) presented with markedly reduced p62 levels compared to the end of ischemia, signifying an initial downregulation of mitophagy at the onset of reperfusion. GRT supplementation in HCD also led to a significant increase in Parkin levels, furthermore implicating preference of Parkin-dependent mitophagy in early reperfusion, as opposed to BNIP3L, which showed no significance.

6.6.3 Late Reperfusion

In late reperfusion, diet had no significant effect on OxPhos as there were no differences between HCD and controls (**Table 5.10**). HCD hearts retained greater OxPhos effiency (elevated coupling) in palmitate compared to glutamate (**Figure 5.37**). Furthermore, at this late stage, GRT supplementation only had a significant effect in controls which resulted in decreased OxPhos rates and RCI in both mediums throughout the protocol, which could potentially infer that cellular homeostasis was restored in this GRT treated group first, followed by controls.

Towards late reperfusion, mitochondria from HCD rats also had significantly increased p62 levels compared to controls, while p62 and BNIP3L levels was still higher compared to pre-ischemia. It has been shown in a control mouse model that 45 min ischemia followed by 0 – 24 h of reperfusion led to progressive increases in FUNDC1 (an alternative mitophagy pathway), correlating with infarct size, till at least 3h post reperfusion (Zhou *et al.*, 2018). Therefore, it could also be inferred that following 30 min of reperfusion, the amount of damage incurred would still be increasing and the role of mitophagy as a whole remains essential – albeit varying in specificity for which autophagy pathway. Parkin and BNIP3L was significantly reduced towards late reperfusion in controls while GRT supplementation further decreased Parkin, BNIP3L and p62 levels. The severe reduction in mitophagy in these animals and the low infarct size, together with better functional recovery all point to the increased robustness of these hearts to endure a 20 min global ischemic insult. Inversely, this also point to the heightened susceptibility of insulin-resistant obese rats to I/R-I damage and subsequent mitochondrial dysfunction during late reperfusion. Mitochondria-bound LC3-II, used as steady state mitophagy indicator, also remained significantly elevated in GRT supplemented HCD since ischemia.

6.7 Summary of Findings

- **Insulin-resistant model**

Young control rats administered a high-caloric diet for 16 weeks compared to a normal rat chow diet presented with in an average 24% higher daily food intake and 37% lower water intake, resulting in 8% higher body weight, 69% higher visceral fat, 10% increased fasting blood glucose, 44% higher fasting blood insulin and elevated blood lipids – and collectively deemed pre-diabetic. This manifested in a 15% poorer heart function when stabilized, and a 26% poorer heart function after a 20 min ischemic period, and 14% poorer heart recovery compared to controls indicating cardiac dysfunction. In response to a 35-min regional ischemia, 60

min reperfusion protocol the hearts from pre-diabetic rats also had a 113% greater infarct size (meaning a more than doubling in non-viable heart tissue) showing a severe lack of cardioprotection. Furthermore, mitochondria isolated from pre-diabetic hearts did not yet show mitochondrial dysfunction but did show elevated OxPhos in a FA medium compared to a carbohydrate medium, showing a greater reliance on β-oxidation. Prior to ischemia (**Figure 6.1**), these hearts showed a decreased dependence on insulin-independent AMPK, had increased inflammation through upregulated p38, and presented with an increase in mitophagy through Parkin (less reliant on BNIP3) and autophagy through LC3 signaling. Following 20 min of ischemia (**Figure 6.2**), mitochondrial dysfunction was still not present, but the elevated β-oxidation rates remained. Insulin-independent AMPK was upregulated together with ATM while insulin-dependent PKB was downregulated together with GSK3β phosphorylation. Mitophagy was also upregulated through PINK1 and p62, but autophagy in general was low as LC3 remained low, plausibly because mitophagy is an energy-dependent process and substrates needed for efficient mitophagy are not abundant in ischemia. Upon reperfusion (**Figure 6.3**), nearly all protective signals were downregulated including AMPK, PKB, AS160, GSK3β and ATM. Mitophagy was also highly upregulated via increased Parkin, p62 and LC3. Surprisingly, these hearts had a greater mitochondrial OxPhos capacity early into reperfusion – which would implicate either efficient mitophagy or elevated ischemia-induced stress. The reasoning for improved mitophagy relates to maintaining the energy demand required to combat I/R-I induction of ROS and Ca^{2+} influx (which would all be aimed at destroying the Δψm) through upregulating antioxidant systems and efficiently restoring ion channel activity (possibly due to high substrate availability in energy-rich foods and high sustained activity levels (Menshikova *et al.*, 2006)). To the contrary, higher stress induced by ischemia requires more energy intensive OxPhos resulting in substrate exhaustion and subsequent ROS production, which could trigger not only the increased mitophagy levels witnessed, but also result in cell death (as seen from the increased infarct size). It was shown towards late reperfusion that hearts from pre-diabetic rats had lower ERK1/2 activation, and therefore less protection against prolonged reperfusion damage, while also retaining elevated β-oxidation. However, mitochondrial dysfunction seemed to improve towards late reperfusion as there was no significant difference in OxPhos potential between mitochondria from HCD and controls.

- **GRT in insulin-resistant model**

Administration of potentially cardioprotective, “hypoglycemic”, antioxidant-rich GRT treatment for 6 weeks to rats at risk for developing pre-diabetes (10 weeks of HCD at commencement of GRT treatment, followed by an additional 6 weeks of HCD), resulted in no change in biometric parameters (e.g. equal daily food and water intake compared to HCD, no difference in body weight or visceral fat, no difference in fasting blood glucose or insulin levels). However, isolated hearts had a 10 bpm lower heart rate and 12% improved heart function when stabilized, a 23% better heart function after a 20 min ischemic period, implicating GRT as a potent cardiotonic. Furthermore, in response to a 35-min regional ischemia, 60 min reperfusion protocol the hearts from pre-diabetic rats also had a 62% reduction in infarct size (meaning half the non-viable heart tissue compared to the untreated pre-diabetic rats), implicating GRT as a potent cardioprotective agent. Prior to ischemia (**Figure 6.1**), these hearts showed a decreased dependence on insulin-dependent PKB together with decreased glucose uptake through AS160 (which also corrolated with a higher mitochondrial uncoupling and preference for OxPhos in FA compared to glucose) and presented with decreased GSK3β inhibition but had decreased inflammation evident by downregulated p38, confirming GRT’s previously reported anti-inflammatory effects. No significant effects on mitophagy were recorded prior to reperfusion. After 20 min of

ischemia (**Figure 6.2**), insulin-independent AMPK was downregulated together with ERK1/2 signaling and autophagy through downregulated LC3. Once reperfusion was initiated (**Figure 6.3**), insulin-independent AMPK and mitophagy through Parkin was upregulated, while the stress markers JNK1/2 and inflammatory markers p38 was significantly decreased, further showing GRT's effect on reducing oxidative stress and inflammation. Surprisingly also ERK1/2 and LC3 were decreased compared to the HCD. OxPhos prior to reperfusion remained similar to HCD, however upon reperfusion OxPhos was significantly reduced in GRT treated rats, while a preference for FA was still maintained over carbohydrates. Towards late reperfusion insulin-dependent PKB signaling was also attenuated.

- **GRT in insulin-sensitive model**

Administration of potentially cardioprotective, "hypoglycemic", antioxidant-rich GRT treatment for 6 weeks to control rats (10 weeks of standard rat chow at commencement of GRT treatment, followed by an additional 6 weeks of standard rat chow), resulted in no change in biometric parameters (e.g. equal daily food and water intake compared to HCD, no difference in body weight or visceral fat, no difference in fasting blood glucose or insulin levels). However, isolated hearts had a 9 bpm lower heart rate and 10% improved heart function when stabilized, a 7% better heart function after a 20 min ischemic period, implicating GRT as a cardiotonic even in rats absent of CVD. However, in response to a 35-min regional ischemia, 60 min reperfusion protocol the hearts from GRT treated control rats presented with no additional infarct size reduction, potentially indicating that control rats absent of CVD are already optimally protected. Prior to ischemia (**Figure 6.1**), these hearts showed an increase in both insulin-dependent PKB and insulin-independent AMPK signaling but presented with decreased glucose uptake through AS160 (and elevated mitochondrial uncoupling resulting in reduced metabolic rate) – potentially explaining why GRT treatment did not have a hypoglycemic effect. GRT supplemented controls presented with elevated ERK1/2 activation, which can be considered preconditioning against I/R-I, however in the present study it did not confer additional cardioprotection. GRT treatment in controls resulted in a potential upregulation in mitophagy as evidenced by an observed increase in mitochondria-bound LC3. However, since all the specific mitophagy proteins investigated were downregulated (BNIP3L, Parkin, p62) this would indicate either an AMPK-dependent or additional unknown mechanism. After 20 min of ischemia (**Figure 6.2**), insulin-independent AMPK was upregulated together with AS160 (potentially indicating an increase in glucose oxidation during ischemia which could be beneficial in maintaining cell housekeeping and ATP production). This allowed mitophagy to remain upregulated as increased PINK1, p62 and BNIP3L was also found. However, LC3-II remained extremely low in both GRT treated and untreated controls compared to HCD counterparts, thereby implicating a reduction in, albeit more efficient mitophagy. Once reperfusion was initiated (**Figure 6.3**), ATM and ATM-dependent PKB activation were both downregulated, whereas pro-survival signals such as ERK1/2 was upregulated, however stress signals, JNK1/2 and inflammatory markers, p38 were also upregulated which is an opposite profile as was seen in the GRT treated pre-diabetic rats. For JNK1/2 it is argued that the presence of antioxidants conferred by the GRT treatment resulted in an elevated propensity to deal with stress-induced damage, and even though these hearts presented with high stress, it is more indicative of the stress-response signaling than the subsequent damage to be incurred. Regarding the p38, a marker of inflammation, we pose that since p38 had been upregulated since stabilization, GRT was able to act as a preconditioning agent against subsequent inflammatory-induced damage, and thereby still be cardiotonic, as was seen from increased heart function, and cardioprotective, as seen from no additional infarct size increases. GRT supplemented controls did not

show significant difference in mitochondrial function, arguably because control rats did not have dysfunctional mitochondria induced by a 20 min global ischemia insults. The known mitophagy markers investigated, BNIP3L, Parkin and p62 were all downregulated, even though LC3-II was once again upregulated pointing to a separate mechanism of mitophagy being retained in late reperfusion.

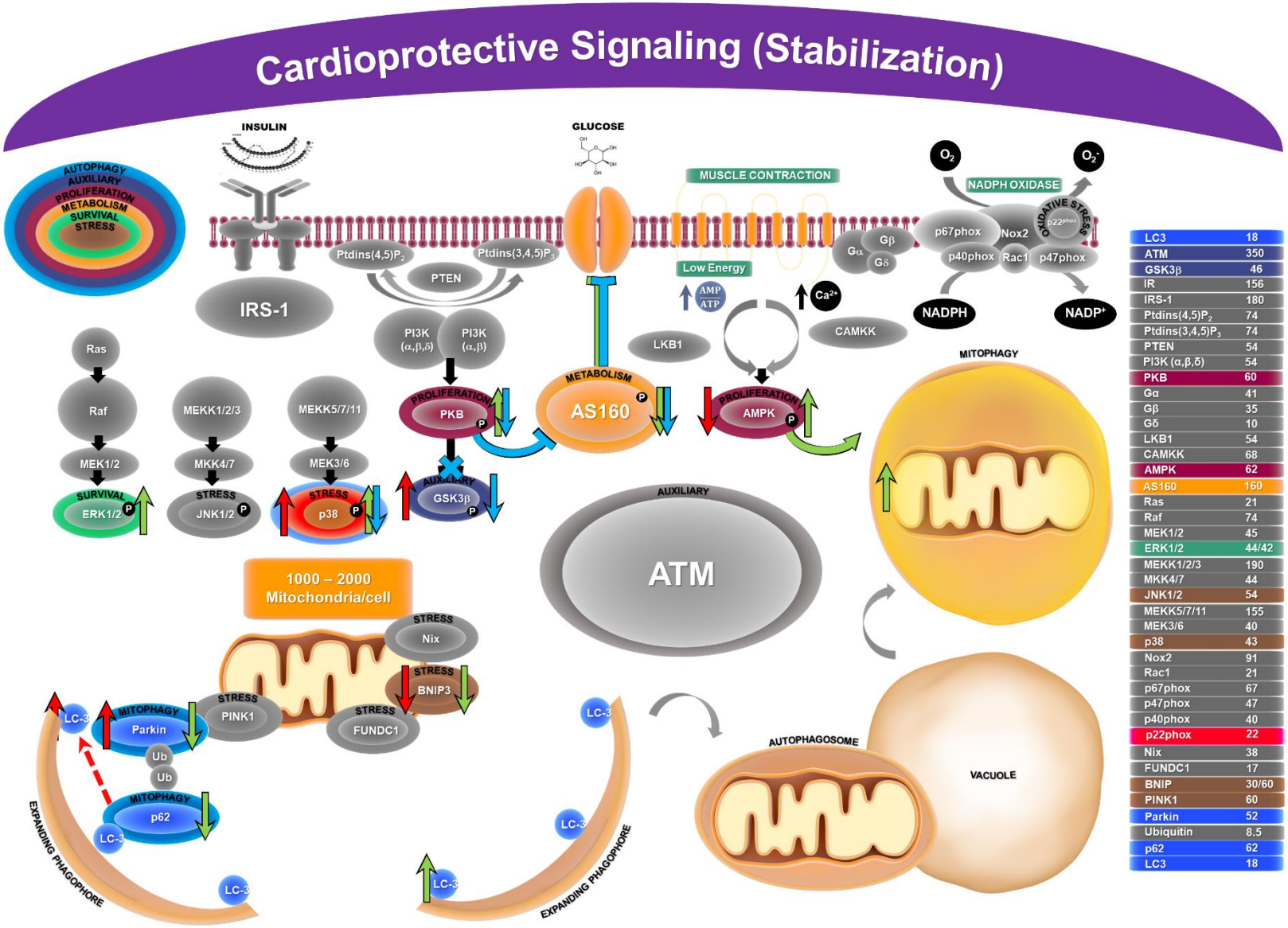

Figure 6.1 Cardioprotective signaling during stabilization. Effect of: HCD (red arrow); GRT in control (green arrow); GRT in HCD (blue arrow).

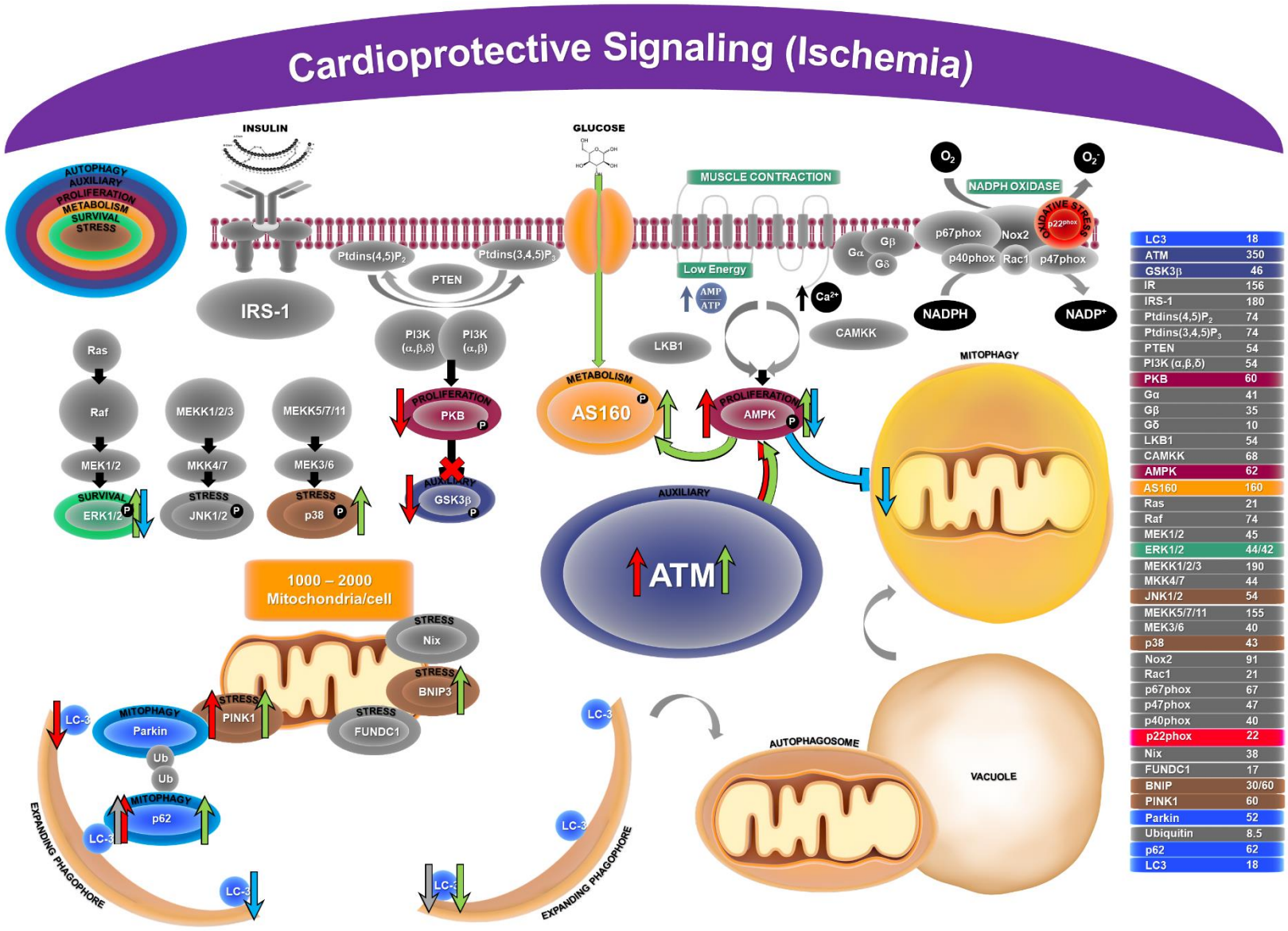

Figure 6.2 Cardioprotective signaling during ischemia. Effect of: HCD (red arrow); GRT in control (green arrow); GRT in HCD (blue arrow).

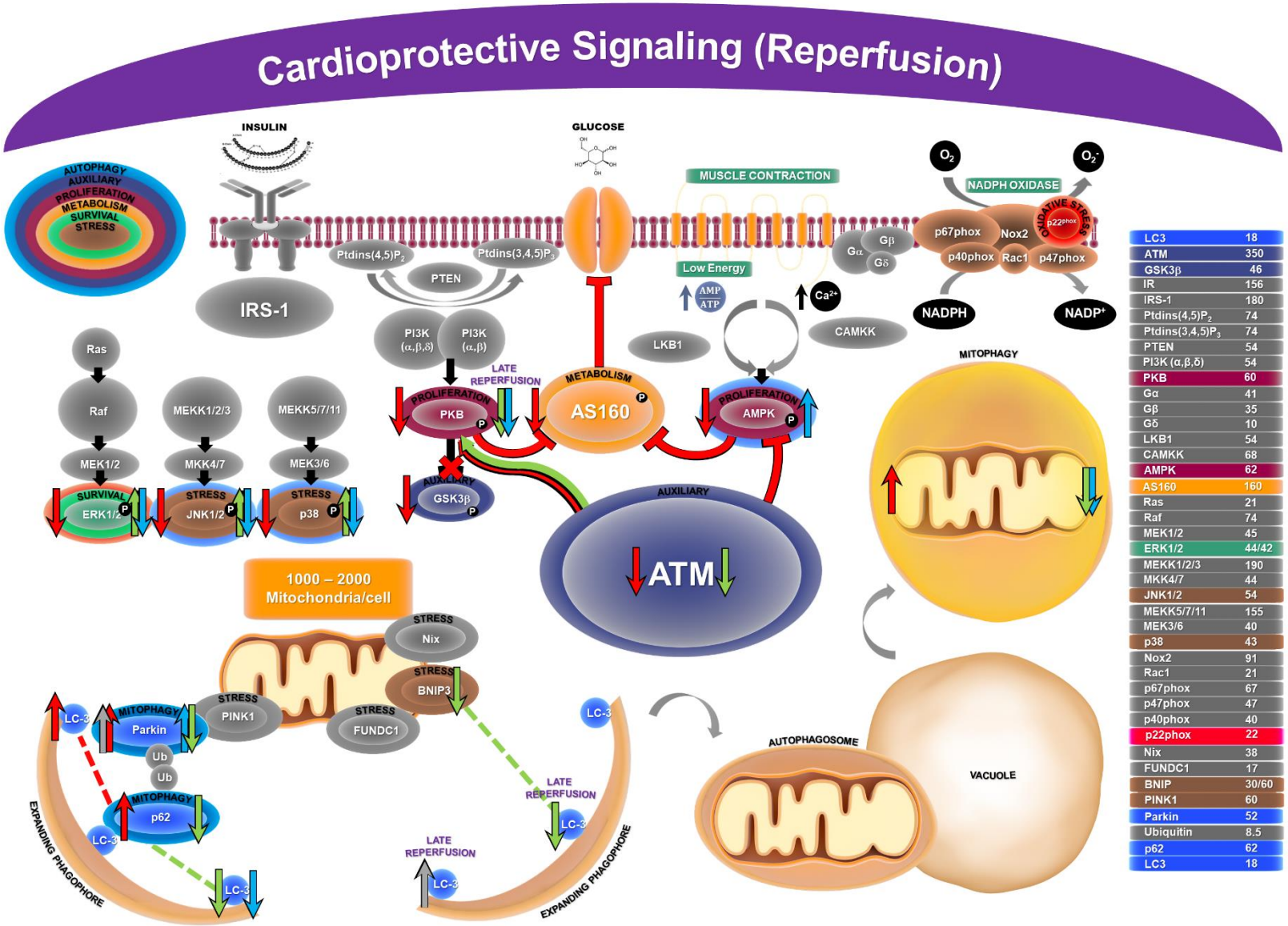

Figure 6.3 Cardioprotective signaling during reperfusion. Effect of: HCD (red arrow); GRT in control (green arrow); GRT in HCD (blue arrow).

6.8 STUDY LIMITATIONS

The rats used in the study were housed in a controlled environment without exposure to toxins, environmental hazards, and related factors that would further exacerbate obesity and insulin resistance in humans (Murea *et al.*, 2012). We also recognize using male only rats is a limitation to extrapolation of the results. For the purposes of the research question it was decided not to double the sample size, cost and effort required in using female subjects with potential confounding endocrine function on CVD progression (Rice *et al.*, 2014).

As described in **Section 4.3.2.3**. in the current study, a rat age of 22 weeks equates to approximately 13 human years and is therefore not yet fully-grown. This does not consider the development of cellular ageing of the rat being studied potentially resulting in decreased scientific validity. In most studies, rodents under the age of 20 weeks are often used to limit cost of maintenance and allow data comparability with a historical database of rodent studies (Jackson *et al.*, 2017). Therefore, the use of older animals may be beneficial and would increase scientific rigour accelerating translation of therapies to humans. However, since obesity and its comorbidities are becoming a growing concern especially in younger children (**Section 1.3.4.1.)** it remains important to investigate the therapeutic reversibility of early risk factors.

It has been shown that performing identical protocols on different species result in significantly different outcomes, as demonstrated in isolated heart perfusions from rabbits, hamsters, ferrets, gerbils, rats, mice and guinea pigs (Galinanes & Hearse, 1990). Furthermore, different strains of the same species have also been shown to have significantly different outcomes in response to I/R-I (Barnabei *et al.*, 2010) which can be a serious experimental limitation and need to be considered.

In the past, mitochondrial oxidative capacity used to be a measure of the maximal mitochondrial enzyme activities (Lanza & Nair, 2009). This approach assumed that the activity or expression of one enzyme accurately reflects the overall function of the mitochondrion and could thus be indicative of OxPhos. Nevertheless, it led to the development of a technique to measure oxygen consumption in isolated mitochondria and was first established 60 years ago (Chance & Williams, 1956). Different substrates were used to measure mitochondrial function in response to different energy states, favouring electron flow through specific mitochondrial complexes and coupling oxygen consumption to ATP production (Lanza & Nair, 2009). The limitations of this technique include exposure of mitochondria to non-physiological conditions, such that:

- isolated mitochondria in vitro are subject to oxygen levels way above physiological oxygen concentrations *in vivo*.
- substrate and ADP concentrations are also added in saturating quantities which far exceed its inherent microcellular environment (Lanza & Nair, 2009).

Nevertheless, isolating mitochondria allowed for detailed OxPhos capacity determination without confounding factors such as blood flow, oxygen and substrate delivery or mitochondrial density volume (Lanza & Nair, 2009).

There is an ongoing debate regarding the probability of observed direct antioxidant activities *in vivo*, since supra-physiological concentrations (100–400 µM) of polyphenols were often used *in vitro* tests determining their antioxidant properties (Goszcz *et al.*, 2015). Furthermore, the low bioavailability (~1 µM) of phenolic

compounds seriously questions their ability to engage in direct antioxidant potential in the *in vivo* scenario. Presently, we did not measure antioxidant capacity in the blood and only inferred that some of the cardioprotective effects observed is plausibly due to antioxidant effects of GRT. Furthermore, an argument has been put forth that the antioxidant activity of polyphenols could be irrelevant to their protective effects – to the contrast it is reasoned to be due to their toxic effect which upregulate endogenous antioxidant systems properties (Goszcz *et al.*, 2015). This analogy can be thought of in the same manner as how bouts of exercise preconditions the body to handle subsequent exercise 'insults' (van Vilsteren *et al.*, 2005). To verify either an elevated anti- or pro-oxidant state, blood samples would need to be analysed for TBARS, total and reduced glutathione (GSH + GSSG), glutathione peroxidase activity and SOD, as well as urine samples analysed for ascorbic and uric acid.

CHAPTER 7
CONCLUSION AND FUTURE RESEARCH

Ancient wisdom withstanding the test of time:
*Hippocrates asserted in ~400 BC: "**Let food be thy medicine and medicine be thy food.**"*
*Ezekiel's vision in ~580 BC on heavenly trees: "**Their fruit will be for food, and their leaves for healing.**"*

Therefore, it is up to modern day researchers and physicians to figure out the dosing, duration of treatment and contra-indications when used in conjunction with other medications.

In the present study we aimed to answer three questions:

1. What is the effect of 6-weeks of high-dose Afriplex GRT treatment on heart function pre- and post-ischemia in a pre-diabetic Wistar rat model?

In establishing our pre-diabetic model, we found that 16 weeks of high-caloric diet feeding resulted in significant increases in body weight, body fat, elevated fasting serum triglycerides, glucose and insulin levels, worse glucose tolerance and elevated HOMA-IR - inferring insulin resistance. Furthermore, the elevated risk for CVD imposed on these rats also resulted in increased heart mass, worse heart function and recovery post-ischemia, and increased infarct sizes. Without significantly affecting any of the biometric parameters, GRT treatment for 6 weeks improved heart function pre- and post-ischemia, improved heart recovery post-ischemia and significantly reduced infarct size. Furthermore, GRT treatment lowered heart rate pre-ischemia, while improving cardiac contractility, showing additional cardiotonic properties.

2. How does this relate to cardioprotection following an ischemic event?

Mechanistically, we found that GRT treatment pre-conditioned the pre-diabetic hearts to I/R-I by inhibition of GSK3β, sustaining anti-inflammatory (↓p38 activation), and switched metabolism to insulin-independent (↓PKB activation) and glucose-independent (↓AS160 activation) mechanisms. Early into reperfusion, GRT's anti-inflammatory effect was still evident (↓p38 and ERK1/2 activation), while also improving resilience to oxidative stress (↓JNK activation) and favouring insulin-independent mechanism (↑AMPK and ↓PKB activation).

3. How does GRT treatment effect mitochondrial function in I/R-I?

In the present study, pre-diabetic hearts did not present with significant mitochondrial dysfunction prior to reperfusion, but retained greater reliance on β-oxidation, indicative of FA accumulation in the heart and an independent indicator for poorer cardiac recovery post ischemia (Fillmore *et al.*, 2014). These hearts also had elevated mitophagy through a Parkin mediated mechanism (and less reliant on BNIP3L) and autophagy through LC3 signaling. GRT treatment did not significantly alter the preference for β-oxidation, but did result in mitochondrial uncoupling, leading to a reduction in OxPhos, thereby reducing basal metabolic rate – and ultimately less ROS production (Mookerjee *et al.*, 2010). GRT did not significantly alter mitophagy prior to reperfusion. Early into reperfusion, pre-diabetic rats presented with elevated OxPhos, increasing ROS production and plausibly one of the greatest contributors to the cell death that caused the severely increased

infarct size. GRT treatment was able to inhibit OxPhos, thereby preventing additional ROS-induced cell death, and reducing infarct size. Mitophagy was also highly upregulated via increased Parkin, p62 and LC3.

Surprisingly in the present study, GRT did not have a hypoglycemic effect, neither played a role in resensitizing insulin signaling. One limitation to this regard was addressed, in that previous studies showed a dose-specific hypoglycemic effect that could only be sustained for 6 hours maximum and dissipated with increasing dosages of GRE (Muller *et al.*, 2012). This could mean the high-aspalathin content in the present daily GRT extract supplemented could have potentially overwhelmed the pancreas, or insulin-sensitive tissues and transport mechanisms and thereby nullify the beneficial hypoglycemic effects. To test this hypothesis, future studies would need to use varying daily dosages ranging from 10-60 mg GRT/kg BW to potentially investigate this claim. Furthermore, GRE has presented with strong α-glucosidase inhibitory effects leading to reduced blood glucose elevations after a meal (Miller *et al.*, 2018). This mechanism of managing hyperglycemia would encourage multiple GRT dosages (or dissolving the GRT in water) to be administered throughout the day in hyperphagia high-caloric-induced pre-diabetic rats.

Second only to revascularization, ischemic preconditioning remains the most effective cardioprotective intervention to reduce I/R-I (Cohen & Downey, 2015). Currently, in patients with coronary occlusion and acute myocardial infarction, the coronary artery is opened and the damaged ischemic myocardium reperfused. It is important to understand why cardioprotective agents has mostly failed to provide the theoretical relief for I/R-I and become an effective therapy. A multi-target hypothesis has been suggested by (Rossello & Yellon, 2018). Future research should not solely focus on improving the potency of RISK pathway kinases, but also study the compounding effect of combination therapies to maximize cellular survival.

Making sense of the mitophagy results in the present study posed to be quite challenging. For the interpretation of results to be sensible there must be certain trends that can be appreciated. If, however, one sees various up and down phenomenas at play regardless of how these hearts were perfused before isolation of mitochondria it readily implicates mitochondrial dynamics as more complex than initially realized. Mitochondria are independent organelles with one goal in mind: produce energy through OxPhos. To maintain a favourable work environment, it can undergo structural changes, mitophagy, fission, fusion and biogenesis. Thus, at any given time a ‘colony’ of mitochondria can be in either of these states depending on the need for energy production and the need for cell survival. To reach more certainty on the cellular mechanisms involved during different pathological states one would need to investigate all these phenomena together – as aiming at simply one could result in tunnel vision, and worse: being stuck in the tunnel while the train is approaching. To clarify, the train is the investigative need to understand signalling dynamics; the tunnel is using either a sniper or a shotgun to investigate signalling phenomena. It is recommended that one rather use surveillance and exhaustively follow the flux of each protein at multiple time points following the onset of reperfusion. Regardless, this study has improved our understanding of the complexity of mitochondrial dynamics in I/R-I in response to both high-caloric diets and phytochemical therapy.

In conclusion, I will sign off with my answer to the question: What did I learn from doing this study?

Firstly, excessive sugar intake is bad for the heart (as inferred by the nutritional make-up of the current diet used to induce pre-diabetes). Not only does it result in declining function and poor recovery after an ischemic event, it can also cause irreversible damage to the heart (the shear magnitude of infarcted tissue present following an ischemic event). This necessitates the need to exercise self-control when considering and partaking in overindulgence of sweet treats. The human body is an amazing machine, and it will serve you well initially. But when ignorance continuously wins the battle against symptomatic gluttony, and sound wisdom such as everything in moderation is downplayed, a harsh reality of primary medication dependence, and secondary side-effects awaits.

Secondly, rooibos has a future in primary health care. The reasoning is as follow: rooibos can be a harsh plant to cultivate evident from its preference to only grow in its indigenous scorched earth climate. Somehow this results in unique polyphenols capable of scavenging stress and inflammation (primarily to the benefit of the rooibos plant itself). This resistance can be transferred when rooibos phytochemicals are consumed in adequate concentrations which makes it especially beneficial to alleviate stress induced by our modern lifestyles. In the present study we have shown the cardioprotective benefit of high rooibos intake, through a commercial product called Afriplex GRT, which aids in bridging the gap between the pre-diabetic heart and a normal healthy heart. Surprisingly, rooibos also lowered resting heart - a proven favourable indicator of cardiovascular health. This is on par with cardio-exercise which is arguably the best cardiopreserving therapy. Even though exercise raises heart rate initially, its benefit is a result of lowering resting heart rate and thereby lowering the overall strain placed on the heart in the long run. Moreover, the one trait that all centenarians have in common is a well-preserved heart molded by a peaceful life. Therefore, rooibos is not only beneficial to protect the heart against impending cardiac risk, but also confers a soothing or calming effect which is synonymous with longevity. As the findings in this study has only been confirmed in a pre-diabetic rat model, it remains to be determined what the potential benefits of Afriplex GRT will be in humans. However, as a personal inference in the meantime, if you had to snack on something… feel free to make it a cup of rooibos.

APPENDIX

A1) TRANSMISSION AND 3D SCANNING ELECTRON MICROSCOPY OF MITOCHONDRIA IN CARDIOMYOPATHY PATIENT

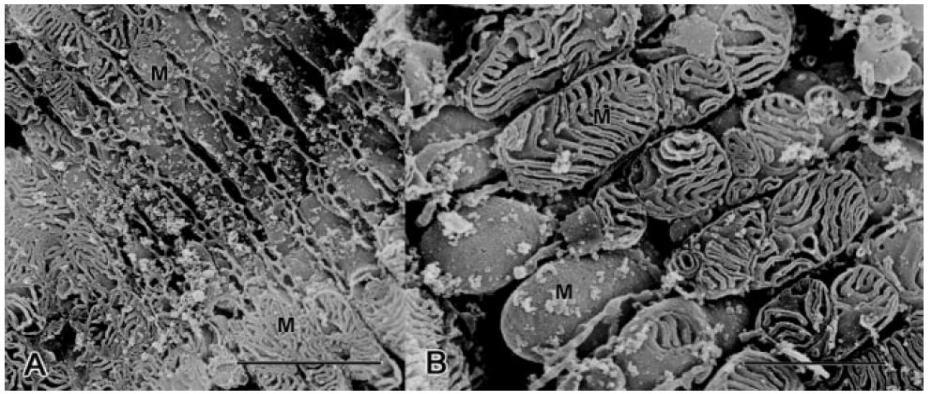

Figure 1. Scanning electron micrographs of membrane system in left ventricular myocardium with normal histology. A, Continuous rows of normal mitochondria in subsarcolemmal lesion are presented. Bar, 2 μm; magnification, 15 000×. B, Normal cardiac mitochondria with lamelliform cristae showing its unit membrane substructure. Bar, 1 μm; magnification, 30 000× (M indicates mitochondria).

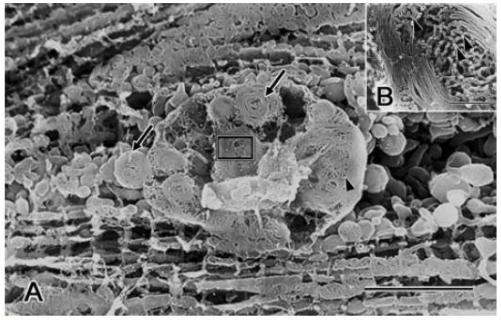

Figure 2. A, Mitochondria in cardiomyocytes are in various sizes and shapes. Note that some of these mitochondria are relatively large and have concentric circular cristae (arrows). A giant mitochondrion is surrounded by numerous mitochondria of normal size and appears to consist of several mitochondria showing concentric circular cristae around central tubular cristae (arrowheads). Bar, 5 μm; magnification, 6000×. B, Boxed area in A. The tubular profiles of the cristae are clearly observed (arrowheads). Bar, 600 nm; magnification, 50 000×.

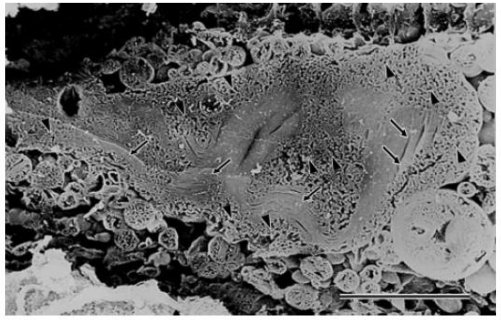

Figure 3. A huge, irregularly shaped mitochondrion containing abundant tubular (arrowheads) and lamellar undulated cristae (arrows) closely packed together. Bar, 5 μm; magnification, 6000×.

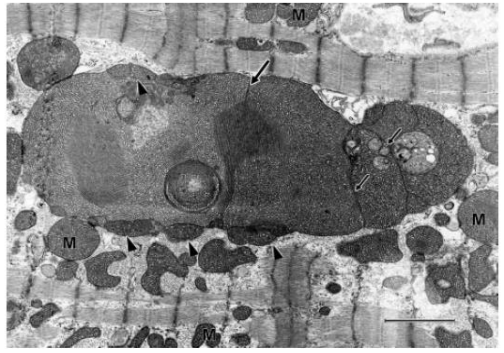

Figure 4. A huge mitochondrion that appears to have been formed from the fusion of several large mitochondria (arrows) with mitochondria of normal size (arrowheads). Bar, 2 μm; magnification, 6000× (M indicates mitochondria).

Figure A1 Scanning electron micrographs showing cardiac mitochondrial colonies (1), shapes and sizes (2), irregular shapes (3) and huge fused mitochondria (4). From Kanzaki *et al.* (2010).

A2) MITOCHONDRIA ONLY PRESENT IN OOCYTE POST FERTILIZATION

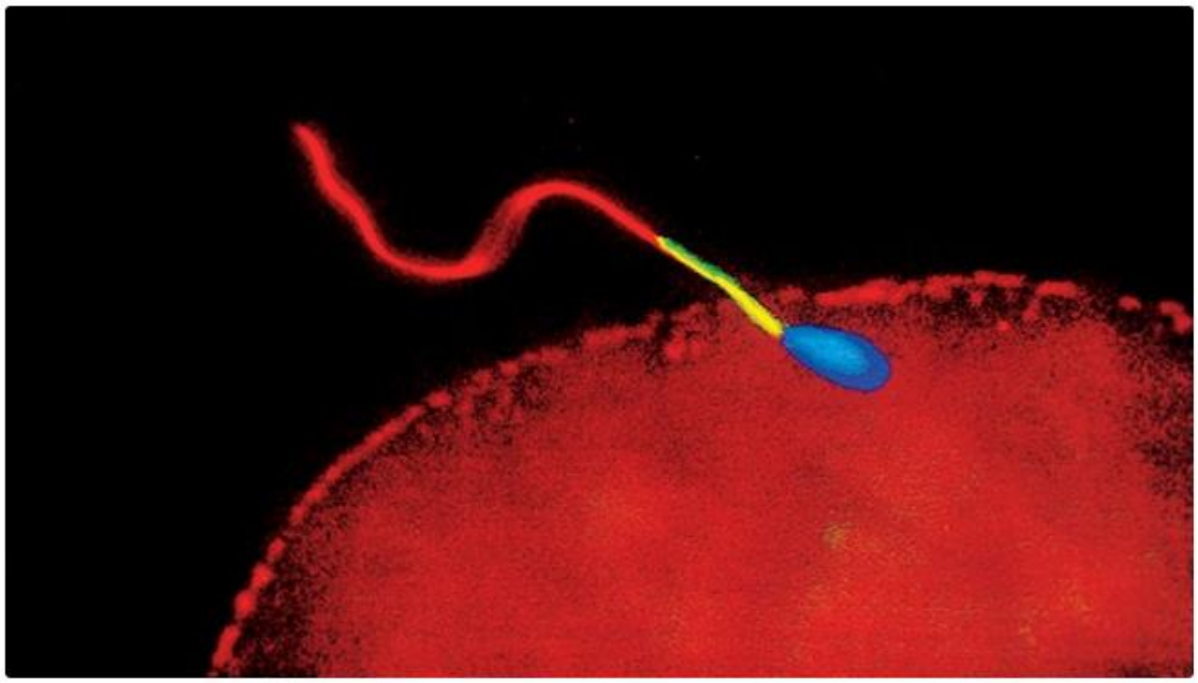

Bull sperm prelabeled with MitoTracker® Green FM and used for in vitro fertilization of bovine oocytes. Bull sperm prelabeled with MitoTracker® Green FM (Cat. no. M7514) and used for in vitro fertilization of bovine oocytes (Biol Reprod 55, 1195 (1996)). After fertilization, eggs with bound or incorporated sperm were fixed in 2% formaldehyde, made permeable with Triton X-100 and labeled with an anti-tubulin antibody followed by a tetramethylrhodamine-labeled secondary antibody and counterstained with DAPI (Cat. no. D1306, D3571, D21490). Image contributed by Peter Sutovsky, University of Wisconsin.

Figure A2 Paternal mitochondria only present to power sperm journey

A3) AFRIPLEX GREEN ROOIBOS EXTRACT COMPOSITIONAL ANALYSIS

Afriplex PHARMACEUTICALS

CERTIFICATE OF ANALYSIS

Product Name: Afriplex GRT Extract
Product Code: CPE--03287
Product Batch Number: 730330
Product Manufacturing date: September 2015
Product Expiry Date: August 2017

CHARACTERISTIC	SPECIFICATION	RESULTS
Analytical parameters		
Definition	Needle-like leaves and fine stems	Conforms
Characteristics	Reddish brown fine powder. Aroma is typical to Rooibos	Conforms
Appearance	Appearance complies	Conforms
Identification (FT-IR)	≥ 95.00 %	First Reference
Loss on Drying	≤ 5.0 % (m/m)	2.2 % (m/m)
Bulk Density	0.20 - 0.45 g/ ml	0.32 g/ ml
Extract Yield	> 15 % (g/ 100g)	16.84 %
Soluble Solids content	> 2 % (g/ 100g)	2.12 %
Aspalathin Content	> 15 % (g/ 100g)	12.36 %
Pesticides	Meets Ph. Eur. requirements	Conforms
Heavy Metal parameters		
Heavy Metals	≤ 10 ppm	Conforms
Cadmium	≤ 1.0 ppm	< 0.01 ppm
Lead	≤ 3.0 ppm	0.07 ppm
Mercury	≤ 0.1 ppm	0.02 ppm
Arsenic	≤ 1.0 ppm	0.09 ppm
Microbial parameters		
Total aerobic count	< 2 000 cfu/ g	65 cfu/ g
Total combined yeast and mould count	< 100 cfu/ g	No growth
Escherichia coli	Absent/ g	No growth
Coliforms	Absent/ g	No growth
Salmonella	Absent/ 25 g	Absent

STORAGE REQUIREMENTS
Store in a cool dry place protected from temperature extremes and direct light.

PAARL, 23 September 2015

Quality Control Department

A4) STANDARD RAT CHOW DIET COMPOSITION

microchem
Specialized Lab Services
Co .Reg. 2007/010539/07 Vat No. 4330239049

1st Floor, Fairweather House,
176 Sir Lowry Road,
Cape Town
8001
Telephone : +27 21 465-6996/7
E-mail: chem@microchem.co.za

ilac-MRA sanas Testing Laboratory T0393

CERTIFICATE OF ANALYSIS

Client's Reporting Address:
Department of Food Science
Private Bag X1
Matieland
7602

Client's Telephone #: 021 938 9391
Client's Fax #:

Our Lab Ref #: 2013-06-25-039 **Our Sample ID :** AC92365
Client: Stellenbosch University
Requested by: Prof A Lochner
E-mail address: alo@sun.ac.za
Product: Control Chow
Sampling Method
Barcode
No of Samples:
Production Date: 24/06/2013
Sample Condition: SEALED
Date Received: 25/06/2013
Date Validated: 16/07/2013

Client Samp #: 1
Batch Code:
Sell By Date:
Order Number: PROF A LOCHNER

ANALYSIS RESULTS	1	2	Average	MoU (%)	Test Method Ref
Moisture (g/100g)	10.95	10.84	10.9	0.70	S.O.P.C. No. 1#
Ash (g/100g)	5.66	5.72	5.7	5.00	S.O.P.C. No. 2#
Total Fat (g/100g)	4.65	4.91	4.8	2.60	S.O.P.C. No. 25#
Saturated Fat (g/100g)	0.87	0.91	0.9	2.60	S.O.P.C. No. 25#
Mono-Unsaturated Fat (g/100g)	1.42	1.51	1.5	2.60	S.O.P.C. No. 25#
Poly-Unsaturated Fat (g/100g)	2.37	2.50	2.4	2.60	S.O.P.C. No. 25#
Trans Fatty Acids (g/100g)	0.000	0.000	0.00	2.60	S.O.P.C. No. 25#
Omega 3 Fatty Acids (g/100g)	0.23	0.25	0.2	2.60	S.O.P.C. No. 25#
ALA (g/100g)	0.23	0.25	0.2	2.60	S.O.P.C. No. 25#
EPA (g/100g)	0.00	0.00	0.0	2.60	S.O.P.C. No. 25#
DHA (g/100g)	0.00	0.00	0.0	2.60	S.O.P.C. No. 25#
DPA (g/100g)	0.00	0.00	0.0		S.O.P.C. No. 25#
Omega 6 Fatty acids (g/100g)	2.13	2.25	2.2	2.60	S.O.P.C. No. 25#
Cholesterol (mg/100 g)	2.99	2.94	3	4.70	S.O.P.C. No. 26#
% Protein (6.25)	16.96	17.22	17.1	1.90	S.O.P.C. No. 36#
Nitrogen (g/100g)	2.71	2.75	2.7	1.90	S.O.P.C. No. 36#
Total Dietary Fibre (g/100g)	26.98	26.88	26.9	1.30	S.O.P.C. No. 20#
% Carbohydrate	34.80	34.43	34.6	C*	S.O.P.C. No. 21
Total Sugar (g/100g)	6.65	6.54	6.6	2.90	S.O.P.C. No. 27#
Fructose (g/100g)	0.51	0.49	0.5	2.90	S.O.P.C. No. 27#
Glucose (g/100g)	0.76	0.77	0.8	2.90	S.O.P.C. No. 27#
Sucrose (g/100g)	5.39	5.28	5.3	2.90	S.O.P.C. No. 27#
Maltose (g/100g)	0.00	0.00	0.0	2.90	S.O.P.C. No. 27#
Lactose (g/100g)	0.00	0.00	0.0	2.90	S.O.P.C. No. 27#
Energy (kJ/100 g)	1268	1275	1272		S.O.P.C. No. 22
Sodium (mg/100 g)	188.75	178.40	184	7.56	S.O.P.C. No. 45#

COMMENTS

Confirmed by: P Rubuz Date: 16-Jul-13
Technical Signatory

These results relate only to the items tested. Total Dietary Fibre content determined by AOAC Method 991.43
MoU = Measurement of Uncertainty. C* = By calculation.
 # = SANAS Accredited Method.
Tests without the # mark in this report are "Not SANAS Accredited" and are not included in the SANAS Schedule of Accreditation for this laboratory.
Opinions and interpretations expressed herein are outside the scope of SANAS accreditation. This certificate shall not be reproduced except with the approval of the laboratory. The integrity of results reported are only valid from sample receipt by the laboratory.

Page 1 of 1

A5) HIGH-CALORIC DIET COMPOSITION

microchem
Specialized Lab Services
Co .Reg. 2007/010539/07 Vat No. 4330239049

1st Floor, Fairweather House,
176 Sir Lowry Road,
Cape Town
8001
Telephone : +27 21 465-6996/7
E-mail: chem@microchem.co.za

ilac-MRA sanas Testing Laboratory T0393

CERTIFICATE OF ANALYSIS

Client's Reporting Address:
Department of Food Science
Private Bag X1
Matieland
7602

Client's Telephone #: 021 938 9391
Client's Fax #:

Our Lab Ref #: 2013-06-25-039 **Our Sample ID :** AC92366
Client: Stellenbosch University
Requested by: Prof A Lochner
E-mail address: alo@sun.ac.za
Product: Sucrose Diet
Sampling Method
Barcode
No of Samples:
Production Date: 24/06/2013
Sample Condition: SEALED
Date Received: 25/06/2013
Date Validated: 16/07/2013

Client Samp #: 2
Batch Code:
Sell By Date: 2013/06/26
Order Number: PROF A LOCHNER

ANALYSIS RESULTS	1	2	Average	MoU (%)	Test Method Ref
Moisture (g/100g)	29.83	29.31	29.6	0.70	S.O.P.C. No. 1#
Ash (g/100g)	2.75	2.93	2.8	5.00	S.O.P.C. No. 2#
Total Fat (g/100g)	4.53	4.76	4.6	2.60	S.O.P.C. No. 25#
Saturated Fat (g/100g)	2.74	2.92	2.8	2.60	S.O.P.C. No. 25#
Mono-Unsaturated Fat (g/100g)	1.05	1.12	1.1	2.60	S.O.P.C. No. 25#
Poly-Unsaturated Fat (g/100g)	0.75	0.73	0.7	2.60	S.O.P.C. No. 25#
Trans Fatty Acids (g/100g)	0.032	0.044	0.04	2.60	S.O.P.C. No. 25#
Omega 3 Fatty Acids (g/100g)	0.07	0.07	0.1	2.60	S.O.P.C. No. 25#
ALA (g/100g)	0.07	0.07	0.1	2.60	S.O.P.C. No. 25#
EPA (g/100g)	0.00	0.00	0.0	2.60	S.O.P.C. No. 25#
DHA (g/100g)	0.00	0.00	0.0	2.60	S.O.P.C. No. 25#
DPA (g/100g)	0.00	0.00	0.0		S.O.P.C. No. 25#
Omega 6 Fatty acids (g/100g)	0.68	0.66	0.7	2.60	S.O.P.C. No. 25#
Cholesterol (mg/100 g)	10.32	10.46	10	4.70	S.O.P.C. No. 26#
% Protein (6.25)	9.23	9.61	9.4	1.90	S.O.P.C. No. 36#
Nitrogen (g/100g)	1.48	1.54	1.5	1.90	S.O.P.C. No. 36#
Total Dietary Fibre (g/100g)	7.69	7.68	7.7	1.30	S.O.P.C. No. 20#
% Carbohydrate	45.97	45.71	45.8	C*	S.O.P.C. No. 21
Total Sugar (g/100g)	28.06	27.43	27.7	2.90	S.O.P.C. No. 27#
Fructose (g/100g)	0.76	0.78	0.8	2.90	S.O.P.C. No. 27#
Glucose (g/100g)	0.90	0.91	0.9	2.90	S.O.P.C. No. 27#
Sucrose (g/100g)	23.58	22.99	23.3	2.90	S.O.P.C. No. 27#
Maltose (g/100g)	0.00	0.00	0.0	2.90	S.O.P.C. No. 27#
Lactose (g/100g)	2.82	2.75	2.8	2.90	S.O.P.C. No. 27#
Energy (kJ/100 g)	1168	1178	1173		S.O.P.C. No. 22
Sodium (mg/100 g)	91.7	103	97.4	7.56	S.O.P.C. No. 45#

COMMENTS

Confirmed by: P Rubuz Date: 16-Jul-13
Technical Signatory

These results relate only to the items tested. Total Dietary Fibre content determined by AOAC Method 991.43
MoU = Measurement of Uncertainty. C* = By calculation.
 # = SANAS Accredited Method.
Tests without the # mark in this report are "Not SANAS Accredited" and are not included in the SANAS Schedule of Accreditation for this laboratory.

A6) WESTERN BLOT WORK FLOW AND NORMALIZATION

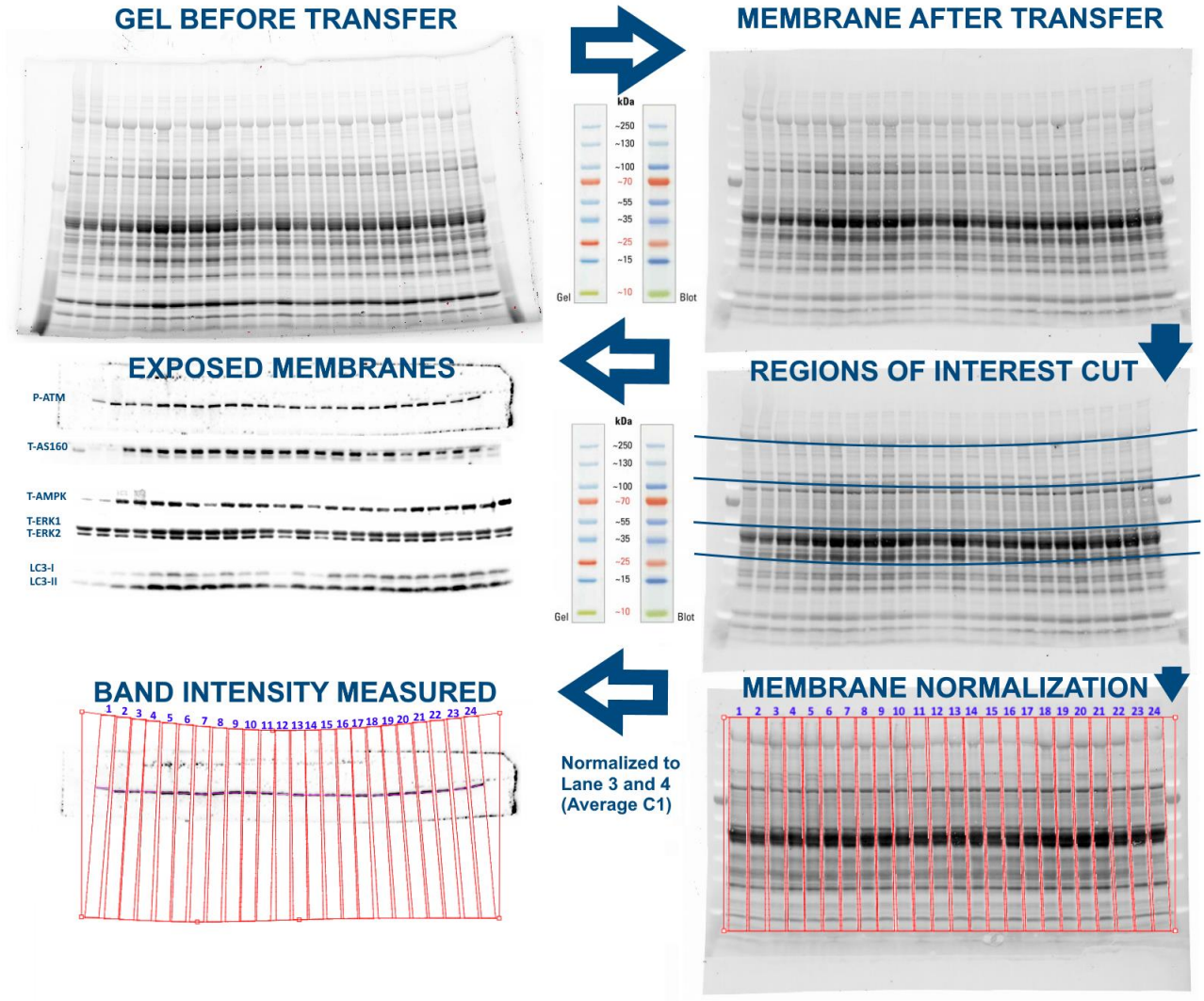

Figure A3 Western blotting work-flow and normalization. C1: 30 min stabilized control. Lanes 1 and 2: 30 min young control stabilized; Lanes 3 and 4: C1; Lanes 5 – 9: Control samples; Lanes 10 – 14: Control + GRT samples; Lanes 15-19: HCD samples; Lanes 20-24: HCD + GRT samples.

A7) SUMMARY OF MITOCHONDRIAL FUNCTIONAL PARAMETERS IN GLUTAMATE AND PALMITATE

Table A1 Summary of mitochondrial functional parameters in glutamate and palmitate

Parameter	Time Point	GLUTAMATE				PALMITATE			
		CONTROL	CONTROL+GRT	HCD	HCD+GRT	CONTROL	CONTROL+GRT	HCD	HCD+GRT
		MEAN±SEM	MEAN±SEM	MEAN±SEM	MEAN±SEM	MEAN±SEM	MEAN±SEM	MEAN±SEM	MEAN±SEM
ADP/O Ratio	S	2.53±0.08	2.17±0.11 (*) ↓	2.33±0.12	1.97±0.13 (p=0.066) ↓	2.76±0.01	2.37±0.05 (***) ↓	2.58±0.10	2.47±0.13
	I	2.29±0.14	2.33±0.11	2.45±0.07	2.08±0.11	2.65±0.09	2.61±0.09	2.78±0.26	2.46±0.07 (p=0.065)
	ER	2.61±0.20	2.36±0.06	2.41±0.06	2.32±0.05	2.73±0.09	2.90±0.17	2.89±0.23	3.05±0.09 (♥)
	LR	2.53±0.15	2.51±0.09	2.19±0.16	2.50±0.11	2.70±0.07	2.60±0.10	2.75±0.18 (♣)	2.76±0.14
State 3 (nAtoms O /mg/min)	S	297.05±38.14	291.69±25.95	248.28±42.51	277.34±19.18	313.35±13.09	358.92±12.71 (*) ↑	341.21±40.39	300.17±30.5
	I	177.82±21.37	280.45±17.34 (**) ↑	272.81±25.6 (*) ↑	243.54±27.88	245.96±26.73	318.09±5 (p=0.053) ↑	299.76±13.65	309.65±16.6
	ER	344.98±25.52	331.69±32.08	392.34±10.44	275.61±37.77 (*) ↓	368.84±10.77	332.43±19.7	446.68±26.38 (*) ↑	297.88±26.53 (**) ↓
	LR	305.2±19.03	227.09±14.49 (*) ↓	239.86±41.91	198.77±24.39	314.9±6.51	259.76±6.34 (***) ↓	254.1±40.78	263.27±18.42
State 4 (nAtoms O /mg/min)	S	92.81±8.4	83.72±2.36	64.53±8.99 (*) ↓	59.97±2.65	88.8±4.04	81.23±2.7	89.38±11.59	66.67±2.76 ↓
	I	46.31±5.19	69.51±5.36 (*) ↑	64.44±3.64 (*) ↑	61.93±5.34	65.76±4.98	87.77±5.69 (*) ↑	75.83±1.8	81.73±6.52
	ER	75.17±8.17	71.47±8.31	78.31±3.32	63.46±6.32 (p=0.083)	87.31±3.49	84.41±3.97	107.27±8.86 (♣)	76.16±3.37 (**) ↓
	LR	61.79±5.17	60.08±2.7	62.19±10.13	63.11±4.3	76.45±4.3	85.1±3.39	69.83±7.62	70.78±5.09
State 5 (nAtoms O /mg/min)	S	255.55±41.43	329.59±27.05	278.34±36.14	341.11±40.51	419.64±22.56 (♦)	447.65±8.24	274.1±44 (*) ↓	392.13±17.28 (p=0.053) ↑
	I	200.52±33.7	314.7±26.3 (*) ↑	311.04±31.57 (*) ↑	290.24±34.22	263.71±54.28	351.38±24.87	372.89±20.83	288.58±56.1
	ER	370.92±26.63	367.22±41.69	396.25±26.27	298.89±43.83	399.15±32.34	372.33±26.46	468.71±9.81 (p=0.098)	352.65±26.72 (**) ↓
	LR	383.46±35.35	277.88±26.39 (*) ↓	298.6±41.07	272.72±27.87	416.2±9.56	356.74±5.42 (**) ↓	369.11±49.77	362.97±29.17

S: Stabilization; I: Ischemia; ER: Early Reperfusion; LR: Late Reperfusion; HCD: High-caloric diet, GRT: Afriplex green rooibos extract; Control + GRT significance compared to Control, HCD significance compared to Control, HCD + GRT significance compared to HCD; *p<0.05, **p<0.01, ***p<0.001, ****p<0.0001.

Table A2 Summary of mitochondrial functional parameters in glutamate and palmitate (Continued)

Parameter	Time Point	GLUTAMATE				PALMITATE			
		CONTROL	CONTROL+GRT	HCD	HCD+GRT	CONTROL	CONTROL+GRT	HCD	HCD+GRT
		MEAN±SEM	MEAN±SEM	MEAN±SEM	MEAN±SEM	MEAN±SEM	MEAN±SEM	MEAN±SEM	MEAN±SEM
%Respiratory Recovery	S	86.07±5.92	115.6±10.26 (*) ↑	118.4±11.59 (*) ↑	126.16±19.14	133.45±2.06 (♦)	125.17±2.72	89.14±21.44 (*) ↓	134.67±10.32 (*) ↑
	I	108.72±5.45	112.08±5.9	113.93±3.58	120.21±8.27	100.2±12.02	110.71±8.42	124.36±5.16	114.63±7.15
	ER	107.87±3.2	110.35±4.8	100.87±5.41	108.08±4.16	116.73±2.7	112.21±5.98	106.47±6.77	119.15±3.21
	LR	125.5±8.54	121.98±6.28	132.05±20.52	139.1±7.17	132.23±2.2	137.63±3.11	148.62±9.72	137.62±5.37
RCI	S	3.17±0.25	3.47±0.26	3.93±0.71	4.62±0.26	3.55±0.19	4.46±0.28 (*) ↑	3.84±0.16	4.53±0.47
	I	3.9±0.26	4.09±0.28	4.21±0.26	3.94±0.33	3.72±0.21	3.69±0.25	3.94±0.12	3.87±0.32
	ER	4.71±0.26	4.84±0.65	5.06±0.29	4.46±0.6	4.24±0.15	3.95±0.22	4.21±0.23	3.95±0.42
	LR	5.05±0.45	3.84±0.34 (p=0.065) ↓	3.91±0.46	3.2±0.45	4.16±0.17	3.06±0.07 (**) ↓	3.58±0.3	3.73±0.12
Oxphos S3 (moles ADP /mg/min)	S	659.17±130.65	586.83±72.7	579.11±106.35	542.43±43.67	758.4±92.18	774.06±78.77 ↑	879.23±101.5 (♣)	739.55±76.02
	I	355±37.38	653.83±58.72 (**) ↑	523.16±83.35	441.14±38.77	578.04±106.03	830.26±36.8 (p=0.075) ↑	780.28±97.22	724.49±41.41 (♥)
	ER	894.89±85.29	781.07±74.34	943.19±28.14	641.21±92.55 (*) ↓	1007.01±51.39	953.78±44.92	1276.93±70.55 (♣) (*) ↑	913.69±92.23 (*) ↓
	LR	760.98±24.93	635.21±79.29	511.31±73.96 (*) ↓	446.09±63.35	853.09±38.38	717.37±47.61 (p=0.059) ↓	719.58±150.87	651.41±106.97
Oxphos S4 (moles ADP /mg/min)	S	203.43±35.32	164.56±17.21	149.51±20.53	117.6±7.29	211.31±25.73	184.18±13.59	230.25±29.53 (♣)	163.9±8.02
	I	112.19±10.48	163.28±18.76 (p=0.053) ↑	130.03±12.66	124.43±7.34	169.86±19.33	229.65±19.02 (p=0.059) ↑	202.41±26.53 (♣)	196.59±20.07 (♥)
	ER	197.63±31.44	169.41±21.9	189.11±12.17	147.76±16.14 (p=0.078) ↓	238.03±12.52	242.84±11.75	306.79±23.57 (♣) (*) ↑	231.53±6.43 (♥) (*) ↓
	LR	156.08±15.68	156.84±10.13	133.99±20.11	141.4±22.77	207.62±16.25	221.91±10.18	196.57±32.9	183.94±19.98

S: Stabilization; I: Ischemia; ER: Early Reperfusion; LR: Late Reperfusion; HCD: High-caloric diet, GRT: Afriplex green rooibos extract; Control + GRT significance compared to Control, HCD significance compared to Control, HCD + GRT significance compared to HCD; *p<0.05, **p<0.01, ***p<0.001, ****p<0.0001, ♦p<0.05 (Palmitate vs Glutamate in Control), ♣p<0.05 (Palmitate vs Glutamate in HCD), ♥p<0.05 (Palmitate vs Glutamate in HCD + GRT)

A8) UNDISCLOSED TOTAL LIPID FATTY ACID CONTENT

Table A3 Fasting Serum Total Lipid Fatty Acid Content

Chemical Name	Common Name	Control (n = 8)	Control + GRT (n = 8)		HCD (n = 8)		HCD + GRT (n = 8)	
Monounsaturated fatty acids (MUFAs)								
			n-7 Series					
C16:1 n-7 PTA	Palmitoleic acid	1.927±0.273	1.974±0.333		1.99±0.253		3.221±0.646	
C18:1 n-7 VA	Vaccenic acid	2.45±0.161	2.767±0.133		2.35±0.162		3.375±0.341 (*)	↑
			n-9 Series					
C18:1 n-9 OA	Oleic acid	12.158±1.133	10.623±0.451		18.725±0.513 (***)	↑	19.196±0.251	
C20:1 n-9 GA	Gadoleic acid	0.236±0.011	0.269±0.022		0.264±0.015		0.299±0.027	
C22:1 n-9 EA	Erucic acid	0.003±0.003	0.028±0.011		0.027±0.007 (*)	↑	0.023±0.005	
C24:1 n-9 NA	Nervonic acid	0.282±0.017	0.276±0.034		0.25±0.018		0.204±0.018	
Polyunsaturated fatty acids (PUFAs)								
			n-3 Series					
C18:3 n-3 ALA	Alpha-linolenic acid	0.957±0.076	1.197±0.14		0.583±0.042 (***)	↓	0.654±0.067	
C20:3 n-3 ETA	Eicosatrienoic acid	0.017±0.008	0.027±0.008		0.026±0.006		0.025±0.006	
C20:5 n-3 EPA	Eicosapentaenoic acid	2.612±0.521	4.31±0.455 (*)	↑	1.873±0.121		2.133±0.161	
C22:5 n-3 DPA	Docosapentaenoic acid	1.187±0.1	1.923±0.137 (***)	↑	1.227±0.067		1.393±0.123	
C22:6 n-3 DHA	Docosahexaenoic acid	3.464±0.354	4.605±0.159 (*)	↑	4.182±0.214		4.312±0.303	
			n-6 Series					
C18:2 n-6 LA	Linoleic acid	22.06±1.105	22.734±0.507		17.829±0.498 (**)	↓	16.288±0.577	
C18:3 n-6 GLA	Gamma linolenic acid	0.634±0.029	0.322±0.016 (****)	↓	0.288±0.012 (***)	↓	0.277±0.017	
C20:2 n-6 EDA	Eicosadienoic acid	0.313±0.021	0.297±0.007		0.206±0.01 (***)	↓	0.203±0.013	
C20:3 n-6 DGLA	Dihomo-gamma-linolenic acid	0.718±0.051	0.73±0.024		1.101±0.057 (***)	↑	1.121±0.045	
C20:4 n-6 AA	Arachidonic acid	16.607±0.655	17.077±1.079		12.194±0.748 (***)	↓	10.441±0.671	
C22:2 n-6 DDA	Docosadienoic acid	0±0	0.01±0.01		0.013±0.013		0±0	
C22:4 n-6 ADA	Adrenic acid	0.254±0.05	0.201±0.008		0.207±0.012		0.188±0.013	
C22:5 n-6 DPA	Docosapentaenoic acid	0.109±0.018	0.098±0.03		0.142±0.011		0.109±0.012	
Saturated fatty acid								
C12:0 LA	Lauric acid	0.024±0.007	0.022±0.007		1.355±0.258 (***)	↑	1.319±0.097	
C14:0 MA	Myristic acid	0±0	0.722±0.126 (***)	↑	2.403±0.287 (***)	↑	3.09±0.258	
C16:0 PA	Palmitic acid	20.382±0.571	17.899±0.386 (**)	↓	19.899±0.165		19.685±0.452	
C17:0 HAD	Heptadecanoic acid	0.583±0.039	0.564±0.017		0.346±0.022 (***)	↓	0.365±0.023	
C18:0 SA	Stearic acid	12.279±0.455	10.666±0.45 (*)	↓	11.83±0.191		11.466±0.144	
C20:0 ARA	Arachidic acid	0.168±0.009	0.167±0.021		0.187±0.018		0.198±0.009	
C22:0 BA	Behenic acid	0.168±0.011	0.148±0.01		0.176±0.007		0.146±0.008 (*)	↓
C24:0 LGA	Lignoceric acid	0.407±0.022	0.342±0.028		0.326±0.013 (**)	↓	0.27±0.018 (*)	↓
Calculations								
Total Saturated Fatty Acids		34.011±0.937	30.53±0.48 (**)	↓	36.522±0.543 (*)	↑	36.54±0.405	
Total n-7-MUFA		4.378±0.425	4.742±0.449		4.339±0.392		6.596±0.984	
Total n-9-MUFA		12.68±1.122	11.196±0.459		19.265±0.51 (***)	↑	19.721±0.257	
Total Monounsaturated Fatty Acids		17.058±1.51	15.938±0.842		23.605±0.801 (**)	↑	26.317±1.034	
Total Polyunsaturated Fatty Acids		48.932±1.797	53.532±0.982 (*)	↑	39.873±1.163 (***)	↓	37.143±1.131	
Total n-6-PUFA		40.695±1.159	41.47±1.403		31.981±1.241 (***)	↓	28.626±1.108	
Total n-3-PUFA		8.237±0.956	12.062±0.809 (**)	↑	7.892±0.366		8.517±0.602	
PUFA/SFA Ratio		1.451±0.077	1.758±0.05 (**)		1.096±0.047	↓	1.018±0.036	
Total n-6/Total n-3 Ratio		5.355±0.565	3.61±0.385 (*)	↓	4.139±0.319	↓	3.491±0.294	
GLA:LA		0.029±0.002	0.014±0.001 (***)	↓	0.016±0.001 (***)	↓	0.017±0.002	
DGLA:GLA		1.13±0.054	2.278±0.052 (***)	↑	3.926±0.381 (***)	↑	4.111±0.174	
DGLA:LA		0.034±0.004	0.032±0.002		0.062±0.003 (***)	↑	0.07±0.005	
AA:DGLA		23.838±1.691	23.488±1.551		11.193±0.734 (***)	↓	9.505±0.835	
AA:LA		0.766±0.046	0.75±0.043		0.68±0.025		0.639±0.029	
n-6DPA:DHA		0.036±0.008	0.022±0.008		0.035±0.004		0.026±0.002	

REFERENCES

Abdelaal, M., le Roux, C.W. & Docherty, N.G. 2017. Morbidity and mortality associated with obesity. *Annals of translational medicine*. 5(7):161.

Abdurrachim, D., Luiken, J.J.F.P., Nicolay, K., Glatz, J.F.C., Prompers, J.J. & Nabben, M. 2015. Good and bad consequences of altered fatty acid metabolism in heart failure: evidence from mouse models. *Cardiovascular Research*. 106(2):194–205.

Abounit, K., Scarabelli, T.M. & McCauley, R.B. 2012. Autophagy in mammalian cells. *World journal of biological chemistry*. 3(1):1–6.

Abozguia, K., Shivu, G.N., Ahmed, I., Phan, T.T. & Frenneaux, M.P. 2009. The heart metabolism: pathophysiological aspects in ischaemia and heart failure. *Current pharmaceutical design*. 15(8):827–35.

Achari, A.E. & Jain, S.K. 2017. Adiponectin, a Therapeutic Target for Obesity, Diabetes, and Endothelial Dysfunction. *International journal of molecular sciences*. 18(6).

Aguirre, V., Uchida, T., Yenush, L., Davis, R. & White, M.F. 2000. The c-Jun NH2-terminal kinase promotes insulin resistance during association with insulin receptor substrate-1 and phosphorylation of Ser307. *Journal of Biological Chemistry*. 275(12):9047–9054.

Ahrén, B.O. & Taborsky, G.J. 1986. The Mechanism of Vagal Nerve Stimulation of Glucagon and Insulin Secretion in the Dog*. *Endocrinology*. 118(4):1551–1557.

Akinrinmade, O., Omoruyi, S., Dietrich, D. & Ekpo, O. 2017. Long-term consumption of fermented rooibos herbal tea offers neuroprotection against ischemic brain injury in rats. *Acta neurobiologiae experimentalis*. 77(1):94–105.

Alberts, B., Johnson, A., Lewis, J., Raff, M., Roberts, K. & Walter, P. 2002. *Molecular biology of the cell*. Garland Science.

Alexandre, A., Reynafarje, B. & Lehninger, A.L. 1978. Stoichiometry of vectorial H+ movements coupled to electron transport and to ATP synthesis in mitochondria. *Proceedings of the National Academy of Sciences of the United States of America*. 75(11):5296–300.

Ali, A., Hoeflich, K.P. & Woodgett, J.R. 2001. Glycogen synthase kinase-3: Properties, functions, and regulation. *Chemical Reviews*. 101(8):2527–2540.

Altomare, D.A., Guo, K., Cheng, J.Q., Sonoda, G., Walsh, K. & Testa, J.R. 1995. Cloning, chromosomal localization and expression analysis of the mouse Akt2 oncogene. *Oncogene*. 11(6):1055–1060.

American Diabetes Association, A.D. 2014. Standards of medical care in diabetes--2014. *Diabetes care*. 37 Suppl 1(Supplement 1):S14-80.

An, D. & Rodrigues, B. 2006. Role of changes in cardiac metabolism in development of diabetic cardiomyopathy. *American journal of physiology.Cell physiology.* 60(4):H1489.

Anderson, E.J., Kypson, A.P., Rodriguez, E., Anderson, C.A., Lehr, E.J. & Neufer, P.D. 2009. Substrate-Specific Derangements in Mitochondrial Metabolism and Redox Balance in the Atrium of the Type 2 Diabetic Human Heart. *Journal of the American College of Cardiology*. 54(20):1891–1898.

Andreollo, A.N., Dos Santos, F.E., Araujo, R.M. & Lopes, R.L. 2012. Rat's age versus human's age: what is the relationship? *ABCD Arq Bras Cir Dig*. 25(1):49–51.

Andres, A.M., Kooren, J.A., Parker, S.J., Tucker, K.C., Ravindran, N., Ito, B.R., Huang, C., Venkatraman, V., et al. 2016. Discordant signaling and autophagy response to fasting in hearts of obese mice: Implications for ischemia tolerance. *American Journal of Physiology-Heart and Circulatory Physiology*. 311(1):H219–H228.

Anjana, R.M., Unnikrishnan, R., Mugilan, P., Jagdish, P.S., Parthasarathy, B., Deepa, M., Loganathan, G., Kumar, R.A., et al. 2018. Causes and predictors of mortality in Asian Indians with and without diabetes–10 year follow-up of the Chennai Urban Rural Epidemiology Study (CURES - 150). *PLOS ONE*. 13(7):e0197376.

Anonymous. 2007. South Africa Sector Report Food and Beverages Industry. Swiss Business Hub South Africa. *Food Chemistry*. 108:55–63.

Antunes, L.C., Elkfury, J.L., Jornada, M.N., Foletto, K.C. & Bertoluci, M.C. 2016. Validation of HOMA-IR in a model of insulin-resistance induced by a high-fat diet in Wistar rats. *Archives of Endocrinology and Metabolism*. 60(2):138–142.

Anzell, A.R., Maizy, R., Przyklenk, K. & Sanderson, T.H. 2018. Mitochondrial Quality Control and Disease: Insights into Ischemia-Reperfusion Injury. *Molecular Neurobiology*. 55(3):2547–2564.

Arts, I.C. & Hollman, P.C. 2005. Polyphenols and disease risk in epidemiologic studies. *The American Journal of Clinical Nutrition*. 81(1 Suppl):317S–325S.

Ashcroft, F. 1996. Mechanisms of the Glycaemic Effects of Sulfonylureas. *Hormone and Metabolic Research*. 28(09):456–463.

Association American Diabetes. 2003. Gestational Diabetes Mellitus. *Diabetes care*. 26(Supplement 1):S103–S105.

Augustin, R. 2010. The protein family of glucose transport facilitators: It's not only about glucose after all. *IUBMB life*. 62(5):315–333.

Azevedo, P.S., Polegato, B.F., Minicucci, M.F., Paiva, S.A.R. & Zornoff, L.A.M. 2016. Cardiac Remodeling: Concepts, Clinical Impact, Pathophysiological Mechanisms and Pharmacologic Treatment. *Arquivos brasileiros de cardiologia*. 106(1):62–9.

Baggio, L.L. & Drucker, D.J. 2007. Biology of Incretins: GLP-1 and GIP. *Gastroenterology*. 132(6):2131–2157.

Baggish, A.L. & Wood, M.J. 2011. Athlete's Heart and Cardiovascular Care of the Athlete: Scientific and Clinical Update. *Circulation*. 123(23):2723–2735.

Balaban, R.S., Kantor, H.L., Katz, L.A. & Briggs, R.W. 1986. Relation between work and phosphate metabolite in the in vivo paced mammalian heart. *Science (New York, N.Y.)*. 232(4754):1121–3. [Online], Available: http://www.ncbi.nlm.nih.gov/pubmed/3704638 [2018, November 01].

Bandyopadhyay, G.K., Yu, J.G., Ofrecio, J. & Olefsky, J.M. 2005. Increased p85/55/50 expression and decreased phosphotidylinositol 3-kinase activity in insulin-resistant human skeletal muscle. *Diabetes*. 54(8):2351–9.

Barker, D.J.P. 2007. The origins of the developmental origins theory. *Journal of Internal Medicine*. 261(5):412–417.

Barnabei, M.S., Palpant, N.J. & Metzger, J.M. 2010. Influence of genetic background on ex vivo and in vivo cardiac function in several commonly used inbred mouse strains. *Physiological Genomics*. 42A(2):103–113.

Baxter, G.F., Mocanu, M.M., Brar, B.K., Latchman, D.S. & Yellon, D.M. 2001. Cardioprotective Effects of Transforming Growth Factor-β1 During Early Reoxygenation or Reperfusion Are Mediated by p42/p44 MAPK. *Journal of Cardiovascular Pharmacology*. 38(6):930–939.

Bazotte, R.B., Silva, L.G. & Schiavon, F.P. 2014. Insulin resistance in the liver: deficiency or excess of insulin? *Cell cycle (Georgetown, Tex.)*. 13(16):2494–500.

Beale, E.G. 2013. Insulin signaling and insulin resistance. *Journal of Investigative Medicine*. 61(1):11–14.

Beaser, R.S., Hollander, P.A. & Silvestri, R. 2015. Inhaled Insulin: Pulmonary Considerations. *Medscape*. [Online], Available: http://www.medscape.org/viewarticle/556041.

Beauloye, C., Bertrand, L., Krause, U., Marsin, A.S., Dresselaers, T., Vanstapel, F., Vanoverschelde, J.L. & Hue, L. 2001. No-flow ischemia inhibits insulin signaling in heart by decreasing intracellular pH. *Circulation research*. 88(5):513–9.

Beer, D. De, Malherbe, C.J., Beelders, T., Willenburg, E.L., Brand, D.J. & Joubert, E. 2015. Isolation of aspalathin and nothofagin from rooibos (Aspalathus linearis) using high-performance countercurrent chromatography : Sample loading and compound stability considerations ☆. *Journal of Chromatography A*. 1381:29–36.

De Beer, D., Joubert, E., Viljoen, M. & Manley, M. 2012. Enhancing aspalathin stability in rooibos (Aspalathus linearis) ready-to-drink iced teas during storage: The role of nano-emulsification and beverage ingredients, citric and ascorbic acids. *Journal of the Science of Food and Agriculture*. 92(2):274–282.

Bell, R.M., Mocanu, M.M. & Yellon, D.M. 2011. Retrograde heart perfusion: The Langendorff technique of isolated heart perfusion. *Journal of Molecular and Cellular Cardiology*. 50(6):940–950.

Beltrán-Debón, R., Rull, A., Rodríguez-Sanabria, F., Iswaldi, I., Herranz-López, M., Aragonès, G., Camps, J., Alonso-Villaverde, C., et al. 2011. Continuous administration of polyphenols from aqueous rooibos (Aspalathus linearis) extract ameliorates dietary-induced metabolic disturbances in hyperlipidemic mice. *Phytochemistry*. 18:414–424.

Benito, M. 2011. Tissue specificity on insulin action and resistance: past to recent mechanisms. *Acta Physiologica*. 201(3):297–312.

Berg, J.M., Tymoczko, J.L. & Stryer, L. 2002. Each Organ Has a Unique Metabolic Profile Biochemistry. 5th edition. New York: W H Freeman; 2002. Section 30.2.

Bergmann, O., Bhardwaj, R.D., Bernard, S., Zdunek, S., Barnabe-Heider, F., Walsh, S., Zupicich, J., Alkass, K., et al. 2009. Evidence for Cardiomyocyte Renewal in Humans. *Science*. 324(5923):98–102.

Bertrand, L., Horman, S., Beauloye, C. & Vanoverschelde, J.-L. 2008. Insulin signalling in the heart. *Cardiovascular Research*. 79(2):238–248.

Bertsch, R.A. & Merchant, M.A. 2015. Study of the Use of Lipid Panels as a Marker of Insulin Resistance to Determine Cardiovascular Risk. *The Permanente journal*. 19(4):4–10.

Beznak, M. 1954. The behaviour of the weight of the heart and the blood pressure of albino rats under different conditions. *J Physiol*. 124(1): 44–63.

Bhatt, D.L., Stone, G.W., Mahaffey, K.W., Gibson, C.M., Steg, P.G., Hamm, C.W., Price, M.J., Leonardi, S., et al. 2013. Effect of Platelet Inhibition with Cangrelor during PCI on Ischemic Events. *New England Journal of Medicine*. 368(14):1303–1313.

Bhattacharya, S., Dey, D. & Roy, S.S. 2007. Molecular mechanism of insulin resistance. *J Biosci*. 32(2):405–

413.

Bhatti, J.S., Bhatti, G.K. & Reddy, P.H. 2017. Mitochondrial dysfunction and oxidative stress in metabolic disorders — A step towards mitochondria based therapeutic strategies. *Biochimica et Biophysica Acta (BBA) - Molecular Basis of Disease*. 1863(5):1066–1077.

Bijur, G.N. & Jope, R.S. 2003. Rapid accumulation of Akt in mitochondria following phosphatidylinositol 3-kinase activation. *Journal of neurochemistry*. 87(6):1427–35.

Bing, R.J., Siegel, A., Ungar, I. & Gilbert, M. 1954. Metabolism of the human heart. II. Studies on fat, ketone and amino acid metabolism. *The American Journal of Medicine*. 16(4):504–515.

Bischoff, H. 1995. The mechanism of alpha-glucosidase inhibition in the management of diabetes. *Clinical and investigative medicine. Medecine clinique et experimentale*. 18(4):303–11.

Bode, A.M. & Dong, Z. 2007. The functional contrariety of JNK. *Molecular Carcinogenesis*. 46(8):591–598.

Boden, G. 1999. Free Fatty Acids, Insulin Resistance, and Type 2 Diabetes Mellitus. *Proceedings of the Association of American Physicians*. 111(3):241–248.

Boden, G. 2008. Obesity and Free Fatty Acids. *Endocrinology and Metabolism Clinics of North America*. 37(3):635–646.

Boden, G. 2011. Obesity, insulin resistance and free fatty acids. *Current Opinion in Endocrinology, Diabetes and Obesity*. 18(2):139–143.

Boengler, K., Schulz, R. & Heusch, G. 2009. Loss of cardioprotection with ageing. *Cardiovascular Research*. 83(2):247–261.

Boldt, A., Gergs, U., Pönicke, K., Simm, A., Silber, R.-E. & Neumann, J. 2010. Inotropic effects of ivabradine in the mammalian heart. *Pharmacology*. 86(5–6):249–58.

Bonadonna, R.C., Del Prato, S., Saccomani, M.P., Bonora, E., Gulli, G., Ferrannini, E., Bier, D., Cobelli, C., et al. 1993. Transmembrane glucose transport in skeletal muscle of patients with non-insulin-dependent diabetes. *Journal of Clinical Investigation*. 92(1):486–494.

Borbély, A.A., Huston, J.P. & Waser, P.G. 1975. Control of sleep states in the rat by short light-dark cycles. *Brain Research*. 95(1):89–101.

Borer, J.S. & Heuzey, J.-Y. Le. 2008. Characterization of the Heart Rate-Lowering Action of Ivabradine, a Selective If Current Inhibitor. *American Journal of Therapeutics*. 15(5):461–473.

Borga, M., West, J., Bell, J.D., Harvey, N.C., Romu, T., Heymsfield, S.B. & Dahlqvist Leinhard, O. 2018. Advanced body composition assessment: from body mass index to body composition profiling. *Journal of investigative medicine : the official publication of the American Federation for Clinical Research*. 66(5):1–9.

Boudina, S., Sena, S., O'Neill, B.T., Tathireddy, P., Young, M.E. & Abel, E.D. 2005. Reduced Mitochondrial Oxidative Capacity and Increased Mitochondrial Uncoupling Impair Myocardial Energetics in Obesity. *Circulation*. 112(17):2686–2695.

Bourogaa, E., Bertrand, J., Despeaux, M., Jarraya, R., Fabre, N., Payrastre, L., Demur, C., Fournié, J.-J., et al. 2011. Hammada scoparia flavonoids and rutin kill adherent and chemoresistant leukemic cells. *Leukemia Research*. 35(8):1093–1101.

Bradford, M. 1976. A Rapid and Sensitive Method for the Quantitation of Microgram Quantities of Protein Utilizing the Principle of Protein-Dye Binding. *Analytical Biochemistry*. 72(1–2):248–254.

Bramati, L., Minoggio, M., Gardana, C., Simonetti, P., Mauri, P. & Pietta, P. 2002. Quantitative

characterization of flavonoid compounds in Rooibos tea (Aspalathus linearis) by LC-UV/DAD. *Journal of Agricultural and Food Chemistry*. 50(20):5513–5519.

Brand, M.D. & Nicholls, D.G. 2011. Assessing mitochondrial dysfunction in cells. *The Biochemical journal*. 435(2):297–312.

Bratic, I. & Trifunovic, A. 2010. Mitochondrial energy metabolism and ageing. *Biochimica et Biophysica Acta (BBA) - Bioenergetics*. 1797(6–7):961–967.

Bray, G.A. & Hamman, R.F. 2015. Insulin Resistance and Prediabetes. *National Institutes of Health*. 14(4893). [Online], Available: http://www.niddk.nih.gov/health-information/health-topics/Diabetes/insulin-resistance-prediabetes/Pages/index.aspx.

Breet, P., Kruger, H.S., Jerling, J.C. & Oosthuizen, W. 2005. Actions of black tea and Rooibos on iron status of primary school children. *Nutrition Research*. 25(11):983–994.

Breiter, T., Laue, C., Kressel, G., Gröll, S., Engelhardt, U.H. & Hahn, A. 2011. Bioavailability and antioxidant potential of rooibos flavonoids in humans following the consumption of different rooibos formulations. *Food Chemistry*. 128(2):338–347.

Bright, R., Raval, A.P., Dembner, J.M., Pérez-Pinzón, M.A., Steinberg, G.K., Yenari, M.A. & Mochly-Rosen, D. 2004. Protein Kinase C Mediates Cerebral Reperfusion Injury In Vivo. *Journal of Neuroscience*. 24(31):6880–6888.

Bueno, O.F., De Windt, L.J., Tymitz, K.M., Witt, S.A., Kimball, T.R., Klevitsky, R., Hewett, T.E., Jones, S.P., et al. 2000. The MEK1-ERK1/2 signaling pathway promotes compensated cardiac hypertrophy in transgenic mice. *The EMBO Journal*. 19(23):6341–6350.

Burgering, B.M.T. & Coffer, P.J. 1995. Protein kinase B (c-Akt) in phosphatidylinositol-3-OH kinase signal transduction. *Nature*. 376(6541):599–602.

Buscà, R., Pouysségur, J. & Lenormand, P. 2016. ERK1 and ERK2 Map Kinases: Specific Roles or Functional Redundancy? *Frontiers in Cell and Developmental Biology*. 4(June):1–23.

Busiello, R.A., Savarese, S. & Lombardi, A. 2015. Mitochondrial uncoupling proteins and energy metabolism. *Frontiers in physiology*. 6:36.

Calvert, J.W., Gundewar, S., Jha, S., Greer, J.J.M., Bestermann, W.H., Tian, R. & Lefer, D.J. 2008. Acute Metformin Therapy Confers Cardioprotection Against Myocardial Infarction Via AMPK-eNOS–Mediated Signaling. *Diabetes*. 57(3):696–705.

Calvo, S.E. & Mootha, V.K. 2010. The Mitochondrial Proteome and Human Disease. *Annual Review of Genomics and Human Genetics*. 11(1):25–44.

Campello, S., Strappazzon, F. & Cecconi, F. 2014. Mitochondrial dismissal in mammals, from protein degradation to mitophagy. *Biochimica et Biophysica Acta (BBA) - Bioenergetics*. 1837(4):451–460.

Canda, B.D., Oguntibeju, O.O. & Marnewick, J.L. 2014. Effects of consumption of rooibos (Aspalathus linearis) and a rooibos-derived commercial supplement on hepatic tissue injury by tert-butyl hydroperoxide in Wistar rats. *Oxidative medicine and cellular longevity*. 2014:716832.

Carbone, A., D'Andrea, A., Riegler, L., Scarafile, R., Pezzullo, E., Martone, F., America, R., Liccardo, B., et al. 2017. Cardiac damage in athlete's heart: When the "supernormal" heart fails! *World Journal of Cardiology*. 9(6):470.

Carloni, S., Girelli, S., Scopa, C., Buonocore, G., Longini, M. & Balduini, W. 2010. Activation of autophagy and Akt/CREB signaling play an equivalent role in the neuroprotective effect of rapamycin in neonatal

hypoxia-ischemia. *Autophagy*. 6(3):366–77.

Carpenter, K., Kent-Jones, D.W., Weininger, J. & Truswell, A.S. 2018. *Human nutrition*. [Online], Available: https://www.britannica.com/science/human-nutrition [2018, October 08].

De Carvalho, C.A.M. & Thomazini, J.A. 2014. Study of Wistar Rats Heart at Different Stages in the Evolutionary Cycle. *International Journal of Morphology*. 32(2):614–617.

Cavaghan, M.K., Ehrmann, D.A. & Polonsky, K.S. 2000a. Interactions between insulin resistance and insulin secretion in the development of glucose intolerance. *The Journal of clinical investigation*. 106(3):329–33.

Cavaghan, M.K., Ehrmann, D.A. & Polonsky, K.S. 2000b. Interactions between insulin resistance and insulin secretion in the development of glucose intolerance. *Journal of Clinical Investigation*. 106(3):329–333.

Chai, W., Wu, Y., Li, G., Cao, W., Yang, Z. & Liu, Z. 2008. Activation of p38 mitogen-activated protein kinase abolishes insulin-mediated myocardial protection against ischemia-reperfusion injury. *American Journal of Physiology-Endocrinology and Metabolism*. 294(1):E183–E189.

Chambers, J.W. & LoGrasso, P. V. 2011. Mitochondrial c-Jun N-terminal kinase (JNK) signaling initiates physiological changes resulting in amplification of reactive oxygen species generation. *The Journal of biological chemistry*. 286(18):16052–62.

Chambers, J.W., Pachori, A., Howard, S., Iqbal, S. & LoGrasso, P. V. 2013. Inhibition of JNK Mitochondrial Localization and Signaling Is Protective against Ischemia/Reperfusion Injury in Rats. *Journal of Biological Chemistry*. 288(6):4000–4011.

Chamie, K., Oberfoell, S., Kwan, L., Labo, J., Wei, J.T. & Litwin, M.S. 2013. Body Mass Index and Prostate Cancer Severity: Do Obese Men Harbor More Aggressive Disease on Prostate Biopsy? *Urology*. 81(5):949–955.

Chance, B. & Williams, G.R. 1956. The respiratory chain and oxidative phosphorylation. *Advances in enzymology and related subjects of biochemistry*. 17:65–134.

Chandel, N.S. 2014. Mitochondria as signaling organelles. *BMC Biology*. 12(1):34.

Chang, W., Zhang, M., Li, J., Meng, Z., Xiao, D., Wei, S., Chen, L., Wang, C., et al. 2012. Berberine Attenuates Ischemia-Reperfusion Injury Via Regulation of Adenosine-5′-monophosphate Kinase Activity in Both Non-ischemic and Ischemic Areas of the Rat Heart. *Cardiovascular Drugs and Therapy*. 26(6):467–478.

Chen, L. & Knowlton, A.A. 2010. Mitochondria and heart failure: new insights into an energetic problem. *Minerva cardioangiologica*. 58(2):213–29.

Chen, W., Sudji, I.R., Wang, E., Joubert, E., Van Wyk, B.-E. & Wink, M. 2013. Ameliorative effect of aspalathin from rooibos (Aspalathus linearis) on acute oxidative stress in Caenorhabditis elegans. *Phytomedicine*. 20(3–4):380–386.

De Chiara, G., Marcocci, M.E., Torcia, M., Lucibello, M., Rosini, P., Bonini, P., Higashimoto, Y., Damonte, G., et al. 2006. Bcl-2 Phosphorylation by p38 MAPK: identification of target sites and biologic consequences. *The Journal of biological chemistry*. 281(30):21353–61.

Chimhashu, T., Malan, L., Baumgartner, J., van Jaarsveld, P.J., Galetti, V., Moretti, D., Smuts, C.M. & Zimmermann, M.B. 2018. Sensitivity of fatty acid desaturation and elongation to plasma zinc concentration: a randomised controlled trial in Beninese children. *British Journal of Nutrition*. 119(6):610–619.

Chin, J.T., Troke, J.J., Kimura, N., Itoh, S., Wang, X., Palmer, O.P., Robbins, R.C. & Fischbein, M.P. 2011. A novel cardioprotective agent in cardiac transplantation: metformin activation of AMP-activated protein kinase decreases acute ischemia-reperfusion injury and chronic rejection. *The Yale journal of biology and medicine*. 84(4):423–32.

Cho, H., Mu, J., Kim, J.K., Thorvaldsen, J.L., Chu, Q., Crenshaw, E.B., Kaestner, K.H., Bartolomei, M.S., et al. 2001. Insulin Resistance and a Diabetes Mellitus-Like Syndrome in Mice Lacking the Protein Kinase Akt2 (PKBbeta). *Science*. 292(5522):1728–1731.

Clarke, S.J., McStay, G.P. & Halestrap, A.P. 2002. Sanglifehrin A Acts as a Potent Inhibitor of the Mitochondrial Permeability Transition and Reperfusion Injury of the Heart by Binding to Cyclophilin-D at a Different Site from Cyclosporin A. *Journal of Biological Chemistry*. 277(38):34793–34799.

Coats, A.J.S. 2004. Anaemia and heart failure. *Heart (British Cardiac Society)*. 90(9):977–9.

Cohen, M. V. & Downey, J.M. 2015. Signalling pathways and mechanisms of protection in pre- and postconditioning: Historical perspective and lessons for the future. *British Journal of Pharmacology*. 172(8):1913–1932.

Cohen, P., Alessi, D.R. & Cross, D.A.E. 1997. PDK1, one of the missing links in insulin signal transduction? *FEBS Letters*. 410(1):3–10.

Coimbra, S., Santos-Silva, A., Rocha-Pereira, P., Rocha, S. & Castro, E. 2006. Green tea consumption improves plasma lipid profiles in adults. *Nutrition Research*. 26(11):604–607.

Consitt, L.A., Van Meter, J., Newton, C.A., Collier, D.N., Dar, M.S., Wojtaszewski, J.F.P., Treebak, J.T., Tanner, C.J., et al. 2013. Impairments in site-specific AS160 phosphorylation and effects of exercise training. *Diabetes*. 62(10):3437–47.

Contreras, L., Drago, I., Zampese, E. & Pozzan, T. 2010. Mitochondria: The calcium connection. *Biochimica et Biophysica Acta (BBA) - Bioenergetics*. 1797(6–7):607–618.

Corbucci, G.G., Perrino, C., Donato, G., Ricchi, A., Lettieri, B., Troncone, G., Indolfi, C., Chiariello, M., et al. 2004. Transient and reversible deoxyribonucleic acid damage in human left ventricle under controlled ischemia and reperfusion. *Journal of the American College of Cardiology*. 43(11):1992–1999.

Cornier, M.-A., Dabelea, D., Hernandez, T.L., Lindstrom, R.C., Steig, A.J., Stob, N.R., Van Pelt, R.E., Wang, H., et al. 2008. The Metabolic Syndrome. *Endocrine reviews*. 29(7):777–822.

Courts, F.L. & Williamson, G. 2009. The C -glycosyl flavonoid, aspalathin, is absorbed, methylated and glucuronidated intact in humans. *Molecular Nutrition & Food Research*. 53(9):1104–1111.

Crouser, E.D. & Parinandi, N. 2011. Mitochondrial mechanisms are at the 'heart' of novel ischemia–reperfusion therapies*. *Critical Care Medicine*. 39(3):593–595.

Dahlgren, C. & Karlsson, A. 1999. Respiratory burst in human neutrophils. *Journal of immunological methods*. 232(1–2):3–14.

Dai, S., Xu, Q., Liu, S., Yu, B., Liu, J. & Tang, J. 2017. Role of autophagy and its signaling pathways in ischemia/reperfusion injury. *American journal of translational research*. 9(10):4470–4480.

Davidson, M.W. 2015. *Cell Biology: Mitochondria*. [Online], Available: https://micro.magnet.fsu.edu/cells/mitochondria/mitochondria.html [2018, October 12].

Davidson, S.M., Hausenloy, D., Duchen, M.R. & Yellon, D.M. 2006. Signalling via the reperfusion injury signalling kinase (RISK) pathway links closure of the mitochondrial permeability transition pore to cardioprotection. *The International Journal of Biochemistry & Cell Biology*. 38(3):414–419.

Day, A.J., Bao, Y., Morgan, M.R.A. & Williamson, G. 2000. Conjugation position of quercetin glucuronides and effect on biological activity. *Free Radical Biology and Medicine*. 29(12):1234–1243.

DeBerardinis, R.J., Mancuso, A., Daikhin, E., Nissim, I., Yudkoff, M., Wehrli, S. & Thompson, C.B. 2007. Beyond aerobic glycolysis: Transformed cells can engage in glutamine metabolism that exceeds the requirement for protein and nucleotide synthesis. *Proceedings of the National Academy of Sciences*. 104(49):19345–19350.

Decker, R.S. & Wildenthal, K. 1980. Lysosomal alterations in hypoxic and reoxygenated hearts. I. Ultrastructural and cytochemical changes. *The American journal of pathology*. 98(2):425–44. [Online], Available: http://www.ncbi.nlm.nih.gov/pubmed/7355988 [2018, October 20].

DeFronzo, R.A. 1999. Pathogenesis of Type 2 Diabetes. *Drugs*. 58(Supplement 1):29–30.

DeFronzo, R.A. & Tripathy, D. 2009. Skeletal Muscle Insulin Resistance Is the Primary Defect in Type 2 Diabetes. *Diabetes care*. 32(suppl_2):S157–S163.

Deng, M., Deng, L. & Xue, Y. 2012. MAP Kinase-Mediated and MLCK-Independent Phosphorylation of MLC20 in Smooth Muscle Cells. *Current Basic and Pathological Approaches to the Function of Muscle Cells and Tissues - From Molecules to Humans*.

Depre, C., Rider, M.H. & Hue, L. 1998. Mechanisms of control of heart glycolysis. *Eur J Biochem*. 258(2):277–290.

Depre, C., Vanoverschelde, J.L. & Taegtmeyer, H. 1999. Glucose for the heart. *Circulation*. 99(4):578–88.

Depre, C., Vatner, S.F. & Gross, G.J. 2011. Coronary Blood Flow and Myocardial Ischemia. In 13th ed. J.W. Hurst et al. (eds.). McGraw-Hill Medical *Hurst's the heart*. 80.

Derosa, G. & Maffioli, P. 2012. α-Glucosidase inhibitors and their use in clinical practice. *Archives of medical science : AMS*. 8(5):899–906.

Dhanasekaran, D.N. & Reddy, P. 2011. JNK Signaling in Apoptosis. 27(48):6245–6251.

Diabetes Prevention Program Research Group. 2012. Long-Term Safety, Tolerability, and Weight Loss Associated With Metformin in the Diabetes Prevention Program Outcomes Study. *Diabetes Care*. 35(4):731–737.

Dicker, D. 2011. DPP-4 Inhibitors: Impact on glycemic control and cardiovascular risk factors. *Diabetes care*. 34(SUPPL. 2):S276–S278.

Dinauer, M.C., Pierce, E.A., Bruns, G.A., Curnutte, J.T. & Orkin, S.H. 1990. Human neutrophil cytochrome b light chain (p22-phox). Gene structure, chromosomal location, and mutations in cytochrome-negative autosomal recessive chronic granulomatous disease. *Journal of Clinical Investigation*. 86(5):1729–1737.

Ding, W.-X. & Yin, X.-M. 2012. Mitophagy: mechanisms, pathophysiological roles, and analysis. *Biological Chemistry*. 393(7):547–64.

Ding, L., Song, A., Dai, M., Xu, M., Sun, W., Xu, B., Sun, J., Wang, T., et al. 2015. Serum lipoprotein (a) concentrations are inversely associated with T2D, prediabetes, and insulin resistance in a middle-aged and elderly Chinese population. *J.Lipid Res.* 56(4):920–926.

Dludla, P. V., Muller, C.J.F., Louw, J., Joubert, E., Salie, R., Opoku, A.R. & Johnson, R. 2014. The cardioprotective effect of an aqueous extract of fermented rooibos (Aspalathus linearis) on cultured cardiomyocytes derived from diabetic rats. *Phytomedicine*. 21(5):595–601.

Dolman, N.J., Chambers, K.M., Mandavilli, B., Batchelor, R.H. & Janes, M.S. 2013. Tools and techniques to

measure mitophagy using fluorescence microscopy. *Autophagy*. 9(11):1653–1662.

Donner, D.G., Elliott, G.E., Beck, B.R., Bulmer, A.C. & Du Toit, E.F. 2015. Impact of Diet-Induced Obesity and Testosterone Deficiency on the Cardiovascular System: A Novel Rodent Model Representative of Males with Testosterone-Deficient Metabolic Syndrome (TDMetS). *PLOS ONE*. 10(9):e0138019.

Duthie, S.J., Jenkinson, A.M., Crozier, A., Mullen, W., Pirie, L., Kyle, J., Yap, L.S., Christen, P., et al. 2005. The effects of cranberry juice consumption on antioxidant status and biomarkers relating to heart disease and cancer in healthy human volunteers. *European journal of nutrition*. 45(2):113–122.

Eckel, R.H. 1997. Obesity and Heart Disease : A Statement for Healthcare Professionals From the Nutrition Committee, American Heart Association. *Circulation*. 96(9):3248–3250.

Eiselein, L., Schwartz, H.J. & Rutledge, J.C. 2004. The Challenge of Type 1 Diabetes Mellitus. *ILAR Journal*. 45(3):231–236.

Ekor, M. 2014. The growing use of herbal medicines: issues relating to adverse reactions and challenges in monitoring safety. *Frontiers in pharmacology*. 4:177.

Eldar-Finkelman, H. & Krebs, E.G. 1997. Phosphorylation of insulin receptor substrate 1 by glycogen synthase kinuse 3 impairs insulin action. *Proceedings of the National Academy of Sciences of the United States of America*. 94(18):9660–9664.

Eldar-Finkelman, H., Schreyer, S.A., Shinohara, M.M., LeBoeuf, R.C. & Krebs, E.G. 1999. Increased glycogen synthase kinase-3 activity in diabetes- and obesity-prone C57BL/6J mice. *Diabetes*. 48(8):1662–6.

Eltzschig, H.K. & Eckle, T. 2011. Ischemia and reperfusion—from mechanism to translation. *Nature Medicine*. 17(11):1391–1401.

Engels, M., Wang, C., Matoso, A., Maidan, E. & Wands, J. 2013. Tea not Tincture: Hepatotoxicity Associated with Rooibos Herbal Tea. *ACG case reports journal*. 1(1):58–60.

Espach, Y. 2017. An investigation into the importance of the ATM protein in the myocardial pathology associated with insulin resistance and type 2 diabetes.

Essop, M.F., Anna Chan, W.Y., Valle, A., García-Palmer, F.J. & Du Toit, E.F. 2009. Impaired contractile function and mitochondrial respiratory capacity in response to oxygen deprivation in a rat model of pre-diabetes. *Acta Physiologica*. 197(4):289–296.

Fajans, S.S., Bell, G.I. & Polonsky, K.S. 2001. Molecular mechanisms and clinical pathophysiology of maturity-onset diabetes of the young. *New England Journal of Medicine*. 345(13):971–980.

Fan, W. 2017. Effect of different substrates on functional performance and kinase activation during reperfusion after ischaemia in hearts from obese insulin resistant rats

Fan, M., Du, L., Stone, A.A., Gilbert, K.M. & Chambers, T.C. 2000. Modulation of mitogen-activated protein kinases and phosphorylation of Bcl-2 by vinblastine represent persistent forms of normal fluctuations at G2-M1. *Cancer research*. 60(22):6403–7.

Ferdinandy, P., Schulz, R. & Baxter, G.F. 2007. Interaction of Cardiovascular Risk Factors with Myocardial Ischemia/Reperfusion Injury, Preconditioning, and Postconditioning. *Pharmacological Reviews*. 59(4):418–458.

Ferreira, D., Marais, C., Steenkamp, J. & Joubert, E. 1995. *Rooibos tea as a likely health food supplement. Proceedings of Recent Development of Technologies on Fundamental Foods for Health.* Seoul, Korea.

Fillmore, N., Mori, J. & Lopaschuk, G.D. 2014. Mitochondrial fatty acid oxidation alterations in heart failure,

ischaemic heart disease and diabetic cardiomyopathy. *British journal of pharmacology*. 171(8):2080–90.

Flepisi, T.B., Lochner, A. & Huisamen, B. 2013. The Consequences of Long-Term Glycogen Synthase Kinase-3 Inhibition on Normal and Insulin Resistant Rat Hearts. *Cardiovasc Drugs Ther*. 27(5):381–392.

Folch, J., Lees, M. & Sloane Stanley, G.H. 1957. A simple method for the isolation and purification of total lipides from animal tissues. *The Journal of biological chemistry*. 226(1):497–509.

Förster, K., Paul, I., Solenkova, N., Staudt, A., Cohen, M. V., Downey, J.M., Felix, S.B. & Krieg, T. 2006. NECA at reperfusion limits infarction and inhibits formation of the mitochondrial permeability transition pore by activating p70S6 kinase. *Basic Research in Cardiology*. 101(4):319–326.

Foster, C.R., Zha, Q., Daniel, L.L., Singh, M. & Singh, K. 2012. Lack of ataxia telangiectasia mutated kinase induces structural and functional changes in the heart: role in β-adrenergic receptor-stimulated apoptosis. *Experimental physiology*. 97(4):506–15.

Frank, A., Bonney, M., Bonney, S., Weitzel, L., Koeppen, M. & Eckle, T. 2012. Myocardial ischemia reperfusion injury: from basic science to clinical bedside. *Seminars in cardiothoracic and vascular anesthesia*. 16(3):123–32.

Frederich, M. & Balschi, J.A. 2002. The relationship between AMP-activated protein kinase activity and AMP concentration in the isolated perfused rat heart. *Journal of Biological Chemistry*. 277(3):1928–1932.

Frémin, C., Saba-El-Leil, M.K., Lévesque, K., Ang, S.-L. & Meloche, S. 2015. Functional Redundancy of ERK1 and ERK2 MAP Kinases during Development. *Cell Reports*. 12(6):913–921.

Fu, Z., Gilbert, E.R. & Liu, D. 2013. Regulation of insulin synthesis and secretion and pancreatic Beta-cell dysfunction in diabetes. *Current diabetes reviews*. 9(1):25–53.

Fujio, Y., Nguyen, T., Wencker, D., Kitsis, R.N. & Walsh, K. 2000. Akt promotes survival of cardiomyocytes in vitro and protects against Ischemia-reperfusion injury in mouse heart. *Circulation*. 101(6):660–667.

Fukuda, M. 2011. TBC proteins: GAPs for mammalian small GTPase Rab? *Bioscience Reports*. 31(3):159–168.

Fukui, T., Yoshiyama, M., Hanatani, A., Omura, T., Yoshikawa, J. & Abe, Y. 2001. Expression of p22-phox and gp91-phox, Essential Components of NADPH Oxidase, Increases after Myocardial Infarction. *Biochemical and Biophysical Research Communications*. 281(5):1200–1206.

Fuster, V. 2014. Top 10 cardiovascular therapies and interventions for the next decade. *Nature Reviews Cardiology*. 11(11):671–683.

Galinanes, M. & Hearse, D.J. 1990. Assessment of ischemic injury and protective interventions: the Langendorff versus the working rat heart preparation. *The Canadian journal of cardiology*. 6(2):83–91.

Gao, F., Yue, T.-L., Shi, D.-W., Christopher, T.A., Lopez, B.L., Ohlstein, E.H., Barone, F.C. & Ma, X.L. 2002. p38 MAPK inhibition reduces myocardial reperfusion injury via inhibition of endothelial adhesion molecule expression and blockade of PMN accumulation. *Cardiovascular research*. 53(2):414–22.

GDC. 2015. Body Mass Index Calculator. *Global Diabetes Community*. [Online], Available: http://www.diabetes.co.uk/bmi.html.

George, C., Lochner, A. & Huisamen, B. 2011. The efficacy of Prosopis glandulosa as antidiabetic treatment in rat models of diabetes and insulin resistance. *Journal of Ethnopharmacology*. 137(1):298–304.

George, S., Rochford, J.J., Wolfrum, C., Gray, S.L., Schinner, S., Wilson, J.C., Soos, M.A., Murgatroyd, P.R.,

et al. 2004. A Family with Severe Insulin Resistance and Diabetes Due to a Mutation in AKT2. *Science*. 304(5675):1325–1328.

Ghaderi, S., Alidadiani, N., Dilaver, N., Heidari, H.R., Parvizi, R., Rahbarghazi, R., Soleimani-Rad, J. & Baradaran, B. 2017a. Role of glycogen synthase kinase following myocardial infarction and ischemia–reperfusion. *Apoptosis*. 22(7):887–897.

Ghaderi, S., Alidadiani, N., Dilaver, N., Heidari, H.R., Parvizi, R., Rahbarghazi, R., Soleimani-Rad, J. & Baradaran, B. 2017b. Role of glycogen synthase kinase following myocardial infarction and ischemia–reperfusion. *Apoptosis*. 22(7):887–897.

Ghasemi, A. & Jeddi, S. 2017. Anti-obesity and anti-diabetic effects of nitrate and nitrite. *Nitric Oxide*. 70:9–24.

Gnaiger, E. 2014. *Mitochondrial Pathways and Respiratory Control An Introduction to OXPHOS Analysis*. [Online], Available: http://wiki.oroboros.at/images/f/fc/Gnaiger_2014_Mitochondr_Physiol_Network_MitoPathways.pdf.

Golan, R., Shelef, I., Rudich, A., Gepner, Y., Shemesh, E., Chassidim, Y., Harman-Boehm, I., Henkin, Y., et al. 2012. Abdominal superficial subcutaneous fat: a putative distinct protective fat subdepot in type 2 diabetes. *Diabetes care*. 35(3):640–7.

Gonsolin, D., Couturier, K., Garait, B., Rondel, S., Novel-Chaté, V., Peltier, S., Faure, P., Gachon, P., et al. 2007. High dietary sucrose triggers hyperinsulinemia, increases myocardial β-oxidation, reduces glycolytic flux and delays post-ischemic contractile recovery. *Molecular and Cellular Biochemistry*. 295(1–2):217–228.

Gonzalez, E. & McGraw, T.E. 2009. Insulin-modulated Akt subcellular localization determines Akt isoform-specific signaling. *Proceedings of the National Academy of Sciences*. 106(17):7004–7009.

Goszcz, K., Deakin, S.J., Duthie, G.G., Stewart, D., Leslie, S.J. & Megson, I.L. 2015. Antioxidants in Cardiovascular Therapy: Panacea or False Hope? *Frontiers in Cardiovascular Medicine*. 2(July):1–22.

Gottlieb, R.A. & Mentzer, R.M. 2010. Autophagy During Cardiac Stress: Joys and Frustrations of Autophagy. *Annual Review of Physiology*. 72(1):45–59.

Gottlieb, R.A. & Thomas, A. 2017. Mitophagy and Mitochondrial Quality Control Mechanisms in the Heart. *Current Pathobiology Reports*. 5(2):161–169.

Gottlieb, R.A., Mentzer, R.M., Linton, P.-J. & Linton, P.-J. 2011. Impaired mitophagy at the heart of injury. *Autophagy*. 7(12):1573–4.

Gouws, P., Hartel, T. & van Wyk, R. 2014. The influence of processing on the microbial risk associated with Rooibos (Aspalathus linearis) tea. *Journal of the science of food and agriculture*. 94(15):3069–3078.

Granger, D.N. 1988. Role of xanthine oxidase and granulocytes in ischemia-reperfusion injury. *American Journal of Physiology-Heart and Circulatory Physiology*. 255(6):H1269–H1275.

Gray, D.S., Bray, G.A., Bauer, M., Kaplan, K., Gemayel, N., Wood, R., Greenway, F. & Kirk, S. 1990. Skinfold thickness measurements in obese subjects. *American Journal of Clinical Nutrition*. 51(4):571–577.

Gray, M.W., Lang, B.F., Cedergren, R., Golding, G.B., Lemieux, C., Sankoff, D., Turmel, M., Brossard, N., et al. 1998. Genome structure and gene content in protist mitochondrial DNAs. *Nucleic acids research*. 26(4):865–78.

Greenfield, J.R., Chisholm, D.J. & Endocrinology, D. of. 2004. Experimental and clinical pharmacology:

Thiazolidinediones - mechanisms of action. *Australian Prescriber*. 27(3):67–70.

Gregory, A.B., Lester, K.K., Gregory, D.M., Twells, L.K., Midodzi, W.K. & Pearce, N.J. 2017. The Relationship between Body Mass Index and the Severity of Coronary Artery Disease in Patients Referred for Coronary Angiography. *Cardiology Research and Practice*. 2017:1–10.

Grover, G.J., Atwal, K.S., Sleph, P.G., Wang, F.-L., Monshizadegan, H., Monticello, T. & Green, D.W. 2004. Excessive ATP hydrolysis in ischemic myocardium by mitochondrial F_1F_0-ATPase: effect of selective pharmacological inhibition of mitochondrial ATPase hydrolase activity. *American Journal of Physiology-Heart and Circulatory Physiology*. 287(4):H1747–H1755.

Grundy, S.M. 2004. Definition of Metabolic Syndrome: Report of the National Heart, Lung, and Blood Institute/American Heart Association Conference on Scientific Issues Related to Definition. *Circulation*. 109(3):433–438.

Grundy, S.M. 2012. Pre-Diabetes, Metabolic Syndrome, and Cardiovascular Risk. *Journal of the American College of Cardiology*. 59(7):635–643.

Gupte, A.A., Minze, L.J., Reyes, M., Ren, Y., Wang, X., Brunner, G., Ghosn, M., Cordero-Reyes, A.M., et al. 2013. High-Fat Feeding-Induced Hyperinsulinemia Increases Cardiac Glucose Uptake and Mitochondrial Function Despite Peripheral Insulin Resistance. *Endocrinology*. 154(8):2650–2662.

Gustafsson, A.B. & Gottlieb, R.A. 2009. Autophagy in ischemic heart disease. *Circulation research*. 104(2):150–8.

Hagan, S. & Niswender, K.D. 2012. Neuroendocrine regulation of food intake. *Pediatric Blood & Cancer*. 58(1):149–153.

Halestrap, A.P. 2010. A pore way to die: the role of mitochondria in reperfusion injury and cardioprotection. *Biochemical Society Transactions*. 38(4):841–860.

Halestrap, A.P. & Wilson, M.C. 2012. The monocarboxylate transporter family-Role and regulation. *IUBMB Life*. 64(2):109–119.

Halse, R., Fryer, L.G.D., McCormack, J.G., Carling, D. & Yeaman, S.J. 2003. Regulation of glycogen synthase by glucose and glycogen: a possible role for AMP-activated protein kinase. *Diabetes*. 52(1):9–15.

Haq, S., Choukroun, G., Lim, H., Tymitz, K.M., del Monte, F., Gwathmey, J., Grazette, L., Michael, A., et al. 2001. Differential activation of signal transduction pathways in human hearts with hypertrophy versus advanced heart failure. *Circulation*. 103(5):670–7.

Hardie, D.G. & Carling, D. 1997. The AMP-Activated Protein Kinase. Fuel Gauge of the Mammalian Cell? *Eur J Biochem*. 246(2):259–273.

Hardie, D.G., Hawley, S.A. & Scott, J.W. 2006. AMP-activated protein kinase - Development of the energy sensor concept. *Journal of Physiology*. 574(1):7–15.

Harding, S.J., Browne, G.J., Miller, B.W., Prigent, S.A. & Dickens, M. 2010. Activation of ASK1, downstream MAPKK and MAPK isoforms during cardiac ischaemia. *Biochimica et Biophysica Acta (BBA) - Molecular Basis of Disease*. 1802(9):733–740.

Hasima, N. & Ozpolat, B. 2014. Regulation of autophagy by polyphenolic compounds as a potential therapeutic strategy for cancer. *Cell death & disease*. 5(11):e1509.

Hausenloy, D. & Yellon, D.M. 2004. New directions for protecting the heart against ischaemia–reperfusion injury: targeting the Reperfusion Injury Salvage Kinase (RISK)-pathway. *Cardiovascular Research*.

61(3):448–460.

Hausenloy, D.J. & Yellon, D.M. 2013. Myocardial ischemia-reperfusion injury: a neglected therapeutic target. *Journal of Clinical Investigation*. 123(1):92–100.

Hausenloy, D., Duchen, M.R. & Yellon, D.M. 2003. Inhibiting mitochondrial permeability transition pore opening at reperfusion protects against ischaemia–reperfusion injury. *Cardiovascular Research*. 60(3):617–625.

Hausenloy, D.J., Tsang, A., Mocanu, M.M. & Yellon, D.M. 2005. Ischemic preconditioning protects by activating prosurvival kinases at reperfusion. *American Journal of Physiology-Heart and Circulatory Physiology*. 288(2):H971–H976.

Hawley, S.A., Gadalla, A.E., Olsen, G.S. & Hardie, D.G. 2002. The antidiabetic drug metformin activates the AMP-activated protein kinase cascade via an adenine nucleotide-independent mechanism. *Diabetes*. 51(8):2420–5.

Heise, T., Zijlstra, E., Nosek, L., Heckermann, S., Plum-Mörschel, L. & Forst, T. 2016. Euglycaemic glucose clamp: what it can and cannot do, and how to do it.

Hesseling, P.B., Klopper, J.F. & Van Heerden, P.D.R. 1979. Die effek van rooibostee op ysterabsorpsie. *South African Medical Journal*. 55:631–632.

Heusch, G. & Gersh, B.J. 2016. The pathophysiology of acute myocardial infarction and strategies of protection beyond reperfusion: a continual challenge. *European Heart Journal*. 38(11):ehw224.

Heusch, G., Musiolik, J., Kottenberg, E., Peters, J., Jakob, H. & Thielmann, M. 2012. STAT5 activation and cardioprotection by remote ischemic preconditioning in humans: short communication. *Circulation research*. 110(1):111–5.

Heymsfield, S.B., Gallagher, D., Kotler, D.P., Wang, Z., Allison, D.B. & Heshka, S. 2002. Body-size dependence of resting energy expenditure can be attributed to nonenergetic homogeneity of fat-free mass. *American journal of physiology. Endocrinology and metabolism*. 282(1):E132-8.

Hillis, W.E. & Inoue, T. 1967. The polyphenols of Nothofagus species II. The heartwood of Nothofagus fusca. *Phytochemistry*. 6:59–67.

Himsworth, H.P. 1936. Diabetes Mellitus. Its differentiation into insulin-sensitive and insulin-insensitive types. *The Lancet*. 227(5864):127–130.

Hirasawa, K., Sugimoto, T., Nohara, T., Ohya, N., Inasaka, T., Kaseno, K. & Takeuchi, J. 1974. Influence of changes in heart rate, aortic pressure and flow rate upon experimental coronary insufficiency. *Cardiology*. 59(4):213–21.

Hon, G., Hassan, M., van Rensburg, S.J., Abel, S., Marais, D.W., van Jaarsveld, P., Smuts, C., Henning, F., et al. 2009. Immune cell membrane fatty acids and inflammatory marker, C-reactive protein, in patients with multiple sclerosis. *The British journal of nutrition*. 102(9):1334–40.

Hou, W.-L., Yin, J., Alimujiang, M., Yu, X.-Y., Ai, L.-G., Bao, Y.-Q., Liu, F. & Jia, W.-P. 2018. Inhibition of mitochondrial complex I improves glucose metabolism independently of AMPK activation. *Journal of cellular and molecular medicine*. 22(2):1316–1328.

How, O.-J., Aasum, E., Severson, D.L., Chan, W.Y.A., Essop, M.F. & Larsen, T.S. 2006. Increased myocardial oxygen consumption reduces cardiac efficiency in diabetic mice. *Diabetes*. 55(2):466–473.

Hu, F.B. 2003. Plant-based foods and prevention of cardiovascular disease: an overview. *Am.J.Clin.Nutr*. 78:544S–551S.

Hu, F.B. 2008. *Obesity epidemiology*. Oxford University Press.

Huang, C.F., Gan, X.W., Bai, H.Y., Ma, L. & Hu, L.H. 2008. Schoepfin A, B, C: three new chalcone C-glycosides from Schoepfia chinensis. *Natural Product Research*. 22:623–627.

Huang, E.S., Basu, A., O'Grady, M. & Capretta, J.C. 2009. Projecting the Future Diabetes Population Size and Related Costs for the U.S. *Diabetes care*. 32(12):2225–2229.

Hue, L. & Rider, M.H. 2007. The AMP-activated protein kinase: more than an energy sensor. *Essays in biochemistry*. 43:121–37.

Huisamen, B. & Flepisi, B. 2014. P757 * Chronic GSK-3 inhibition may be good for diabetes, but is bad for the heart. *Cardiovascular research*. 103(suppl 1):S138–S139.

Huisamen, B. & Lochner, A. 2005. Exercise modulates myocardial protein kinase B/Akt in Zucker obese rats. *Heart (British Cardiac Society)*. 91(2):227–8.

Huisamen, B. & Lochner, A. 2010. GSK-3 protein and the heart: friend or foe? *SAHeart*. 7:48–57.

Huisamen, B., Genis, A., Marais, E. & Lochner, A. 2011. Pre-treatment with a DPP-4 Inhibitor is Infarct Sparing in Hearts from Obese, Pre-diabetic Rats. *Cardiovasc Drugs Ther*. 25(1):13–20.

Huisamen, B., Dietrich, D., Bezuidenhout, N., Lopes, J., Flepisi, B., Blackhurst, D. & Lochner, A. 2012. Early cardiovascular changes occurring in diet-induced, obese insulin-resistant rats. *Molecular and cellular biochemistry*. 368(1–2):37–45.

Huisamen, B., George, C., Dietrich, D. & Genade, S. 2013. Cardioprotective and anti-hypertensive effects of Prosopis glandulosa in rat models of pre-diabetes : cardiovascular topics. *Cardiovascular Journal Of Africa*. 24(2):10–16.

Hussain, T., Tan, B., Yin, Y., Blachier, F., Tossou, M.C.B. & Rahu, N. 2016. Oxidative Stress and Inflammation: What Polyphenols Can Do for Us? *Oxidative medicine and cellular longevity*. 2016:7432797.

Iliadis, F., Kadoglou, N. & Didangelos, T. 2011. Insulin and the heart. *Diabetes Research and Clinical Practice*. 93(SUPPL. 1):S86–S91.

International Diabetes Foundation. 2018. [Online], Available: http://www.diabetesatlas.org/ [2018, October 08].

Ip, Y.T. & Davis, R.J. 1998. Signal transduction by the c-Jun N-terminal kinase (JNK) - From inflammation to development. *Current Opinion in Cell Biology*. 10(2):205–219.

Ishikura, S., Bilan, P.J. & Klip, A. 2007. Rabs 8A and 14 are targets of the insulin-regulated Rab-GAP AS160 regulating GLUT4 traffic in muscle cells. *Biochemical and Biophysical Research Communications*. 353(4):1074–1079.

Jackson, S.J., Andrews, N., Ball, D., Bellantuono, I., Gray, J., Hachoumi, L., Holmes, A., Latcham, J., et al. 2017. Does age matter? The impact of rodent age on study outcomes. *Laboratory animals*. 51(2):160–169.

Jang, S. & Javadov, S. 2014. Inhibition of JNK Aggravates the Recovery of Rat Hearts after Global Ischemia: The Role of Mitochondrial JNK. *PLoS ONE*. 9(11):e113526.

Janssen, X., Basterfield, L., Parkinson, K.N., Pearce, M., Reilly, J.K., Adamson, A.J. & Reilly, J.J. 2015. Determinants of changes in sedentary time and breaks in sedentary time among 9 and 12 year old children. *Preventive Medicine Reports*. 2:880–885.

Javadov, S., Jang, S., Parodi-rullan, R., Khuchua, Z., Andrey, V., Rico, P. & Medical, I. 2018. *HHS Public*

Access. Vol. 74.

Jennings, J.H. & Lesser, M. 2012. Weight Loss and Calorie Restriction at 50% Fasting Rate. *Pakistan J.of Nutrition*. 11(3):282–287.

Jennings, R.B. & Reimer, K. a. 1981. Lethal myocardial ischemic injury. *The American journal of pathology*. 102(2):241–255.

Jeon, J.Y., Ko, S.-H., Kwon, H.-S., Kim, N.H., Kim, J.H., Kim, C.S., Song, K.-H., Won, J.C., et al. 2013. Prevalence of Diabetes and Prediabetes according to Fasting Plasma Glucose and HbA1c. *Diabetes & metabolism journal*. 37(5):349–57.

Ji, L., Fu, F., Zhang, L., Liu, W., Cai, X., Zhang, L., Zheng, Q., Zhang, H., et al. 2010. Insulin attenuates myocardial ischemia/reperfusion injury via reducing oxidative/nitrative stress. *American Journal of Physiology-Endocrinology and Metabolism*. 298(4):E871–E880.

Jiang, M., Liu, K., Luo, J. & Dong, Z. 2010. Autophagy is a renoprotective mechanism during in vitro hypoxia and in vivo ischemia-reperfusion injury. *The American journal of pathology*. 176(3):1181–92.

Jing, M., Cheruvu, V.K. & Ismail-Beigi, F. 2008. Stimulation of glucose transport in response to activation of distinct AMPK signaling pathways. *American Journal of Physiology-Cell Physiology*. 295(5):C1071–C1082.

Jo, J., Gavrilova, O., Pack, S., Jou, W., Mullen, S., Sumner, A.E., Cushman, S.W. & Periwal, V. 2009. Hypertrophy and/or Hyperplasia: Dynamics of Adipose Tissue Growth. *PLoS Computational Biology*. 5(3):e1000324.

Johnson, R., Dludla, P. V, Muller, C.J.F., Huisamen, B., Faadiel Essop, M. & Louw, J. 2017. molecules The Transcription Profile Unveils the Cardio-Protective Effect of Aspalathin against Lipid Toxicity in an In Vitro H9c2 Model. *Molecules*. 22(219).

Johnson, R., Beer, D. de, Dludla, P., Ferreira, D., Muller, C. & Joubert, E. 2018. Aspalathin from Rooibos (Aspalathus linearis): A Bioactive C-glucosyl Dihydrochalcone with Potential to Target the Metabolic Syndrome. *Planta Medica*. 84(09/10):568–583.

Jonassen, A.K., Sack, M.N., Mjøs, O.D. & Yellon, D.M. 2001. Myocardial protection by insulin at reperfusion requires early administration and is mediated via Akt and p70s6 kinase cell-survival signaling. *Circulation research*. 89(12):1191–8.

Jose, A.D. & Collison, D. 1970. The normal range and determinants of the intrinsic heart rate in man. *Cardiovascular research*. 4(2):160–167.

Joubert, E. 1996. HPLC quantification of the dihydrochalcones, aspalathin and nothofagin in rooibos tea (Aspalathus linearis) as affected by processing. *Food Chemistry*. 55(4):403–411.

Joubert, E. & de Beer, D. 2012a. Phenolic content and antioxidant activity of rooibos food ingredient extracts. *Journal of Food Composition and Analysis*. 27(1):45–51.

Joubert, E. & de Beer, D. 2012b. Phenolic content and antioxidant activity of rooibos food ingredient extracts. *Journal of Food Composition and Analysis*. 27(1):45–51.

Joubert, E. & De Beer, D. 2011. Rooibos (Aspalathus linearis) beyond the farm gate : From herbal tea to potential phytopharmaceutical. *South African Journal of Botany*. 77(4):869–886.

Joubert, E. & Schulz, H. 2006. Production and quality aspects of rooibos tea and related products. A review. *Journal of Applied Botany and Food Quality*. 80(2):138–144.

Joubert, E., Gelderblom, W.C.A. & De Beer, D. 2009. Phenolic contribution of South African herbal teas to a

healthy diet. *Natural Product Communications*. 4(5):701–718.

Joubert, E., Viljoen, M., De Beer, D., Malherbe, C.J., Brand, D.J. & Manley, M. 2010. Use of green rooibos (Aspalathus linearis) extract and water-soluble nanomicelles of green rooibos extract encapsulated with ascorbic acid for enhanced aspalathin content in ready-to-drink iced teas. *Journal of Agricultural and Food Chemistry*. 58(20):10965–10971.

Kadowaki, M. & Karim, M.R. 2009. Chapter 13 Cytosolic LC3 Ratio as a Quantitative Index of Macroautophagy. In Vol. 452 *Methods in enzymology*. 199–213.

Kahn, C.R., Chen, L. & Cohen, S.E. 2000. Unraveling the mechanism of action of thiazolidinediones. *Journal of Clinical Investigation*. 106(11):1305–1307.

Kalogeris, T., Baines, C.P., Krenz, M. & Korthuis, R.J. 2012. *Cell Biology of Ischemia/Reperfusion Injury*. Vol. 298.

Kalogeris, T., P.Baines, C., Krenz, M. & J.Korthuis, R. 2017. Ischemia/Reperfusion. *Comprehensive Physiology*. 7(1):113–170.

Kamakura, R., Son, M.J., de Beer, D., Joubert, E., Miura, Y. & Yagasaki, K. 2015. Antidiabetic effect of green rooibos (Aspalathus linearis) extract in cultured cells and type 2 diabetic model KK-Aymice. *Cytotechnology*. 67(4):699–710.

Kamau, F.M. 2018. Contribution of highly active anti-retroviral therapy to the development of non-alcoholic fatty liver disease with concomitant cardiovascular dysfunction in an obese rat model. [Online], Available: http://scholar.sun.ac.za/handle/10019.1/103335 [2018, October 18].

Kang, J. 2012. *Nutrition and metabolism in sports, exercise and health*. Routledge.

Kang, Y.E., Kim, J.M., Joung, K.H., Lee, J.H., You, B.R., Choi, M.J., Ryu, M.J., Ko, Y.B., et al. 2016. The Roles of Adipokines, Proinflammatory Cytokines, and Adipose Tissue Macrophages in Obesity-Associated Insulin Resistance in Modest Obesity and Early Metabolic Dysfunction. *PloS one*. 11(4):e0154003.

Kannel, W.B. & McGee, D.L. 1979. Diabetes and Glucose Tolerance as Risk Factors for Cardiovascular Disease: The Framingham Study. *Diabetes care*. 2(2):120–126.

Kannengiesser, G.J., Opie, L.H. & van der Werff, T.J. 1979. Impaired cardiac work and oxygen uptake after reperfusion of regionally ischaemic myocardium. *Journal of molecular and cellular cardiology*. 11(2):197–207. [Online], Available: http://www.ncbi.nlm.nih.gov/pubmed/423263 [2018, October 09].

Kanzaki, Y., Terasaki, F., Okabe, M., Otsuka, K., Katashima, T., Fujita, S., Ito, T. & Kitaura, Y. 2010. Giant mitochondria in the myocardium of a patient with mitochondrial cardiomyopathy: Transmission and 3-dimensional scanning electron microscopy. *Circulation*. 121(6):831–832.

Karch, J., Kanisicak, O., Brody, M.J., Sargent, M.A., Michael, D.M. & Molkentin, J.D. 2015. Necroptosis Interfaces with MOMP and the MPTP in Mediating Cell Death. *PloS one*. 10(6):e0130520.

Karlsson, H.K.R., Zierath, J.R., Kane, S., Krook, A., Lienhard, G.E. & Wallberg-Henriksson, H. 2005. Insulin-stimulated phosphorylation of the Akt substrate AS160 is impaired in skeletal muscle of type 2 diabetic subjects. *Diabetes*. 54(6):1692–7.

Kaur, J. 2014. A comprehensive review on metabolic syndrome. *Cardiology research and practice*. 2014:943162.

Kawano, A., Nakamura, H., Hata, S., Minakawa, M., Miura, Y. & Yagasaki, K. 2009. Hypoglycemic effect of aspalathin, a rooibos tea component from Aspalathus linearis, in type 2 diabetic model db/db mice.

Phytomedicine. 16(5):437–443.

Kershaw, E.E. & Flier, J.S. 2004. Adipose tissue as an endocrine organ. *Journal of Clinical Endocrinology and Metabolism*. 89(6):2548–2556.

Khan, A.U.H., Rathore, M.G., Allende-Vega, N., Vo, D.-N., Belkhala, S., Orecchioni, S., Talarico, G., Bertolini, F., et al. 2016. Human Leukemic Cells performing Oxidative Phosphorylation (OXPHOS) Generate an Antioxidant Response Independently of Reactive Oxygen species (ROS) Production. *EBioMedicine*. 3:43–53.

King, L.A., Toledo, A.H., Rivera-Chavez, F.A. & Toledo-Pereyra, L.H. 2009. Role of p38 and JNK in liver ischemia and reperfusion. *Journal of Hepato-Biliary-Pancreatic Surgery*. 16(6):763–770.

Kjems, L.L., Holst, J.J., Volund, A. & Madsbad, S. 2003. The Influence of GLP-1 on Glucose-Stimulated Insulin Secretion: Effects on -Cell Sensitivity in Type 2 and Nondiabetic Subjects. *Diabetes*. 52(2):380–386.

Klappan, A.K., Hones, S., Mylonas, I. & Brüning, A. 2012. Proteasome inhibition by quercetin triggers macroautophagy and blocks mTOR activity. *Histochemistry and Cell Biology*. 137(1):25–36.

Kleindienst, A., Battault, S., Belaidi, E., Tanguy, S., Rosselin, M., Boulghobra, D., Meyer, G., Gayrard, S., et al. 2016. Exercise does not activate the β3 adrenergic receptor–eNOS pathway, but reduces inducible NOS expression to protect the heart of obese diabetic mice. *Basic Research in Cardiology*. 111(4):40.

Klok, M.D., Jakobsdottir, S. & Drent, M.L. 2007. The role of leptin and ghrelin in the regulation of food intake and body weight in humans: a review. *Obesity Reviews*. 8(1):21–34.

Kloner, R.A. & Jennings, R.B. 2001. Consequences of brief ischemia: stunning, preconditioning, and their clinical implications: part 2. *Circulation*. 104(25):3158–67.

Knekt, P., Kumpulainen, J., JÃ¤rvinen, R., Rissanen, H., HeliÃ¶vaara, M., Reunanen, A., Hakulinen, T. & Aromaa, A. 2002. Flavonoid intake and risk of chronic diseases. *American Journal of Clinical Nutrition*. 76(3):560–568.

Koch, I.S., Muller, N., de Beer, D., Næs, T. & Joubert, E. 2013. Impact of steam pasteurization on the sensory profile and phenolic composition of rooibos (Aspalathus linearis) herbal tea infusions. *Food Research International*. 53(2):704–712.

Koeppen, B.H. & Roux, D.G. 1965. Aspalathin : a novel C-glycosylflavonoid from aspalathus linearis. *Tetrahedron Letters*. 6(39):3497–3503.

Koeppen, B.H. & Roux, D.G. 1966. C -glycosylflavonoids. The chemistry of aspalathin. *Biochem.J.* 99(3):604–609.

Koeppen, B.H., Smit, C.J.B. & Roux, D.G. 1962. he flavone C-glycosides and the flavonol O-glycosides of Aspalathus acuminatus (Rooibos tea). *Biochemical Journal*. 83:507–511.

Konhilas, J.P., Widegren, U., Allen, D.L., Paul, A.C., Cleary, A. & Leinwand, L.A. 2005. Loaded wheel running and muscle adaptation in the mouse. *American Journal of Physiology - Heart and Circulatory Physiology*. 289(1 58-1):H455–H465.

Konstantinidis, K., Whelan, R.S. & Kitsis, R.N. 2012. Mechanisms of cell death in heart disease. *Arteriosclerosis, thrombosis, and vascular biology*. 32(7):1552–62.

Korb, A., Tohidast-Akrad, M., Cetin, E., Axmann, R., Smolen, J. & Schett, G. 2006. Differential tissue expression and activation of p38 MAPK α, β, γ, and δ isoforms in rheumatoid arthritis. *Arthritis and Rheumatism*. 54(9):2745–2756.

Kotecki, J.E. 2011. *Physical Activity & Health: An Interactive Approach: An Interactive Approach*. Jones & Bartlett Publishers.

Koutsari, C. & Jensen, M.D. 2006. Free fatty acid metabolism in human obesity. *Journal of Lipid Research*. 47(8):1643–1650.

Krafczyk, N. & Glomb, M.A. 2008. Characterization of phenolic compounds in rooibos tea. *Journal of Agricultural and Food Chemistry*. 56(9):3368–3376.

Kreuz, S., Joubert, E., Waldmann, K.-H. & Ternes, W. 2008. Aspalathin, a flavonoid in Aspalathus linearis (rooibos), is absorbed by pig intestine as a C-glycoside. *Nutrition Research*. 28(10):690–701.

von Kriegsheim, A., Baiocchi, D., Birtwistle, M., Sumpton, D., Bienvenut, W., Morrice, N., Yamada, K., Lamond, A., et al. 2009. Cell fate decisions are specified by the dynamic ERK interactome. *Nature Cell Biology*. 11(12):1458–1464.

Ku, S.-K., Kwak, S., Kim, Y. & Bae, J.-S. 2015. Aspalathin and Nothofagin from Rooibos (Aspalathus linearis) Inhibits High Glucose-Induced Inflammation In Vitro and In Vivo. *Inflammation*. 38(1):445–455.

Kubli, D.A., Cortez, M.Q., Moyzis, A.G., Najor, R.H., Lee, Y. & Gustafsson, Å.B. 2015. PINK1 Is Dispensable for Mitochondrial Recruitment of Parkin and Activation of Mitophagy in Cardiac Myocytes. *PloS one*. 10(6):e0130707.

Kudo, N., Barr, A.J., Barr, R.L., Desai, S. & Lopaschuk, G.D. 1995. High rates of fatty acid oxidation during reperfusion of ischemic hearts are associated with a decrease in malonyl-CoA levels due to an increase in 5'-AMP-activated protein kinase inhibition of acetyl-CoA carboxylase. *The Journal of biological chemistry*. 270(29):17513–20.

Kühlbrandt, W. 2015. Structure and function of mitochondrial membrane protein complexes. *BMC Biology*. 13(1):1–11.

Kumar, D., Menon, V., Ford, W.R., Clanachan, A.S. & Jugdutt, B.I. 2004. Effect of angiotensin II type 2 receptor blockade on mitogen activated protein kinases during myocardial ischemia-reperfusion. *Molecular and cellular biochemistry*. 258(1–2):211–8.

Kumar, N.T., Liestøl, K., Løberg, E.M., Reims, H.M. & Maehlen, J. 2014. Postmortem heart weight: relation to body size and effects of cardiovascular disease and cancer.

Kurian, G.A., Rajagopal, R., Vedantham, S. & Rajesh, M. 2016. The Role of Oxidative Stress in Myocardial Ischemia and Reperfusion Injury and Remodeling: Revisited. *Oxidative medicine and cellular longevity*. 2016:1656450.

Kurien, V.A. & Oliver, M.F. 1971. Free fatty acids during acute myocardial infarction. *Progress in Cardiovascular Diseases*. 13(4):361–373.

Kusuoka, H. & Marban, E. 1994. Mechanism of the diastolic dysfunction induced by glycolytic inhibition. Does adenosine triphosphate derived from glycolysis play a favored role in cellular Ca2+ homeostasis in ferret myocardium? *Journal of Clinical Investigation*. 93(3):1216–1223.

Kwan, A.C., May, H.T., Cater, G., Sibley, C.T., Rosen, B.D., Lima, J.A.C., Rodriguez, K., Lappe, D.L., et al. 2014. Coronary Artery Plaque Volume and Obesity in Patients with Diabetes: The Factor-64 Study. *Radiology*. 272(3):690–699.

Lackner, L.L. 2014. Shaping the dynamic mitochondrial network. *BMC Biology*. 12(1):35.

Lahlou, M. 2013. The Success of Natural Products in Drug Discovery. *Pharmacology & Pharmacy*. 04(03):17–31.

Lambeth, D.O. 2006. Reconsideration of the significance of substrate-level phosphorylation in the citric acid cycle. *Biochemistry and Molecular Biology Education*. 34(1):21–29.

Langley-Evans, S.C. & McMullen, S. 2010. Developmental Origins of Adult Disease. *Medical Principles and Practice*. 19(2):87–98.

Lanza, I.R. & Nair, K.S. 2009. Functional Assessment of Isolated Mitochondria In Vitro. *Methods*. 6879(09):1–19.

Laue, E., Gröll, S., Breiter, T. & Engelhardt, U.H. 2009. Bioverfügbarkeit von Flavonoiden aus grünem Rooibos. *Lebensmittelchemi*. 64:259.

Laughlin, M.R. & Taylor, J. 1994. Non-glucose substrates increase glycogen synthesis in vivo in dog heart. *Am J Physiol*. 267:H219–H223.

LeBrasseur, N.K., Kelly, M., Tsao, T.-S., Farmer, S.R., Saha, A.K., Ruderman, N.B. & Tomas, E. 2006. Thiazolidinediones can rapidly activate AMP-activated protein kinase in mammalian tissues. *American Journal of Physiology-Endocrinology and Metabolism*. 291(1):E175–E181.

Lecour, S. 2009. Activation of the protective Survivor Activating Factor Enhancement (SAFE) pathway against reperfusion injury: Does it go beyond the RISK pathway? *Journal of Molecular and Cellular Cardiology*. 47(1):32–40.

Lecour, S., Suleman, N., Deuchar, G.A., Somers, S., Lacerda, L., Huisamen, B. & Opie, L.H. 2005. Pharmacological Preconditioning With Tumor Necrosis Factor- Activates Signal Transducer and Activator of Transcription-3 at Reperfusion Without Involving Classic Prosurvival Kinases (Akt and Extracellular Signal-Regulated Kinase). *Circulation*. 112(25):3911–3918.

Ledwig, D., Müller, H., Bischoff, H. & Eckel, J. 2002. Early acarbose treatment ameliorates resistance of insulin-regulated GLUT4 trafficking in obese Zucker rats. *European journal of pharmacology*. 445(1–2):141–8.

Lee, J.-H. & Paull, T.T. 2007. Activation and regulation of ATM kinase activity in response to DNA double-strand breaks. *Oncogene*. 26(56):7741–7748.

Leibiger, I.B., Leibiger, B. & Berggren, P.-O. 2008. Insulin signaling in the pancreatic beta-cell. *Annu Rev Nutr*. 2008;28:233-51.

Leichman, J.G., Aguilar, D., King, T.M., Vlada, A., Reyes, M. & Taegtmeyer, H. 2006. Association of plasma free fatty acids and left ventricular diastolic function in patients with clinically severe obesity. *American Journal of Clinical Nutrition*. 84(2):336–341.

Lenormand, P., Sardet, C., Pagès, G., L'Allemain, G., Brunet, A. & Pouysségur, J. 1993. Growth factors induce nuclear translocation of MAP kinases (p42mapk and p44mapk) but not of their activator MAP kinase kinase (p45mapkk) in fibroblasts. *The Journal of cell biology*. 122(5):1079–88.

Lesnefsky, E.J., Moghaddas, S., Tandler, B., Kerner, J. & Hoppel, C.L. 2001. Mitochondrial Dysfunction in Cardiac Disease: Ischemia–Reperfusion, Aging, and Heart Failure. *Journal of Molecular and Cellular Cardiology*. 33(6):1065–1089.

Levine, R. & Sobel, G.W. 1957. The mechanism of action of the sulfonylureas in diabetes mellitus. *Diabetes*. 6(3):263–9.

Levy, J.C., Matthews, D.R. & Hermans, M.P. 1998. Correct Homeostasis Model Assessment (HOMA) Evaluation Uses the Computer Program. *Diabetes care*. 21(12):2191–2192.

Li, J., Zhong, L., Wang, F. & Zhu, H. 2017. Dissecting the role of AMP-activated protein kinase in human

diseases. *Acta pharmaceutica Sinica. B*. 7(3):249–259.

Li, R., Luo, X., Zhu, Y., Zhao, L., Li, L., Peng, Q., Ma, M. & Gao, Y. 2017. ATM signals to AMPK to promote autophagy and positively regulate DNA damage in response to cadmium-induced ROS in mouse spermatocytes. *Environmental Pollution*. 231(Pt 2):1560–1568.

Li, S., Xiao, J., Ji, L., Weng, J., Jia, W., Lu, J., Zhou, Z., Guo, X., et al. 2014. BMI and waist circumference are associated with impaired glucose metabolism and type 2 diabetes in normal weight Chinese adults. *Journal of Diabetes and its Complications*. 28(4):470–476.

Libman, I.M., Barinas-Mitchell, E., Bartucci, A., Chaves-Gnecco, D., Robertson, R. & Arslanian, S. 2010. Fasting and 2-hour plasma glucose and insulin: relationship with risk factors for cardiovascular disease in overweight nondiabetic children. *Diabetes care*. 33(12):2674–6.

Liemburg-Apers, D.C., Willems, P.H.G.M., Koopman, W.J.H. & Grefte, S. 2015. Interactions between mitochondrial reactive oxygen species and cellular glucose metabolism. *Archives of toxicology*. 89(8):1209–26.

Liochev, S.I. 2013. Reactive oxygen species and the free radical theory of aging. *Free Radical Biology and Medicine*. 60:1–4.

Lips, D.J., Bueno, O.F., Wilkins, B.J., Purcell, N.H., Kaiser, R.A., Lorenz, J.N., Voisin, L., Saba-El-Leil, M.K., et al. 2004. MEK1-ERK2 Signaling Pathway Protects Myocardium From Ischemic Injury In Vivo. *Circulation*. 109(16):1938–1941.

Di Lisa, F., Canton, M., Menabò, R., Dodoni, G. & Bernardi, P. 2003. Mitochondria and reperfusion injury. The role of permeability transition. *Basic research in cardiology*. 98(4):235–41.

Di Lisa, F., Kaludercic, N., Carpi, A., Menabò, R. & Giorgio, M. 2009. Mitochondria and vascular pathology. *Pharmacological reports : PR*. 61(1):123–30.

Liu, Z. & Cao, W. 2009. p38 Mitogen-Activated Protein Kinase: A Critical Node Linking Insulin Resistance and Cardiovascular Diseases in Type 2 Diabetes Mellitus. *Endocr Metab Immune Disord Drug Targets*. 2009 Mar;9(1):38-46.

Liu, J., Minemoto, Y. & Lin, A. 2004. c-Jun N-terminal protein kinase 1 (JNK1), but not JNK2, is essential for tumor necrosis factor alpha-induced c-Jun kinase activation and apoptosis. *Molecular and cellular biology*. 24(24):10844–56.

Liu, J., Wang, P., Zou, L., Qu, J., Litovsky, S., Umeda, P., Zhou, L., Chatham, J., et al. 2014. High-fat, low-carbohydrate diet promotes arrhythmic death and increases myocardial ischemia-reperfusion injury in rats. *AJP: Heart and Circulatory Physiology*. 307(4):H598–H608.

Liu, J., Wang, P., Douglas, S.L., Tate, J.M., Sham, S. & Lloyd, S.G. 2016. Impact of high-fat, low-carbohydrate diet on myocardial substrate oxidation, insulin sensitivity, and cardiac function after ischemia-reperfusion. *American Journal of Physiology - Heart and Circulatory Physiology*. 311(1):H1–H10.

Lochner, A., Genade, S., Hattingh, S., Marais, E., Huisamen, B. & Moolman, J.A. 2003. Comparison between ischaemic and anisomycin-induced preconditioning: role of p38 MAPK. *Cardiovascular drugs and therapy*. 17(3):217–30.

Lodish, H.F. 2000. *Molecular cell biology*. W.H. Freeman.

Lopaschuk, G., Folmes, C., Jaswal, J., Stanley, W. & Ussher, J.R. 2010. Myocardial fatty acid metabolism in health and disease. *Physiological Reviews*. 90(1):207–258.

Lopaschuk, G.D., Ussher, J.R., Folmes, C.D.L., Jaswal, J.S. & Stanley, W.C. 2010. Myocardial Fatty Acid Metabolism in Health and Disease. *Physiological Reviews*. 90(1):207–258.

Losada-Barreiro, S. & Bravo-Díaz, C. 2017. Free radicals and polyphenols: The redox chemistry of neurodegenerative diseases. *European Journal of Medicinal Chemistry*. 133:379–402.

Lotito, S. & Frei, B. 2006. Consumption of flavonoid-rich foods and increased plasma antioxidant capacity in humans: Cause, consequence, or epiphenomenon? *Free Radical Biology and Medicine*. 41(12):1727–1746.

Lu, K., Cho, C.-L., Liang, C.-L., Chen, S.-D., Liliang, P.-C., Wang, S.-Y. & Chen, H.-J. 2007. Inhibition of the MEK/ERK pathway reduces microglial activation and interleukin-1-beta expression in spinal cord ischemia/reperfusion injury in rats. *The Journal of Thoracic and Cardiovascular Surgery*. 133(4):934–941.

Ma, S., Wang, Y., Chen, Y. & Cao, F. 2015. The role of the autophagy in myocardial ischemia/reperfusion injury. *Biochimica et Biophysica Acta (BBA) - Molecular Basis of Disease*. 1852(2):271–276.

Mackenzie, R.W. & Elliott, B.T. 2014. Akt/PKB activation and insulin signaling: a novel insulin signaling pathway in the treatment of type 2 diabetes. *Diabetes, metabolic syndrome and obesity : targets and therapy*. 7:55–64.

Mailloux, R.J. 2018. Mitochondrial Antioxidants and the Maintenance of Cellular Hydrogen Peroxide Levels. *Oxidative Medicine and Cellular Longevity*. 2018:1–10.

Maiuri, M.C., Zalckvar, E., Kimchi, A. & Kroemer, G. 2007. Self-eating and self-killing: crosstalk between autophagy and apoptosis. *Nature Reviews Molecular Cell Biology*. 8(9):741–752.

Manach, C., Morand, C., Demigné, C., Texier, O., Régérat, F. & Rémésy, C. 1997. Bioavailability of rutin and quercetin in rats. *FEBS letters*. 409(1):12–16.

Manchester, J., Kong, X., Nerbonne, J., Lowry, O.H. & Lawrence, J.C.J. 1994. Glucose transport and phosphorylation in single cardiac myocytes: rate-limiting steps in glucose metabolism. *Am.J.Physiol*. 266:E326–E333.

Marais, C., Steenkamp, J.A., Ferreira, D. 1996. The occurrence of phenylpyruvic acid in woody plants: biosynthetic significance. *Tetrahedron Letters*. 37:5763–5764.

Marais, C., Janse van Rensburg, W., Ferreira, D. & Steenkamp, J.A. 2000. S)- and (R)-Eriodictyol-6-C-β-D-glucopyranoside, novel keys to the fermentation of rooibos (Aspalathus linearis). *Phytochemistry*. 55:43–49.

Marais, E., Genade, S., Huisamen, B., Strijdom, J.G., Moolman, J.A. & Lochner, A. 2001. Activation of p38 MAPK Induced by a Multi-cycle Ischaemic Preconditioning Protocol is Associated with Attenuated p38 MAPK Activity During Sustained Ischaemia and Reperfusion. *Journal of Molecular and Cellular Cardiology*. 33(4):769–778.

Marnewick, J.L., Joubert, E., Swart, P., van der Westhuizen, F. & Gelderblom, W.C. 2003. Modulation of Hepatic Drug Metabolizing Enzymes and Oxidative Status by Rooibos (Aspalathus linearis) and Honeybush (Cyclopia intermedia), Green and Black (Camellia sinensis) Teas in Rats. *J.Agric.Food Chem.* 51(27):8113–8119.

Marnewick, J.L., Rautenbach, F., Venter, I., Neethling, H., Blackhurst, D.M., Wolmarans, P. & Macharia, M. 2011. Effects of rooibos (Aspalathus linearis) on oxidative stress and biochemical parameters in adults at risk for cardiovascular disease. *Journal of ethnopharmacology*. 133(1):46–52.

Marsin, A.S., Bertrand, L., Rider, M.H., Deprez, J., Beauloye, C., Vincent, M.F., Van den Berghe, G., Carling, D., et al. 2000. Phosphorylation and activation of heart PFK-2 by AMPK has a role in the stimulation of glycolysis during ischaemia. *Current biology : CB*. 10(20):1247–55.

Matés, J.M., Segura, J.A., Martín-Rufián, M., Campos-Sandoval, J.A., Alonso, F.J. & Márquez, J. 2013. Glutaminase isoenzymes as key regulators in metabolic and oxidative stress against cancer. *Current molecular medicine*. 13(4):514–34.

Matsuoka, S., Ballif, B.A., Smogorzewska, A., McDonald, E.R., Hurov, K.E., Luo, J., Bakalarski, C.E., Zhao, Z., et al. 2007. ATM and ATR Substrate Analysis Reveals Extensive Protein Networks Responsive to DNA Damage. *Science*. 316(5828):1160–1166.

Mayo Foundation for Medical Education and Research. 2018. *Diabetes - Diagnosis and treatment - Mayo Clinic*. [Online], Available: https://www.mayoclinic.org/diseases-conditions/diabetes/diagnosis-treatment/drc-20371451 [2018, June 29].

Mazibuko, S.E., Muller, C.J.F., Joubert, E., De Beer, D., Johnson, R., Opoku, A.R. & Louw, J. 2013. Amelioration of palmitate-induced insulin resistance in C2C12 muscle cells by rooibos (Aspalathus linearis). *Phytomedicine*. 20(10):813–819.

McCall, A.L. 2012. Insulin therapy and hypoglycemia. *Endocrinology and metabolism clinics of North America*. 41(1):57–87.

McGurk, K.A., Brierley, C.H. & Burchell, B. 1998. Drug Glucuronidation by Human Renal UDP-Glucuronosyltransferases. *Biochemical pharmacology*. 55(7):1005–1012.

McLaughlin, T., Abbasi, F., Cheal, K., Chu, J., Lamendola, C. & Reaven, G. 2003. Use of metabolic markers to identify overweight individuals who are insulin resistant. *Annals of internal medicine*. 139(10):802–9.

McLaughlin, T., Allison, G., Abbasi, F., Lamendola, C. & Reaven, G. 2004. Prevalence of insulin resistance and associated cardiovascular disease risk factors among normal weight, overweight, and obese individuals. *Metabolism*. 53(4):495–499.

Mcmurray, R.G., Soares, J., Caspersen, C.J., Mccurdy, T. & Hill, C. 2015. Examining Variations of Resting Metabolic Rate of Adults: A Public Health Perspective. 46(7):1352–1358.

Meares, G.P. & Jope, R.S. 2007. Resolution of the Nuclear Localization Mechanism of Glycogen Synthase Kinase-3. *Journal of Biological Chemistry*. 282(23):16989–17001.

Meerman, R. & Brown, A.J. 2014. When somebody loses weight, where does the fat go? *BMJ (Clinical research ed.)*. 349:g7257.

Meeusen, S., McCaffery, J.M. & Nunnari, J. 2004. Mitochondrial Fusion Intermediates Revealed in Vitro. *Science*. 305(5691):1747–1752.

Meldrum, D.R., Dinarello, C.A., Cleveland, J.C., Cain, B.S., Shames, B.D., Meng, X. & Harken, A.H. 1998. Hydrogen peroxide induces tumor necrosis factor alpha-mediated cardiac injury by a P38 mitogen-activated protein kinase-dependent mechanism. *Surgery*. 124(2):291–6; discussion 297.

Mennen, L.I., Walker, R., Bennetau-Pelissero, C. & Scalbert, A. 2005. Risks and safety of polyphenol consumption. *American Journal of Clinical Nutrition*. 81(Suppl.1):326S–329S.

Menshikova, E. V, Ritov, V.B., Fairfull, L., Ferrell, R.E., Kelley, D.E. & Goodpaster, B.H. 2006. Effects of exercise on mitochondrial content and function in aging human skeletal muscle. *The journals of gerontology. Series A, Biological sciences and medical sciences*. 61(6):534–40.

Merghani, T.H., Alawad, A.O., Ibrahim, R.M. & Abdelmoniem, A.M. 2015. Prediction of basal metabolic rate

in overweight/obese and non-obese subjects and its relation to pulmonary function tests. *BMC Research Notes*. 8(1):4–9.

Merlotti, C., Ceriani, V., Morabito, A. & Pontiroli, A.E. 2017. Subcutaneous fat loss is greater than visceral fat loss with diet and exercise, weight-loss promoting drugs and bariatric surgery: a critical review and meta-analysis. *International Journal of Obesity*. 41(5):672–682.

van der Merwe, J.D., Joubert, E., Richards, E.S., Manley, M., Snijman, P.W., Marnewick, J.L. & Gelderblom, W.C.A. 2006. A comparative study on the antimutagenic properties of aqueous extracts of Aspalathus linearis (rooibos), different Cyclopia spp. (honeybush) and Camellia sinensis teas. *Mutation Research - Genetic Toxicology and Environmental Mutagenesis*. 611(1–2):42–53.

Van Der Merwe, J.D., Joubert, E., Manley, M., De Beer, D., Malherbe, C.J. & Gelderblom, W.C.A. 2010. In vitro hepatic biotransformation of aspalathin and nothofagin, dihydrochalcones of rooibos (Aspalathus linearis), and assessment of metabolite antioxidant activity. *Journal of Agricultural and Food Chemistry*. 58(4):2214–2220.

Metukuri, M.R., Beer-Stolz, D., Namas, R.A., Dhupar, R., Torres, A., Loughran, P.A., Jefferson, B.S., Tsung, A., et al. 2009. Expression and subcellular localization of BNIP3 in hypoxic hepatocytes and liver stress. *American journal of physiology. Gastrointestinal and liver physiology*. 296(3):G499-509.

Metzger, B.E. & Coustan, D.R. 1998. Proceedings of the Fourth International Work-shop-Conference on Gestational Diabetes Mellitus. *Diabetes care*. 21(Suppl. 2):B1–B167.

Meyer, K.D. & Zhang, L. 2009. Short- and long-term adverse effects of cocaine abuse during pregnancy on the heart development. *Therapeutic advances in cardiovascular disease*. 3(1):7–16.

Mîinea, C.P., Sano, H., Kane, S., Sano, E., Fukuda, M., Peränen, J., Lane, W.S. & Lienhard, G.E. 2005. AS160, the Akt substrate regulating GLUT4 translocation, has a functional Rab GTPase-activating protein domain. *Biochem.J.* 391(1):87–93.

Mikami, N., Tsujimura, J., Sato, A., Narasada, A., Shigeta, M., Kato, M., Hata, S. & Hitomi, E. 2015. Green Rooibos Extract from <i>Aspalathus linearis</i>, and its Component, Aspalathin, Suppress Elevation of Blood Glucose Levels in Mice and Inhibit α-amylase and α-glucosidase Activities <i>in vitro</i> *Food Science and Technology Research*. 21(2):231–240.

Milano, G., Morel, S., Bonny, C., Samaja, M., von Segesser, L.K., Nicod, P. & Vassalli, G. 2007. A peptide inhibitor of c-Jun NH_2 -terminal kinase reduces myocardial ischemia-reperfusion injury and infarct size in vivo. *American Journal of Physiology-Heart and Circulatory Physiology*. 292(4):H1828–H1835.

Miles, M.P. & Clarkson, P.M. 1994. Exercise-induced muscle pain, soreness, and cramps. *The Journal of sports medicine and physical fitness*. 34(3):203–16.

Miller, N., De Beer, D., Aucamp, M., Malherbe, C.J. & Joubert, E. 2018. Inulin as microencapsulating agent improves physicochemical properties of spray-dried aspalathin-rich green rooibos (Aspalathus linearis) extract with α-glucosidase inhibitory activity. *Journal of Functional Foods*. 48:400–409.

Miyazaki, S., Fujiwara, H., Onodera, T., Kihara, Y., Wu, D.-J., Nakamura, Y., Kumada, T., Sasayama, S., et al. 1987. Quantitative analysis of contraction band and coagulation necrosis after ischemia and reperfusion in the porcine heart. *Circulation*, 75 5, 1074-82 .

Mnatsakanyan, N., Beutner, G., Porter, G.A., Alavian, K.N. & Jonas, E.A. 2017. Physiological roles of the mitochondrial permeability transition pore. *Journal of Bioenergetics and Biomembranes*. 49(1):13–25.

Mocanu, M.M., Baxter, G.F. & Yellon, D.M. 2000. Caspase inhibition and limitation of myocardial infarct size:

protection against lethal reperfusion injury. *British Journal of Pharmacology*. 130(2):197–200.

Mookerjee, S.A., Divakaruni, A.S., Jastroch, M. & Brand, M.D. 2010. Mitochondrial uncoupling and lifespan. *Mechanisms of ageing and development*. 131(7–8):463–72.

Morgan, H.E. & Parmeggiani, A. 1964. Regulation of glycogenolysis in muscle. II. Control of glycogen phosphorylase reaction in isolated perfused heart. *J.Biol.Chem*. 239:2435–2439.

Morgan, M.J., Kim, Y.-S. & Liu, Z. 2008. TNFα and reactive oxygen species in necrotic cell death. *Cell Research*. 18(3):343–349.

Morigny, P., Houssier, M., Mouisel, E. & Langin, D. 2016. Adipocyte lipolysis and insulin resistance. *Biochimie*. 125:259–266.

Morton, J.F. 1983. Rooibos tea, Aspalathus linearis, a caffeineless, low-tannin beverage. *Economic Botany*. 37:164–173.

Moule, S.K. & Denton, R.M. 1997. Multiple Signaling Pathways Involved in the Metabolic Effects of Insulin. *The American Journal of Cardiology*. 80(3):41A–49A.

Muller, C.J.F., Joubert, E., de Beer, D., Sanderson, M., Malherbe, C.J., Fey, S.J. & Louw, J. 2012. Acute assessment of an aspalathin-enriched green rooibos (Aspalathus linearis) extract with hypoglycemic potential. *Phytomedicine*. 20(1):32–39.

Muller, C.J.F., Malherbe, C.J., Chellan, N., Yagasaki, K., Miura, Y. & Joubert, E. 2018. Potential of rooibos, its major *C* -glucosyl flavonoids, and *Z* -2-(**β** -D-glucopyranosyloxy)-3-phenylpropenoic acid in prevention of metabolic syndrome. *Critical Reviews in Food Science and Nutrition*. 58(2):227–246.

Mungai, P.T., Waypa, G.B., Jairaman, A., Prakriya, M., Dokic, D., Ball, M.K. & Schumacker, P.T. 2011. Hypoxia Triggers AMPK Activation through Reactive Oxygen Species-Mediated Activation of Calcium Release-Activated Calcium Channels. *Mol Cell Biol.* 31(17):3531–3545.

Murea, M., Ma, L. & Freedman, B.I. 2012. Genetic and environmental factors associated with type 2 diabetes and diabetic vascular complications. *The Review of Diabetic Studies*. 9(1):6–22.

Murphy, E. & Steenbergen, C. 2007. Preconditioning: The Mitochondrial Connection. *Annual Review of Physiology*. 69(1):51–67.

Murphy, L.O., MacKeigan, J.P. & Blenis, J. 2004. A network of immediate early gene products propagates subtle differences in mitogen-activated protein kinase signal amplitude and duration. *Molecular and cellular biology*. 24(1):144–53.

Naga Prasad, S. V, Esposito, G., Mao, L., Koch, W.J. & Rockman, H.A. 2000. Gβγ-dependent phosphoinositide 3-kinase activation in hearts with in vivo pressure overload hypertrophy. *Journal of Biological Chemistry*. 275(7):4693–4698. [Online], Available: http://www.scopus.com/inward/record.url?eid=2-s2.0-0034681226&partnerID=40&md5=36c09c7bba75846bc9612b619eb6c9df.

Nagoshi, T., Matsui, T., Aoyama, T., Leri, A., Anversa, P., Li, L., Ogawa, W., del Monte, F., et al. 2005. PI3K rescues the detrimental effects of chronic Akt activation in the heart during ischemia/reperfusion injury. *The Journal of clinical investigation*. 115(8):2128–38.

Nair, A. & Jacob, S. 2016. A simple practice guide for dose conversion between animals and human. *Journal of Basic and Clinical Pharmacy*. 7(2):27.

Najafian, M., Najafian, B. & Najafian, Z. 2016. The Effect of Aspalathin on Levels of Sugar and Lipids in Streptozotocin-Induced Diabetic and Normal Rats. *Zahedan Journal of Research in Medical Sciences*.

In Press(In Press).

Nam, H.K., Cho, W.K., Kim, J.H., Rhie, Y.J., Chung, S., Lee, K.H. & Suh, B.K. 2018. HbA1c Cutoff for Prediabetes and Diabetes Based on Oral Glucose Tolerance Test in Obese Children and Adolescents. *Journal of Korean medical science*. 33(12):e93.

National Institute of Health. 2009. Insulin Resistance and Pre-diabetes. *Diabetes*. 09:1–19. [Online], Available: http://diabetes.niddk.nih.gov/DM/pubs/insulinresistance/insulinresistance.pdf.

Nduhirabandi, F. 2014. The role of melatonin in cardioprotection : an investigation into the mechanisms involved in glucose homeostasis, microvascular endothelial function and mitochondrial function in normal and insulin resistant states. [Online], Available: http://scholar.sun.ac.za/handle/10019.1/86332 [2018, October 18].

Nduhirabandi, F., Huisamen, B., Strijdom, H. & Lochner, A. 2017. Role of melatonin in glucose uptake by cardiomyocytes from insulin-resistant Wistar rats. *Cardiovascular Journal of Africa*. 28(6):362–369.

Nediani, C., Borchi, E., Giordano, C., Baruzzo, S., Ponziani, V., Sebastiani, M., Nassi, P., Mugelli, A., et al. 2007. NADPH oxidase-dependent redox signaling in human heart failure: Relationship between the left and right ventricle. *Journal of Molecular and Cellular Cardiology*. 42(4):826–834.

Neely, J.R., Liebermeister, H., Battersby, E. & Morgan, H. 1967. Effect of pressure development on oxygen consumption by isolated rat heart. *American Journal of Physiology-Legacy Content*. 212(4):804–814.

Neubauer, S. 2007. The Failing Heart — An Engine Out of Fuel. *New England Journal of Medicine*. 356(11):1140–1151.

Newsholme, P., Lima, M.M.R., Procopio, J., Pithon-Curi, T.C., Doi, S.Q., Bazotte, R.B. & Curi, R. 2003. Glutamine and glutamate as vital metabolites. *Braz J Med Biol Res*. 36(2):153–163.

Nikoulina, S.E., Ciaraldi, T.P., Mudaliar, S., Mohideen, P., Carter, L. & Henry, R.R. 2000. Potential role of glycogen synthase kinase-3 in skeletal muscle insulin resistance of type 2 diabetes. *Diabetes*. 49(2):263–71.

Noble, R.E. 2001. Waist-to-hip ratio versus BMI as predictors of cardiac risk in obese adult women. *Western Journal of Medicine*. 174(4):240–241.

Norris, J.M. & Rich, S.S. 2012. Genetics of Glucose Homeostasis: Implications for Insulin Resistance and Metabolic Syndrome. *Arteriosclerosis, Thrombosis, and Vascular Biology*. 32(9):2091–2096.

Novak, I. & Dikic, I. 2011. Autophagy receptors in developmental clearance of mitochondria. *Autophagy*. 7(3):301–3.

Novak, I., Kirkin, V., McEwan, D.G., Zhang, J., Wild, P., Rozenknop, A., Rogov, V., Löhr, F., et al. 2010. Nix is a selective autophagy receptor for mitochondrial clearance. *EMBO reports*. 11(1):45–51.

Nsiah-Sefaa, A. & McKenzie, M. 2016. Combined defects in oxidative phosphorylation and fatty acid -oxidation in mitochondrial disease. *Bioscience Reports*. 36(2):e00313–e00313.

Nunes, S., Soares, E., Fernandes, J., Viana, S., Carvalho, E., Pereira, F.C. & Reis, F. 2013. Early cardiac changes in a rat model of prediabetes: brain natriuretic peptide overexpression seems to be the best marker. *Cardiovascular diabetology*. 12:44.

O'Leary, K.A., Day, A.J., Needs, P.W., Mellon, F.A., O'Brien, N.M. & Williamson, G. 2003. Metabolism of quercetin-7- and quercetin-3-glucuronides by an in vitro hepatic model: the role of human ß-glucuronidase, sulfotransferase, catechol-O-methyltransferase and multi-resistant protein 2 (MRP2) in flavonoid metabolism. *Biochemical pharmacology*. 65(3):479–491.

O'Shea, J.J., Holland, S.M. & Staudt, L.M. 2013. JAKs and STATs in Immunity, Immunodeficiency, and Cancer. *New England Journal of Medicine*. 368(2):161–170.

O'Shea, J.J., Schwartz, D.M., Villarino, A. V, Gadina, M., McInnes, I.B. & Laurence, A. 2015. The JAK-STAT pathway: impact on human disease and therapeutic intervention. *Annual review of medicine*. 66:311–28.

Ogden, C.L., Carroll, M.D., Kit, B.K. & Flegal, K.M. 2014. Prevalence of Childhood and Adult Obesity in the United States, 2011–2012. *Survey of Anesthesiology*. 58(4):206.

Oh, S.-H., Choi, Y.-B., Kim, J.-H., Weihl, C.C. & Ju, J.-S. 2017. Quantification of autophagy flux using LC3 ELISA. *Analytical Biochemistry*. 530:57–67.

Okwuosa, T.M., Soliman, E.Z., Lopez, F., Williams, K.A., Alonso, A. & Ferdinand, K.C. 2015. Left ventricular hypertrophy and cardiovascular disease risk prediction and reclassification in blacks and whites: the Atherosclerosis Risk in Communities Study. *American heart journal*. 169(1):155–61.e5.

Olefsky, J.M. & Glass, C.K. 2010. Macrophages, Inflammation, and Insulin Resistance. *Annual Review of Physiology*. 72(1):219–246.

Olfson, M. & Marcus, S.C. 2013. Decline In Placebo-Controlled Trial Results Suggests New Directions For Comparative Effectiveness Research. *Health Affairs*. 32(6):1116–1125.

Ong, S.-B. & Gustafsson, A.B. 2012. New roles for mitochondria in cell death in the reperfused myocardium. *Cardiovascular Research*. 94(2):190–196.

Ong, S.-B. & Hausenloy, D.J. 2010. Mitochondrial morphology and cardiovascular disease. *Cardiovascular Research*. 88(1):16–29.

Opie, L.H. 1968. Metabolism of the heart in health and disease. Part I. *American Heart Journal*. 76(5):685–698.

Opie, L.H. 1969a. Metabolism of the heart in health and disease. Part II. *American Heart Journal*. 77(1):100–122.

Opie, L.H. 1969b. Metabolism of the heart in health and disease. Part III. *American Heart Journal*. 77(3):383–410. [Online], Available: http://www.scopus.com/inward/record.url?eid=2-s2.0-0014478336&partnerID=40&md5=ca2f3d2ba716bcfa1c2eb4fd2944b11e.

Ouwens, D.M., Boer, C., Fodor, M., de Galan, P., Heine, R.J., Maassen, J.A. & Diamant, M. 2005. Cardiac dysfunction induced by high-fat diet is associated with altered myocardial insulin signalling in rats. *Diabetologia*. 48(6):1229–1237.

Owen, O.E., Kalhan, S.C. & Hanson, R.W. 2002. The key role of anaplerosis and cataplerosis for citric acid cycle function. *Journal of Biological Chemistry*. 277(34):30409–30412.

Pallauf, K. & Rimbach, G. 2013. Autophagy, polyphenols and healthy ageing. *Ageing Research Reviews*. 12(1):237–252.

Pampel, F.C., Denney, J.T. & Krueger, P.M. 2012. Obesity, SES, and economic development: A test of the reversal hypothesis. *Social science & medicine*. 74(7):1073–1081.

Pandey, K.B. & Rizvi, S.I. 2009. Plant polyphenols as dietary antioxidants in human health and disease. *Oxidative medicine and cellular longevity*. 2(5):270–8.

Pantsi, W.G., Marnewick, J.L., Esterhuyse, A.J., Rautenbach, F. & Van Rooyen, J. 2011. Rooibos (Aspalathus linearis) offers cardiac protection against ischaemia/reperfusion in the isolated perfused rat heart. *Phytomedicine*. 18(14):1220–1228.

Di Paola, M. & Lorusso, M. 2006. Interaction of free fatty acids with mitochondria: Coupling, uncoupling and permeability transition. *Biochimica et Biophysica Acta (BBA) - Bioenergetics*. 1757(9–10):1330–1337.

Papadopoulou, L.C., Theophilidis, G., Thomopoulos, G.N. & Tsiftsoglou, A.S. 1999. Structural and functional impairment of mitochondria in adriamycin-induced cardiomyopathy in mice: suppression of cytochrome c oxidase II gene expression. *Biochemical pharmacology*. 57(5):481–9.

Pareek, M., Bhatt, D.L., Nielsen, M.L., Jagannathan, R., Eriksson, K.-F., Nilsson, P.M., Bergman, M. & Olsen, M.H. 2018. Enhanced Predictive Capability of a 1-Hour Oral Glucose Tolerance Test: A Prospective Population-Based Cohort Study. *Diabetes care*. 41(1):171–177.

Patel, D.K., Prasad, S.K., Kumar, R. & Hemalatha, S. 2012. An overview on antidiabetic medicinal plants having insulin mimetic property. *Asian Pacific Journal of Tropical Biomedicine*. 2(4):320–330.

Patterson, A.J. & Zhang, L. 2010. Hypoxia and fetal heart development. *Current molecular medicine*. 10(7):653–66.

Pellegrino, M.W. & Haynes, C.M. 2015. Mitophagy and the mitochondrial unfolded protein response in neurodegeneration and bacterial infection. *BMC biology*. 13:22.

Perrelli, M.-G., Pagliaro, P. & Penna, C. 2011. Ischemia/reperfusion injury and cardioprotective mechanisms: Role of mitochondria and reactive oxygen species. *World Journal of Cardiology*. 3(6):186.

Persson, I.A.-L., Persson, K., Hägg, S. & Andersson, R.G. 2010. Effects of green tea, black tea and Rooibos tea on angiotensin-converting enzyme and nitric oxide in healthy volunteers. *Public Health Nutrition*. 13(05):730.

Pickavance, L.C., Tadayyon, M., Widdowson, P.S., Buckingham, R.E. & Wilding, J.P.H. 1999. Therapeutic index for rosiglitazone in dietary obese rats: Separation of efficacy and haemodilution. *British Journal of Pharmacology*. 128(7):1570–1576.

Polonsky, K.S. 2012. The past 200 years in diabetes. *New England Journal of Medicine*. 367(14):1332–1340.

Popkin, B.M. 2009. The World is Fat: The Fads, Trends, Policies, and Products that Are Fattening the Human Race. *New York: Avery*.

Popkin, B.M., D'Anci, K.E. & Rosenberg, I.H. 2010. Water, hydration, and health. *Nutrition Reviews*. 68(8):439–458.

Povlsen, J.A., Løfgren, B., Dalgas, C., Birkler, R.I.D., Johannsen, M., Støttrup, N.B. & Bøtker, H.E. 2013. Protection against Myocardial Ischemia-Reperfusion Injury at Onset of Type 2 Diabetes in Zucker Diabetic Fatty Rats Is Associated with Altered Glucose Oxidation. *PLoS ONE*. 8(5):e64093.

Prasad, K.N., Cole, W.C., Kumar, B. & Che Prasad, K. 2002. Pros and cons of antioxidant use during radiation therapy. *Cancer treatment reviews*. 28(2):79–91.

Prior, R.L., Gu, L., Wu, X., Jacob, R.A., Sotoudeh, G., Kader, A.A. & Cook, R.A. 2007. Plasma Antioxidant Capacity Changes Following a Meal as a Measure of the Ability of a Food to Alter In Vivo Antioxidant Status. *Journal of the American College of Nutrition*. 26(2):170–181.

Puchowicz, M.A., Varnes, M.E., Cohen, B.H., Friedman, N.R., Kerr, D.S. & Hoppel, C.L. 2004. Oxidative phosphorylation analysis: assessing the integrated functional activity of human skeletal muscle mitochondria—case studies. *Mitochondrion*. 4(5–6):377–385.

Qi, D. & Young, L.H. 2015. AMPK: energy sensor and survival mechanism in the ischemic heart. *Trends in endocrinology and metabolism: TEM*. 26(8):422–9.

Quattrocchi, U. 2012. *CRC world dictionary of medicinal and poisonous plants*. CRC.

Rabe, C., Steenkamp, J.A., Joubert, E., Burger, J.F.W. & Ferreira, D. 1994. Phenolic metabolites from rooibos tea (Aspalathus linearis). *Phytochemistry*. 35:1559–1565.

Raedschelders, K., Ansley, D.M. & Chen, D.D.Y. 2012. The cellular and molecular origin of reactive oxygen species generation during myocardial ischemia and reperfusion. *Pharmacology & Therapeutics*. 133(2):230–255.

Ravnskov, U., de Lorgeril, M., Diamond, D.M., Hama, R., Hamazaki, T., Hammarskjöld, B., Hynes, N., Kendrick, M., et al. 2018. LDL-C does not cause cardiovascular disease: a comprehensive review of the current literature. *Expert Review of Clinical Pharmacology*. 11(10):959–970.

Rayasam, G. V, Tulasi, V.K., Sodhi, R., Davis, J.A. & Ray, A. 2009. Glycogen synthase kinase 3: More than a namesake. *British Journal of Pharmacology*. 156(6):885–898.

Reddy, V.P. & Reddy, V.P. 2015. Fluorinated Compounds in Enzyme-Catalyzed Reactions. *Organofluorine Compounds in Biology and Medicine*. (January, 1):29–57.

Rena, G., Hardie, D.G. & Pearson, E.R. 2017. The mechanisms of action of metformin. *Diabetologia*. 60(9):1577–1585.

Reynolds, L.P., Borowicz, P.P., Caton, J.S., Vonnahme, K.A., Luther, J.S., Hammer, C.J., Maddock Carlin, K.R., Grazul-Bilska, A.T., et al. 2010. Developmental programming: The concept, large animal models, and the key role of uteroplacental vascular development1,2. *Journal of Animal Science*. 88(suppl_13):E61–E72.

Rial, E., Rodríguez-Sánchez, L., Gallardo-Vara, E., Zaragoza, P., Moyano, E. & González-Barroso, M.M. 2010. Lipotoxicity, fatty acid uncoupling and mitochondrial carrier function. *Biochimica et Biophysica Acta (BBA) - Bioenergetics*. 1797(6–7):800–806.

Riccioni, G. 2009. Focus on ivabradine: a new heart rate-controlling drug. *Expert Review of Cardiovascular Therapy*. 7(2):107–113.

Rice, K.M., Fannin, J.C., Gillette, C. & Blough, E.R. 2014. Efficacy of female rat models in translational cardiovascular aging research. *Journal of aging research*. 2014:153127.

Richter, E.A. & Ruderman, N.B. 2009. AMPK and the biochemistry of exercise: implications for human health and disease. *Biochemical Journal*. 418(2):261–275.

Rizzuto, R., De Stefani, D., Raffaello, A. & Mammucari, C. 2012. Mitochondria as sensors and regulators of calcium signalling. *Nature Reviews Molecular Cell Biology*. 13(9):566–578.

Rosano, G.M.C., Fini, M., Caminiti, G. & Barbaro, G. 2008. Cardiac metabolism in myocardial ischemia. *Current pharmaceutical design*. 14(25):2551–62.

Rosca, M.G., Vazquez, E.J., Kerner, J., Parland, W., Chandler, M.P., Stanley, W., Sabbah, H.N. & Hoppel, C.L. 2008. Cardiac mitochondria in heart failure: Decrease in respirasomes and oxidative phosphorylation. *Cardiovascular Research*. 80(1):30–39.

Roskoski, R. 2012. ERK1/2 MAP kinases: Structure, function, and regulation. *Pharmacological Research*. 66(2):105–143.

Ross, F.A., MacKintosh, C. & Hardie, D.G. 2016. AMP-activated protein kinase: a cellular energy sensor that comes in 12 flavours. *The FEBS journal*. 283(16):2987–3001.

Rossello, X. & Yellon, D.M. 2016. A critical review on the translational journey of cardioprotective therapies! *International Journal of Cardiology*. 220:176–184.

Rossello, X. & Yellon, D.M. 2018. The RISK pathway and beyond. *Basic Research in Cardiology*. 113(1):2.

Rossello, X., Riquelme, J.A., Davidson, S.M. & Yellon, D.M. 2017. Role of PI3K in myocardial ischaemic preconditioning: mapping pro-survival cascades at the trigger phase and at reperfusion. *Journal of Cellular and Molecular Medicine*. 22(2):926–935.

Saboor Aftab, S.A., Reddy, N., Smith, E. & Barber, T.M. 2014. Obesity and Type 2 Diabetes Mellitus. *Intern Med*. S6(002).

Sakamoto, K. & Holman, G.D. 2008. Emerging role for AS160/TBC1D4 and TBC1D1 in the regulation of GLUT4 traffic. *American Journal of Physiology-Endocrinology and Metabolism*. 295(1):E29–E37.

Salabei, J.K., Gibb, A.A. & Hill, B.G. 2014. Comprehensive measurement of respiratory activity in permeabilized cells using extracellular flux analysis. *Nature protocols*. 9(2):421–38.

Salie, R., Huisamen, B. & Lochner, A. 2014. High carbohydrate and high fat diets protect the heart against ischaemia/reperfusion injury. *Cardiovascular Diabetology*. 13(1):1–12.

Salpeter, S.R., Greyber, E., Pasternak, G.A. & Salpeter, E.E. 2006. Risk of fatal and nonfatal lactic acidosis with metformin use in type 2 diabetes mellitus. In S.R. Salpeter (ed.). Chichester, UK: John Wiley & Sons, Ltd *The Cochrane Database of Systematic Reviews (Complete Reviews)*. CD002967.

Samocha-Bonet, D., Chisholm, D.J., Tonks, K., Campbell, L.V. & Greenfield, J.R. 2012. Insulin-sensitive obesity in humans – a 'favorable fat' phenotype? *Trends in Endocrinology & Metabolism*. 23(3):116–124.

Samovski, D., Su, X., Xu, Y., Abumrad, N.A. & Stahl, P.D. 2012. Insulin and AMPK regulate FA translocase/CD36 plasma membrane recruitment in cardiomyocytes via Rab GAP AS160 and Rab8a Rab GTPase. *Journal of Lipid Research*. 53(4):709–717.

Sanada, S., Komuro, I. & Kitakaze, M. 2011. Pathophysiology of myocardial reperfusion injury: preconditioning, postconditioning, and translational aspects of protective measures. *American Journal of Physiology-Heart and Circulatory Physiology*. 301(5):H1723–H1741.

Sanderson, M., Mazibuko, S.E., Joubert, E., de Beer, D., Johnson, R., Pheiffer, C., Louw, J. & Muller, C.J.F. 2014. Effects of fermented rooibos (Aspalathus linearis) on adipocyte differentiation. *Phytomedicine*. 21(2):109–117.

Sasaoka, T., Wada, T. & Tsuneki, H. 2006. Lipid phosphatases as a possible therapeutic target in cases of type 2 diabetes and obesity. *Pharmacology and Therapeutics*. 112(3):799–809.

Sattur, S., Brener, S.J. & Stone, G.W. 2015. Pharmacologic therapy for reducing myocardial infarct size in clinical trials: Failed and promising approaches. *Journal of Cardiovascular Pharmacology and Therapeutics*. 20(1):21–35.

Scalbert, A. & Williamson, G. 2000. Dietary Intake and Bioavailability of Polyphenols. *The Journal of Nutrition*. 130(8):2073S–2085S.

Scalbert, A., Morand, C., Manach, C. & Rémésy, C. 2002. Absorption and metabolism of polyphenols in the gut and impact on health. *Biomedicine & Pharmacotherapy*. 56(6):276–282.

Schloms, L., Smith, C., Storbeck, K.-H., Marnewick, J.L., Swart, P. & Swart, A.C. 2014. Rooibos influences glucocorticoid levels and steroid ratios in vivo and in vitro: A natural approach in the management of stress and metabolic disorders? *Molecular Nutrition & Food Research*. 58(3):537–549.

Schneider, C.A., Nguyêñ, V.T.B. & Taegtmeyer, H. 1991. Feeding and fasting determine postischemic glucose utilization in isolated working rat hearts. *Am J Physiol*. 260:H542–H548.

Schulman, D., Latchman, D.S. & Yellon, D.M. 2002. Urocortin protects the heart from reperfusion injury via upregulation of p42/p44 MAPK signaling pathway. *American Journal of Physiology-Heart and Circulatory Physiology*. 283(4):H1481–H1488.

Schulz, H., Joubert, E. & Schütze, W. 2003. Quantification of quality parameters for reliable evaluation of green rooibos (Aspalathus linearis). *European Food Research and Technology*. 216(6):539–543.

Sciarretta, S., Hariharan, N., Monden, Y., Zablocki, D. & Sadoshima, J. 2011. Is autophagy in response to ischemia and reperfusion protective or detrimental for the heart? *Pediatric cardiology*. 32(3):275–81.

Scorrano, L., Oakes, S.A., Opferman, J.T., Cheng, E.H., Sorcinelli, M.D., Pozzan, T. & Korsmeyer, S.J. 2003. BAX and BAK Regulation of Endoplasmic Reticulum Ca2+: A Control Point for Apoptosis. *Science*. 300(5616):135–139.

Seo, A.Y., Joseph, A.-M., Dutta, D., Hwang, J.C.Y., Aris, J.P. & Leeuwenburgh, C. 2010. New insights into the role of mitochondria in aging: mitochondrial dynamics and more. *Journal of Cell Science*. 123(15):2533–2542.

Sequeira, I.R. & Poppitt, S.D. 2017. Unfolding Novel Mechanisms of Polyphenol Flavonoids for Better Glycaemic Control: Targeting Pancreatic Islet Amyloid Polypeptide (IAPP). *Nutrients*. 9(7).

Sesti, G. 2006. Pathophysiology of insulin resistance. *Best Practice and Research: Clinical Endocrinology and Metabolism*. 20(4):665–679.

Shah, A. & Shannon, R.P. 2003. Insulin resistance in dilated cardiomyopathy. *Reviews in cardiovascular medicine*. 4 Suppl 6:S50-7.

Shanik, M.H., Xu, Y., Skrha, J., Dankner, R., Zick, Y. & Roth, J. 2008. Insulin Resistance and Hyperinsulinemia: Is hyperinsulinemia the cart or the horse? *Diabetes care*. 31(Supplement 2):S262–S268.

Sharma, S., Adrogue, J. V, Golfman, L., Uray, I., Lemm, J., Youker, K., Noon, G.P., Frazier, O.H., et al. 2004. Intramyocardial lipid accumulation in the failing human heart resembles the lipotoxic rat heart. *FASEB Journal*. 18(14):1692–1700.

Shaul, Y.D. & Seger, R. 2007. The MEK/ERK cascade: From signaling specificity to diverse functions. *Biochimica et Biophysica Acta (BBA) - Molecular Cell Research*. 1773(8):1213–1226.

Shelley, H.J. 1961. Cardiac glycogen in different species before and after birth. *Br Med Bull*. 17:137–156.

Shimamura, N., Miyase, T., Umehara, K., Warashina, T. & Fujii, S. 2006. Phytoestrogens from Aspalathus linearis. *Biological & pharmaceutical bulletin*. 29(6):1271–4.

Shiojima, I., Yefremashvili, M., Luo, Z., Kureishi, Y., Takahashi, A., Tao, J., Rosenzweig, A., Ronald Kahn, C., et al. 2002. Akt signaling mediates postnatal heart growth in response to insulin and nutritional status. *Journal of Biological Chemistry*. 277(40):37670–37677.

Shvedova, M., Anfinogenova, Y., Atochina-Vasserman, E.N., Schepetkin, I.A. & Atochin, D.N. 2018. c-Jun N-Terminal Kinases (JNKs) in Myocardial and Cerebral Ischemia/Reperfusion Injury. *Frontiers in pharmacology*. 9:715.

Simpson, M.J., Hjelmqvist, D., López-Alarcón, C., Karamehmedovic, N., Minehan, T.G., Yepremyan, A., Salehani, B., Lissi, E., et al. 2013. Anti-peroxyl radical quality and antibacterial properties of rooibos infusions and their pure glycosylated polyphenolic constituents. *Molecules*. 18(9):11264–11280.

Sinisalo, M., Enkovaara, A.-L. & Kivistö, K.T. 2010. Possible hepatotoxic effect of rooibos tea: a case report. *European journal of clinical pharmacology*. 66(4):427–428.

Sinjman, P.W., Joubert, E., Ferreira, D., Li, X.C., Ding, Y., Green, I.R. & Gelderblom, W.C.A. 2009. Antioxidant activity of the dihydrochalcones aspalathin and nothofagin and their corresponding flavones in relation to other rooibos (Aspalathus linearis) flavonoids, epigallocatechin gallate, and Trolox. *Journal of Agricultural and Food Chemistry*. 57(15):6678–6684.

Skyschally, A., van Caster, P., Boengler, K., Gres, P., Musiolik, J., Schilawa, D., Schulz, R. & Heusch, G. 2008. Ischemic Postconditioning in Pigs: No Causal Role for RISK Activation. *Circulation Research*. 104(1):15–18.

Skyschally, A., van Caster, P., Boengler, K., Gres, P., Musiolik, J., Schilawa, D., Schulz, R. & Heusch, G. 2009. Ischemic Postconditioning in Pigs. *Circulation Research*. 104(1):15–18.

Slegtenhorst, B.R., Dor, F.J., Rodriguez, H., Voskuil, F.J. & Tullius, S.G. 2014. Ischemia/reperfusion Injury and its Consequences on Immunity and Inflammation. *Current transplantation reports*. 1(3):147–154.

Smit, S., Johnson, R., Van Vuuren, M. & Huisamen, B. 2018. Myocardial Glucose Clearance by Aspalathin Treatment in Young, Mature, and Obese Insulin-Resistant Rats. *Planta Medica*. 84(02):75–82.

Smith, G.C., Cary, R.B., Lakin, N.D., Hann, B.C., Teo, S.H., Chen, D.J. & Jackson, S.P. 1999. Purification and DNA binding properties of the ataxia-telangiectasia gene product ATM. *Proceedings of the National Academy of Sciences of the United States of America*. 96(20):11134–9.

Snijman, P.W., Swanevelder, S., Joubert, E., Green, I.R. & Gelderblom, W.C.A. 2007. The antimutagenic activity of the major flavonoids of rooibos (Aspalathus linearis): Some dose-response effects on mutagen activation-flavonoid interactions. *Mutation Research - Genetic Toxicology and Environmental Mutagenesis*. 631(2):111–123.

Sola, D., Rossi, L., Schianca, G.P.C., Maffioli, P., Bigliocca, M., Mella, R., Corlianò, F., Fra, G.P., et al. 2015. Sulfonylureas and their use in clinical practice. *Archives of medical science : AMS*. 11(4):840–8.

Son, M.J., Minakawa, M., Miura, Y. & Yagasaki, K. 2013. Aspalathin improves hyperglycemia and glucose intolerance in obese diabetic ob/ob mice. *European Journal of Nutrition*. 52(6):1607–1619.

Song, M., Mihara, K., Chen, Y., Scorrano, L., Dorn, G.W. & II. 2015. Mitochondrial fission and fusion factors reciprocally orchestrate mitophagic culling in mouse hearts and cultured fibroblasts. *Cell metabolism*. 21(2):273–286.

Sriwijitkamol, A., Coletta, D.K., Wajcberg, E., Balbontin, G.B., Reyna, S.M., Barrientes, J., Eagan, P.A., Jenkinson, C.P., et al. 2007. Effect of Acute Exercise on AMPK Signaling in Skeletal Muscle of Subjects With Type 2 Diabetes: A Time-Course and Dose-Response Study. *Diabetes*. 56(3):836–848.

Stalmach, A., Mullen, W., Pecorari, M., Serafini, M. & Crozier, A. 2009. Bioavailability of C-linked dihydrochalcone and flavanone glucosides in humans following ingestion of unfermented and fermented rooibos teas. *Journal of Agricultural and Food Chemistry*. 57(15):7104–7111.

Stanford, K.I., Middelbeek, R.J.W., Townsend, K.L., An, D., Nygaard, E.B., Hitchcox, K.M., Markan, K.R., Nakano, K., et al. 2012. Brown adipose tissue regulates glucose homeostasis and insulin sensitivity. *Journal of Clinical Investigation*. 123(1):215–223.

Stanley, W. 1997. Regulation of energy substrate metabolism in the diabetic heart. *Cardiovascular research*. 34(1):25–33.

Stanley, W.C., Recchia, F.A. & Lopaschuk, G.D. 2005. Myocardial Substrate Metabolism in the Normal and Failing Heart. *Physiological Reviews*. 85(3):1093–1129.

Stewart, J.T., Grbic, M. & Sigwart, U. 1992. Left atrial and left ventricular diastolic function during acute

myocardial ischaemia. *British heart journal*. 68(4):377–81.

Stowe, D. 1999. Understanding the temporal relationship of ATP loss, calcium loading, and rigor contracture during anoxia, and hypercontracture after anoxia in cardiac myocytes. *Cardiovascular Research*. 43(2):285–287.

Stowe, D.F. & Camara, A.K.S. 2009. Mitochondrial Reactive Oxygen Species Production in Excitable Cells: Modulators of Mitochondrial and Cell Function. *Antioxidants & Redox Signaling*. 11(6):1373–1414.

Støy, J., Steiner, D.F., Park, S.-Y., Ye, H., Philipson, L.H. & Bell, G.I. 2010. Clinical and molecular genetics of neonatal diabetes due to mutations in the insulin gene. *Reviews in Endocrine and Metabolic Disorders*. 11(3):205–215.

Surinkaew, S., Kumphune, S., Chattipakorn, S. & Chattipakorn, N. 2013. Inhibition of p38 MAPK During Ischemia, But Not Reperfusion, Effectively Attenuates Fatal Arrhythmia in Ischemia/Reperfusion Heart. *Journal of Cardiovascular Pharmacology*. 61(2):133–141.

Suzuki, T., Bridges, D., Nakada, D., Skiniotis, G., Morrison, S.J., Lin, J.D., Saltiel, A.R. & Inoki, K. 2013. Inhibition of AMPK catabolic action by GSK3. *Molecular cell*. 50(3):407–19.

Szczepaniak, L.S., Dobbins, R.L., Metzger, G.J., Sartoni-D'Ambrosia, G., Arbique, D., Vongpatanasin, W., Unger, R. & Victor, R.G. 2003. Myocardial triglycerides and systolic function in humans: In vivo evaluation by localized proton spectroscopy and cardiac imaging. *Magnetic Resonance in Medicine*. 49(3):417–423.

Takagi, H., Matsui, Y., Hirotani, S., Sakoda, H., Asano, T. & Sadoshima, J. 2007. AMPK mediates autophagy during myocardial ischemia in vivo. *Autophagy*. 3(4):405–7.

Talmor, D., Applebaum, A., Rudich, A., Shapira, Y. & Tirosh, A. 2000. Activation of mitogen-activated protein kinases in human heart during cardiopulmonary bypass. *Circulation research*. 86(9):1004–7.

Taniyama, Y., Ito, M., Sato, K., Kuester, C., Veit, K., Tremp, G., Liao, R., Colucci, W.S., et al. 2005. Akt3 overexpression in the heart results in progression from adaptive to maladaptive hypertrophy. *Journal of Molecular and Cellular Cardiology*. 38(2):375–385.

Tewari, N., Awad, S., Macdonald, I.A. & Lobo, D.N. 2015. Obesity-related insulin resistance: implications for the surgical patient. *International Journal of Obesity*. 39(11):1575–1588.

"The Normal Size of the Heart Muscle Weight". 1951. *Acta Medica Scandinavica*. 139(S257):15–19.

Thilakarathna, S.H. & Rupasinghe, H.P.V. 2013. Flavonoid bioavailability and attempts for bioavailability enhancement. *Nutrients*. 5(9):3367–87.

Thorell, A., Hirshman, M.F., Nygren, J., Jorfeldt, L., Wojtaszewski, J.F.P., Dufresne, S.D., Horton, E.S., Ljungqvist, O., et al. 1999. Exercise and insulin cause GLUT-4 translocation in human skeletal muscle. *American Journal of Physiology-Endocrinology and Metabolism*. 277(4):E733–E741.

Thornburg, K.L., O'Tierney, P.F. & Louey, S. 2010. Review: The placenta is a programming agent for cardiovascular disease. *Placenta*. 31 Suppl(Suppl):S54-9.

Du Toit, E.F., Smith, W., Muller, C., Strijdom, H., Woodiwiss, A.J., Norton, G.R., Lochner, A. & Stouthammer, B. 2008. Myocardial susceptibility to ischemic-reperfusion injury in a prediabetic model of dietary-induced obesity. *American journal of physiology. Heart and circulatory physiology*. 294(5):H2336-43.

Trifunovic, A. 2006. Mitochondrial DNA and ageing. *Biochimica et Biophysica Acta (BBA) - Bioenergetics*. 1757(5–6):611–617.

Tsatsoulis, A., Mantzaris, M.D., Bellou, S. & Andrikoula, M. 2013. Insulin resistance: An adaptive mechanism

becomes maladaptive in the current environment — An evolutionary perspective. *Metabolism*. 62(5):622–633.

Unwin, N., Shaw, J., Zimmet, P. & Alberti, K.G.M.M. 2002. Impaired glucose tolerance and impaired fasting glycaemia: the current status on definition and intervention. *Diabetic medicine : a journal of the British Diabetic Association*. 19(9):708–23.

Uusitalo, A., Uusitalo, A. & Rusko, H. 1998. Exhaustive Endurance Training for 6-9 Weeks did not Induce Changes in Intrinsic Heart Rate and Cardiac Autonomic Modulation in Female Athletes. *International Journal of Sports Medicine*. 19(08):532–540.

Valentim, L., Laurence, K.M., Townsend, P.A., Carroll, C.J., Soond, S., Scarabelli, T.M., Knight, R.A., Latchman, D.S., et al. 2006. Urocortin inhibits Beclin1-mediated autophagic cell death in cardiac myocytes exposed to ischaemia/reperfusion injury. *Journal of Molecular and Cellular Cardiology*. 40(6):846–852.

Vandenabeele, P., Declercq, W., Van Herreweghe, F. & Vanden Berghe, T. 2010. The Role of the Kinases RIP1 and RIP3 in TNF-Induced Necrosis. *Science Signaling*. 3(115):re4-re4.

Vassalli, G., Milano, G. & Moccetti, T. 2012. Role of Mitogen-Activated Protein Kinases in Myocardial Ischemia-Reperfusion Injury during Heart Transplantation. *Journal of Transplantation*. 2012:1–16.

Vaughan-Jones, R.D., Spitzer, K.W. & Swietach, P. 2009. Intracellular pH regulation in heart. *Journal of Molecular and Cellular Cardiology*. 46(3):318–331.

Veeresham, C. 2012. Natural products derived from plants as a source of drugs. *Journal of advanced pharmaceutical technology & research*. 3(4):200–1.

Vella, C.A., Burgos, X., Ellis, C.J., Zubia, R.Y., Ontiveros, D., Reyes, H. & Lozano, C. 2013. Associations of insulin resistance with cardiovascular risk factors and inflammatory cytokines in normal-weight Hispanic women. *Diabetes care*. 36(5):1377–83.

Vendelbo, M.H., Clasen, B.F.F., Treebak, J.T., Møller, L., Krusenstjerna-Hafstrøm, T., Madsen, M., Nielsen, T.S., Stødkilde-Jørgensen, H., et al. 2012. Insulin resistance after a 72-h fast is associated with impaired AS160 phosphorylation and accumulation of lipid and glycogen in human skeletal muscle. *American Journal of Physiology-Endocrinology and Metabolism*. 302(2):E190–E200.

Verkerk, A.O., Wilders, R., Van Borren, M.M.G.J., Peters, R.J.G., Broekhuis, E., Lam, K., Coronel, R., De Bakker, J.M.T., et al. 2007. Clinical research Arrhythmia/electrophysiology Pacemaker current (If) in the human sinoatrial node. *European Heart Journal*. 28:2472–2478.

Villaño, D., Pecorari, M., Testa, M.F., Raguzzini, A., Stalmach, A., Crozier, A., Tubili, C. & Serafini, M. 2010. Unfermented and fermented rooibos teas (Aspalathus linearis) increase plasma total antioxidant capacity in healthy humans. *Food Chemistry*. 123(3):679–683.

van Vilsteren, M.C.B.A., de Greef, M.H.G. & Huisman, R.M. 2005. The effects of a low-to-moderate intensity pre-conditioning exercise programme linked with exercise counselling for sedentary haemodialysis patients in The Netherlands: results of a randomized clinical trial. *Nephrology Dialysis Transplantation*. 20(1):141–146.

Viniegra, J.G., Martínez, N., Modirassari, P., Losa, J.H., Cobo, C.P., Lobo, V.J.S.-A., Luquero, C.I.A., Álvarez-Vallina, L., et al. 2005. Full Activation of PKB/Akt in Response to Insulin or Ionizing Radiation Is Mediated through ATM. *Journal of Biological Chemistry*. 280(6):4029–4036.

Viollet, B., Guigas, B., Sanz Garcia, N., Leclerc, J., Foretz, M. & Andreelli, F. 2012. Cellular and molecular

mechanisms of metformin: An overview. *Clinical science*. 122(6):253–270.

Van Der Vusse, G.J., Van Bilsen, M. & Glatz, J.F.C. 2000. Cardiac fatty acid uptake and transport in health and disease. *Cardiovascular Research*. 45(2):279–293.

Wagner, C., Tillack, D., Simonis, G., Strasser, R.H. & Weinbrenner, C. 2010. Ischemic post-conditioning reduces infarct size of the in vivo rat heart: role of PI3-K, mTOR, GSK-3β, and apoptosis. *Molecular and Cellular Biochemistry*. 339(1–2):135–147.

Waisundara, V.Y. & Hoon, L.Y. 2015. Free radical scavenging ability of Aspalathus linearis in two in vitro models of diabetes and cancer. *Journal of Traditional and Complementary Medicine*. 5(3):174–178.

Walczak, J., Partyka, M., Duszyński, J. & Szczepanowska, J. 2017. Implications of mitochondrial network organization in mitochondrial stress signalling in NARP cybrid and Rho0 cells. *Scientific Reports*. 7(1):14864.

Walsh, K. 2006. Akt Signaling and Growth of the Heart. *Circulation*. 113(17):2032–2034.

Wang, Y., Ji, H.-X., Xing, S.-H., Pei, D.-S. & Guan, Q.-H. 2007. SP600125, a selective JNK inhibitor, protects ischemic renal injury via suppressing the extrinsic pathways of apoptosis. *Life Sciences*. 80(22):2067–2075.

Wang, Z., Yang, Y., Xiang, X., Zhu, Y., Men, J. & He, M. 2010. [Estimation of the normal range of blood glucose in rats]. *Wei sheng yan jiu = Journal of hygiene research*. 39(2):133–7, 142. [Online], Available: http://www.ncbi.nlm.nih.gov/pubmed/20459020 [2018, October 09].

Watson, S. 2009. Amazing Facts About Heart Health and Heart Disease. *WEBMD*. [Online], Available: http://www.webmd.com/heart/features/amazing-facts-about-heart-health-and-heart-disease_.

Webster, I., Salie, R., Marais, E., Fan, W.J., Maarman, G., Huisamen, B. & Lochner, A. 2017. Myocardial susceptibility to ischaemia/reperfusion in obesity: a re-evaluation of the effects of age. *BMC Physiology*. 17(1):1–13.

Weiss, J. & Hiltbrand, B. 1985. Functional compartmentation of glycolytic versus oxidative metabolism in isolated rabbit heart. *Journal of Clinical Investigation*. 75(2):436–447.

Whelan, R.S., Kaplinskiy, V. & Kitsis, R.N. 2010. Cell Death in the Pathogenesis of Heart Disease: Mechanisms and Significance. *Annual Review of Physiology*. 72(1):19–44.

“WHO | Cardiovascular diseases (CVDs)”. 2018. *WHO*. [Online], Available: http://www.who.int/cardiovascular_diseases/en/ [2018, October 08].

“WHO | GKT1 Activity and Practices”. 2013. *WHO*. [Online], Available: http://www.who.int/transplantation/gkt/statistics/en/ [2018, July 01].

“WHO | Obesity”. 2014. *WHO*. [Online], Available: http://www.who.int/topics/obesity/en/ [2018, October 08].

“WHO | Obesity”. 2015. *WHO*. [Online], Available: http://www.who.int/gho/ncd/risk_factors/obesity_text/en/ [2018, October 08].

WHO | Obesity and overweight. 2018. [Online], Available: http://www.who.int/news-room/fact-sheets/detail/obesity-and-overweight [2018, October 08].

Widlansky, M.E., Duffy, S.J., Hamburg, N.M., Gokce, N., Warden, B.A., Wiseman, S., Keaney, J.F., Frei, B., et al. 2005. Effects of black tea consumption on plasma catechins and markers of oxidative stress and inflammation in patients with coronary artery disease. *Free Radical Biology and Medicine*. 38(4):499–506.

Wieser, V., Moschen, A.R. & Tilg, H. 2013. Inflammation, Cytokines and Insulin Resistance: A Clinical

Perspective. *Arch.Immunol.Ther.Exp.* 61(2):119–125.

Wilcox, G. 2005. Insulin and Insulin Resistance. *Clin Biochem Rev.* 26(2):19–39. [Online], Available: http://www.ncbi.nlm.nih.gov/pmc/articles/PMC1204764/.

Wilhelm, M.J. 2015. Long-term outcome following heart transplantation: current perspective. *Journal of thoracic disease*. 7(3):549–51.

Willms, B., Lubke, D., Ahrens, K. & Arends, J. 1991. Delayed resorption of carbohydrates in type 2 diabetes: Dietetic measure (musli) compared with Î±-glucosidase inhibition [Resorptionsverzogerung der kohlenhydrate in der therapie des typ-II-diabetes: vergleich zwischen diatetischer (musli) und pharmakolog. *Schweizerische medizinische Wochenschrift*. 121(38):1379–1382.

Witters, L.A. 2001. The blooming of the French lilac. *The Journal of clinical investigation*. 108(8):1105–7.

Wolf, P.S., Merry, H.E., Farivar, A.S., McCourtie, A.S. & Mulligan, M.S. 2008. Stress-activated protein kinase inhibition to ameliorate lung ischemia reperfusion injury. *The Journal of Thoracic and Cardiovascular Surgery*. 135(3):656–665.

Wong, E.D., Wagner, J.A., Gorsich, S.W., McCaffery, J.M., Shaw, J.M. & Nunnari, J. 2000. The dynamin-related GTPase, Mgm1p, is an intermembrane space protein required for maintenance of fusion competent mitochondria. *The Journal of cell biology*. 151(2):341–52.

Woodgett, J.R. 1990. Molecular cloning and expression of glycogen synthase kinase-3/factor A. *EMBO J.* 9(8):2431–2438.

Woods, A., Johnstone, S.R., Dickerson, K., Leiper, F.C., Fryer, L.G.D., Neumann, D., Schlattner, U., Wallimann, T., et al. 2003. LKB1 Is the Upstream Kinase in the AMP-Activated Protein Kinase Cascade. *Current Biology*. 13(22):2004–2008.

World Economic Outlook. 2018. [Online], Available: https://www.imf.org/external/pubs/ft/weo/2018/01/weodata/download.aspx [2018, October 08].

Wu, M.-Y., Yiang, G.-T., Liao, W.-T., Tsai, A.P.-Y., Cheng, Y.-L., Cheng, P.-W., Li, C.-Y. & Li, C.-J. 2018. Current Mechanistic Concepts in Ischemia and Reperfusion Injury. *Cellular physiology and biochemistry : international journal of experimental cellular physiology, biochemistry, and pharmacology*. 46(4):1650–1667.

Xie, L., Pi, X., Wang, Z., He, J., Willis, M.S. & Patterson, C. 2015. Depletion of PHD3 protects heart from ischemia/reperfusion injury by inhibiting cardiomyocyte apoptosis. *Journal of molecular and cellular cardiology*. 80:156–65.

Xu, H., Barnes, G.T., Yang, Q., Tan, G., Yang, D., Chou, C.J., Sole, J., Nichols, A., et al. 2003. Chronic inflammation in fat plays a crucial role in the development of obesity-related insulin resistance. *Journal of Clinical Investigation*. 112(12):1821–1830.

Xu, Q., Yuan, F., Shen, X., Wen, H., Li, W., Cheng, B. & Wu, J. 2014. Polymorphisms of C242T and A640G in CYBA Gene and the Risk of Coronary Artery Disease: A Meta-Analysis. *PLoS ONE*. 9(1):e84251.

Xu, X.J., Valentine, R.J. & Ruderman, N.B. 2014. AMP-activated Protein Kinase (AMPK): Does This Master Regulator of Cellular Energy State Distinguish Insulin Sensitive from Insulin Resistant Obesity? *Current obesity reports*. 3(2):248–55.

Yadav, A., Kataria, M.A., Saini, V. & Yadav, A. 2013. Role of leptin and adiponectin in insulin resistance. *Clinica Chimica Acta*. 417:80–84.

Yang, Z. & Klionsky, D.J. 2010. Eaten alive: a history of macroautophagy. *Nature Cell Biology*. 12(9):814–

822.

Yang, C., Sudderth, J., Dang, T., Bachoo, R.M., Bachoo, R.G., McDonald, J.G. & DeBerardinis, R.J. 2009. Glioblastoma cells require glutamate dehydrogenase to survive impairments of glucose metabolism or Akt signaling. *Cancer research*. 69(20):7986–93.

Yang, C., Ko, B., Hensley, C.T., Jiang, L., Wasti, A.T., Kim, J., Sudderth, J., Calvaruso, M.A., et al. 2014. Glutamine oxidation maintains the TCA cycle and cell survival during impaired mitochondrial pyruvate transport. *Molecular cell*. 56(3):414–24.

Yang, X., Liu, Y., Yang, X.-M., Hu, F., Cui, L., Swingle, M.R., Honkanen, R.E., Soltani, P., et al. 2011. Cardioprotection by mild hypothermia during ischemia involves preservation of ERK activity. *Basic research in cardiology*. 106(3):421–30.

Yau, Y.H.C. & Potenza, M.N. 2013. Stress and eating behaviors. *Minerva endocrinologica*. 38(3):255–67.

Yellon, D.M. & Baxter, G.F. 1999. Reperfusion injury revisited: is there a role for growth factor signaling in limiting lethal reperfusion injury? *Trends in cardiovascular medicine*. 9(8):245–9.

Yellon, D.M. & Hausenloy, D.J. 2007. Myocardial Reperfusion Injury. *New England Journal of Medicine*. 357(11):1121–1135.

Yoshida, M., Shiojima, I., Ikeda, H. & Komuro, I. 2009. Chronic doxorubicin cardiotoxicity is mediated by oxidative DNA damage-ATM-p53-apoptosis pathway and attenuated by pitavastatin through the inhibition of Rac1 activity. *Journal of Molecular and Cellular Cardiology*. 47(5):698–705.

Youle, R.J. & van der Bliek, A.M. 2012. Mitochondrial Fission, Fusion, and Stress. *Science*. 337(6098):1062–1065.

Zang, M., Xu, S., Maitland-Toolan, K.A., Zuccollo, A., Hou, X., Jiang, B., Wierzbicki, M., Verbeuren, T.J., et al. 2006. Polyphenols Stimulate AMP-Activated Protein Kinase, Lower Lipids, and Inhibit Accelerated Atherosclerosis in Diabetic LDL Receptor-Deficient Mice. *Diabetes*. 55(8):2180–2191.

Zatroch, K.K., Knight, C.G., Reimer, J.N. & Pang, D.S.J. 2016. Refinement of intraperitoneal injection of sodium pentobarbital for euthanasia in laboratory rats (Rattus norvegicus). *BMC Veterinary Research*. 13(1):60.

Zhang, C., Skamagki, M., Liu, Z., Ananthanarayanan, A., Zhao, R., Li, H. & Correspondence, K.K. 2017. Biological Significance of the Suppression of Oxidative Phosphorylation in Induced Pluripotent Stem Cells.

Zhang, L., Zuo, Z. & Lin, G. 2007. Intestinal and Hepatic Glucuronidation of Flavonoids. *Mol.Pharmaceutics*. 4(6):833–845.

Zhao, Z.-Q., Nakamura, M., Wang, N.-P., Velez, D.A., Hewan-Lowe, K.O., Guyton, R.A. & Vinten-Johansen, J. 2000. Dynamic Progression of Contractile and Endothelial Dysfunction and Infarct Extension in the Late Phase of Reperfusion. *Journal of Surgical Research*. 94(2):133–144.

Zhou, H., Zhu, P., Wang, J., Zhu, H., Ren, J. & Chen, Y. 2018. Pathogenesis of cardiac ischemia reperfusion injury is associated with CK2α-disturbed mitochondrial homeostasis via suppression of FUNDC1-related mitophagy. *Cell Death & Differentiation*. 25(6):1080–1093.

Zhou, L., Deepa, S.S., Etzler, J.C., Ryu, J., Mao, X., Fang, Q., Liu, D.D., Torres, J.M., et al. 2009. Adiponectin Activates AMP-activated Protein Kinase in Muscle Cells via APPL1/LKB1-dependent and Phospholipase C/Ca^{2+} /Ca^{2+} /Calmodulin-dependent Protein Kinase Kinase-dependent Pathways. *Journal of Biological Chemistry*. 284(33):22426–22435.

Zhou, T., Prather, E.R., Garrison, D.E. & Zuo, L. 2018. Interplay between ROS and Antioxidants during Ischemia-Reperfusion Injuries in Cardiac and Skeletal Muscle. *International journal of molecular sciences*. 19(2).

Zhu, J., Su, X., Li, G., Chen, J., Tang, B. & Yang, Y. 2014. The incidence of acute myocardial infarction in relation to overweight and obesity: a meta-analysis. *Archives of medical science : AMS*. 10(5):855–62.

Zhu, Y., Wu, J. & Yuan, S.-Y. 2013. MCT1 and MCT4 Expression During Myocardial Ischemic-Reperfusion Injury in the Isolated Rat Heart. *Cellular Physiology and Biochemistry*. 32(3):663–674.

Zordoky, B.N.M., Nagendran, J., Pulinilkunnil, T., Kienesberger, P.C., Masson, G., Waller, T.J., Kemp, B.E., Steinberg, G.R., et al. 2014. AMPK-Dependent Inhibitory Phosphorylation of ACC Is Not Essential for Maintaining Myocardial Fatty Acid Oxidation. *Circulation Research*. 115(5):518–524.

Zorov, D.B., Juhaszova, M. & Sollott, S.J. 2014. Mitochondrial Reactive Oxygen Species (ROS) and ROS-Induced ROS Release. *Physiological Reviews*. 94(3):909–950.

Zorzano, A. 2017. Modulation of Parkin-dependent mitophagy and mitochondrial health. *Free Radical Biology and Medicine*. 108:S4.